Regulation of the ‘molecular scissor’ ADAM10 by tetraspanin Tspan15

by

JUSTYNA SZYROKA

A thesis submitted to The University of Birmingham for the degree of DOCTOR OF PHILOSOPHY

School of Biosciences
College of Life and Environmental Sciences
The University of Birmingham
May 2019

Abstract

ADAM10 is a ubiquitously-expressed ‘molecular scissor’ that regulates a variety of important transmembrane proteins by proteolytically cleaving their extracellular regions. The cellular localisation and substrate specificity of ADAM10 is regulated by one of six tetraspanin membrane proteins, termed TspanC8s, comprising Tspan5, 10, 14, 15, 17 and 33. This has led to the hypothesis that ADAM10 exists as six different scissors, depending on its interacting TspanC8. This thesis investigates the function of Tspan15, which is of interest due to its recent implication in cancer, deep vein thrombosis and bacterial infection. The new discoveries of this study are as follows. (1) Tspan15 expression is dependent on ADAM10. (2) Tspan15 is required for cleavage of neural-, epithelial- and vascular endothelial-cadherin in cell lines. (3) Two of four newly-generated anti-Tspan15 monoclonal antibodies have inhibitory activity directed against ADAM10-mediated cleavage of VE-cadherin, which cannot be explained by recognition of different epitopes or differential effects on Tspan15 internalisation or ADAM10 expression. (4) Loss of ADAM10 in human endothelial cells promotes migration, increases proliferation and impairs network formation, but loss of Tspan15 has no effect. These findings support the six-scissor hypothesis, suggest that the major function of Tspan15 is to regulate ADAM10, and demonstrate the therapeutic potential of TspanC8 monoclonal antibodies.

Dedication

This thesis is dedicated to my mum, Anna

Dla mamy

Acknowledgement

I would like to say thank you to my supervisor Dr Mike Tomlinson for the opportunity to join the group. Thank you for your constant help, support and knowledge throughout the PhD. I would like to thank you to my co-supervisor Dr Victoria Heath, for your valuable input in the project.

To Tomlinson group members, Ally, Connie and Neale, thank you for your kindness, moral support, scientific discussions and being all great round friends.

Ola, to była miłość od pierwszego wyjścia na piwo. Jestem wdzięczna Beacie, że nas poznała. Bez Ciebie PhD nie byłoby takie same ;*

Jas, thank you for your support and enthusiastic discussions throughout my mini-project and PhD, and always having time to help me out.

To all my friends on the 8th floor, thank you for putting up with me as fellow PhD students. You made this experience unforgettable.

Finally, I would like to thank my mum, who has supported me so much over these years, this could not have been done without you.

Table of Contents

List of figures

List of tables

Abbreviations

ADAM: A disintegrin and metalloprotease

ADAMTS: A disintegrin and metalloprotease with thrombospondin motifs

Ang1 and 2: Angiopoietin 1 and 2

AP: Adaptor protein

APP: Amyloid precursor protein

DAPT: N-[N-(3,5-difluorophenacetyl)-L-alanyl]-S-phenylglycine t-butyl ester

DLL4: Delta-like ligand 4

E-cadherin: Epithelial-cadherin

ECM: Extracellular matrix

EGF: Epidermal growth factor

FGF: Fibroblast growth factor

GPVI: Glycoprotein VI

GPCR: G protein-coupled receptor

HEK-293T: Human embryonic kidney-293 cells expressing the large T-antigen of simian virus 40

HIF-1: Hypoxia induced factor 1 alpha

HMVEC: Human microvascular endothelial cell

HUVEC: Human umbilical vein endothelial cell

JAM: Junctional adhesion molecule

MT1-MMP: Membrane type 1 matrix metalloprotease

N-cadherin: Neural cadherin

NEM: N-ethylmaleimide

NEXT: Notch extracellular truncation

NICD: Notch intracellular domain

Nrarp: Notch-regulated ankyrin repeat protein

OSCC: Oesophageal squamous cell carcinoma

PDGF/PDGFR: Platelet-derived growth factor/receptor

PECAM: Platelet endothelial cell adhesion molecule

PMA: phorbol 12-myristate 13-acetate

SAP97: Synapse-associated protein 97

SP1: Specificity protein 1

TGFβ: Transforming growth factor β

TIMP: Tissue inhibitor of metalloproteinase

TSP1: Thrombospondin 1

UP: Uroplakin

USF: Upstream stimulatory factor

UTR: Untranslated region

VE-cadherin: Vascular endothelial cadherin

VEGF: Vascular endothelial growth factor

VEGFR2: Vascular endothelial growth factor receptor 2

XBP-1: X-box binding protein 1

ZO-1: Zona occludens protein

CHAPTER 1
GENERAL INTRODUCTION

1.1 A disintegrin and metalloproteases (ADAMs)

1.1.1 Shedding overview

The landscape of proteases on the cell surface adds variety to the repertoire of surface proteins and their functions. Indeed, membrane proteases contribute towards the activation or inhibition of signalling cascades, and also form a part of the degradation machinery for unwanted proteins to maintain proper physiological function (Lopez-Otin and Bond, 2008). Thus, proteolytic release of the ectodomains, or 'shedding', of membrane proteins emerges as an essential mechanism in controlling various biological events including embryonic development, cell adhesion, migration and differentiation, necessary for the life of all organisms (Weber and Saftig, 2012). Dysregulation of proteolytic systems is associated with many pathological conditions like cancer, neurodegenerative disorders, inflammatory and cardiovascular diseases (Giebeler and Zigrino, 2016). The shedding process is directed towards membrane-tethered proteins. Proteolytic shedding occurs at the juxtamembrane site, freeing a soluble ectodomain and leaving a membrane-associated remnant (Clark, 2014).

In the shedding of cytokines or growth factors, like tumour necrosis factor α (TNFα), transmembrane chemokine (CX3CL1), and the epidermal growth factor (EGF) family, the released extracellular fragment is biologically active and capable of initiating paracrine signalling (Lopez-Otin and Bond, 2008, Clark, 2014). The cleavage is also a prerequisite for intracellular signalling, which is mediated by intracellular protein domain release from the membrane through the action of γ-secretase. This process is known as regulated intramembrane proteolysis (RIP) and has a role in signal transduction and also contributes to the degradation of proteins (Lichtenthaler et al., 2011). A few proteins are known to be subjected to this double cleavage, among them Notch receptors (van Tetering et al., 2009), APP-α (Postina et al., 2004), heparin binding (HB)-EGF (Nanba et al., 2003), the cadherin family of cell-cell ahesion proteins (Maretzky et al., 2005, Reiss et al., 2005, Schulz et al., 2008), the adhesion protein CD44 (Nagano et al., 2004) and a disintegrin and metalloproteases (ADAMs) themselves (Tousseyn et al., 2009). Besides the signalling role, the proteolysis can abolish the function of proteins at the cell surface. This downregulation most commonly happens in *cis*, on the same cell, such as for endothelial adhesion molecule VE-cadherin (Shultz et al., 2008) or growth factor receptor VEGFR2 (Donners et al., 2010), that results in cell detachment or inhibition of signalling, respectively. In one case it has been reported on opposite cells, in *trans*, for ADAM10 cleavage of ephrin-A5 following engagement with its Eph-A3 receptor on an adjacent cell, a process which enables termination of signalling and the contact repulsion of neuronal cells (Janes et al., 2009, Atapattu et al., 2014).

1.1.2 ADAM family

The ADAMs belong to an evolutionarily conserved superfamily of Zn^{2+}-dependent metalloproteinases. They are type I transmembrane glycoproteins of about 750-900 amino acids in length and identified in a broad range of animal classes including nematodes, sea urchins, fruit flies, frogs, birds and mammals (Weber and Saftig, 2012). 22 ADAM members have been identified in human and 12 of them (ADAM 8, 9, 10, 12, 15, 17, 19, 20, 21, 28, 30 and 33) are found to be enzymatically active. Over the years, studies have highlighted their roles as sheddases and modulators of cell-cell adhesion and cell-matrix interactions, with some variations in substrate specificity (Endres and Deller, 2017). Expression profiles of the ADAMs can vary considerably. ADAM9, 10, 15 and 17 are ubiquitous, whereas other ADAMs are expressed in a tissue-type restricted manner like ADAM12 and 19 in muscle, ADAM22 in the brain and ADAM23 in the heart and the brain (Hartmann et al., 2013, Edwards et al., 2008). ADAMs are involved in the shedding of a plethora of transmembrane proteins like growth factors and their receptors, adhesion molecules, as well as cell cytokines, among others (Reiss and Saftig, 2009).

The uniqueness of the structural organisation of ADAMs allows them to exhibit proteolytic activity towards their substrates on the cell surface. Typical ADAM structure shares a modular topology (Figure 1.1). Starting from the N-terminal signal sequence that directs the enzyme through secretory pathways, the first domain is a pro-domain (in the immature form of the protein, which controls enzyme latency and correct folding). This is followed by a metalloprotease domain with Zn^{2+}-binding consensus motif (HExGHxxGxxHD) within the active site and with proteolytic properties (Edwards et al., 2008). Next, there is a

disintegrin domain and cysteine-rich region that together contribute to substrate recognition and ADAM catalytic activity (Janes et al., 2005). This is followed by an EGF domain, except for ADAM10 and 17. This region has been thought to contribute to the regulation of substrate binding to the cysteine-rich domain. Lastly, there is a transmembrane region and cytoplasmic tail equipped with proline-rich motifs, recognising SH3 domain-containing proteins, and phosphorylation sites. The tail has been postulated to facilitate proteolytic activity, signalling and surface localisation of ADAMs (Reiss and Saftig, 2009).

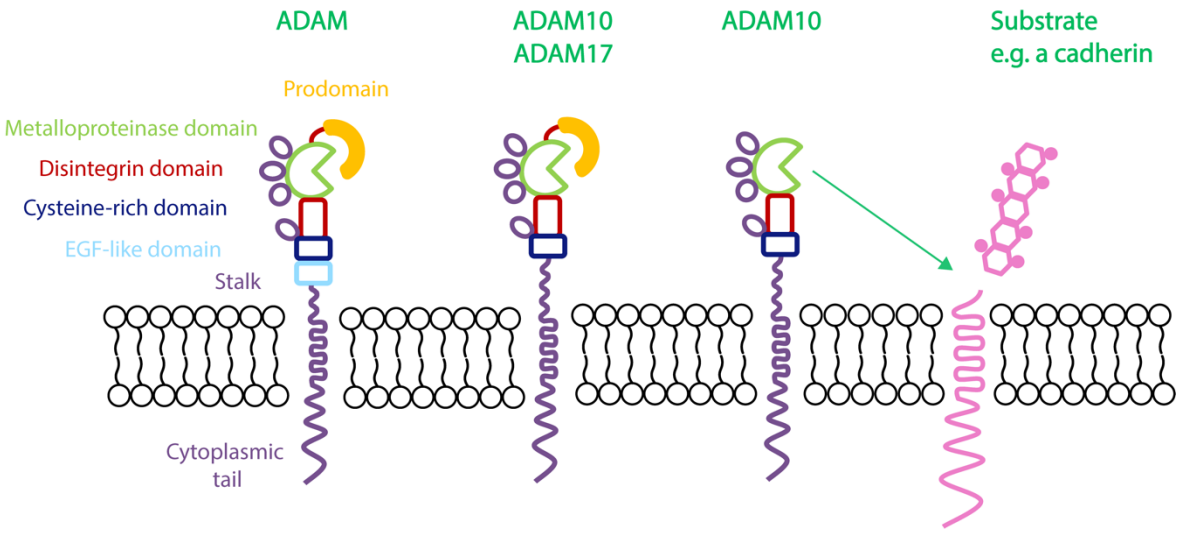

Figure 1.1 Schematic representation of modular domain organisation of ADAM family proteins. N-glycosylation sites represented by ovals.

Metalloproteases are produced as inactive proenzymes in the endoplasmic reticulum (ER). Their activation and subsequent maturation take place in the ER and Golgi network, where the chaperone-like acting prodomain is cleaved by furin or proprotein convertase 7 (PC7).

As a consequence, the active site within the metalloprotease domain is revealed, and the enzymes can exert their proteolytic activity (Wong et al., 2015).

There is no consensus sequence that indicates the cleavage site in the substrates subjected to proteolysis by ADAMs. Nevertheless, the cleavage occurs close to the plasma membrane (Hogl et al., 2011). The proteomic identification of ADAM10 cleavage sites identified specificity for basic and aromatic amino acid residues like leucine, tyrosine and phenylalanine (Tucher et al., 2014). Additionally, other features like the substrate-binding pocket within the metalloprotease domain, the presence of non-catalytic domains and conformational change within the substrate may facilitate substrate recognition (Janes et al., 2005, Caescu et al., 2009).

1.2 ADAM10

1.2.1 Structure and function of ADAM10

To date, ADAM10 (Kuzbanian orthologue in *Drosophila*), along with its close relative ADAM17 (TACE, tumour necrosis factor α (TNFα) converting enzyme), is the best characterised ADAM. ADAM10 has a ubiquitous expression profile in mammalian cell types and a broad list of identified substrates (Hartmann et al., 2013). Additionally, genetic deficiency of the protease yields severe phenotypes during embryogenesis that have lethal consequences for both vertebrates and invertebrates (Dreymueller et al., 2015, Saftig and Lichtenthaler, 2015).

ADAM17 is particularly important for inflammation, immunity and epithelial barrier integrity (Dreymueller et al., 2015). It is critically involved in first line of defence upon injury, by mediating proteolysis of TNFα to stimulate the immune system, and EGFR-ligands to promote epithelial cell proliferation and repair (Le Gall et al., 2010). Indeed, ADAM17-knockout mice die perinatally with defects in eyes, hair and in morphogenesis of multiple organs (heart, lung and skin), strikingly resembling phenotypes observed in EGF/transforming growth factor α (TGFα)/HB-EGF-deficient mice (Chalaris et al., 2010, Franzke et al., 2012, Jackson et al., 2003, Sternlicht et al., 2005). Mice with tissue specific deletion of ADAM17 are protected from endotoxin-induced septic shock and have reduced inflammation symptoms (Khokha et al., 2013).

Rooke *et al* showed that a loss-of-function mutation in ADAM10 in *Drosophila* was critical for neuronal cell fate decisions (Rooke et al., 1996). These results were in line with those caused by mutations in Notch. In ADAM10-deficient fruit flies, the Notch receptor cannot be shed, which leads to abolished signalling and severe developmental defects (Sotillos et al., 1997). The mechanism underlying Notch signalling and its proteolytic processing is conserved in all multicellular organisms ranging from sea urchins to humans. ADAM10 is responsible for ligand-induced cleavage at the plasma membrane that enables intramembrane proteolysis by γ-secretase, release of the Notch intracellular domain and ultimately gene transcription in the nucleus (van Tetering et al., 2009).

The importance of the protease is emphasized by the fact that ADAM10-deficient mice die at embryonic day 9.5 due to numerous defects in somite, cardiovascular and neuronal systems. This is similar to phenotypes observed in Notch1 and 4 double-knockout mice (Hartmann et al., 2002). Also, conditional deletion of ADAM10 in endothelial cells induces vascular abnormalities like those caused by interference with Notch signalling (Glomski et al., 2011).

A recent discovery based on the first crystal structure of the ADAM10 ectodomain brought new insight into the architecture and domain organisation (Figure 1.2). Interestingly, the protease favours a closed “auto-inhibitory” conformation, where the cysteine-rich domain partially masks the active site within the metalloprotease domain. Therefore, access of the enzyme to substrates is restricted, although the catalytic site is in position to cleave the substrates close to the plasma membrane, presumably following a conformational change (Seegar et al., 2017).

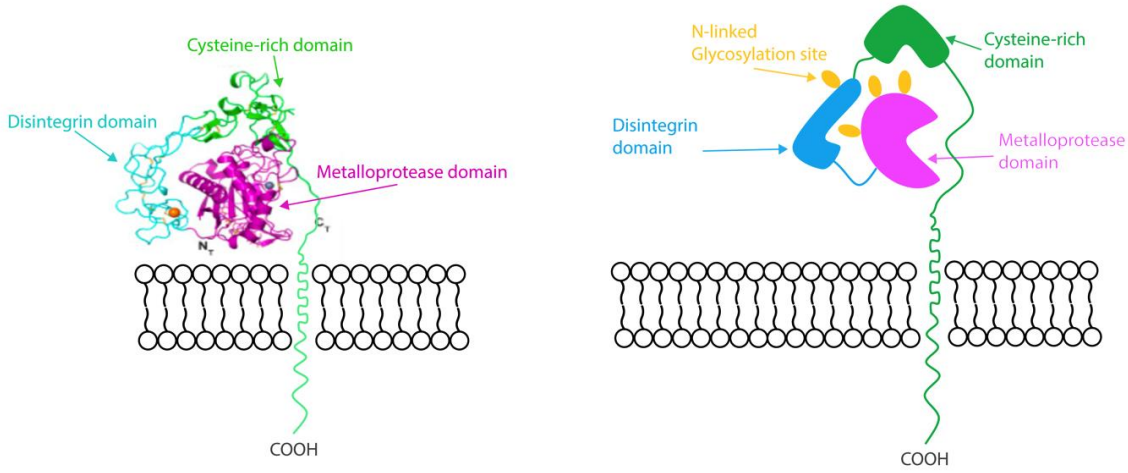

Figure 1.2 ADAM10 ectodomain structure. On the left is the crystal structure of the ADAM10 ectodomain (Seegar et al., 2017) modelled onto the transmembrane region; on the right is a schematic representation of this structure.

1.2.2 Regulation of ADAM10

ADAM10 contributes to a broad range of cellular functions; therefore, its spatial-temporal regulation is of pivotal importance. The activity of the protease can be controlled by several mechanisms including regulation of gene expression, post-translational modifications, compartmentalisation at the plasma membrane and protein-protein interactions (Endres and Deller, 2017). The human ADAM10 gene is evolutionarily conserved, contains 16 exons and spans a total of 154 kb. The promoter region does not comprise a TATA box but has several transcription factors binding sites. The interactions with factors like specificity protein 1 (SP1), upstream stimulatory factor (USF), X-box binding protein-1 (XBP-1) and retinoic acid were found to be important to induce ADAM10 transcription and its availability within the cell, especially during Alzheimer's pathogenesis (Peron et al., 2018). Upregulation of ADAM10 mRNA levels by retinoic acid receptor (RAR) was found to induce ADAM10 α-secretase processing of amyloid precursor protein (APP), so decreasing amyloid-β formation *in vitro* (Lee et al., 2014) and *in vivo* (Tippmann et al., 2009). Translational regulation of ADAM10 includes the interaction of microRNAs (miRNA) with the 3' untranslated region (UTR) of ADAM10 mRNA, and the presence of a GC-rich sequence in the ADAM10 5' UTR region that forms G-quadruplex RNA secondary structures. Both factors act as negative regulators of ADAM10 genes, contributing to the suppression of ADAM10 protein levels (Endres and Deller, 2017, Peron et al., 2018). Depletion of endogenous ADAM10-targeting miR-122 in human hepatic cancer cells promoted a tumorigenic phenotype of the cells (Bai et al., 2009), while destabilisation of the G-quadruplex dysregulated ADAM10-mediated APP processing, leading to synaptic deficits in Fragile X Syndrome (Pasciuto et al., 2015).

ADAM10 is synthesised in the endoplasmic reticulum (ER) as an 85 kDa auto-inhibited pro-enzyme (Anders et al., 2001). After enzymatic removal of the prodomain in the Golgi, a 65 kDa mature and active form of ADAM10 is transported to the cell surface. ADAM10 itself can be proteolytically processed by ADAM9, 15 and γ-secretase, leaving a membrane-bound C-terminal fragment (10 kDa) and releasing a soluble ectodomain of 55 kDa and cytoplasmic fragment (7 kDa) (Tousseyn et al., 2009). However, the physiological relevance of this cleavage is unknown.

Cellular compartmentalisation is thought to be important for ADAM10 regulation and activity. The mature ADAM10 is found to be associated with cellular trafficking regulators. For example, the cytosolic tail of the protease, via a proline-rich motif, binds to the SH3 domain of synaptic proteins like synapse-associated protein 97 (SAP97) (Saraceno et al., 2014) and adaptor protein 2 (AP2) (Marcello et al., 2013), that control transport to the plasma membrane and internalisation, respectively. Rab14 and its effector FAM116 also have been suggested to promote ADAM10 trafficking and surface localisation (Linford et al., 2012). Additionally, ADAM10 was found to interact with tetraspanin trafficking proteins (Arduise et al., 2008), and this association is the only one to known to affect ADAM10 maturation and activity (Saint-Pol et al., 2017b); this is the focus of this thesis and will be introduced later.

The composition of the plasma membrane is another crucial feature in ADAM10 regulation. The association of ADAM10 within cholesterol-rich regions contributes to the downregulation of its catalytic activity (Matthews et al., 2003, Murai et al., 2011). The

increase in cholesterol levels, which often occurs in patients with Alzheimer's disease, reduces the expression of ADAM10 (Sathya et al., 2017). The aforementioned may be one of the factors that prevent the production of a neuroprotective form of APP, instead generating toxic and insoluble Aβ peptides. This has crucial consequences for the progression of a disease state like Alzheimer's disease, where the formation of amyloid plaques is elevated (Sathya et al., 2017). In contrast, cholesterol depletion may affect membrane fluidity and disassembly of membrane micro-platforms, which enhances substrate accessibility and ADAM10 mediated cleavage (Kojro et al., 2010, Peron et al., 2018).

ADAM functions have been shown to be controlled by various inhibitors and stimuli. The naturally occurring inhibitors are the ADAM10 prodomain (Moss et al., 2007) and endogenous tissue inhibitor of metalloproteases (TIMP-1 and -3) (Amour et al., 2000, Murphy, 2011). The synthetic inhibitor GI254023X binds the Zn^{2+} ion within the active site cleft of the metalloprotease domain and blocks its activity (Seegar et al., 2017). Although a broad inhibition of the protease is detrimental, as indicated by the lethal phenotype of the ADAM10-knockout mice, it is thought that a well-controlled dose of inhibitor may be useful for disease treatment (Ludwig et al., 2005).

ADAM10 activity is enhanced by Ca^{2+} ionophores (Sanderson et al., 2005, Maretzky et al., 2005), the alkylating agent N-ethylmaleimide (NEM) (Facey et al., 2016), or growth factors such as vascular endothelial growth factor (VEGF) (Donners et al., 2010). However, the exact mechanisms of their actions remain unknown. Donners *et al* demonstrated the increase in both the expression and activity of ADAM10 upon VEGF stimulation, that consequently promoted shedding of vascular endothelial (VE)-cadherin

and VEGFR2 (Donners et al., 2010). In the aforementioned, ADAM10-mediated cleavage may further depend on activated extracellular signal-regulated kinase (ERK) 1/2 and phosphoinositide 3-kinase (PI3K) signalling pathways. Moreover, the agonists can modulate ADAM10 substrate selectivity. Ionomycin but not phorbol 12-myristate 13-acetate (PMA) may stimulate the activity of ADAM10 towards TNFα, TGFα and L-selectin in the absence of their principal sheddase, ADAM17 (Le Gall et al., 2009). The mechanism behind the inducible shedding is not well understood, but it may depend on the structural domains. Maretzky *et al* showed that the cytoplasmic domain negatively contributes to the constitutive activity of ADAM10 via an ER retention motif, but it is dispensable for rapid activation of the protease by NEM and ionomycin towards betacellulin. Instead, the authors emphasised the importance of the transmembrane region in this process (Maretzky et al., 2015). The results were in line with those previously reported by Horiuchi *et al*. The authors have shown that expression of an ADAM10 mutant with a truncated cytoplasmic domain partially rescue Ca^{2+}-stimulated shedding of BTC in ADAM10-deficient cells (Horiuchi et al., 2007). This suggests that regulation may occur on the plasma membrane through interactions with putative ADAM10 binding partners and may be independent of trafficking.

1.2.3 ADAM10 substrates

1.2.3.1 Overview of ADAM10 substrates

ADAM10 is a primary sheddase for more than 40 substrates; many of which have an impact on health and disease. These include the Notch cell fate regulator (van Tetering et al., 2009), junctional adhesion molecule VE-cadherin (Schulz et al., 2008), transmembrane chemokines CX3CL1 and CXCL16 (Hundhausen et al., 2007), APP (Postina et al., 2004); glycoprotein VI (GPVI) (Bender et al., 2010, Gardiner et al., 2007), EGF receptor (EGFR) ligands betacellulin and EGF (Yan et al., 2002, Sahin et al., 2004, Sanderson et al., 2005, Blobel, 2005), cellular prion protein (Altmeppen et al., 2015), cadherin and CD44 adhesion molecules (Nagano et al., 2004, Reiss et al., 2005, Schulz et al., 2008), the low affinity immunoglobulin E receptor CD23 (Lemieux et al., 2007), vascular endothelial growth factor receptor 2 (VEGFR2) (Donners et al., 2010) and many others. The ubiquitous expression and the substrate repertoire of ADAM10 contribute to a variety of biological processes, including cell fate and differentiation, chemotaxis, receptor-ligand signalling, vascular permeability, migration, proliferation and immunity (Pruessmeyer and Ludwig, 2009, van der Vorst et al., 2012). Due to the biological importance of substrates cleaved by ADAM10, dysregulation of ADAM activity has been associated with pathologies such as cancer, cardiovascular disease, inflammation and neurodegeneration. Thus, targeting ADAM10 could have therapeutic potential (Wetzel et al., 2017). Many conditions, including cancer, inflammation, asthma and skin disorders, could potentially benefit from the inhibition of ADAM10 activity (Saftig and Lichtenthaler, 2015). For example, some breast tumours are characterised by an increased level of ADAM10, which contributes to cancer progression and poor prognosis in patients. Mullooly *et al* have shown that

inactivation of ADAM10 reduces breast cancer cell migration and invasion *in vitro.* Therefore, downregulation may be regarded as an approach that carries therapeutic benefit (Mullooly et al., 2015). In contrast, many disorders can benefit from induction of ADAM10 activity. These include Alzheimer's disease, heart attack and stroke caused by thrombosis (Saftig and Lichtenthaler, 2015, Induruwa et al., 2016). For example, in an Alzheimer's disease mouse model, the neuronal overexpression of ADAM10 was associated with a reduction of the pathologies associated with deposition of the amyloidogenic Aβ peptides (Postina et al., 2004).

1.2.3.2 *Notch*

One of the most important and well-studied ADAM10 substrates is Notch, for which there are four family members, Notch 1-4. Notch signalling is evolutionarily conserved within the animal kingdom, is involved in cell fate decisions and is a crucial developmental process (Weber and Saftig, 2012). Upon binding of a Notch ligand (for example Delta-like ligand 1) to the Notch receptor, ADAM10 liberates the Notch ectodomain. The remaining membrane-anchored fragment is processed by the γ-secretase complex that releases a Notch intracellular domain (NICD). The NICD fragment translocate to the nucleus where it is involved in transcription of Notch target genes (Kopan and Ilagan, 2009). Global ADAM10 inactivation is lethal at the embryonic stage (E9.5) in mice due to developmental defects in the neuronal and cardiovascular system (Hartmann et al., 2002), which is comparable to the features observed in Notch1 and 4 double-knockout mice (Krebs et al., 2000). In angiogenesis, vessel sprouting and branching, as well as tip and stalk cell phenotype differentiation, depends on functional Notch signalling (Herbert and Stainier,

2011). Indeed, in mice with ADAM10-deficient endothelial cells, vascular integrity is impaired through hyper-sprouting of poorly perfused vessels and increased numbers of endothelial cells and cells displaying tip cell characteristics (Glomski et al., 2011, Caolo et al., 2015). This is consistent with the findings of Lucitti *et al* where an increased number of collateral vessel formations was observed in mice with ADAM10-deficient endothelial cells, due to aberrant sprouting and branching (Lucitti et al., 2012). Indeed, expression of Notch target genes (the *Snail* transcriptional factor and bone morphogenetic protein 2 *(Bmp2)*) is impaired in ADAM10-deficient endothelial cells, supporting the notion of ADAM10 involvement in Notch signalling (Zhang et al., 2010).

1.2.3.3 *Amyloid precursor protein (APP)*

Two alternative proteases mediate APP proteolytic processing: ADAM10 (α-secretase) or β-secretase (BACE 1), which lead to soluble APPα (sAPPα) or Aβ peptide, respectively. The ectodomain cleavage leaves a membrane-tethered fragment that is further processed by γ-secretase, releasing an APP intracellular domain (Kogel et al., 2012). However, its exact role is still under discussion. Pathogenesis of Alzheimer's disease is associated with the accumulation of toxic amyloidogenic Aβ peptides in the cerebral cortex, which can be prevented by enhanced cleavage by ADAM10 and the subsequent generation of the neuroprotective sAPPα (Marcello et al., 2017). Consistent with this, overexpression of ADAM10 in an Alzheimer's disease mouse model reduced memory loss and neurodegeneration (Postina et al., 2004). Besides its well-established role in the brain, APP is abundantly expressed on platelets, where it limits venous thrombosis by inhibiting the coagulation cascade. Indeed, APP-knockout mice developed significantly larger blood

clots compared to littermates, and were more susceptible to embolization (Canobbio et al., 2017).

1.2.3.4 *VE-cadherin*

Vascular permeability, integrity and migration are the crucial characteristics of the blood vessel endothelium. To uphold function of the vascular barrier these features must be finely tuned at the right time and place. Endothelial guardians for the aforementioned functions are present within the cadherin superfamily of Ca^{2+}-dependent adhesion molecules (Figure 1.3) (Dejana and Orsenigo, 2013).

Cadherins are type 1 single-pass transmembrane proteins which mediate cell-cell adhesion via trans-homodimerization and through cis-clustering of the cadherins at the cell junctions. While the extracellular domain drives adhesion from outside the cell, the intracellular domain mediates interaction with the actin cytoskeleton which induces changes to cell migration and morphology. To support the aforementioned functions, interaction between the cadherin intracellular domain and cytoplasmic binding partner proteins, p120-catenin and β-catenin, is essential (Gartner et al., 2015). The interaction of p120 with the membrane-proximal region of the cadherin is required for stabilising cadherins at the cell surface, which enhances their adhesion strength and prevents endocytosis. Also, p120 was found to interact with Rho GTPases, which affects actin assembly and dynamics (Shapiro and Weis, 2009). As a component of adherens junctions, the adaptor β-catenin has a dual function: it directly links cadherins to the cytoskeleton via α-catenin, and also regulates gene transcription on the Wnt signalling pathway, when uncoupled from cadherins (Reiss et al., 2005, Nusse and Clevers, 2017).

VE-cadherin is a crucial component of endothelial adherens junctions that mediates homotypic interactions and adhesion between endothelial cells. Therefore, it is required for the establishment of a stable vascular network by inducing contact inhibition of growth, regulation of endothelial permeability and leukocyte transmigration (Giannotta et al., 2013). *In vivo*, intravenous administration of anti-VE-cadherin antibody induced redistribution of the protein from cell-cell junctions and increased permeability of the vascular layer (Corada et al., 1999). VE-cadherin gene deletion (or mutation) do not affect the early stages of *de novo* formation of blood vessels. However, the consequence is lethality at embryonic day 9.5, due to impaired maintenance and remodelling of endothelial cells into vascular structures (Carmeliet et al., 1999, Crosby et al., 2005).

VE-cadherin function and expression at the cell surface are regulated through permeability-increasing agents (inflammatory cytokines, histamine, thrombin and VEGF). The VEGF/VEGFR2-activated signalling pathways promote uncoupling of the VEGFR2/VE-cadherin complex at the cell surface. Subsequent phosphorylation of the constituents and endocytosis of VE-cadherin contribute to the disruption of the cell-cell contacts and increased permeability of the vasculature (Gavard and Gutkind, 2006). Also, VEGF-induced endothelial cell survival requires formation of the complex between VE-cadherin, catenin and VEGFR2. Carmeliet *et al* showed that deficiency of the cadherin gene, or truncation of its cytosolic domain in mice, impairs cell survival and induces apoptosis which in turn prevents angiogenesis (Carmeliet et al., 1999). VE-cadherin clustering induces contact inhibition of endothelial cells and subsequently blocks proliferation. Therefore, confluent cells poorly respond to VEGF signalling via the VEGFR2 receptor (Lampugnani et al., 2003).

Shulz *et al* showed that VE-cadherin is shed by ADAM10, and that thrombin-induced ADAM10 shedding of VE-cadherin contributes to endothelial cell dissociation. Furthermore, siRNA knockdown of ADAM10 on endothelial cells increased VE-cadherin expression and decreased permeability of the endothelial barrier. In fact, elevated levels of soluble VE-cadherin and increased vessel leakage accompany vascular disorders like atherosclerosis and diabetic retinopathy (Schulz et al., 2008). Following up the Schulz publication, Donners *et al* demonstrated VEGF-induced VE-cadherin shedding by ADAM10, and its requirement for endothelial cell migration and vascular permeability (Donners et al., 2010). *In vitro* and *in vivo* studies also investigated histamine as an inducer of vascular permeability. This was effected by phosphorylation and delocalisation of VE-cadherin, activation of protein kinase C (PKC) signalling pathways and cytoskeletal rearrangements (Ashina et al., 2015). In sepsis, increased levels of soluble VE-cadherin are associated with inflammation-induced endothelial barrier breakdown through the interference with binding affinities of endogenous VE-cadherin. The application of an ADAM10 inhibitor confirmed the proteolytic origin of the released fragment, and impaired the formation of the cleaved cadherin and endothelial barrier phenotype (Flemming et al., 2015).

1.2.3.5 *N-cadherin*

A second cadherin expressed on endothelial cells is N-cadherin, but it is best characterised on other cell types such as epithelial cells, fibroblasts, neurons and cardiac myocytes (Uhlen et al., 2015). N-cadherin is known as the junctional adhesion molecule that

maintains barrier function and as a positive regulator of proliferation, migration and invasion (Wheelock et al., 2008, Hazan et al., 2000, Vassilev et al., 2012). N- and VE-cadherin share 38% amino acid sequence identity, and the cytoplasmic regions are most similar, at over 47% (Ferreri et al., 2008). Despite the close homology, N-cadherin differs in having diffuse distribution along the endothelium and mediating heterotypic interactions between endothelial cells and mural cells (Figure 1.3) (Salomon et al., 1992, Giampietro et al., 2012). The interruption of the heterotypic interactions between endothelial cells and pericytes, for example, leads to poor pericyte adhesion to endothelium, disturbed vascular morphogenesis and vessel elongation (Gerhardt et al., 2000). Previous work has shown that VE-cadherin's presence at the junctions excludes N-cadherin from these sites, due to its higher affinity for p120-catenin (Navarro et al., 1998, Giampietro et al., 2012). However, in a separate study, N-cadherin was portrayed as a significant modulator of endothelial cell function and behaviour that localises to endothelial junctions. Indeed, endothelial cell-specific inactivation of the N-cadherin gene causes embryonic lethality at day 9.5 in mice due to severe vascular defects including abnormal vessel organisation, endothelial cell death and impaired development of the heart (Radice et al., 1997, Luo and Radice, 2005). This, in fact, corresponds to the phenotype seen in VE-cadherin-deficient mice (Carmeliet et al., 1999). Interestingly, embryonic death happened before engagement of pericytes in the vasculature, implying that besides the role in vessel maturation, N-cadherin has a direct role in endothelial function (Luo and Radice, 2005, Ferreri et al., 2008). Luo and Radice *et al* concluded that N-cadherin regulates angiogenesis upstream of VE-cadherin, as N-cadherin loss significantly reduced VE-cadherin and p120 surface expression (Luo and Radice, 2005). In the same study, the inactivation of N-cadherin by siRNA resulted in cell proliferation arrest and increased cell motility, with subsequent increase in β1-integrin

expression. Similar to promoting cell motility on endothelial cells, N-cadherin can stimulate epithelial cell behaviour. The cadherin switching (cadherin isoform switching) that occurs during epithelial-mesenchymal transition (EMT) contributes to upregulation of N-cadherin, that in turn modulates many aspects of epithelial cell behaviour in physiopathology (Wheelock et al., 2008). Finally, N-cadherin is functional on neuronal cells (Radice et al., 1997), and has a role in neuro-epithelial cell-cell adhesion, regulation of synaptic development, axonal extension and polarity (Huntley, 2002, Gartner et al., 2015).

Reiss *et al* have identified ADAM10 as the specific sheddase for N-cadherin (Reiss et al., 2005), but the importance of N-cadherin shedding remains poorly understood. In fibroblasts and neuronal cells, N-cadherin processing by ADAM10 is thought to play a role in cell adhesion, migration and signalling. ADAM10-deficient fibroblasts showed upregulated adhesive behaviour and impaired β-catenin-dependent signalling due to the accumulation of full-length cadherin and β-catenin in intact adherent junctions. As a result, β-catenin was inaccessible for Wnt signalling which is essential for proliferation and cell survival (Reiss et al., 2005). Not only full-length, but also shed N-terminal fragments of the cadherin, retain biological activities. Derycke *et al* reported that the cleaved, soluble fragment of N-cadherin promotes angiogenesis *in vivo* and wound healing *in vitro,* through N-cadherin/fibroblast growth factor (FGF)-receptor complex activation. Upon binding of the soluble fragment to the complex, expression of matrix metalloproteases (MMPs) and plasmin was upregulated, which in return induced angiogenesis (Derycke et al., 2006). Likewise, another study showed that N-cadherin expression induces cell motility by maintaining a high level of FGF signalling, leading to upregulation of migration-related genes (Giampietro et al., 2012).

1.2.3.6 *E-cadherin*

E-cadherin has been identified as one of the most important ADAM10 substrates involved in epithelial morphogenesis, repair and integrity. E-cadherin is exclusively expressed on epithelial tissues. Mice with global E-cadherin deletion are embryonic lethal, highlighting its importance in development and tissue homeostasis. Also, tissue and organ-specific loss of the protein leads to early death due to aberrant cell morphology, increased permeability and tissue damage (Schneider and Kolligs, 2015, Schnoor, 2015). E-cadherin is cleaved specifically by ADAM10. E-cadherin shedding is associated with loss of cell adhesion and increased cell migration and proliferation *in vitro* and *in vivo*. Moreover, E-cadherin processing by ADAM10, and then γ-secretase, results in translocation of β-catenin to the nucleus to activate Wnt signalling. This contributes to epithelial-mesenchymal transition (EMT) and invasive behaviour of tumour cells (Maretzky et al., 2005). Sorting and compartmentalisation of cells in epithelial tissue relies on strong adhesion between them. ADAM10-mediated shedding of E-cadherin influence asymmetric localisation of the protein and restricted boundary formation caused by scattered cells. This dispositioning of cells carries important consequences for tissue morphogenesis and homeostasis (Solanas et al., 2011). E-cadherin is known as a tumour suppressor gene, as mutations are associated with gastric, breast, collateral, thyroid and ovarian cancers (Pecina-Slaus, 2003). The loss of function or downregulation of E-cadherin is also associated with poor outcomes and survival in patients. Conversely, upregulation of E-cadherin on cells prevents carcinogenesis due to growth inhibition, cell cycle arrest and reduced invasiveness (Wong et al., 2018). Additionally, elevated levels of the soluble E-cadherin are a vital diagnostic marker in skin diseases. The role of E-cadherin is critically dependent on its regulation of

β-catenin, by keeping the junctions intact and stopping β-catenin entering the nucleus to affect gene expression. Upon pro-inflammatory stimuli, such as TGFβ and cytokines, the areas affected by eczema lesions show upregulation of active ADAM10 and downregulation of E-cadherin, which correlates with impaired keratinocyte cohesion (Maretzky et al., 2008).

Tissue integrity shaped by homotypic interactions between the cadherins on neighbouring cells is essential to hinder spread of pathogens such as bacteria. Identification of ADAM10 as a receptor for *Staphylococcus aureus* α-toxin raised significant interest in exploiting its activity as a therapeutic target. ADAM10-bound α-toxin forms pores in the plasma membrane to induce Ca^{2+} influx and activate ADAM10. Subsequent E-cadherin shedding compromises the epithelial barrier allowing the bacteria to spread (Berube and Bubeck Wardenburg, 2013, Virreira Winter et al., 2016). Indeed, mice with conditional deletion of ADAM10 in respiratory epithelium were resistant to lethal pneumonia (Inoshima et al., 2011). A similar process can occur on endothelial cells, but in this case α-toxin induces ADAM10 shedding of VE-cadherin and subsequent breakdown of endothelial barrier function, followed by vascular injury and sepsis (Powers et al., 2012).

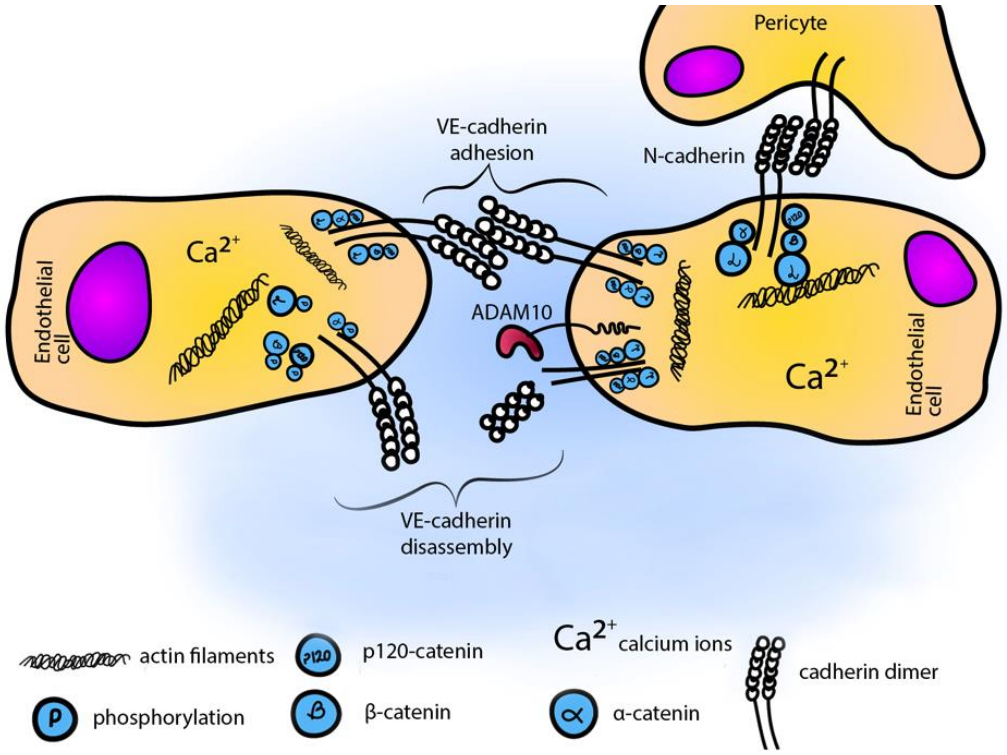

Figure 1.3 Schematic representation of VE-cadherin and N-cadherin regulation of homotypic and heterotypic interactions on endothelial cells, respectively. VE-cadherin is localised at adherens junctions between adjacent endothelial cells and mediates homotypic cell interactions. N-cadherin is dispersed along the endothelial surface and facilities heterotypic interactions between endothelial cells and pericytes. The mature cadherin forms Ca^{2+}-dependent *trans* dimers between two adjacent cells via the extracellular domains. The highly conserved cytoplasmic domain forms a complex with armadillo family proteins (β-catenin, plakoglobin, p120) that link to the actin filaments via α-catenin. These structural units together contribute to the core functions of the cadherins, like maintaining and stabilising the adherens junctions and signal transduction between the cells.

1.3 Tetraspanins as plasma membrane 'organisers'

1.3.1 Function and structure of tetraspanins

Tetraspanins form a superfamily of evolutionary conserved transmembrane proteins with four transmembrane domains and a characteristic structure that will be discussed later (Figure 1.4). They are commonly expressed across animal and plant kingdoms with 33 expressed in humans. Many tetraspanins are widely expressed, like CD9 and CD81. However, a number of them have a tissue or cell-specific expression, like CD37 and CD53 on leukocytes, uroplakin (UP) 1a and UP1b on urothelium, or peripherin and ROM-1 on the retina (Hemler, 2005). Tetraspanins contribute to plasma membrane organisation through the ability to associate with one another and with interacting 'partner' proteins to form nanoclusters (Charrin et al., 2014). The current notion states that separate nanoclusters are devoted to a single type of tetraspanin. However, they can share recruited partner proteins like immunoglobulin superfamily members, integrins, proteases and intracellular signalling proteins (Zuidscherwoude et al., 2015). This spatial organization generates a dynamic network of interactions across the plasma membrane through which tetraspanins are believed to facilitate intracellular trafficking, signalling, clustering, lateral mobility and membrane compartmentalization of their partners. This can lead to the regulation of vital cellular events like adhesion, spreading, migration, fusion and signalling (Charrin et al., 2014).

A relatively well-studied example of tetraspanin function is CD151 regulation of laminin-binding integrins (α3β1, α6β1, α6β4 and α7β1) (Sterk et al., 2002, Hemler, 2014). Indeed, CD151 restricts integrin diffusion mode to random-confined movements that facilitate integrin outside-in signalling and the availability to participate in cell adhesion and spreading functions (Yang et al., 2012). Loss of CD151 also decreases the adhesion strengthening towards laminins by an altered dynamic of integrin clustering (Lammerding et al., 2003). In addition, CD151 knockdown causes a reduction in integrin clustering that accompanies the effects on lateral diffusion (Yang et al., 2012), along with impaired recycling and redistribution of integrins away from the tetraspanin microdomains during cell migration (Winterwood et al., 2006, Yang et al., 2008). CD151-knockout mice have phenotypes consistent with impaired function of laminin-binding integrins, including kidney failure due to defective epithelial cell binding to basement membrane (Sachs et al., 2006). Similarly, CD151 deficiency in humans leads to kidney dysfunction and skin blistering disease (Karamatic Crew et al., 2004).

A second relatively well-studied tetraspanin is CD81, one function of which is to complex with B-cell co-receptor CD19 to regulate its glycosylation profile and trafficking from the ER to the cell surface. CD81-knockout mice, and a human patient with loss of CD81 due to a mutation, show reduced surface expression of CD19 (Shoham et al., 2003, Levy, 2014). As a result, B cell receptor signalling is impaired and the mice and human have impaired antibody responses, so phenocopying loss of CD19 (van Zelm et al., 2010, Levy, 2014).

A third example of tetraspanin function is Tspan12 regulation of Wnt receptor Frizzled-4 clustering and signalling via the Norrin ligand. Tspan12 is relatively highly expressed by endothelial cells in the retina, and loss of Tspan12 in mice results in impaired vascular development in the retina, which phenocopies deletion of Frizzled-4 (Junge et al., 2009). Moreover, in a mouse model of vasoproliferative retinopathy, anti-Tspan12 mAbs inhibit Frizzled-4/Tspan12-mediated β-catenin signalling and prevent abnormal vessel growth (Bucher et al., 2018). In humans, mutations in Tspan12 and Frizzled-4 lead to the human disease familial exudative vitreoretinopathy, characterised by defective retinal vasculature and ultimately blindness (Poulter et al., 2010).

An additional aspect of tetraspanins is that several of them are utilised by infectious pathogens to promote disease dissemination. Some pathogens interact directly with tetraspanins and use them as a means of spreading infections, while others exploit the cellular processes that tetraspanins are involved in, like exosome release, vesicle trafficking, internalisation and adhesion (Hemler, 2008, Monk and Partridge, 2012). For example, CD81-dependent entry and trafficking of the hepatitis C virus into hepatocytes has been well-studied. The virus entry is a multistage process and involves many proteins, including scavenger receptor class B type I (SR-BI), CD81, claudin-1 and occludins (Feneant et al., 2014). Furthermore, CD81 is a co-receptor for the protozoan *Plasmodium* (which is responsible for malaria), and is required for hepatocyte invasion in their sporozoite form, which sustains malaria infection. CD81 is crucial for the formation of parasitophorous vacuole, where the parasite acquires its exoerythrocytic form necessary for the disease (Silvie et al., 2003). Finally, adhesion of *Neisseria meningitidis, Staphylococcus aureus, Neisseria lactamica, E. coli* and *Streptococcus pneumoniae* to

epithelial cells involves their interaction with CD9, CD63 and CD151, and *Salmonella typhimurium* binding to macrophages involves CD63 (Green et al., 2011, Hassuna et al., 2017). Tetraspanin knockdown, or pre-treatment of the epithelial cells with tetraspanin mAbs or recombinant forms of the major extracellular regions of tetraspanins, reduced adhesion of the bacteria (Green et al., 2011). More recently, peptides from the major extracellular region of CD9 were shown to inhibit *S. aureus* binding to keratinocytes (Ventress et al., 2016). The mechanism of action behind this striking finding remains unclear, but the data suggest that tetraspanin targeting has great potential as an anti-bacterial therapeutic strategy.

1.3.2 Structure of tetraspanins

Tetraspanins are small molecules of 204 - 355 amino acids long with only a 5 nm projection over the plasma membrane. Tetraspanin structure comprises four transmembrane regions, two extracellular loops that are distinct in size, one inner loop, and N- and C- cytoplasmic tails (Figure 1.4). The structure of the tetraspanins supports intramolecular interactions mediated by features in the large extracellular loop and transmembrane regions. The large extracellular loop holds structurally essential cysteine residues (between 4 to 8), including a characteristic CCG motif, and disulphide bridges - a hallmark of the group. It is also the most diverse domain in the family and is where the functionally important variable region is located. The transmembrane domains include conserved polar and hydrophobic residues and are important for proper packaging and trafficking of the entire structure (van Deventer et al., 2017). Previous studies have shown

that tetraspanins with mutations in the transmembranes were unable to exit the ER and had impaired folding of the extracellular regions (Kovalenko et al., 2005). The intracellular events and protein organisation below the plasma membrane are believed to be regulated by the tetraspanin cytoplasmic tails, which are diverse in size and sequence homology. The C-terminus tail holds the YXXϕ and/or PZD-binding motifs in some tetraspanins, responsible for endocytosis, signalling and intracellular localisation of certain cytoplasmic proteins (Stipp et al., 2003). This aspect of tetraspanins remains understudied, but interactions between the N-terminal tail of CD53 and PKC-β (Zuidscherwoude et al., 2017), or C-terminal tail of CD81 and Rac (Tejera et al., 2013), have been noted. In addition, tetraspanins are subjected to post-translational modification, such as palmitoylation of cytosolic membrane-proximal cysteine residues, N-glycosylation in the large extracellular region and ubiquitination at cytoplasmic tails (van Deventer et al., 2017). In particular, palmitoylation was shown to contribute to tetraspanin-tetraspanin interactions and tetraspanin web formation as a whole (Israels and McMillan-Ward, 2010), whereas N-glycosylation contributes to tetraspanin-partner protein interactions (Yoshida et al., 2009).

Recently the structure of the first full length tetraspanin was solved, for CD81, which revealed a cone-like architecture where the large extracellular loop overshadows the four transmembrane domains arranged as separate pairs of helices, forming an intramembranous ligand-binding cavity (Figure 1.4). The study suggests that the lipid composition of the plasma membrane, in particular cholesterol, modulates dynamic structure transitions from a closed, cholesterol-bound form, to an open conformation when

cholesterol is not bound within the cavity. This, in turn, appears to affect tetraspanin function and subcellular localisation of their partner proteins (Zimmerman et al., 2016).

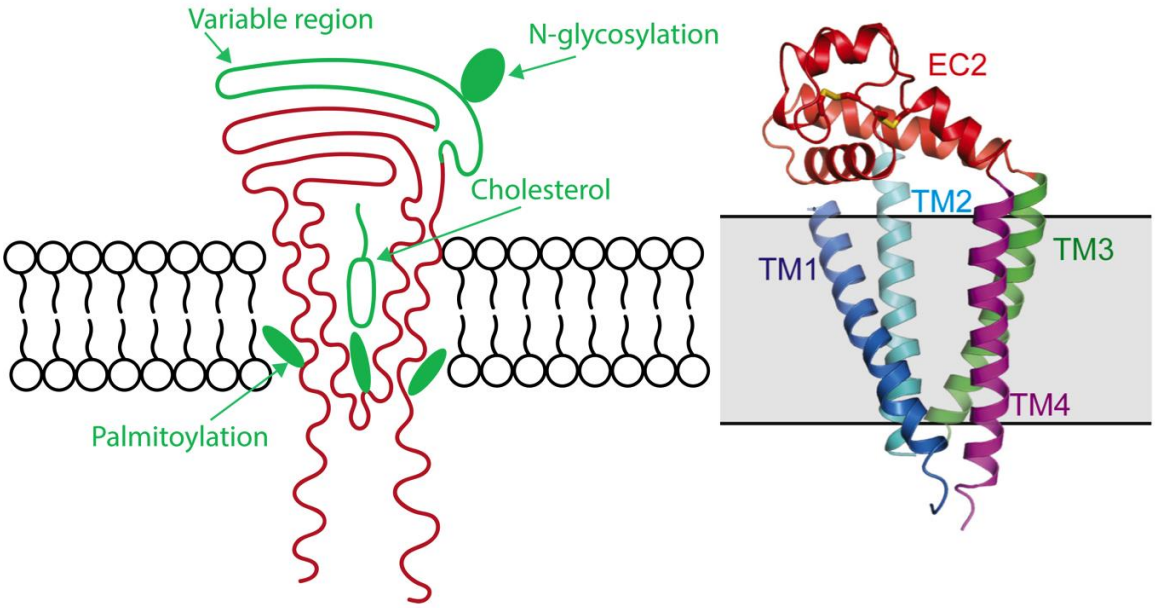

Figure 1.4 Tetraspanin structure: an ice cream cone with a cavity. A schematic representation of human tetraspanin CD81 (left panel) based on the CD81 crystal structure (right panel, Zimmerman et al., 2016).

1.4 The TspanC8 tetraspanins and ADAM10

1.4.1 'Six scissors': TspanC8s regulate ADAM10

ADAM10 has been shown to interact specifically with six different tetraspanins, as determined by co-immunoprecipitation under stringent lysis conditions like 1% digitonin (Dornier et al., 2012, Haining et al., 2012, Prox et al., 2012). These six tetraspanins have been named the TspanC8s, which form a subgroup of evolutionary conserved tetraspanins comprising Tspan5, 10, 14, 15, 17, and 33. Each of them contain eight cysteine residues in the large extracellular loop, a hallmark of the group. Various experimental approaches have shown that these tetraspanins are important for ADAM10 function through regulation of its maturation, trafficking, surface expression, lateral mobility and its activity towards several substrates (Figure 1.5). The findings are consistent in *Drosophila*, primary human endothelial cells, and in mice (Matthews et al., 2017b, Saint-Pol et al., 2017b, Matthews et al., 2018).

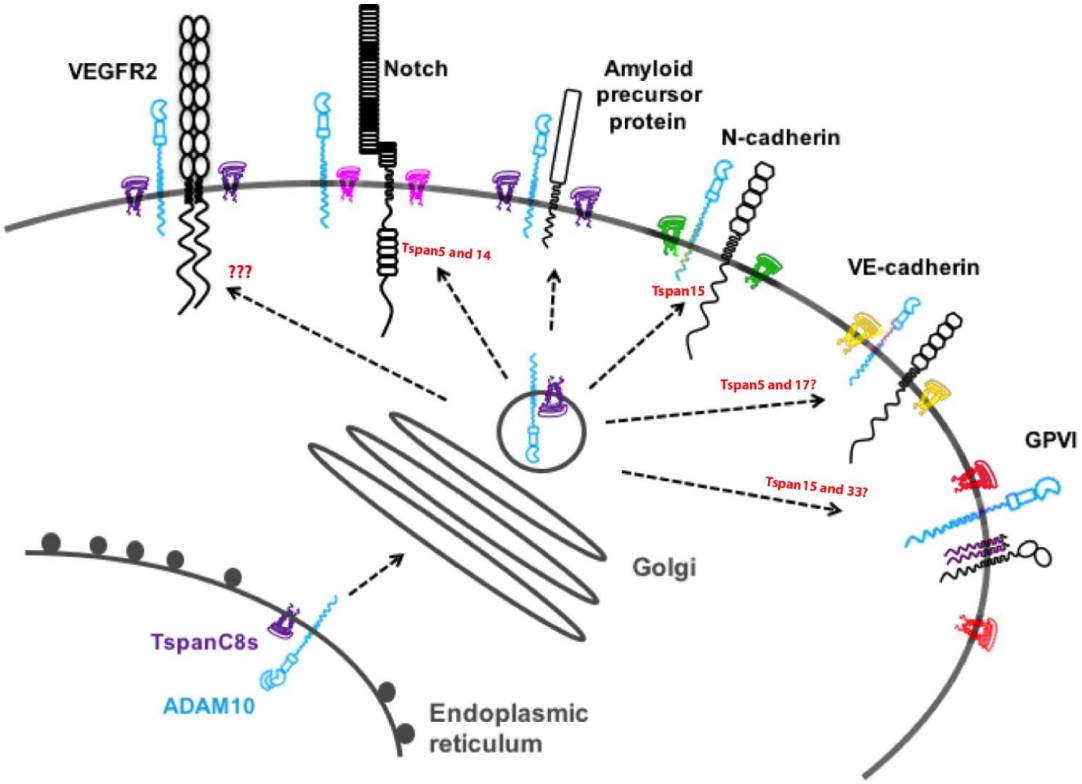

Figure 1.5 Different TspanC8s promote shedding of specific ADAM10 substrates. ADAM10 is synthesised as an inactive precursor in the ER. TspanC8s are required for ADAM10 ER exit and its subsequent maturation in the Golgi, via removal of the inhibitory prodomain. The mature form of ADAM10 is transported to the plasma membrane or intracellular compartments. Emerging evidence suggests that different TspanC8/ADAM10 complexes cleave different substrates such as Notch cell fate regulators, cadherin adhesion molecules and the platelet collagen receptor GPVI.

The depletion of all three TspanC8 gene orthologs (Tsp3A, Tsp86D and Tsp26D) in *Drosophila* resulted in developmental defects that phenocopied ADAM10 and Notch deletion. Weaker effects in single knockdowns suggested functional redundancy amongst these three TspanC8s (Dornier et al., 2012). Moreover, in human cell line models, Tspan5 and Tspan14 were identified as positive regulators of ADAM10-mediated Notch activation, while Tspan15 and Tspan33 appeared to be negative regulators (Dornier et al., 2012, Jouannet et al., 2016, Saint-Pol et al., 2017b); the latter may be due to competition

with Tspan5/14 for ADAM10. In osteoclasts, Zhou *et al* have shown that loss of Tspan5 or Tspan10 expression reduced ADAM10 maturation and consequent Notch2 activity (Zhou et al., 2014). These data suggest that Tspan5, 10 and 14 can each promote ADAM10-mediated Notch activation, but their relative importance will likely depend on expression levels in different cell types. Indeed, different cell types have different TspanC8 repertoires (Haining et al., 2012, Noy et al., 2016, Matthews et al., 2017b, Matthews et al., 2018).

The most definitive example of a TspanC8 specifically promoting shedding of a particular substrate is Tspan15 and N-cadherin, because it has been shown by three different groups (Noy et al., 2016; Jouannet et al., 2016; Prox et al., 2012). This will be covered in the next section on Tspan15. However, other examples are Tspan15/33 and the platelet collagen receptor GPVI (Matthews and Tomlinson, unpublished), and Tspan5/17 and VE-cadherin (Reyat et al., 2017). In the HEK-293T cell line, Tspan14 over-expression appeared to protect GPVI from ADAM10-mediated cleavage, but the other TspanC8s did not have this effect (Noy et al., 2016). More recent data from the Tomlinson lab, using CRISPR/Cas9 knockout megakaryocyte-like cell lines, has shown that Tspan15/ADAM10 and Tspan33/ADAM10 can each promote GPVI cleavage, but Tspan14/ADAM10 and other complexes cannot (Matthews and Tomlinson unpublished). The apparent protection by Tspan14 in the over-expression system was likely due to competition with Tspan15/33 for ADAM10 interaction. For VE-cadherin, our study in HUVECs using combination TspanC8 siRNA knockdowns, showed that Tspan5 and Tspan17, which are the two most highly-related TspanC8s at 72% amino acid identity, limit VE-cadherin expression and promote lymphocyte transmigration, but it was not proven that this was via actual cleavage of VE-cadherin (Reyat et al., 2017).

As previously mentioned, different cell types show different expression patterns of TspanC8s (Haining et al., 2012, Noy et al., 2016, Matthews et al., 2017b, Matthews et al., 2018). For instance, primary HUVECs and the A549 lung epithelial cell line express most of the TspanC8s, although with substantial variation in the relative levels (Haining et al., 2012). In contrast, primary mouse erythroblasts and megakaryocytes express mainly Tspan33 and Tspan14, respectively (Haining et al., 2012). Erythrocytes from Tspan33-knockout mice showed almost a complete loss of ADAM10 surface expression (Haining et al., 2012), that was accomplished by defects in red blood cell development (Heikens et al., 2007), but it is not clear that these are linked. Knockdown of Tspan14, the most highly expressed TspanC8 in HUVECs, was sufficient to reduce ADAM10 surface expression and activity towards VE-cadherin (Haining et al., 2012). TspanC8s also have different subcellular localisations. In the present absence of antibodies to most TspanC8s, this has been investigated using transfected GFP-tagged TspanC8s. For example, Tspan5, 14, 15 and 33 are located mainly at the plasma membrane, whereas Tspan10 and 17 have more intracellular localization (Dornier et al., 2012). However, the mechanism underlying these different localisation patterns is not known.

The mechanisms by which different TspanC8s differentially regulate ADAM10 substrate specificity are not known. It seems likely that TspanC8s exert their functions by trafficking ADAM10 into proximity with substrates and/or by constraining ADAM10 into distinct conformations that favour cleavage of certain substrates. As mentioned in the previous paragraph, TspanC8s do differentially localise ADAM10. Moreover, TspanC8s can differently affect lateral diffusion of ADAM10 in the plasma membrane. This was

measured by single particle tracking of ADAM10 in Tspan5- or Tspan15-over-expressing cells, in which mobility in the membrane increased by 55% in the presence of Tspan15 versus Tspan5 or control cells (Dornier et al., 2012, Jouannet et al., 2016). GFP-tagged Tspan5 and Tspan15 were also shown to co-immunoprecipitate overlapping but somewhat different proteins in 1% Brij97, as detected by mass spectrometry, suggesting that they reside in different membrane microdomain environments (Jouannet et al., 2016). There is also evidence that ADAM10 may adopt distinct conformations in complex with different TspanC8s (Figure 1.6) that in turn could impact the substrate specificity and cellular localization (Jouannet et al., 2016, Noy et al., 2016). Binding regions were mapped using chimeric approaches for both TspanC8s and ADAM10, and the extracellular regions of the two interacting partners seemed to play the most important role (Noy et al., 2016). Indeed, the variable region in the large extracellular region of TspanC8s was necessary but not sufficient to mediate interactions with ADAM10. Furthermore, just the 26 amino acid membrane-proximal stalk region of ADAM10 appeared sufficient for interaction with Tspan15. In contrast, the stalk, cysteine-rich and disintegrin domain were required for interactions with Tspan5, 10, 14 and 33, whereas Tspan17 interaction was impaired by inclusion of the disintegrin domain (Noy et al., 2016). Since there are no specific amino acid sequence motifs identified as an ADAM10 cleavage site, and since the shedding happens at different heights above the plasma membrane (5-15 amino acids for different substrates), it is possible that different TspanC8s ‘lock’ ADAM10 in a conformation that favours cleavage of certain substrates. However, the data underlying these speculations were based entirely on co-immunoprecipitation of over-expressed mutant proteins, and so additional structural studies are required for verification.

Taking together the data that has emerged in the last six years on TspanC8s, the Tomlinson group have proposed the ‘six scissors’ hypothesis, in which ADAM10 can be regarded as six different molecular scissors, depending upon which TspanC8 it is partnered with (Matthews et al., 2017, Mathews et al., 2018). A better understanding of the regulation of ADAM10 by TspanC8s could enable a new avenue of therapy for human disorders by targeting the specific ADAM10-TspanC8 complexes and/or regions of interaction.

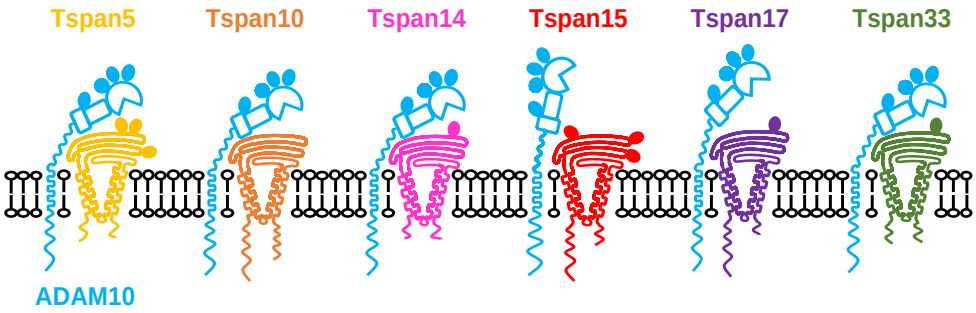

Figure 1.6 'Six scissors' hypothesis. ADAM10 in a complex with different TspanC8 tetraspanins may adopt distinct conformations, which could impact substrate specificity and cellular localization. Therefore, ADAM10 is regarded as six different proteases. Figure taken from Noy et al., 2016.

1.4.2 Tspan15

Tspan15 became the model TspanC8 of focus for this thesis because the Tomlinson group generated the first mAbs to this protein (Noy, unpublished), and because Tspan15 was definitively shown to specifically promote ADAM10 cleavage of N-cadherin (Jouannet et al., 2016, Prox et al., 2012, Noy et al., 2016). Through the generation of a polyclonal antibody to Tspan15, the Saftig group demonstrated Tspan15 expression in most mouse tissues (Seipold et al., 2018). The examination of its expression within the Human Protein Atlas RNA-Seq data indicated that Tspan15 has a relatively restricted expression in epithelial and endothelial cells, and is an unfavourable prognostic marker in liver and kidney cancers (Uhlén et al., 2015). In the Gene Expression Profiling Interactive Analysis (GEPIA) data, Tspan15 is found to be approximately 50-fold, 16-fold and 13-fold upregulated in cholangio carcinoma, ovarian serous cystadenocarcinoma and pancreatic adenocarcinoma, respectively, but not substantially upregulated in most other cancers (Tang, 2017). Furthermore, overexpression of Tspan15 was recently reported in clinical oesophageal squamous cell carcinoma, which correlated with cancer metastasis and poor survival. Further studies suggested an importance of Tspan15 in cancer initiation and development and the possibility of using it as a therapeutic marker (Zhang et al., 2018). Indeed, Tspan15 over-expression in two oesophageal cancer cell lines substantially increased cell migration in vitro and promoted tumour formation in nude mouse lungs by 3-fold following intravenous injection of the cells. Consistent with this, Tspan15 knockdown reduced in vivo tumour formation by 75% (Zhang et al., 2018). To understand mechanism, the authors showed a co-immunoprecipitation of beta-transducin repeat containing E3 ubiquitin protein ligase (BTRC) with Tspan15. BTRC promotes activation

of the transcription factor nuclear factor-κB (NF-κB), by targeting the IκB inhibitory proteins for degradation via ubiquitination. Moreover, knockdown of BTRC, or chemical inhibition of the NF-κB pathway, inhibited the in vitro and in vivo oncogenic effects of Tspan15 (Zhang et al., 2018). However, the co-immunoprecipitation was not fully controlled, for example knockdown cell lines could have been used as negative controls to check antibody specificity, and the BTRC functional effects could be merely downstream effects on signalling induced by Tspan15/ADAM10 activity. The authors acknowledge that ADAM10 presents a mechanistic possibility that they had not investigated and that further study is required to provide a complete understanding (Zhang et al., 2018).

Tspan15 was first identified by Prox *et al* as a specific binding partner of ADAM10 in mammalian cell line models. Furthermore, the overexpression of Tspan15 was found to increase surface levels of ADAM10 and its shedding activity towards N-cadherin. Further data showed that Tspan15 knockdown substantially reduced N-cadherin shedding (Prox et al., 2012). Using over-expression and knockdown in different cell line models, our group and the Rubinstein group confirmed the above findings, and extended them to show that the other five TspanC8s could not promote N-cadherin cleavage (Noy et al., 2016, Jouannet et al., 2016). Analysis of Tspan15-knockout mice agreed with these cell line studies by showing 75-85% decreased N-cadherin cleavage in the brains of Tspan15-knockout mice, an effect that increased with age, and a subtler 25-50% decrease in the percentage of mature ADAM10 (Seipold et al., 2018). A 50-60% decrease in cleavage of cellular prion protein was also observed, but APP cleavage was unaffected. Yet, Tspan15-knockout mice had no obvious functional impairments when compared to wide-type littermates, and mice were born at normal Mendelian ratios. Dendritic spines in the brain,

which are important for memory and learning, were also normal (Seipold et al., 2018), but it may be interesting in future to perform more detailed functional analysis of the brains of these mice or to cross them to a model for prion disease.

In the Seipold study, Tspan15 protein expression levels were shown to be elevated by 25% in the brains of a mouse Alzheimer's disease model, and by 70% in the brains of human Alzheimer's disease patients, as assessed from six patient samples. However, the relevance of these changes is not known. Tspan15 has also been implicated in deep vein thrombosis in a genome-wide association study (Germain et al., 2015). A single nucleotide polymorphism (SNP) in a Tspan15 intron was one of two SNPs identified in this study as being linked to disease susceptibility, but it is not yet known whether this truly impacts on the disease (Germain et al., 2015). More recently, Tspan15 was implicated in *Streptococcus pneumoniae* infection (Salas et al., 2018). Whole exome sequencing of eight patients with complicated cases of pneumococcal pneumonia identified a SNP in the 3' UTR of Tspan15 as the second-best candidate. Although the relevance to the disease is again unknown (Salas et al., 2018), it is interesting that ADAM10-cleavage of cadherins, following activation by the *S. pneumoniae* virulence factor pneumolysin, has been implicated in bacterial spread (Inoshima et al., 2011). This will be discussed later in the thesis as it is relevant to some of the discoveries in the results chapters that follow.

1.5 Endothelial cell function

1.5.1 Overview

Endothelial cells became the cells of choice for functional studies of ADAM10 and Tspan15 in this thesis. Endothelial cells are the building blocks of all blood vessels. Collectively they form a thin monolayer called the endothelium that lines the interior of the entire cardiovascular system (Eelen et al., 2015). The endothelium is heterogenic in both phenotype and functions. This is a consequence of the diversity of endothelial cells that are present in different parts of the vascular system. Thus, it has the capacity to adapt its number and organisation to suit the local environment (Aird, 2012). The endothelium acts not only as a physical barrier between vessel lumen and underlying tissue, but also actively participates in cardiovascular regulation. It maintains vessel integrity and homeostasis by regulating the balance between pro-thrombogenic and fibrinolytic substance release and generating the anti-thrombogenic surface allowing blood to flow freely. Further, it controls vascular tone by releasing vasoactive factors, like nitric oxide, that constrict and dilate the vessels. The endothelium is also an active participant in inflammatory processes via recruiting and regulating transmigration of leukocytes through the vessel wall. It is also playing a necessary role in the regulation of vessel permeability by controlling the crossing of macromolecules back and forth between the bloodstream and tissues (Galley and Webster, 2004).

The industrialisation and globalisation of everyday life contribute to the development and progression of numerous devastating and life-threatening illnesses, including cancer, skin

diseases, blindness, diabetes, obesity, cardiovascular diseases among others. In the last decade, scientists have linked these conditions to the vascular endothelium and blood vessels (Mensah, 2007). Indeed, the homeostasis established by blood vessel integrity is crucial for life, and its dysregulation can be fatal. Abnormalities of blood vessels are present in the majority of malignant, ischemic, inflammatory, infectious and immune conditions (Carmeliet, 2005a). Vascular disorders are hence often reported as the leading cause of death worldwide (WHO, 2007). Angiogenesis, the formation of new blood vessels from existing vasculature, is a major current research focus. The development of angiogenesis-targeting therapies, using suppressors or activators of the vascular beds, could provide a new avenue in combating these diseases (Chu and Wang, 2012). Before developing these therapies, however, more detailed understanding of the vascular system is required.

1.5.2 Endothelial cells in sprouting angiogenesis

In order to grow and survive, any single cell or multicellular entity will require new blood vessels to satisfy constant metabolic demands. Thus, the primitive vascular plexus that was once established during embryogenesis undergoes reorganisation, expansion and maturation into a functional circuit in a process called sprouting angiogenesis (Adair and Montani, 2010). This multi-step process is strictly regulated by a number of pro- and anti-angiogenic molecules (Table 1). The complex interactions between these factors affect the time, place and patterning of the vasculature (Otrock et al., 2007).

Table 1 List of activators and inhibitors of angiogenesis and their function.

ACTIVATORS FUNCTION	INHIBITORS FUNCTION
• VEGF family members: stimulate angiogenesis, permeability, leukocyte transmigration • VEGFR2, NRP-1: integrate angiogenic and survival signals • Angiopoetin1, Tie 2: stabilise vessels, inhibit permeability • PDGF and receptors: recruits pericytes, smooth muscle cells • TGF-β and receptors: stimulate extracellular matrix production, recruit macrophages • Integrin: receptor for matrix macromolecules and proteinases • VE-cadherin, PECAM (CD31): endothelial junctional molecules • Plasminogen activators, MMPs: remodel extracellular matrix, release and activate growth factors • HIF-1: activate pro-angiogenic factors	• VEGFR1: binds VEGF • Angiopoietin 2: agonists for Angiopoietin 1 • Thrombospondin-1, -2: inhibit endothelial migration, growth, adhesion and survival • Angiostatins: suppress tumour angiogenesis • Endostatins: inhibit endothelial survival and migration • TIMPs: inhibit MMPs • IL-4, IL-12, IL-8, IFN-α, -β, -γ: inhibit endothelial migration, downregulate bFGF

In health, quiescent endothelial cells within blood vessels form monolayers on the basement membrane, connected through junctional molecules including VE-cadherin, JAMs, PECAM-1, ZO-1 and claudins. These are enclosed by contractile pericytes/smooth muscle cells. Since the vessels carry oxygen and blood, they are well-equipped with sensors for hypoxia and ischemia (HIF-1). Stimulation of these sensors facilitates the

expression and consequent release of pro-angiogenic factors like VEGF, EGF, Ang2, FGF, TGFβ and chemokines. This triggers morphological and behavioural changes in the vessels, like pericyte detachment from vessel walls, loosening of the cell-cell junctions, vessel dilation and ultimately cell migration and sprouting (Welti et al., 2013).

The individual steps of sprouting angiogenesis, together with key players, are shown in Figure 1.7. During the process of the sprout formation, cells do not move in masses. Specialized cells, called 'tip cells', lead the migration along a concentration gradient of the angiogenic stimuli towards hypoxic regions. These cells are equipped with filopodia and sensors to probe their local environment for guidance. In addition, they release matrix metalloproteases (MMPs) which enable the degradation of extracellular matrix components (laminins, collagens, proteoglycans). The cells that trail behind the tip cells are called 'stalk cells. The differentiation and specification of stalk cells results in a highly proliferative phenotype that facilitates elongation and formation of the main body of the new vessel (Eilken and Adams, 2010). The selection and identity of the endothelial cells are controlled by the interplay between VEGF/VEGFR2 and Notch/DLL4 signalling. These signalling pathways control responsiveness of the cells to growth factors (Phng and Gerhardt, 2009). The tip-stalk cell phenotype is transient and may be reversed upon vessel fusion and cell-cell communication (Jakobsson et al., 2010). In the final phase of angiogenesis, nearby sprouts that invaded the tissue space anastomose with one another. In the newly formed vessel, the cell-cell contacts are re-established by VE-cadherin and Ang-1; the basement membrane is laid down with the help of tissue inhibitors of metalloproteases (TIMPs), which prevent digestion of the extracellular matrix by plasmin. Cell migration and proliferation ceases, and the recruited pericytes further stabilise vessels

in response to TGF-β, PDGFR/PDGF-β and Ang-1. Blood starts to flow, bringing the oxygen level back to normal, the growth factor activity diminishes and the nascent vessel becomes quiescent again (Welti et al., 2013).

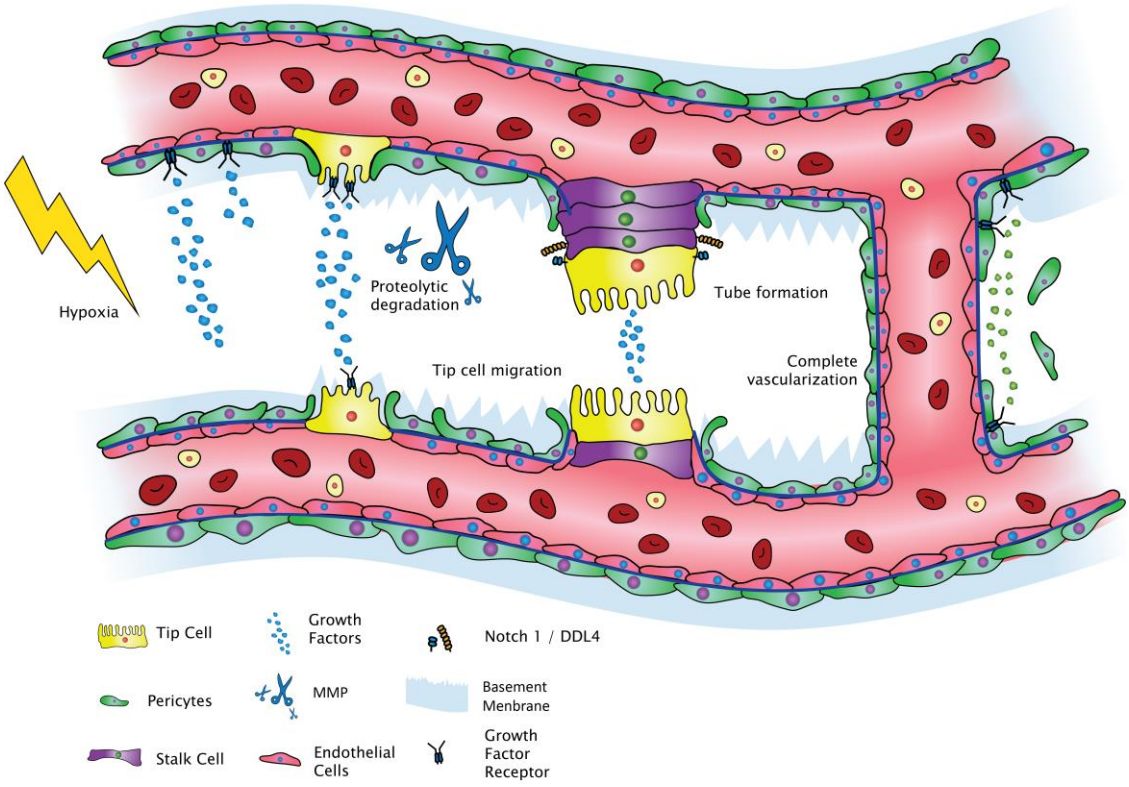

Figure 1.7 Vessel sprouting model. The drawing represents the main steps in vascular morphogenesis: initial tip cell selection and guidance; stalk elongation and lumen formation; anastomosis, maturation and quiescence of the newly formed blood vessel. The key molecular players involved in the process are listed.

During postnatal development, the formation of new blood vessels from pre-existing capillaries occurs rarely and is limited to the menstrual cycle, placenta development, embryo implantation, wound healing, tissue growth and regeneration (Sherer and Abulafia, 2001). However, in pathological conditions, deregulated angiogenesis contributes to sudden enlargement or regression of the existing capillary network. This includes, but is not limited to, cancers, cardiovascular diseases, blindness, arthritis, complications of AIDS (acquired immunodeficiency syndrome), diabetes and Alzheimer's disease (Carmeliet and Jain, 2000).

The early dogma proposed by Judah Folkman presented angiogenesis as an important target for cancer and other diseases (Folkman, 1971). The restriction of blood vessel availability within the whole affected area in the body therefore became a key approach to increase patient survival. Recent discoveries have brought into light the therapeutic potential of targeting angiogenesis whereby the process per se, and its driving factors, could be stimulated or inhibited to treat certain diseases (Ferrara and Kerbel, 2005). Indeed, many diseases, including neurodegenerative illnesses, heart attack, blood clots and limb fractures, could potentially benefit from the administration of pro-angiogenic agents that would stimulate blood vessel growth. In contrast, many disorders can benefit from blocking angiogenesis by introducing anti-angiogenic factors. These include retinal diseases, cancers, arthrosclerosis, obesity and endometriosis (Jain and Carmeliet, 2001).

1.5.3 Crosstalk between VEGF and Notch signalling pathways in regulation of sprouting angiogenesis

Vascular endothelial growth factors (VEGFs) include mammalian VEGFs A-D, and placental growth factor (PIGF), which regulate vasculogenesis, angiogenesis and lymphangiogenesis (Shibuya, 2013). In particular, VEGF-A is crucial for angiogenesis, as a 50% reduction in the level of the ligand is embryonically lethal and associated with various pathologies when bioavailability of VEGF-A decreases (Simons et al., 2016). VEGF and its receptors, the VEGFR1-4 receptor tyrosine kinases, are potent mediators of endothelial cell functions like migration, proliferation and differentiation. Vascular endothelial cells express VEGFR1 and 2, and mice deficient in VEGFR2 die in the uterus due to impaired blood-island formation and vasculogenesis (Shalaby et al., 1995). VEGF and Notch have been identified as crucial regulators of angiogenesis (Figure 1.8). Genetic deficiencies in these genes result in embryonic lethality due to impaired or lack of development of a vasculature (Hofmann and Iruela-Arispe, 2007, Carmeliet, 2005b). Although the two signalling cascades collectively unite through downstream effectors, they differ in temporal and spatial expression and regulation, but are both required for the differential responsiveness of endothelial cells to angiogenic stimuli and correct patterning and assembly of the vasculature (Martin and Murray, 2009). VEGF acts upstream, inducing and controlling expression of Notch signalling components, whereas Notch negatively modulates VEGF pathways. This dependence is coordinated by the feedback loops between expression of the VEGFR2/R1 receptors and activity of the Notch-DLL4 complexes (Blanco and Gerhardt, 2013). In the developing vasculature, VEGF drives the process and is essential for cell migration, proliferation and lumen formation. Notch helps

to guide cell fate decision (arterial-venular and tip-stalk phenotype of endothelial cells) and sprouting, while restricting the angiogenic response to VEGF (Holderfield and Hughes, 2008).

VEGF and Notch/DLL4 are essential drivers of sprouting angiogenesis. Their engagement balances migratory tip cell and proliferating stalk cell phenotypes. Briefly, endothelial cells compete for a tip cell phenotype by over-expressing the VEGFR2/Nrp-1 receptor complex. Nrp-1 is co-receptor for VEGFR2 that is involved in enhancing its binding to VEGF. The absence of Nrp-1 results in embryonic lethality at day 10.5 as a result of impaired heart and blood vessel development and arterial-venous differentiation (Mehta et al., 2018). Hypoxia and binding of VEGF to VEGFR2/Nrp-1 upregulates DLL4 which binds to the Notch1 receptor on a neighbouring cell. This initiates activation and proteolytic cleavages of Notch by ADAM10 and the γ-secretase complex. The resulting intracellular fragment of Notch, named the Notch intracellular domain (NICD), translocate to the nucleus where it interacts with CSL (CBF1/RBP-J, Su(H), Lag-1) transcription factors, which in turn initiates the transcription of Notch target genes. As a consequence, the gene expression profile is altered, including upregulation of VEGFR1, which acts as a VEGF 'trap' to inhibit VEGF activation of VEGFR2 and downregulation of VEGFR2/Nrp-1. As a result, endothelial stalk cells have impaired responsiveness to VEGF, limited filopodia formation and reduced migration. Conversely, locally high VEGF concentration favours signalling pathways that lead to proliferation and migration of the cells with elevated levels of the VEGFR2/Nrp-1 complexes (Li, 2009).

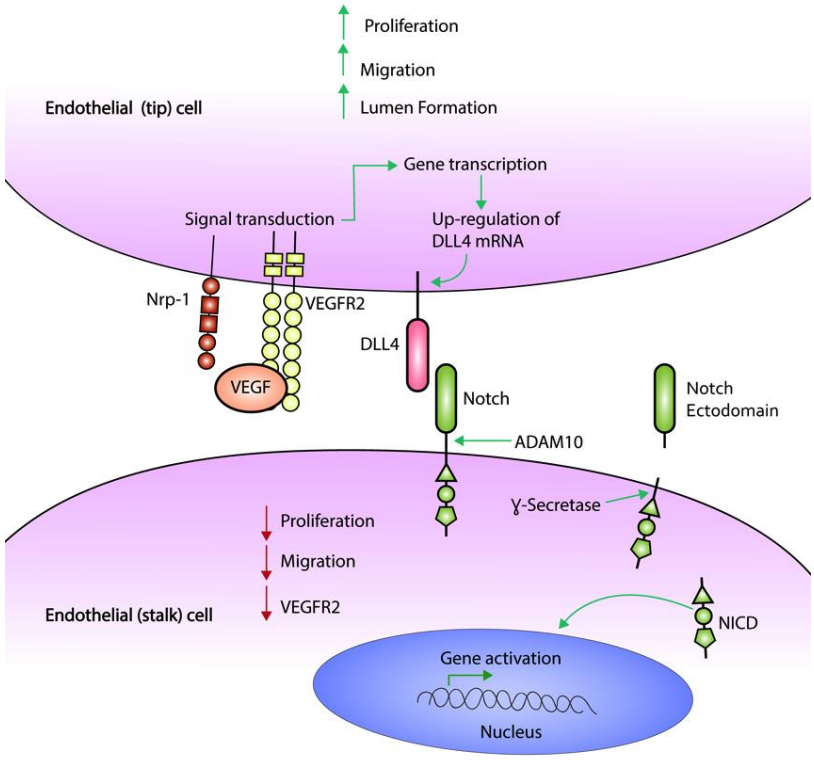

Figure 1.8 VEGF and Notch in the fine-tuning of sprouting angiogenesis. Interplay between VEGF and Notch signalling cascades facilitates vascular development and endothelial cell specification (Alabi et al., 2018).

1.6 Thesis aims

ADAM10 has been shown to be involved in a wide variety of processes including cell adhesion, migration, differentiation and vascular homeostasis, and is known to play an essential role in many pathophysiological conditions. Targeting ADAM10-TspanC8 complexes is therefore a potential therapeutic strategy. Previous studies have made progress towards understanding the mechanism of ADAM10 involvement within these cellular processes, and several key substrates of ADAM10 have been identified. There is, however, still a lack of understanding in how ADAM10 is regulated by tetraspanins. This thesis therefore aims to investigate the regulation of ADAM10 by Tspan15 as a model TspanC8, and to understand how this interaction ultimately modulates cell function.

The main aims of the thesis are as follows:

1. To use four recently-generated anti-Tspan15 mAbs and ADAM10- and Tspan15-knockout cell lines to determine the extent to which Tspan15 regulates cell surface ADAM10 expression, and whether ADAM10 regulates Tspan15 expression.

2. To investigate whether Tspan15 is required for the ADAM10-mediated cleavage of N-, E- and VE-cadherin in cell lines, and whether the Tspan15 mAbs affect their cleavage.

3. To epitope map the four Tspan15 mAbs and to determine their effects on Tspan15 internalisation and ADAM10 cell surface expression.

4. To establish a cell line model for Tspan15 structure/function analyses, by stably reconstituting Tspan15-knockout cells with Tspan15 mutant constructs.

5. To determine whether siRNA knockdown of ADAM10 or Tspan15 in primary endothelial cells affects their migration, proliferation and network formation on Matrigel.

CHAPTER 2
MATERIALS AND METHODS

2.1. List of reagents and antibodies

Table 2 List of reagents and antibodies

Reagent	Source
Ampicillin	Sigma-Aldrich (Poole, Dorset, UK)
Acrylamide	Geneflow (Lichfield, UK)
Ammonium persulfate (APS)	Sigma-Aldrich (Poole, Dorset, UK)
Blasticidin	Sigma-Aldrich (Poole, Dorset, UK)
Bovine brain extract	First Link (UK) Ltd. (Wolverhampton, UK) Gift from Dr V.Heath, UK
Bromophenol Blue	Bio-Rad (Hemel Hempstead, Hertfordshire, UK)
Digitonin	Merck Millipore (Watford, Hertfordshire, UK)
Dimethyl sulfoxide (DMSO)	Sigma-Aldrich (Poole, Dorset, UK)
Dulbecco's Modified Eagles Medium (DMEM) with 1000 mg/L glucose	Sigma-Aldrich (Poole, Dorset, UK)

Ethanol	Fisher Scientific (Loughborough, Leicestershire, UK)
Ethylenediaminetetraacetic acid (EDTA)	Sigma-Aldrich (Poole, Dorset, UK)
10% heat activated fetal bovine serum (FBS)	Gibco (Paisley, UK)
Gelatin	Sigma-Aldrich (Poole, Dorset, UK)
Glycine	Sigma-Aldrich (Poole, Dorset, UK)
GI 254023X	Sigma-Aldrich (Poole, Dorset, UK)
Heparin	Sigma-Aldrich (Poole, Dorset, UK)
L-Glutamine	Gibco (Paisley, UK)
Lipofectamine RNAiMAX	Life Technologies Invitrogen Compounds (Paisley, UK)
Marvel	Premiere Foods (St Albans, Hertfordshire, UK)
Matrigel	BD Bioscience (Oxford, UK)
Methanol	Fisher Scientific (Loughborough, Leicestershire, UK)
β-mercaptoethanol	Sigma-Aldrich (Poole, Dorset, UK)
Mitomicin C	Sigma-Aldrich (Poole, Dorset, UK)
M119 medium	Sigma-Aldrich (Poole, Dorset, UK)
N-[N-(3,5-difluorophenacetyl)-L-alanyl]-S-phenylglycine t-butyl ester (DAPT)	Sigma-Aldrich (Poole, Dorset, UK)
N-ethylmaleimide (NEM)	Sigma-Aldrich (Poole, Dorset, UK)
N, N, N', N'-Tetramethylethylenediamine (TEMED)	Sigma-Aldrich (Poole, Dorset, UK)
OptiMEM	Gibco (Paisley, UK)
Orange G loading buffer (6x)	Fisher Scientific (Loughborough, Leicestershire, UK)
penicillin/streptomycin	Sigma-Aldrich (Poole, Dorset, UK)

Phosphate Buffer Saline (PBS)	Sigma-Aldrich (Poole, Dorset, UK)
Polyethylenimine (PEI)	Sigma-Aldrich (Poole, Dorset, UK)
Polyvinylidene fluoride (PVDF) membrane	Immobilon-FL, Merck Millipore (Watford, Hertfordshire, UK)
Protein G sepharose beads	Generon (Berkshire, UK)
Protease inhibitor cocktail	Sigma-Aldrich (Poole, Dorset, UK)
Protein marker (BLUEye^{TM})	Geneflow (Lichfield, UK)
Sodium azide (NaN_3)	Sigma-Aldrich (Poole, Dorset, UK)
Sodium chloride (NaCl)	Sigma-Aldrich (Poole, Dorset, UK)
Sodium dodecyl sulphate (SDS)	Fisher Scientific (Loughborough, Leicestershire, UK)
SYBR Safe DNA gel stain	Fisher Scientific (Loughborough, Leicestershire, UK)
Tris	Fisher Scientific (Loughborough, Leicestershire, UK)
Triton X-100 lysis buffer	Sigma-Aldrich (Poole, Dorset, UK)
Trypsin-EDTA	Sigma-Aldrich (Poole, Dorset, UK)
Whatman filter paper (3MM)	GE Healthcare (Amersham, Buckinghamshire, UK)
Antibody	**Details and source**
Rabbit anti-HA (C29F4)	Cat No.:3724, Cell Signaling Technology (Danvers, USA) Working dilution: 1:2000 (western blotting)
Mouse anti-FLAG (M2)	Cat No.: F9291, Sigma-Aldrich (Poole, Dorset, UK) Working concentration: 1 µg/ml (western blotting)
Rabbit anti-FLAG	Cat No.: F7425, Sigma-Aldrich

	(Poole, Dorset, UK) Working concentration: 1 µg/ml (western blotting)
Rabbit anti-HA	Cat No.: C29F4, Cell Signaling Technology (Massachusetts, USA) Working concentration: 1 µg/ml (western blotting)
Mouse anti-human ADAM10 (11G2)	Gift from Dr Eric Rubinstein, France Working concentration: 1 µg/ml (western blotting)
Mouse anti-human ADAM10 FITC	R&D Systems (Abingdon, UK) Working dilution: 1:50 (flow cytometry)
Mouse anti-human ADAM10 APC	R&D Systems (Abingdon, UK) Working dilution: 1:50 (flow cytometry)
Mouse IgG (MOPC-21)	Cat No.: 50327, MP Biomedicals Europe (Santa Ana, California, USA) Working concentration: 10µg/ml (flow cytometry)
Mouse anti-human Tspan15 hybridoma tissue culture supernatant 5F4 (IgG2b Kappa) 5D4 (IgG1 Kappa) 1C12 (IgG1 Kappa) 4A4 (IgG1 Kappa)	Abpro (Boston, Massachusetts, USA) Working volume: 50 µl (flow cytometry) *
Mouse anti-human Tspan15 monoclonal antibodies: 5F4 (IgG2b Kappa) 5D4 (IgG1 Kappa) 1C12 (IgG1 Kappa) 4A4 (IgG1 Kappa)	Abpro (Boston, Massachusetts, USA) Working concentration: 10 µg/ml (shedding assay) *

Mouse anti-human Tspan5 (TS5-2)	Gift from Dr Eric Rubinstein, France Working concentration: 10 µg/ml (flow cytometry)
Rabbit VE-cadherin (D87F2) XP	Cat No.: 2500, Cell Signaling Technology (Danvers, USA) Working dilution: 1:1000 (western blotting)
Mouse anti-N-cadherin (13A9)	Cat No.: 14215, Cell Signaling Technology (Danvers, USA) Working dilution: 1:1000 (western blotting)
Rabbit anti-E-cadherin (24E10)	Cat No.: 3195, Cell Signaling Technology (Danvers, USA) Working dilution: 1:1000 (western blotting)
Goat anti-Mouse IgG IRDye 680RD & 800CW	LI-COR (Cambridge, UK) Working dilution: 1:10000 (western blotting)
Goat anti-Rabbit IgG IRDye 680RD & 800CW	LI-COR (Cambridge, UK) Working dilution: 1:10000 (western blotting)
Anti-mouse IgG_{2B}-FITC	Sigma-Aldrich (Poole, Dorset, UK) Working dilution: 1:50 (flow cytometry)
Anti-mouse IgG_{2B}-APC	Sigma-Aldrich (Poole, Dorset, UK) Working dilution: 1:50 (flow cytometry)

* mAb / hybridoma tissue culture supernatant was used at volume that gave saturating binding. No further shift in fluorescence intensity was observed following an increase in the concentration.

2.2 List of buffers

Table 3 List of commonly used buffers

Buffer	Details
2X SDS non-reducing sample buffer	20 ml 1M Tris, pH 6.8 80 ml 10% SDS 40 ml glycerol 60 ml dH_20 4 mg Bromophenol blue 5ml 10% β-mercaptoethanol (only for reducing buffer)
Antibody incubation buffer	3% BSA in PBS 0.02% NaN_3
Blocking buffer (Western blot)	5% Marvel in TBS-T
FACS buffer	0.2% BSA in TBS-T 0.02% NaN_3
Complete M199 (cM199)	M199 media (500 ml) 10% FBS 4 mM glutamine 0.3% bovine brain extract 90 µg/ml heparin 100 U/ml penicillin 100 µg/ml streptomycin
Complete DMEM (cDMEM)	DMEM media (500 ml) 10% FBS 4 mM glutamine 100 U/ml penicillin 100 µg/ml streptomycin
Digitonin	1 % Digitonin (dissolved in methanol 10 % w/v) 10 mM Tris pH 7.5 150 mM NaCl 0.01 % NaN_3
SDS polyacrylamide resolving buffer	30.3 g Tris 2 g SDS pH 8.8 500 ml dH_20

SDS polyacrylamide stacking buffer	30.3 g Tris 2 g SDS pH 6.8 500 ml dH_20
SDS-Page running buffer	15 g Tris 72 g glycine 50 ml 10% SDS 5 L dH_20
TBS buffer	20 mM Tris 137 mM NaCl pH 7.6 2 L dH_20
Triton X-100 lysis buffer	250 ml 1% Triton X-100 1 M Tris, pH 7.5 5 M NaCl 0.5 M EDTA pH 8.0 0.05 g NaN_3 250 ml dH_2O
TBST buffer	20 mM Tris 137 mM NaCl 0.1% Tween pH 7.6 5 L dH_20
TBST high salt wash buffer	TBST containing 500 mM NaCl
Western transfer buffer	15 g Tris 72 g glycine 1 L methanol 5 L dH_20

2.3 Cellular biology methods

2.3.1 Cell culture

Adenocarcinoma Human Alveolar Basal Epithelial (A549) and Human Embryonic Kidney 293T (HEK-293T) cells were obtained from laboratory stocks (Haining et al., 2012) and cultured in complete Dulbecco's Modified Eagle Media (DMEM) (Table 2). ADAM10 and Tspan15 CRISPR/Cas9 knockout A549 and HEK-293T cells were generated previously in the Tomlinson lab. Human umbilical vein endothelial cells (HUVECs) were isolated from human umbilical cords obtained from Human Biomaterials Resource Centre (University of Birmingham) (09/H1010/75) by members of the Tomlinson lab. All cells were cultured in a humidified incubator at 37 ^{0}C with 5% CO_2. HUVECs were used for experiments up to passage six and grown in 10 cm dishes pre-coated with 0.1% gelatine. The remaining cell lines were passaged routinely at a 1 to 10 ratio. The cell culture techniques used for thawing, freezing and general maintenance were performed similarly for all cell types used in the project. Briefly, for sub-culturing cells, the cells were washed with PBS, trypsinised for 1 min at 37 ^{0}C, resuspended in a fresh media and transferred to a new tissue culture dish. For freezing, a confluent monolayer of the cells was collected from 10 cm dishes, spun down at 270 x g for 5 min at room temperature, re-suspended in 1 ml of FBS supplemented with 10% dimethyl sulfoxide (DMSO) and transferred to cryo-vials. The cells were kept at -80^{0}C for 24 hours before moving to liquid nitrogen for long-term storage. To thaw cells, the cells were placed in a 37^{0}C water bath till completely defrosted, transferred to a 15 ml falcon tube filled with a fresh media and centrifuged at 270 x g for 5

min. The supernatant was aspirated, and the cell pellet was resuspended in a fresh media prior to transferring to a new tissue culture vessel.

2.3.2 Transfection of HEK-293T using PEI

Transient transfection of all genotypes of HEK-293T cells was carried out as previously described by Ehrhardt *et al* (Ehrhardt et al., 2006). Briefly, 20 hours prior to transfection, the cells were seeded in 6-well plates at a density of 5 x 10^5 cells per well in 2 ml media. The following day, a mix of Opti-MEM serum-free media, a plasmid DNA and 1mg/ml PEI was added (ratio of each are detailed in Table 4) to the cells for additional 24 hours (for shedding assay) or for 48 hours (for co-immunoprecipitation assay). Following the incubation, the cells were used for further analysis.

The plasmids used for HEK-293T transfections were as follows. Human Tspan15 and human Tspan14 with N-terminal FLAG tag were previously described by Haining *et al* 2012 and produced in pEF6-FLAG vector (a modified version of pEF6/Myc-His A from Invitrogen) (Haining et al., 2012). N-terminal FLAG-tagged human Tspan14/15 chimera series, human Tspan15 cholesterol binding mutants and human Tspan15 tailless were produced in the Tomlinson lab using pEF6-FLAG vector. The HA-tagged bovine ADAM10 in pcDNA3 was previously described (Lammich et al., 1999). The human VE-cadherin in the pWPI (GFP non-tagged) vector was generated by Peter Noy (unpublished).

Table 4 Reagents used for PEI transfection of HEK-293T cells

Plate size	Cells plated	Media volume	Opti-MEM	DNA	PEI (1mg/ml)
6-well	**5 x 10^5**	**2 ml**	**100 µl**	**1 µg**	**4 µl**

2.3.3 Transfection of HUVECs with small interfering RNA (siRNA)

Transient transfection of HUVECs was executed as previously described (Haining et al., 2012) using Lipofectamine RNAiMAX (Life Technologies Invitrogen Compounds), and pre-designed siRNA duplexes to ADAM10 and Tspan15 (Life technologies Ambion Compounds). The reagents and required quantities used in the experiments are shown in Table 5. The day prior to the transfection, cells were plated in a 6-well dish pre-coated with 0.1% gelatine such that the next day thery were about 80% confluent. On the day of the transfection, two separate vials containing siRNA duplexes and RNAiMAX, in Opti-MEM serum free-media, were prepared, mixed and incubated at room temperature (RT) for 10 minutes to allow the complexes to form. While incubating, HUVECs were prepared by washing twice in PBS, and 800 µl of Opti-MEM was added to the cells. Following the incubation, the cells were treated with the siRNA/Lipofectamine mix for 3 hours at 37 ^{0}C and 5% CO_2, before being replaced with appropriate antibiotic-free media for a further 48 to 72 hours. Negative control siRNA duplex was used to account for any effects that the delivery of siRNA into cells may have, and to form a background of basal levels of

analysed proteins. Transfected cells were used in *in vitro* functional and biochemical assays.

Table 5 List of reagents and quantities used for siRNA transfection of HUVECs

Plate size	Cell plated	siRNA mix		Lipofectamine mix		Final volume
		siRNA (10µM)	Opti-MEM	RNAiMAX	Opti-MEM	
6 well	3.6×10^5	2.5 µL	167.5 µl	3 µl	27 µl	1 ml

2.3.4 Stable HEK-293T cell line generation

Tspan15 CRISPR/Cas9 knockout (KO) HEK-293T cells were mock transfected or transfected with the human Tspan15 mutants and human Tspan14/15 chimeras using the PEI method as described above. For information about the mutants and chimera constructs, see figure 5.1. The plasmid vector used encodes the blasticidin-resistant gene as a selectable marker. Therefore at 48-hours post-transfection, the polyclonal cells were trypsinised, spun down at 270 x g for 5 min, the media was removed and replaced with complete DMEM (cDMEM) supplemented with10 µg/ml blasticidin. The cells were then serially diluted in a 96-well plate to isolate monoclones and cultured for 7 to 10 days to allow the clones to grow. The procedure for the serial dilution was as follows: 3 ml of the cell solution was prepared for each 96-well plate. From this, 300µl was transferred to the first column of the plate, while the remaining rows were filled up with 200µl the blasticidin-supplemented cDMEM media. Next, 100µl from the initial wells were

transferred to the second column, mixed well by pipetting up and down, thereby diluting in a ratio of 1:3. The action was repeated for each sequential column. After completing, 100µl was discarded from the last column. Wells were monitored during growth and only those wells where colonies appeared to come from individual cells were further expanded and assessed for the Tspan15 expression using flow cytometry.

2.4 Protein biochemistry methods

2.4.1 Cell-based shedding assay

The cell-based shedding assay was carried out as previously described (Haining et al., 2012) but with the following modifications: the shedding of the endogenous N- and E-cadherin was investigated in wild-type A549 and ADMA10- and Tspan15-KO A549 cells. Prior to the assay, the cells were plated at 80% confluency. The inhibition of γ-secretase activity was achieved by culturing cells for 30 minutes with 10 µM DAPT. Following this incubation, the cells were treated for an additional 30 minutes with 2 mM NEM, a potent ADAM10 agonist, or ethanol vehicle control. The cells were harvested, lysed in 1% Triton 100-X and subjected to western blotting. An antibody to the C-terminal cytoplasmic tail allowed the detection of both full length and cleaved fragments of the cadherins. For antibody selection, see Table 2. The results were imaged using the Odyssey Infrared Imaging System. The intensity of resulting bands, corresponding to full length and cleaved fragments, were quantified, and the percentage shed protein was calculated as follows: [cleaved fragment÷ (cleaved fragment + full length)] * 100, and compared to control, non-treated cells.

A similar protocol was prepared and used for VE-cadherin shedding in HUVECs at day 3 post-siRNA transfection. For details see section 2.6.

Shedding of VE-cadherin was monitored in the wild-type HEK-293T, ADAMA10- and Tspan15-KO HEK-293T cells. The cells were transfected with a plasmid encoding human VE-cadherin, 24 hours prior to the assay, following the standard PEI transfection protocol detailed in section 2.5. The inducible cleavage of VE-cadherin was assessed using DAPT and NEM as described above. This assay was also used to study the effect of Tspan15 monoclonal antibodies (mAbs) on VE-cadherin shedding. Here, the wild-type and ADAM10-KO HEK-293T cells, transfected with VE-cadherin, were pre-treated with anti-human Tspan15 mAbs (10 μg/ml) or MOPC (10μg/ml) control mAb at the point of DAPT (10 μM) addition. After 30 minutes, the cells were stimulated with NEM (2 mM) for an additional 30 minutes. The shedding was measured, and analysis was carried out as aforementioned.

2.4.2 Flow cytometry

Surface expression of ADAM10 and TspanC8s of interest was analysed using BD FACSCalibur Flow Cytometer and its software CellQuest^{TM} Pro (BD Bioscience) as per the manufacturer's instructions. Preceding the analysis, the cells were grown and treated as required for the particular experimental purpose. Briefly, 5 x 10^5 cells were detached (either by scraping for HEK293T and A549 cells or trypsinised for HUVEC cells), and spun for 5 min at 2655 x g at room temprature. The cells were incubated on ice for 30 min in the dark with either primary fluorescent-conjugated mAbs, non-conjugates mAbs, or

hybridoma tissue culture supernatants, along with the appropriate isotype controls (Table 2). Next, the cells were washed in FACS buffer to remove unbound antibodies and stained with species-corresponding secondary antibodies (if non-conjugated mAbs were used in the first stain), as described for the primary antibodies. Live cells were gated by size and granularity, and fluorescence of gated cells was measured. The geometric mean fluorescence intensity was used to assess the surface expression of proteins. The surface expression was calculated by dividing the geometric mean of positive staining by its isotype-matched negative control.

2.4.3 Antibody internalisation assay using flow cytometry

HEK-293T cells were plated in 6-well plate to 80% confluency and used in the assay. All the treatments were performed in duplicate. First, the cells were pre-chilled for 60 minutes at 4 ^{0}C, followed by an additional 30 min incubation in the presence of Tspan15 mAbs (clones 4A4, 5D4, 5F4, 1C12) or MOPC control, each at 10 μg/ml. Next, the unbound mAbs were washed away using ice-cold PBS, and fresh cDMEM media was added. One of the plates was transferred to 37 ^{0}C for 30 min for mAb internalisation to occur, while the other was kept at 4 ^{0}C. After the incubation time, the cells were moved to 4 ^{0}C and stained with corresponding secondary antibodies as described in section 2.4.2. The surface expression of Tspan15 was measured on both duplicate plates using flow cytometry. Only the fluorescence emitted from the live population of the cells was considered for further calculation. The surface expression was calculated by dividing the average geometric mean from positive staining by its negative, isotype control staining.

2.4.4 Immunoprecipitation and western blotting

Co-immunoprecipitation and western blot experiments were conducted as previously described (Haining et al., 2012, Noy et al., 2016). Wild-type or transfected cells were lysed in either 1% Triton X-100 (for western blotting) or 1% digitonin lysis buffer (for co-immunoprecipitation) supplemented with a 1:100 dilution of protease inhibitor cocktail for 30 min on ice. Following centrifugation at 20817 x g for 10 min at 4 ^{0}C to remove insoluble cell derbies; a portion of the soluble lysate was removed as input control. For the co-immunoprecipitation experiments, the lysate was incubated for 90 min at 4 ^{0}C with primary antibody bound to protein G sepharose beads. The beads were washed four times with 0.1% digitonin lysate buffer and the beads were mixed with either 2x SDS non-reducing or reducing sample buffer respectively and boiled for 5 min at 100 ^{0}C to elute and denature bounded proteins prior to gel electrophoresis. Subsequent SDS-PAGE separation and western blot transfer were performed according to standard protocols. For the protein separation, gels with a single polyacrylamide concentration were prepared in-house and ranged from 10 to 12 %. The samples were run at 125V until the dye front reached the bottom of the gel. Next, the separated proteins were transferred onto methanol-activated polyvinylidene difluoride (PVDF) Immobilon-FL membrane and wet-transferred for 90 min at 30 V. Following transfer, the membrane was blocked in 5% milk in TBST for 1 hour at room temperature and then with incubated overnight with primary antibody at 4^{0}C on a rocker. The unbounded antibodies were removed by 3 washes for 10 min each using the high salt TBST wash buffer. Secondary antibodies, conjugated to infrared dye (IR dye) 680 or 800, were added for an additional 2-hour incubation period on a rocker at room

temperature. After the incubation, the membrane was washed 5 times for 5 min each using the high salt TBST wash buffer. The results were visualized and intensities of bands quantified using the Odyssey Infrared Imaging System (LI-COR Bioscience). The selections of the primary and secondary antibodies used in the experiments are specified in Table 2.

2.5 Molecular biology methods

2.5.1 Generation of Tspan15 mutant constructs: point mutations in cholesterol binding sites (Q245E or Q245A) and truncated cytoplasmic N- and C-terminal tails

The tailless form of the human Tspan15 was constructed using a single step PCR-based method (Figure 2.1) in a Veriti® 96-Well Thermal Cycler (Applied Biosystems). The approach utilised the pEF6-FLAG-Tspan15 plasmid previously generated in the laboratory containing the wild-type Tspan15 as a starting template. Specific primers were designed to amplify Tspan15 minus the N- and C-terminal tails. These primers included the restriction sites *Bam*HI and *Not*I (see below) to allow the resulting fragment to be cloned in-frame with the FLAG tag in the pEF6-FLAG plasmid; the reverse primer contained a sequence to introduce a stop codon.

Primers used:

fwd, 5'-TAGTAG GGATCC TGGCTCAAGTTTTCACTTATC-3' (contains *Bam*HI)

rev, 5'-TAGTAG GCGGCCGC TTA ATCAGTGACAGAGTGCTC-3' (contains *Not*I and stop codon TTA)

The point mutations (Q245E and Q245A) for the putative cholesterol binding site were introduced to human Tspan15-FLAG by a two-step PCR strategy (Figure 2.1). The approach required two flanking primers (MT5147 and MT4150), contained within the pEF6-FLAG Tspan15 plasmid, and contained *Bam*HI and *Not*I restriction sites so that the final product could be inserted into the pEF6-FLAG vector. Also, two internal primers were required with complementary ends and carrying a point mutation in the middle of the primer, that hybridised to the region that needed to be altered. The resulting fragment was digested with *Bam*HI and *Not*I and ligated into the pEF6-FLAG plasmid.

Primers used were as follows:

Q245E *fwd* 5'-CATCCTGCTTCCCGAGTTCCTGGGGGTG-3' (contains Q to E mutation CAG -> GAG)

Q245E *rev* 5'-CACCCCGAGGAACTCGGGAAGCAG-3' (contains Q to E mutation CTG -> CTC)

Q245A *fwd* 5'-CATCCTGCTTCCCGCGTTCCTGGGGGTG-3' (contains Q to A mutation CAG -> GCG)

Q245A *rev* 5'-CACCCCCAGGAACGCGGGAAGCAGGATG-3' (contains Q to A mutation GTC -> CGC)

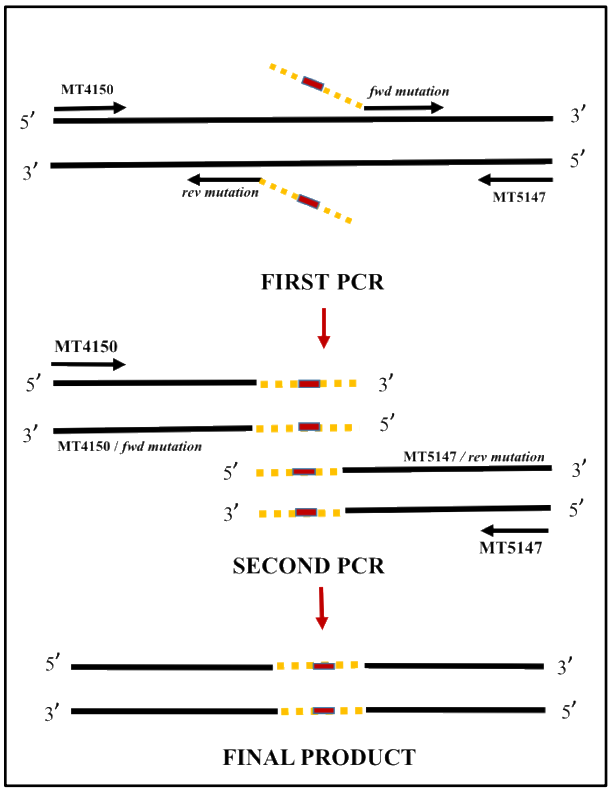

Figure 2.1 Schematic of a PCR-based method for designing Tspan15 with cholesterol binding mutations. The primers were designed and annealed to introduce point mutations to the full-length of Tspan15. The first two PCR reactions were used to generate fragments containing the desired mutation on the wild-type Tspan15 template, using primers pairs: MT5147/*fwd mutation* and MT4150/ *rev mutation.* The two resulting fragments were mixed for the second round of PCR with the flanking primers MT4150 and MT5147.

2.5.2 Polymerase chain reaction (PCR)

All PCR reactions were set up according to the manufacturer's instructions. A typical 50µl reaction contained 25µl KAPA HiFi polymerase ReadyMix (including the polymerase at 0.5 U per 25µl reaction, dNTPs at 0.3 mM, 2.5 mM $MgCL_2$), 1µl DNA template (~ 20 to 50 ng), 1 µl of each forward and reversed primer at 20µM, and 22 µl of PCR grade water. Typical cycling conditions were as follows: [95 ^{0}C, 5 min] for 1 cycle, [98 ^{0}C, 30 sec; 60 ^{0}C, 15 sec; 72 ^{0}C, 60 sec] for 30 cycles, [72 ^{0}C, 5 min] 1 cycle.

2.5.3 Agarose gel electrophoresis

A 1% gel was prepared by dissolving the agarose in 1 x TAE buffer and adding SYBR® Safe DNA Gel Stain (1:10.000 dilution, Invitrogen). The gel was left to set with appropriate combs in place. Next, the samples were mix with 6 x Orange G loading dye and loaded onto the gel along with a 1 kb DNA ladder. The gel was run at 100-150 V until appropriate separation was reached. DNA was visualised on a UV transilluminator.

2.5.4 Purification of PCR products

Prior to using the products of a PCR reaction, the products were purified to remove primers using the QIAquick PCR purification kit (Qiagen), following the manufacturer's protocol, and eluted with 50µl elution buffer (EB) buffer.

2.5.5 Purification of DNA from agarose gel

Prior to cloning, DNA fragments from PCR amplifications and restriction digests were extracted from agarose gels and purified using the GeneJet Gel Extraction Kit (Fermentas), following the manufacturer's protocol, and eluted in 50 µl of EB.

2.5.6 Purification of plasmid DNA

Plasmid DNA was isolated from overnight bacterial cultures (DH5α strain of *E. coli*) using the GeneElute Plasmid DNA Midiprep Kit (Sigma-Aldrich) according to the

manufacturer's protocol. The concentration of the plasmid was measured using a Nanodrop Spectrophotometer.

2.5.7 Digestion of plasmids and PCR products

The digests were set up on ice and carried out in a total volume of 60 µl, containing 48µl of PCR product, or 5 µg of pEF6-FLAG plasmid DNA, 6 µl of 10x NEB buffer, and 3 µl of specific restriction enzymes. When necessary, the remaining volume was made up to 60 µl with sterile water. The digests were left to proceed for 3 hours at 37 ^{0}C.

2.5.8 DNA cloning and *E. coli* transformation

The ligations were set up on ice and incubated at room temperature for 30 min for sticky ends. A ligation reaction included: a digested plasmid DNA and insert DNA, combined in 1:6 ratio, 1 µl of T4 DNA ligase and 2 µl of 10x ligase buffer. The final volume was made up to 20µl with molecular biology-grade water.

A general *E. coli* transformation using DH5α cells (Invitrogen) was carried out as follows. For each transformation, 50 µl of the competent cells was thawed on ice and DNA was added to a maximum of 10% of total bacterial volume. The cells were incubated on the ice for 30 min, next heat shocked in a 42 ^{0}C water bath for 45 seconds, and placed back on the ice for 2 min. 200 µl of SOC media was added and the bacteria further incubated at 37 ^{0}C for 1 hour. Each batch of transformed cells was plated out on LB agar plates with ampicillin antibiotic (100 µg/ml) for selection. The plates were incubated overnight at 37

^{0}C. A single colony of the bacteria was picked up, and a colony PCR reaction was carried out using 25µl of 2x RedTaq® ReadyMix™, 23µl sterile water, 1µl of 20 µM forward and reverse primers. Positive colonies were chosen for plasmid prep and confirmation by DNA sequencing.

2.5.9 DNA sequencing

DNA samples for sequencing were prepared as instructed by the Functional Genomic Facility at the University of Birmingham. In general, 350 ng of DNA was combined with 3.2 pmol of primers in a total reaction volume of 10 µl. The sequencing results were analysed using ChromasPro (Technelysium Pty Ltd) software.

2.6 *In vitro* angiogenesis assays

2.6.1 Scratch wound assay

Prior to the assay, HUVECs were seeded at 90% confluency in a 96-well plate. 24 hours after the seeding, the monolayer was scratched using the 96-pin wound maker tool, followed by image acquisition using the IncuCyte®ZOOM System from Essen BioScience. Mitomycin (5 µg/ml) was included in the media to inhibit proliferation. A time-lapse recording was set up to scan the wounded monolayer every 6 hours until complete wound closure. Two experimental approaches were used to investigate the impact of ADAM10 and Tspan15 on endothelial cell migration. In the first, the wounded

monolayer was incubated with ADAM10 inhibitor (GI254023X at concentrations 2.5 μM) or DMSO as a vehicle control. In the second approach, the ADAM10 and Tspan15 siRNA-transfected HUVECs were used. The changes in the width of the wounded area were analysed over 24 to 30-hour period, using ImageJ plugin. The percentage of the wounded area was measured at a given time point, compared to the initial wound area for each sample.

2.6.2 Endothelial cell proliferation assay

The cell proliferation assay was used to assess the proliferative response of HUVECs to pharmacological inhibition or gene silencing of ADAM10 and Tspan15. The response was monitored by cell counting under an inverted microscope using a hemocytometer. In the gene silencing approach, the cells were transfected with appropriate siRNA duplexes as described in section 2.3.3. One day post-transfection, 2 x 10^5 cells were seeded in a 10 cm plate and incubated for an additional 72-96 hours. For the pharmacological inhibition of ADAM10, the plated cells were maintained in the media containing ADAM10 inhibitor (GI254023X at 2.5 μM) for the duration of the assay alongside with a DMSO as a vehicle control. The cell proliferation in control and treated HUVECs was calculated as the ratio of the number of live cells at the end of the culture period to the number of live cells at the beginning of the experiment. For normalisation of the counts, the cell proliferation for the control was taken as 1, and fold change for the treated samples was calculated accordingly. Cell viability was assessed by the trypan blue exclusion method before and after the treatments. Briefly, 20 μl of the cell suspension was mixed with 20 μl of the trypan blue solution (0.4%) and mixed thoroughly by flicking the tube. Next, 10 μl of cell-trypan blue

suspension was pipetted onto the haemocytometer. The cells were observed using 10x objective magnification settings. Only live cells, that did not take up the dye, were counted and used for the analysis.

2.6.3 2D network formation on Matrigel

The endothelial cell ability to form networks *in vitro* was measured using a 2D tube formation assay on Matrigel. Prior to the assay, HUVECs were transfected with ADAM10, Tspan15 and negative control siRNA duplexes (see section 2.3.3.). 48 hours post-transfection, the cells were plated sparsely at a density of 1.4 x 10^5 cells/ml into 12-well plates pre-coated with 70 µl of the reduced serum Matrigel. The network formation was observed in real-time, using the IncuCyte Imaging System (Essen BioScience), and further analysed using the Angiogenesis Analyser plugin for Image J, by Gilles Carpentier (http://imagej.nih.gov/ij/macros/toolsets/Angiogenesis% 20Analyzer.txt). For ADAM10 pharmacological inhibition analysis, the plated cells were incubated in the presence of 2.5 µM GI254023X or DMSO as a vehicle control. Network formation was determined based on the differences in the number of meshes between control and treated network.

2.7 Statistical analysis

Statistical analyses were completed using GraphPad Prism 7.0 software. All results were from at least 3 independent experiments. Error bars were presented as standard error of the mean (SEM). All relative or percentage data were transformed by arcsine of the square root to normalise them transform prior to parametric statistical tests. Statistical significance between two independent groups was analysed using unpaired two-tailed Student *t*-tests. Comparisons between multiple groups were performed using one-way or two-way analysis of variance (ANOVA) followed by a post hoc multiple comparison test. P-values < 0.05 were considered as significant.

CHAPTER 3
REGULATION OF TSPAN15 BY ADAM10

3.1 Introduction

Previously, Tspan15 has been identified as a member of the group of tetraspanins, termed TspanC8s (Matthews et al., 2017a, Matthews et al., 2017b, Saint-Pol et al., 2017b). These tetraspanins comprise Tspan5, 10, 14, 15, 17 and 33. They are related by protein sequence and characterised by the presence of 8 cysteines in the large extracellular loop (LEL). Notably, Tspan15 was the first tetraspanin identified to co-immunoprecipitate with the 'molecular scissor' ADAM10 in stringent detergents such as 1% digitonin, and promote its maturation, trafficking to the cell surface and substrate specificity (Prox et al., 2012). The other five TspanC8s were then shown to perform a similar function (Dornier et al., 2012, Haining et al., 2012) and, more recently, data has shown that different TspanC8s confer distinct ADAM10 substrate specificities (Jouannet et al., 2016, Noy et al., 2016, Reyat et al., 2017, Saint-Pol et al., 2017a).

The most definite example of a TspanC8 promoting ADAM10 cleavage of a specific substrate is for Tspan15 and the N-cadherin cell-cell adhesion molecule (Prox et al., 2012, Jouannet et al., 2016, Noy et al., 2016). The above findings and the notion of Tspan15 as a central modulator of ADAM10 were recently confirmed *in vivo*. Tspan15-deficient mice showed a substantial reduction of the mature and active form of ADAM10 within the brain that correlated with the reduced shedding of N-cadherin (Seipold et al., 2018). Further, genetic studies implicated Tspan15 in various pathological conditions. Tspan15 was identified as a genetic factor with a single nucleotide polymorphism (SNP) that increases susceptibility to *S. pneumoniae* infections (Salas et al., 2018) and venous thrombotic diseases (Germain et al., 2015), and as an oncogene that promotes oesophageal squamous cancer metastasis (OSCC) (Zhang et al., 2018). Indeed, as summarised by the Human Protein Atlas, the abundance of Tspan15 expression on epithelial cancer cells is consistent with its role in tumour development and progression, particular in pancreatic cancer, and epithelial cell biology (Uhlen et al., 2015). Therefore, the Tspan15-ADAM10 complex is of great interest as a potential therapeutic target.

The current characterisation of Tspan15 is hindered by lack of effective monoclonal antibodies (mAs). To date, the majority of studies on Tspan15 functions have relied on over-expression of epitope-tagged proteins in various cell lines, with potential pitfalls of introducing false positive results. We hypothesised that the difficulty in making tetraspanin mAbs arises from a highly conserved sequence of the protein between the species, a small size of the tetraspanins and subsequent ‘masking’ effect arising from association with larger partner proteins like ADAM10. To address this problem, we have developed a strategy of generating mAbs using a novel immunogen, namely ADAM10-knockout

mouse embryonic fibroblasts stably over-expressing human Tspan15 (Noy and Tomlinson unpublished). In collaboration with Abpro, a Boston-based company, we generated four new mouse anti-human Tspan15 mAbs to the extracellular region of Tspan15 (Figure 3.1). Our new mAbs, together with in-house established ADAM10 and Tspan15 CRISPR/Cas9 knockout cell lines, were used in the investigations forming the basis of the current study and future work.

This chapter aims to determine (1) whether ADAM10 cell surface expression requires Tspan15 in primary human umbilical cord endothelial cells (HUVECs), adenocarcinomic human alveolar basal epithelial (A549) and human embryonic kidney (HEK-293T) cells, and (2) if Tspan15 expression might also require ADAM10.

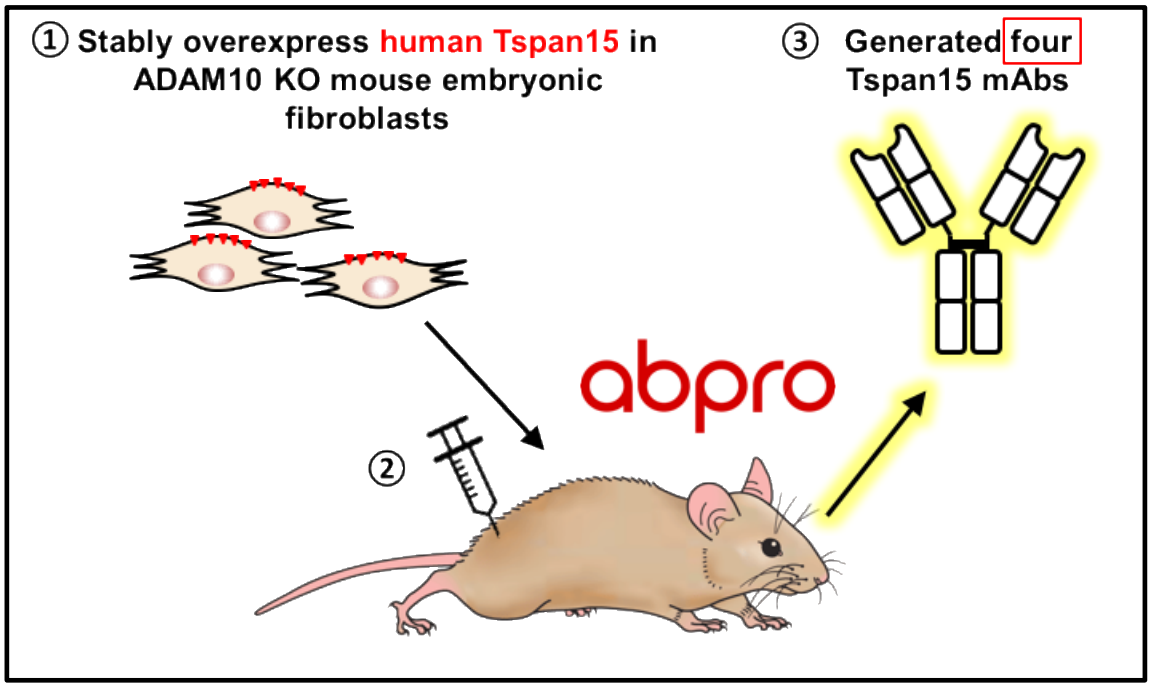

Figure 3.1 A novel method to generate Tspan15 monoclonal antibodies. ADAM10-deficient mouse embryonic fibroblasts stably transfected with human Tspan15 were used as an immunogen for the production of mouse mAbs by the company Abpro. The expression of Tspan15 in ADAM10 knockout mouse cells may prevent the 'masking effect' caused by ADAM10 and enable an antibody response to Tspan15. Four Tspan15 specific mAbs were generated: clone 4A4, 1C12, 5D4 and 5F4 (Noy and Tomlinson unpublished).

3.2 Results

3.2.1 Validation of Tspan15 mAbs

To validate that the new mAbs do indeed recognise the endogenous Tspan15, wild-type (WT) HEK-293T cells, in comparison with their CRISPR/Cas9 Tspan15 knockout (Tspan15 KO) counterparts, were used. As shown in Figure 3.2, all four Tspan15 mAbs were effective in recognising endogenous Tspan15 by flow cytometry. Specificity was confirmed by the lack of antibody reactivity to Tspan15 KO cells.

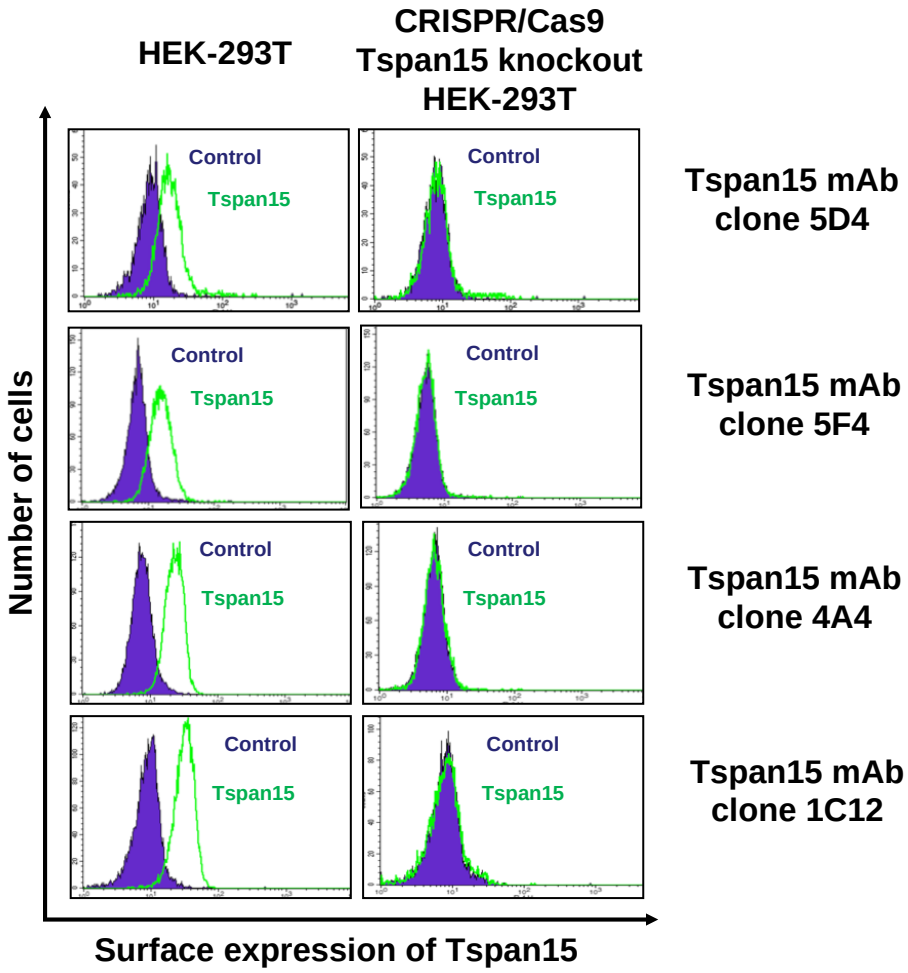

Figure 3.2 Validation of new Tspan15 monoclonal antibodies. The wild-type and Tspan15 CRISPR/Cas9 knockout HEK-293T cell line was stained with four clones of Tspan15 mAbs (clones 4A4, 1C12, 5F4 and 5D4 were used in the form of tissue culture supernatants) and isotype control and subjected to flow cytometry to determine the cell surface expression levels of Tspan15. Each pair of histograms is representative of three independent experiment.

3.2.2 Tspan15 is required for normal ADAM10 cell surface expression

Tspan15 knockdown has previously been shown to reduce ADAM10 cell surface expression in a human prostate carcinoma cells (PC3) by 60% (Jouannet et at., 2016) and by 50% in mouse neuroblastoma cells (N2A) (Prox et al., 2012). To determine the requirement of Tspan15 for ADAM10 expression in HEK-293T and A549 cell lines, a panel of CRISPR/Cas9 KO cell lines were used, in conjunction with the new Tspan15 mAbs. Flow cytometry revealed that in the absence of Tspan15, ADAM10 cell surface expression was reduced by approximately 70% in HEK-293T cells (Figure 3.3A) and by approximately 50% in A549 cells (Figure 3.3B). As a control, no ADAM10 was detected on ADAM10 KO cells (Figure 3.3A-B). To determine whether Tspan15 also affected ADAM10 expression in HUVECs, flow cytometry was performed following siRNA knockdown of Tspan15. ADAM10 cell surface expression was reduced by approximately 30% using two different Tspan15 siRNA duplexes (Figure 3.3C).

The residual ADAM10 expression in the absence of Tspan15 may be due to the expression of other TspanC8s. In the absence of mAbs to most TspanC8s, their expression was compared at the transcriptomic level using data available from the Human Protein Atlas (Uhlen et al., 2015). HEK-293T and A549 cells expressed substantial levels of Tspan15, but other TspanC8s were also expressed at various levels (Figure 3.3D). HUVECs expressed relatively less Tspan15, with higher levels of Tspan5, Tspan14 and Tspan17 (Figure 3.3D). These Protein Atlas data are consistent with our published real-time PCR data (Haining et al., 2012, Matthews et al., 2017b).

Together these data demonstrate that Tspan15 is important for normal ADAM10 cell surface expression, and residual expression is likely due to other TspanC8s that are expressed in a cell type-dependent manner.

A HEK-293T

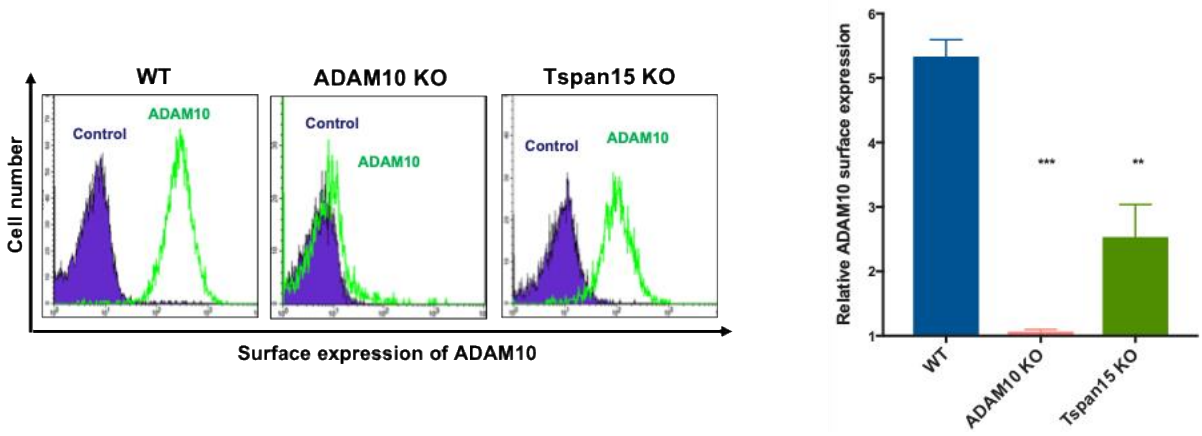

B A549

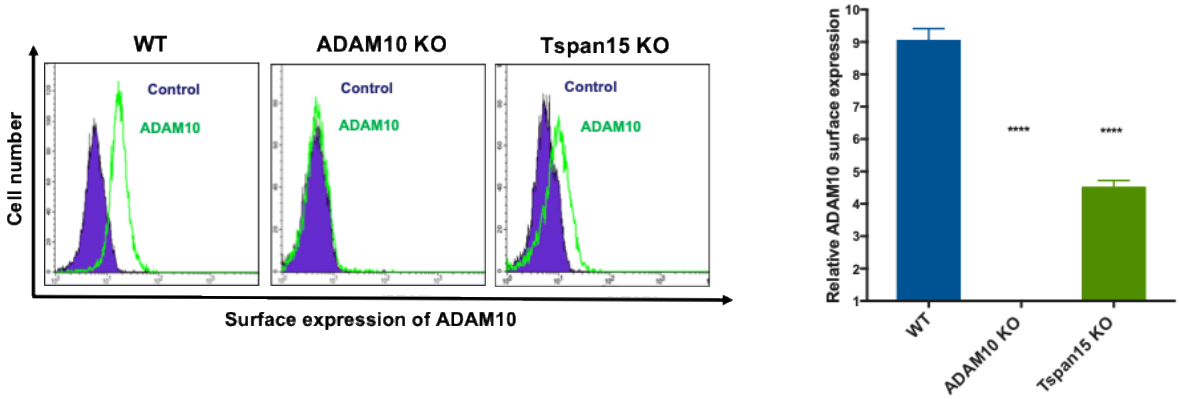

C HUVEC

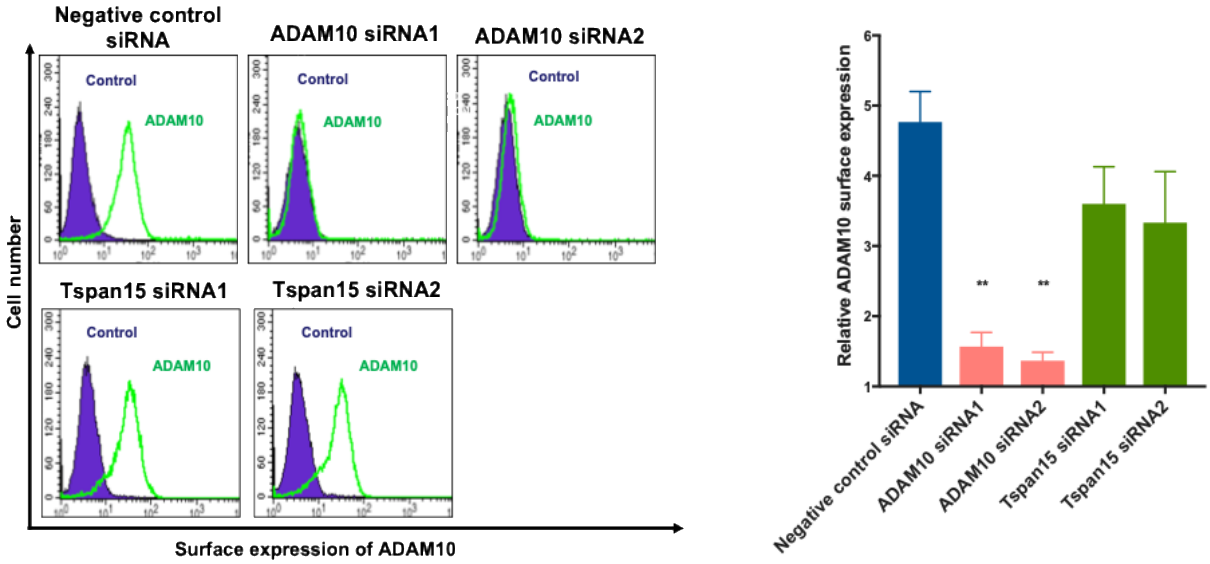

D

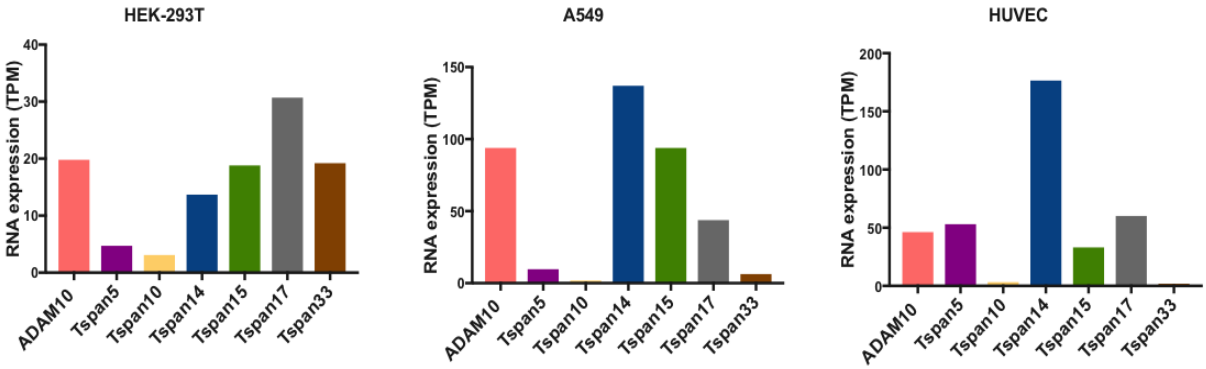

Figure 3.3 Tspan15 is differentially required for ADAM10 cell surface expression in various cell types. [A] HEK-293T and [B] A549 wild-type (WT), ADAM10 KO and Tspan15 KO cells were analysed by flow cytometry using ADAM10 (green histogram) or MOPC negative control (filled purple histogram) mAbs. [C] HUVECs were similarly analysed by flow cytometry, following ADAM10 or Tspan15 knockdown with two different siRNA duplexes. The data in panels A-C were quantitated by dividing the ADAM10 geometric mean fluorescence intensity by the corresponding MOPC value, such that no expression has a value of 1. The bar charts represent the mean expression data from three to four experiments, and error bars are the standard error of the mean. Data were normalised by arcsine transformation of the square root and analysed by a one-way ANOVA and Dunnett's multiple comparison test ($^{**}p < 0.01$, $^{***}p < 0.001$, $^{****}p < 0.0001$). [D] ADAM10 and TspanC8 mRNA expression in HEK-293T, A549 and HUVECs from The Human Protein Atlas. The results are reported as the number of Transcripts per Kilobase Million (TPM).

3.2.3 ADAM10 is required for normal Tspan15 surface expression

ADAM10 knockdown has previously been shown to reduce Tspan5 cell surface expression in U2OS and HCT116 cell lines by 40% (Saint-Pol et al., 2017a), which indicated that regulation within the ADAM10/Tspan5 complex is reciprocal. In order to determine the requirement of ADAM10 for Tspan15 expression, flow cytometry on ADAM10 KO HEK-293T and A549 cell lines and ADAM10 siRNA-transfected HUVEC cells were performed with Tspan15 mAbs. This revealed that in the absence of ADAM10, Tspan15 surface expression was reduced by approximately 80% in ADAM10 KO cell lines (Figure3.4 A-B) and by approximately 90% using two different ADAM10 siRNA duplexes in HUVEC upon quantitation (Figure3.4 C).

Together this data demonstrates that ADAM10 is required for normal Tspan15 surface expression.

A HEK-293T

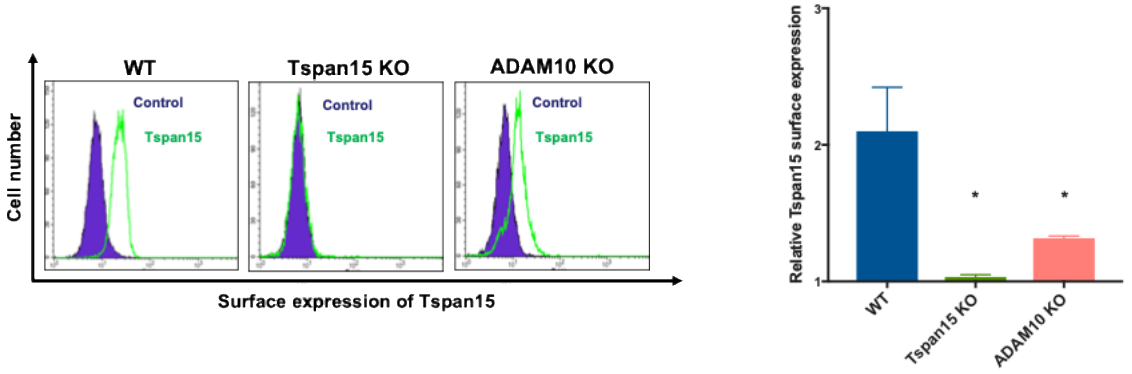

B A549

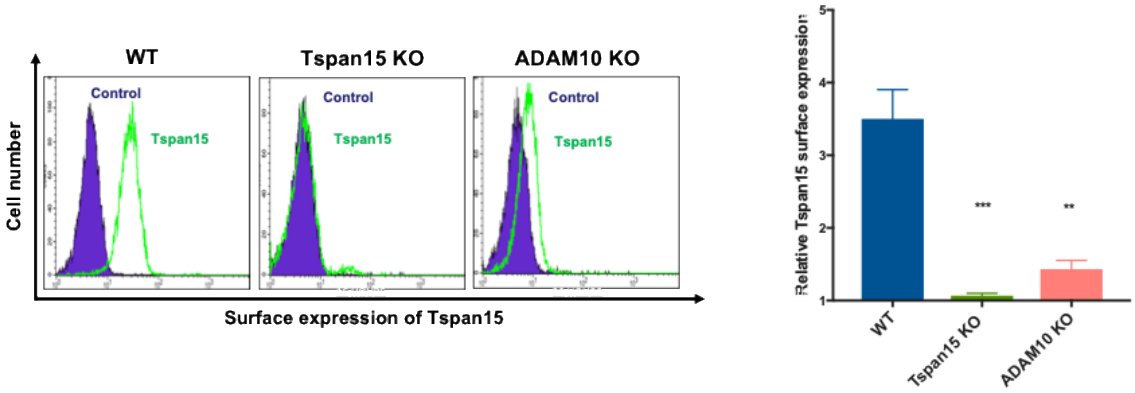

C HUVEC

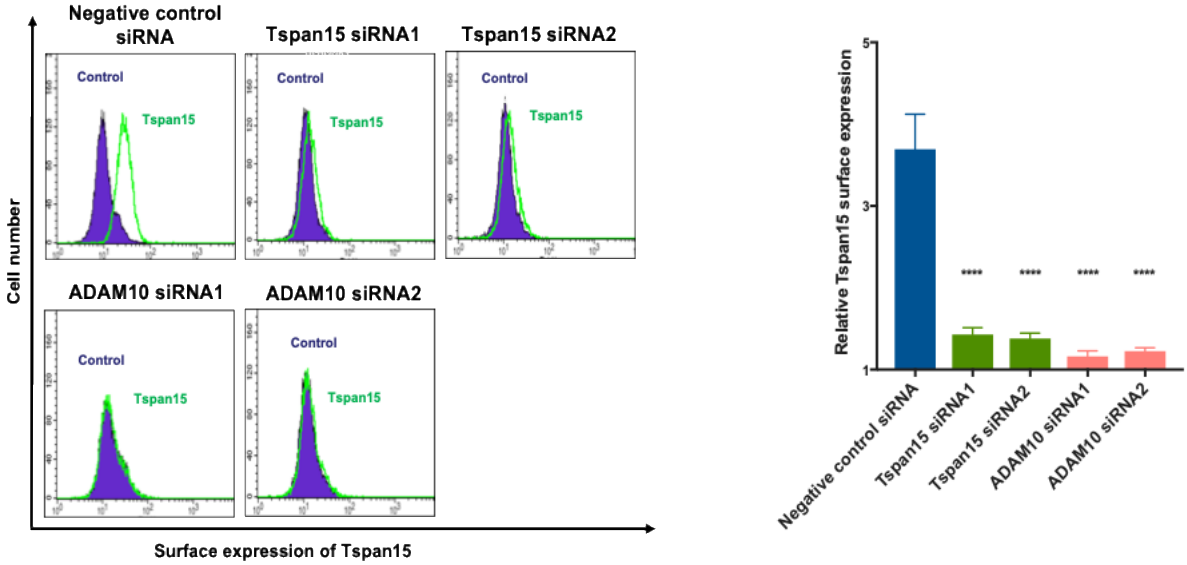

Figure 3.4 Tspan15 cell surface expression is reduced in the absence of ADAM10. [A-C] Flow cytometry was performed as described in Figure 3.3, with the exception that Tspan15 mAb (4A4 clone used in a form of tissue culture supernatant) was used instead of ADAM10. The bar charts represent the mean expression data from three to four experiments, and error bars are the standard error of the mean. Data were normalised by arcsine transformation of the square root and analysed by a one-way ANOVA and Dunnett's multiple comparison test ($^{*}p<0.05$, $^{**}p < 0.01$, $^{***}p < 0.001$, $^{****}p < 0.0001$).

3.3 Discussion

In this chapter, four new Tspan15 mAbs were used in conjunction with ADAM10- and Tspan15-knockout/knockdown cells to investigate the extent to which Tspan15 is required for ADAM10 surface expression and vice versa. Initial validation of the mAbs confirmed their specificity in detecting endogenous levels of Tspan15 by flow cytometry on WT cells, but not on Tspan15-knockout/knockdown cells. Tspan15 was found to be important for normal ADAM10 surface expression on HEK-293T and A549 cells lines, and HUVECs, since ADAM10 was reduced 70%, 50% and 30%, respectively, in the absence of Tspan15. Finally, the discovery that ADAM10 was required for normal Tspan15 surface expression, with an 80% reduction in the absence of ADAM10, was a surprising result. Collectively, the data presented in this chapter indicate the reciprocal relationship between the interacting partners which suggests that the main role of Tspan15 is to regulate ADAM10.

There are well-characterised mAbs to several tetraspanins, in particular, those with CD nomenclature that is given on the basis that mAbs are available: CD9, CD37, CD63, CD81, CD82, CD151 and CD231. However, one problem in the tetraspanin field is the lack of effective antibodies to many of these proteins. Indeed, at the start of this thesis project, there were no mAbs, or even any effective polyclonal antibodies, to any of the TspanC8s. Despite considerable work to develop mAbs, to date, many efforts have failed (Mike Tomlinson, personal communication, following discussions with other tetraspanin researchers). The obstacles in tetraspanin antibody production likely arise from the high sequence conservation between the mouse and human proteins, their relatively small size,

low expression level and/or their association with rather larger partner proteins that may mask a tetraspanin antibody from recognition.

Furthermore, the four-transmembrane structure of tetraspanins, and lack of a modular domain structure in their extracellular regions has hindered efforts to make effective immunogens from soluble recombinant versions of the extracellular region. While such recombinant proteins have proved successful in screening for antibodies (Tomlinson et al., 1993, Tomlinson et al., 1995), for structural studies (Kitadokoro et al., 2001, Rajesh et al., 2012) and in a number of functional studies (Hassuna et al., 2017, Hulme et al., 2014, Green et al., 2011, Barreiro et al., 2008), they have not yet been validated as good immunogens. This is presumably because the antibody response is focussed on unfolded protein or novel epitopes in the recombinant proteins, that do not exist in the full-length protein. In contrast, successful mAb generation projects have used intact cells expressing tetraspanins, or immunoprecipitates of full-length tetraspanins from such cells (Rubinstein et al., 2013).

In this chapter, we have reported the successful generation of four mouse anti-human-Tspan15 mAbs, in collaboration with the antibody company Abpro, using a novel immunogen: ADAM10 KO mouse embryonic fibroblasts stably overexpressing human Tspan15. Western blotting experiments have demonstrated no cross-reactivity of the Tspan15 mAbs with other TspanC8s (Koo, unpublished). The new method likely overcomes the potential problems of low expression or masking by ADAM10, and may have benefited from the eight amino acid differences between human and mouse Tspan15 in the main extracellular region. This region was shown to contain the mAb epitopes (Chapter 4, and Koo, unpublished). The novel immunogen strategy might be useful for generating mAbs to other TspanC8s and tetraspanins in general. Indeed, the emerging

utility of CRISPR/Cas9 genome editing would enable knockout cell lines, for tetraspanin partners, to be readily generated for subsequent over-expression of the tetraspanin. The successful mAb generation could also be attributed to Abpro's proprietary mouse strain, on which the company is based. The ImmunoMax^{TM} Mouse was developed to provide an optimised response and a diversified repertoire of mAbs.

The absence of Tspan15 was sufficient to reduce ADAM10 surface expression on HEK-293T and A549 cells by 70% and 50%, respectively. The remaining ADAM10 is likely to be associated with other TspanC8s since HEK-293T cells express all six TspanC8s (Haining et al., 2012) and A549 express all except Tspan10 (Matthews et al., 2017b). Similarly, Tspan15 knockdown reduced surface ADAM10 by 30% in HUVECs, a primary cell type which expresses all TspanC8s except Tspan33 (Haining et al., 2012). This is in line with a previous study shown by Haining et *al.*, whereby knockdown of the major tetraspanins expressed, such as Tspan33 in erythrocytes or Tspan14 in HUVECs, led to substantial reductions of ADAM10 surface levels (Haining et al., 2012). Also, Dornier et *al*. showed that ADAM10 accumulated in the ER following knockdown of the most highly expressed TspanC8, Tspan14, in HCT116 colon cancer cells (Dornier et al., 2012). Indeed, Prox et al. used pulse-chase experiments to show that Tspan15 promotes ADAM10 exit from the ER and its stabilisation at the cell surface (Prox et al., 2012).

The most striking and surprising result in this chapter was the 80% reduction in surface Tspan15 observed following ADAM10 knockout in HEK-293T, A549 or HUVECs. However, a recent report now suggests that this could be a common feature for all TspanC8/ADAM10 complexes. Saint-Pol et *al* showed that the majority of Tspan5 is

ADAM10-associated in U2OS osteosarcoma cells and HCT116 cells and ADAM10 is required for normal Tspan5 expression and trafficking out of the ER (Saint-Pol et al., 2017a). The important question is what causes the inability of Tspan15 to traffic to the surface? Recent unpublished work in the Tomlinson lab has shown that in the absence of ADAM10, the total Tspan15 protein level was reduced by 80 %, as detected by western blot and there was no difference in Tspan15 mRNA between WT and ADAM10 KO cells (Koo, unpublished). A similar observation was made by Saint-Pol et al., who showed that the total amount of Tspan5 decreased upon ADAM10 knockdown (Saint-Pol et al., 2017a). Thus, the retention of Tspan15 in the ER in the absence of ADAM10 is unlikely to be the mechanism, and instead, it could be that Tspan15 requires ADAM10 for protein stability. This stabilising effect of partners on tetraspanins has not been reported for non-TspanC8 tetraspanins.

While regulation of Tspan15 by ADAM10 is an exciting discovery, it raises the question of how a Tspan15-overexpressing immunogen was created in ADAM10 KO MEFs? One answer could be that the overexpression of Tspan15 yields a large pool of protein that bypasses the need for ADAM10, perhaps by causing Tspan15 clustering. Indeed, it was demonstrated in the Tomlinson lab that, transient over-expression of Tspan15 in WT and ADAM10 KO cells, achieved the same levels of Tspan15 surface expression (Koo, unpublished).

In conclusion, the chapter describes the production of the first mAbs against Tspan15, and their use to characterise the expression of Tspan15/ADAM10 complexes. The data suggest that the Tspan15/ADAM10 complex is a ‘molecular machine’ that only functions as a

whole when both components are present. Indeed, the formation of the complex appears necessary for proteins to exit the ER and be expressed on the cell surface. Moreover, the data strongly suggest that the major role of Tspan15 is to regulate ADAM10.

CHAPTER 4
REGULATION OF CADHERIN SHEDDING BY ADAM10 AND TSPAN15

4.1 Introduction

Cadherins are homophilic cell adhesion molecules and components of cellular adherens junctions. They function through association with the cytoskeleton via interactions between their intracellular tails and β-catenin, a multifunction protein with roles in cell adhesion and gene expression. The interaction maintains structural and functional tissue continuity and integrity that is essential in homeostasis (Leckband and de Rooij, 2014). ADAM10 has been identified as a primary sheddase for several members of the cadherin family (Pruessmeyer and Ludwig, 2009). Analysis of ADAM10-deficient fibroblasts, inhibitor studies and siRNA-mediated ADAM10 downregulation in HUVEC demonstrate that the protease is responsible for N-, E- and VE-cadherin shedding (Reiss et al., 2005, Maretzky et al., 2005, Schulz et al., 2008). ADAM10 can cleave the cadherins at the basal level, and this is increased upon cell stimulation. Shedding of the full-length protein leaves a membrane-bound C-terminal fragment that is a target for intracellular cleavage by the γ-secretase complex. In this context ADAM10 can have at least two effects on cell function namely

loosening of cell-cell junctions to promote cell motility and vessel permeability and signal transduction by release of β-catenin to translocate to the nucleus and regulate gene transcription (Reiss et al., 2005, Maretzky et al., 2005, Schulz et al., 2008). The importance of cadherin cleavage is not fully understood. In the brain, ADAM10 cleavage of N-cadherin induces neuronal progenitor cell migration to promote myelin repair following brain injury (Klingener et al., 2014). Inflammation-induced VE-cadherin shedding is implicated in endothelial barrier disruption and severe increase in sepsis pathogenesis (Flemming et al., 2015). Also, *S. aureus* α-toxin targets ADAM10 to weaken epithelial junctions and promote bacterial spread through a mechanism involving E-cadherin shedding (Inoshima et al., 2011).

Existing evidence in the tetraspanin field indicates that different TspanC8/ADAM10 complexes can cut different cadherins. We and others have reported the effect of Tspan15 specifically on the promotion of N-cadherin shedding in epithelial cell lines. (Prox et al., 2012, Jouannet et al., 2016, Noy et al., 2016). Also, we have shown that Tspan5 and Tspan17 regulate VE-cadherin surface expression and promote T cell transmigration in an inflammatory model while Tspan15 has no effect (Reyat et al., 2017). This study suggested that Tspan5/ADAM10 and Tspan17/ADAM10 were the scissors for VE-cadherin, but only VE-cadherin expression was assessed, not its cleavage (Reyat et al., 2017). The role of TspanC8s in E-cadherin shedding has not been reported. The aim of this chapter was to determine whether Tspan15 is required for N-, E- and VE-cadherin cleavage and to investigate the potential effects of Tspan15 mAbs.

4.2 Results

4.2.1 Tspan15 is required for endogenous N- and E-cadherin shedding in A549 cells and VE-cadherin shedding in transfected HEK-293T cells

To determine the effect of Tspan15 on cadherin cleavage, a panel of CRISPR/Cas9 ADAM10 and Tspan15 KO cell lines were used, all previously generated in the Tomlinson lab. Both constitutive and NEM-stimulated cleavage was investigated for endogenous N- and E-cadherin in A549 cells, and transfected human VE-cadherin in HEK-293T cells, because the latter do not express VE-cadherin. The alkylating agent NEM was chosen to trigger the enzymatic activity of ADAM10, because it is a robust activator, although the mechanism of action is not clear (Gardiner, 2018). Cleavage of the cadherins was determined by western blotting of whole cell lysates with an antibody against the C-terminal tail of the cadherins, to allow detection of both the full length and the truncated transmembrane fragment.

NEM induced a striking increase in N-cadherin cleavage in WT A549 cells, but not in ADAM10- or Tspan15-knockout cells (Figure 4.1A-B). Basal cleavage in the absence of NEM was relatively weak but was also reduced in the absence of ADAM10 or Tspan15 (Figure 4.1A-B). E-cadherin cleavage was similarly dependent on ADAM10 and Tspan15 in A549 cells (Figure 4.1C-D). Furthermore, transfected VE-cadherin cleavage in HEK-293T cells also required ADAM10 and Tspan15 (Figure 4.1E-F). Importantly, Tspan15-knockout A549 and HEK-293T cells still expressed substantial, albeit reduced, levels of

surface ADAM10 (Figure 3.3A-B). Together these data suggest that Tspan15/ADAM10 is a major molecular scissor for cadherins.

A N-cadherin, A549 cells

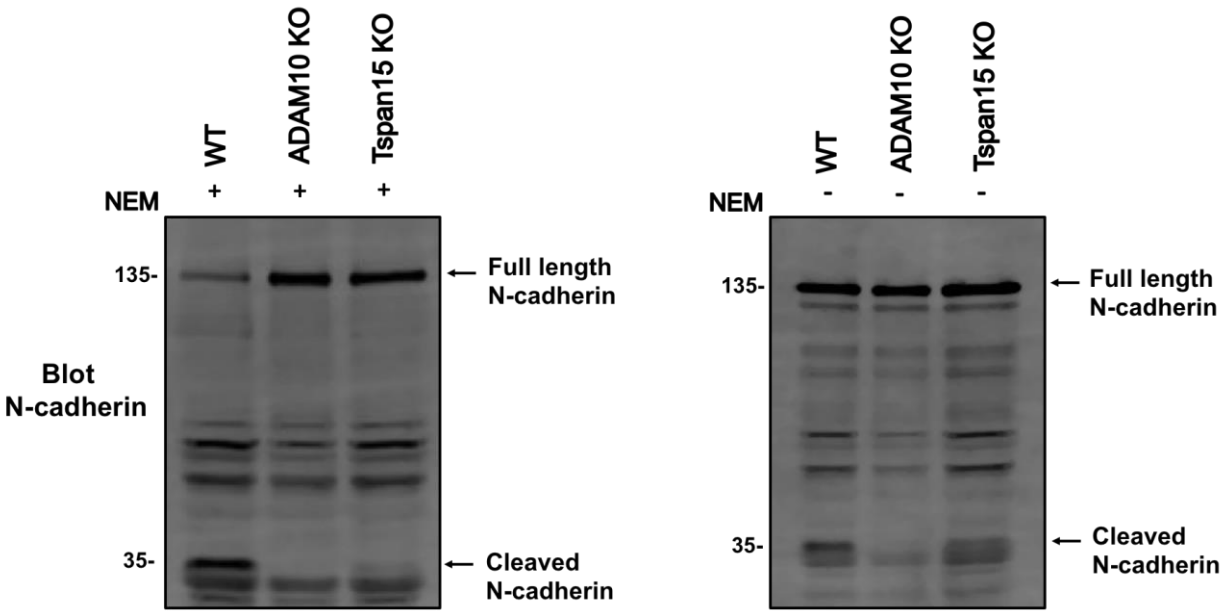

B

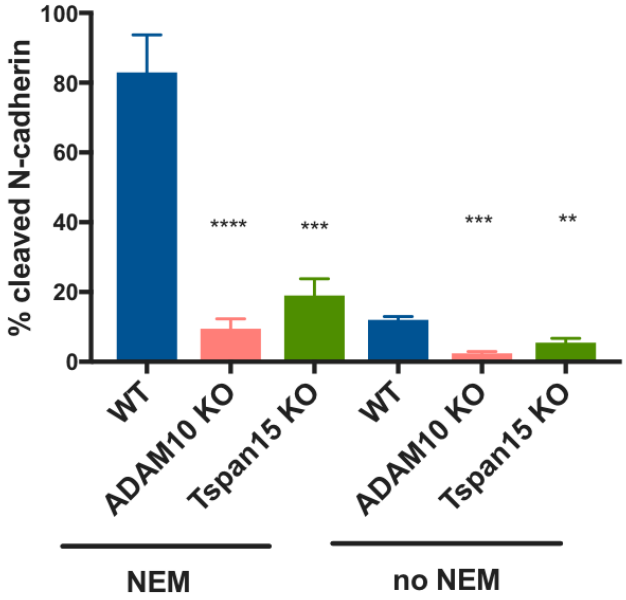

C E-cadherin, A549 cells

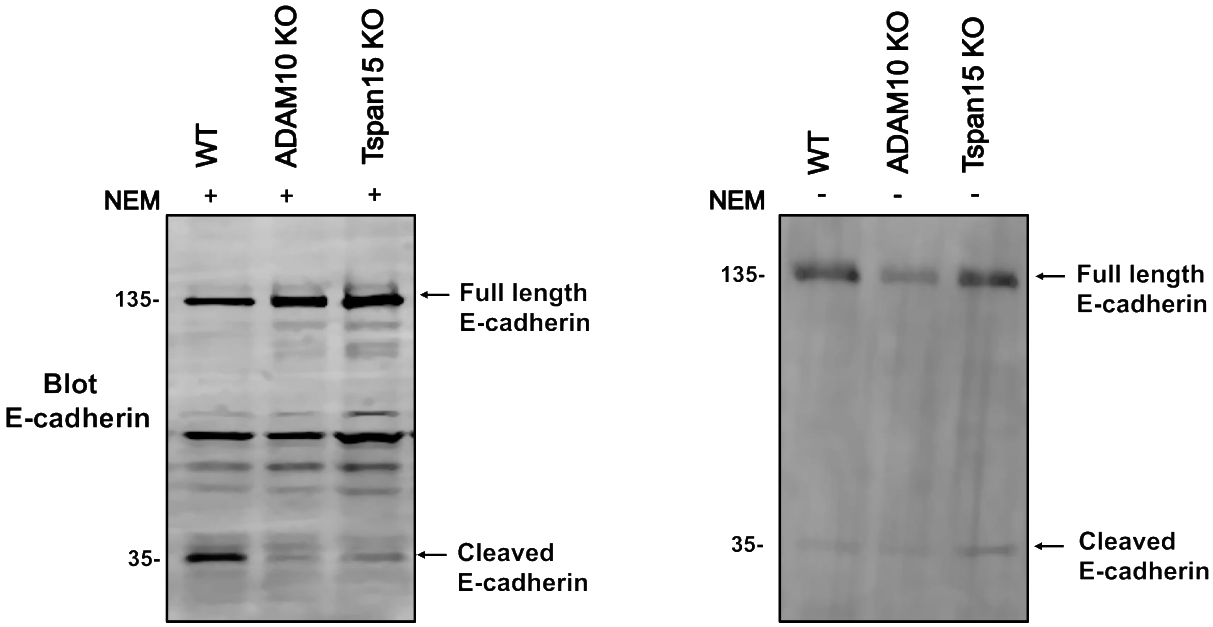

D

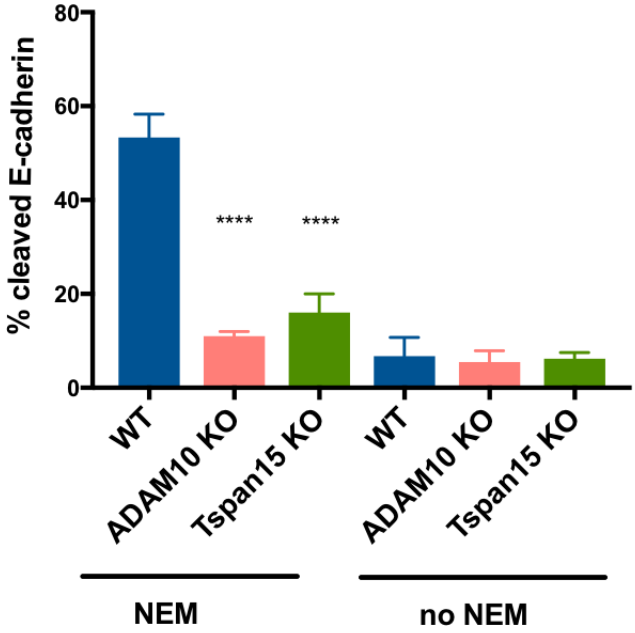

E VE-cadherin, HEK-293T cells

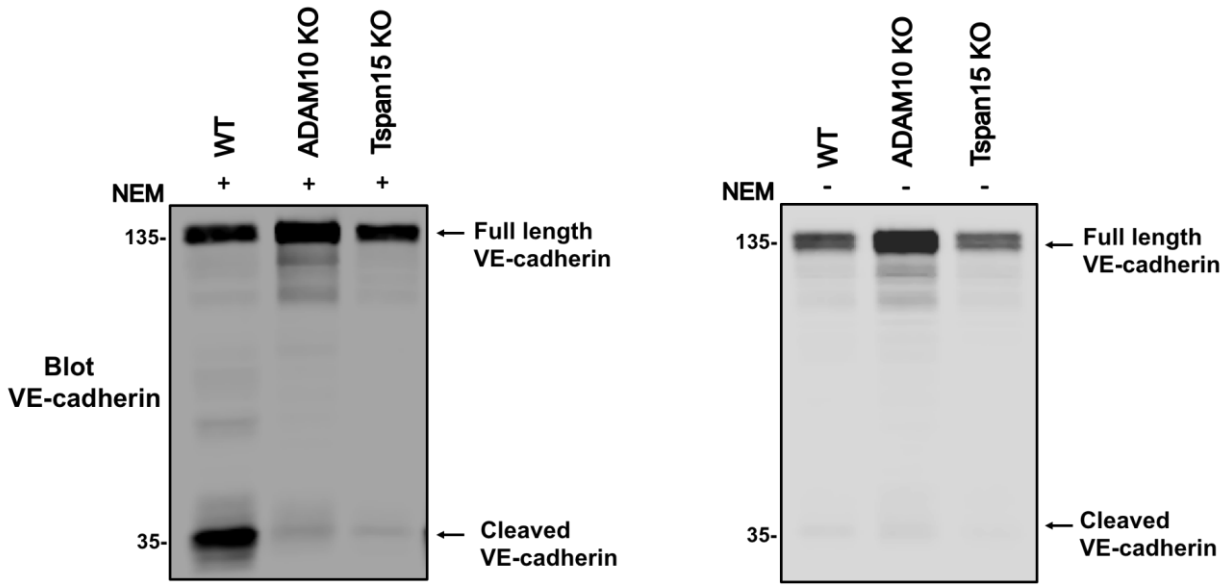

F

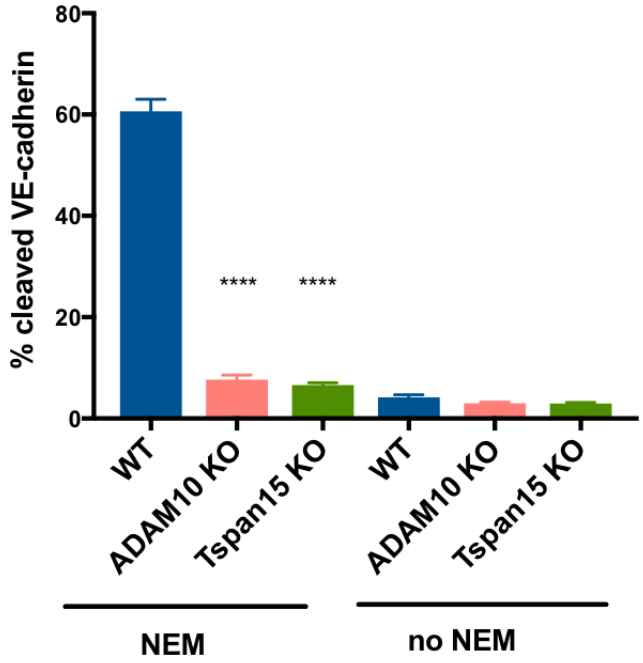

Figure 4.1 ADAM10 and Tspan15 are required for N- and E-cadherin shedding in A549 cells and VE-cadherin shedding in transfected HEK-293T cells. [A-B] N-cadherin and [C-D] E-cadherin shedding were measured in A549 cells, and [E] transfected VE-cadherin shedding was measured in HEK-293T cells. The cells were first treated with DAPT (10μM), to prevent post-ADAM10 proteolysis by γ-secretase, followed by NEM (2mM) to activate ADAM10. Cells were lysed in 1% Triton X-100 and lysates blotted with antibodies against the C-terminal fragments of the cadherins. Representative blots are shown in panels A, C and E, and quantitation of percentage cleavage in panels B, D and F. Error bars represent the standard error of the mean (SEM) of three independent experiments. Before statistical analysis, data were transformed by arcsine of the square root and statistically analysed by a one-way ANOVA followed by Dunnett's multiple comparison test, compared to WT (**$p<0.01$, ***$p<0.001$, ****$p<0.0001$). [E] The blot and quantitation of the E-cadherin shedding without NEM stimulation was done and kindly provided by MSc project student Delia Fernandez De La Fuente.

4.2.2 Tspan15 has a minor role in VE-cadherin shedding on HUVEC cells

We have previously reported that Tspan5 and Tspan17, but not other TspanC8s, affect VE-cadherin expression on HUVECs and might promote VE-cadherin cleavage, but the latter was not formally tested (Reyat et al., 2017). Since Tspan15/ADAM10 appears to be the scissor for transfected VE-cadherin in HEK-293T cells (Figure 4.1E-F), we speculated that Tspan15 might be required for VE-cadherin cleavage in HUVECs. To test this, western blotting of endogenous VE-cadherin was performed following siRNA knockdown of Tspan15 and ADAM10. As shown in Figure 4.2A-B, NEM treatment induced VE-cadherin cleavage in an ADAM10-dependent manner, but knockdown of Tspan15 had only a minor effect in reducing cleavage by approximately 30%. The slight reduction in the cleavage could result from the 30% decrease in ADAM10 surface expression after the Tspan15 knockdown, as shown in Figure 3.3. The efficiency of the knockdown was confirmed by flow cytometry and found to be at least 85% (Figure 4.3C-D).

These results suggest that Tspan15/ADAM10 is not the major scissor for VE-cadherin in HUVEC cells.

A VE-cadherin, HUVEC

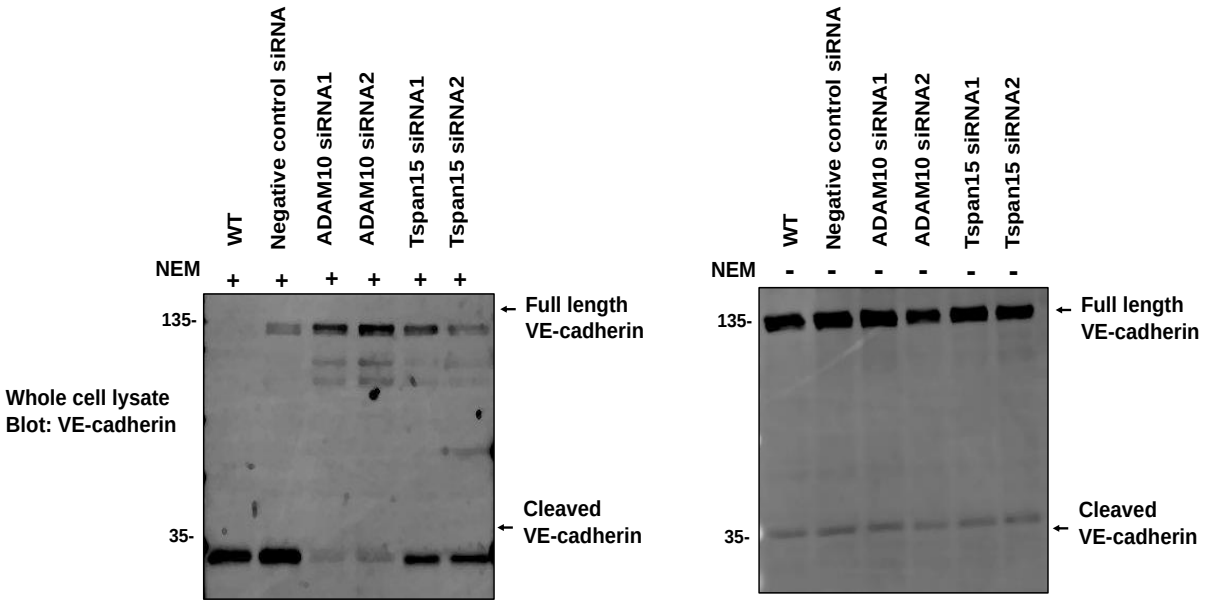

B

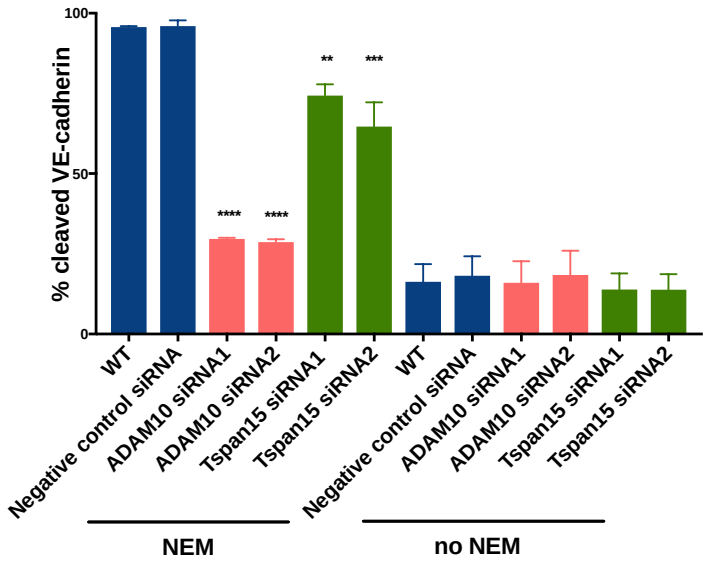

C

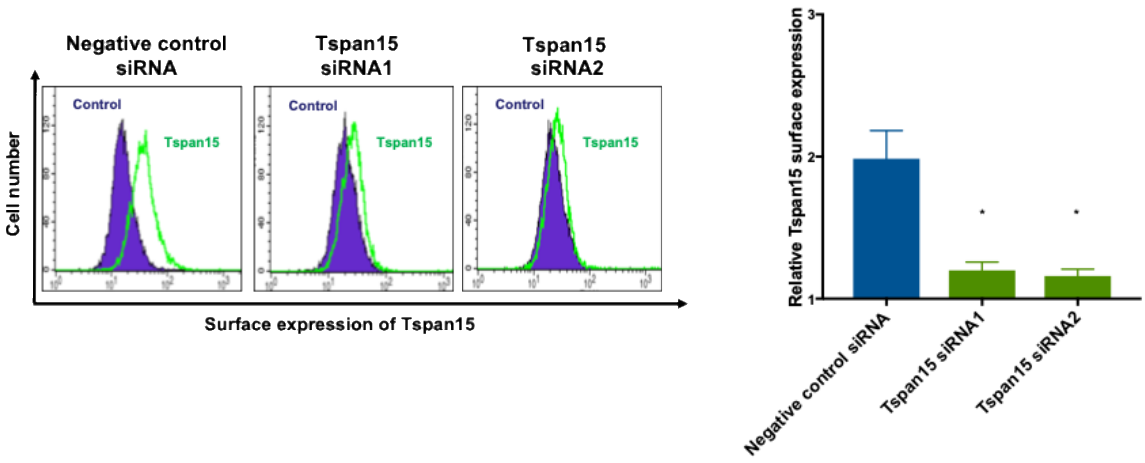

D

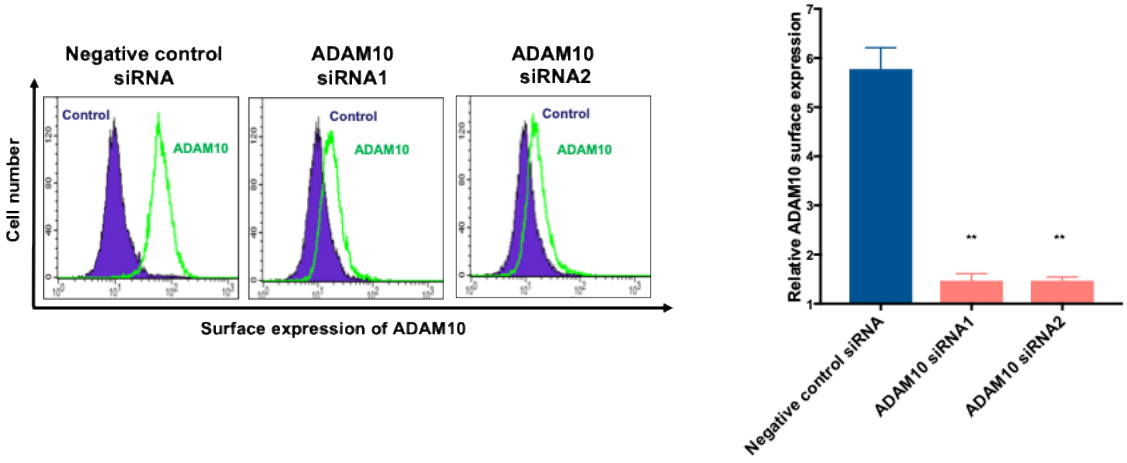

Figure 4.2 ADAM10 is required for VE-cadherin cleavage in HUVEC, but Tspan15 has a minor role. [A] HUVECs were transfected with Tspan15, ADAM10 and negative control siRNAs and cleavage assays were done by western blotting as described in Figure 4.1. [B]The percentage cleaved VE-cadherin was calculated based on the intensities of intact and cleaved fragments of the cadherin. [C-D] Efficiency of ADAM10 and Tspan15 knockdowns were measured by flow cytometry. The blue lines represent isotype control staining and the green lines represent ADAM10 or Tspan15 staining. Tspan15 mAb (clone 4A4) was used in a form of tissue culture supernatant. Error bars represent standard error of the mean for three to four independent experiments. Statistical significance of arcsine-transformed data was analysed by one-way ANOVA followed by Dunnett's multiple comparison test as compared with negative control siRNA (*p<0.05, **p<0.01, ***p<0.001, ****p<0.0001).

4.2.3 Tspan15 mAbs 4A4 and 1C12 inhibit cleavage of transfected VE-cadherin in HEK-293T

A mAb to Tspan5 was reported to inhibit Notch activation (Saint-Pol, 2017). To investigate whether the new Tspan15 mAbs, validated in the previous chapter, might also affect substrate cleavage, VE-cadherin-transfected HEK-293T cells were selected as a model because of the complete Tspan15 dependence in this system (Figure 4.1E-F).

As shown in Figure 4.3A-B, the cells pre-treated with Tspan15 mAb clone 4A4 or 1C12 had inhibited NEM-induced VE-cadherin cleavage as compared to the WT. The phenotype was the most pronounced at a concentration of 10 µg/ml of the mAbs used. Also, the antibody's titration revealed that the cleavage was concentration dependent, and gradually increased as the concentration of the antibodies decreased. In contrast, Tspan15 mAb clones 5F4 and 5D4 had no effect on the shedding (Figure 4.3C-D).

A Tspan15 mAb clone 4A4

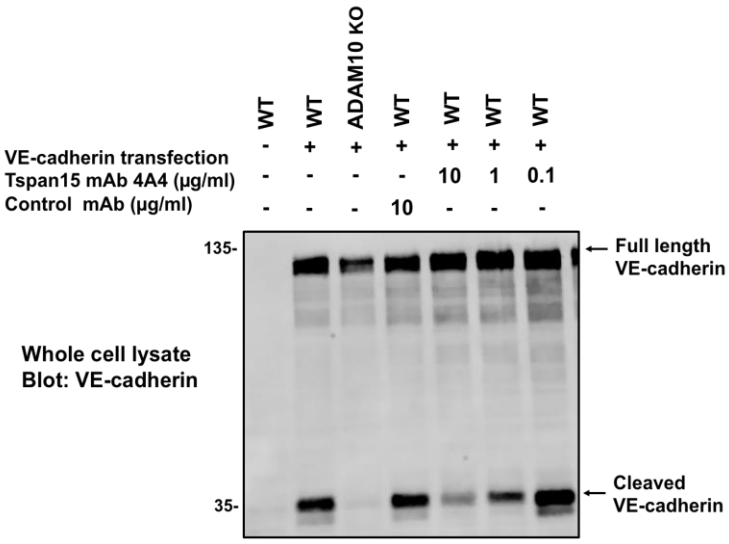

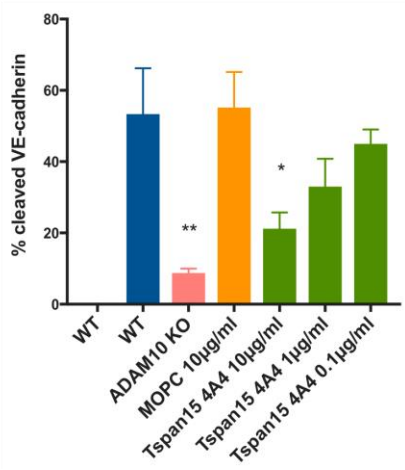

B Tspan15 mAb clone 1C12

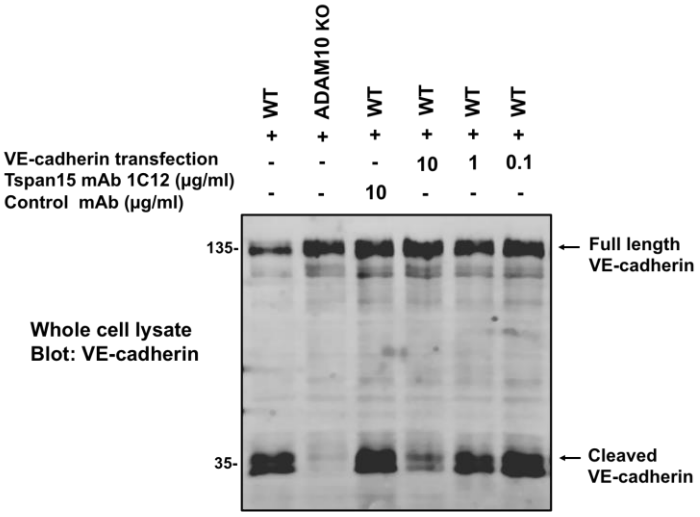

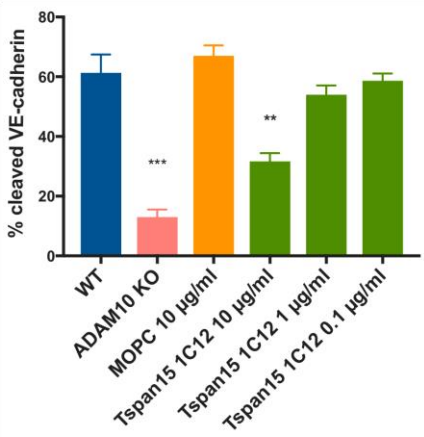

C Tspan15 mAb, clone 5F4

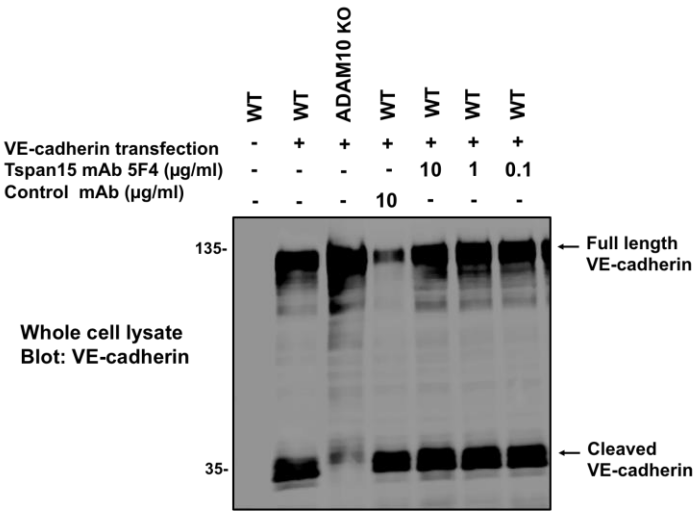

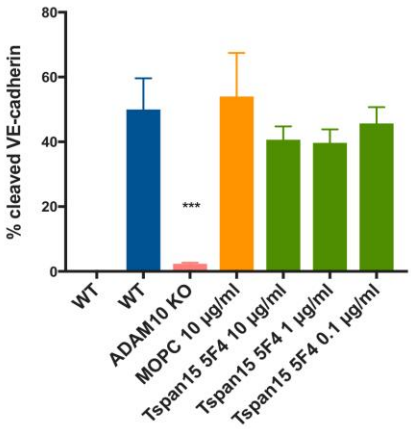

D Tspan15 mAb, clone 5D4

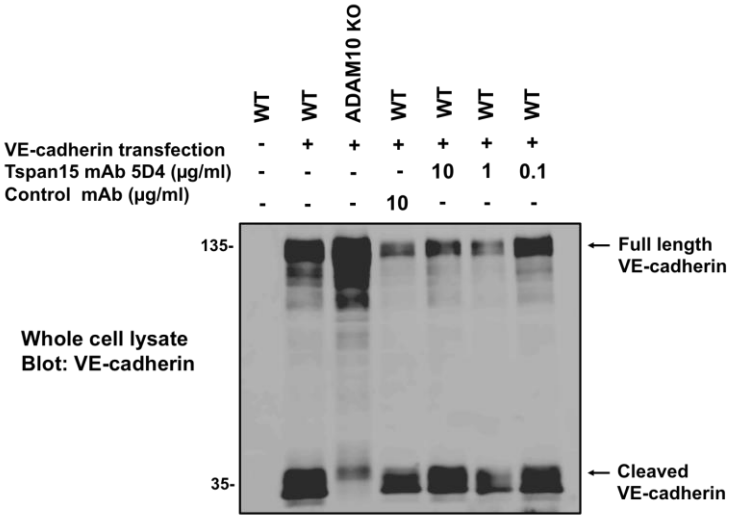

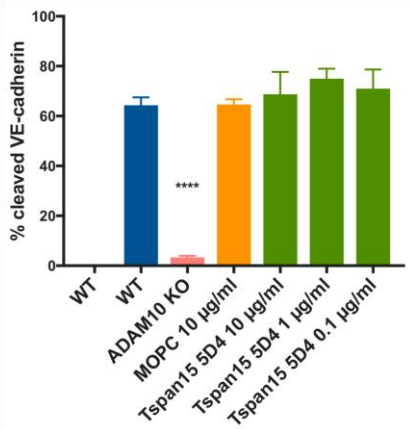

Figure 4.3. Tspan15 mAb clones 4A4 and 1C12 inhibit transfected VE-cadherin cleavage in HEK-293T cells, but clones 5F4 and 5D4 do not. VE-cadherin-transfected HEK-293T cells were treated with Tspan15 mAbs or MOPC control mAb for 30 minutes followed by NEM stimulation for an additional 30 minutes. The cleavage of VE-cadherin was detected by western blotting as described in Figure 4.1E. The data are presented in the form of a representative western blot and quantitation for [A] clone 4A4, [B] 1C12, [C] 5F4 and [D] 5D4. Tspan15 mAbs were used in a form of purified antibodies. Error bars represent SEM for three independent experiments. Statistical significance was measured on arcsine-transformed data using one-way ANOVA and a Dunnett's multiple comparison test as compared with WT control (*$p<0.05$, **$p<0.01$, ***$p<0.001$, ****$p<0.0001$).

4.2.4 Evidence that the four Tspan15 mAbs share a common epitope

Since two of the Tspan15 mAbs (4A4 and 1C12) appear to be inhibitory, but the other two (5F4 and 5D4) do not this could be due to the recognition of different epitopes. Epitope is likely to be within the main extracellular region of Tspan15 since this is the target for most other tetraspanin mAbs that have been epitope mapped. A previously reported method for tetraspanin mAb epitope mapping used chimeras of two different species of CD53, given that the mAbs recognised one species but not the other (Tomlinson et al., 1993, Tomlinson et al., 1995). The four mouse anti-Tspan15 mAbs western blot human but not mouse Tspan15 (Tomlinson lab, unpublished). Sequence analysis showed that human and mouse Tspan15 orthologues share 95% sequence homology (Figure 4.4A). The main difference falls within the main extracellular region and contains eight amino acids that vary between mouse and human which were divided into four regions for chimera generation (Figure 4.4B). Each of the four chimeras comprised human Tspan15 with the designated mouse sequences introduced (Figure 4.5A); these were generated as expression constructs by project student Mike Sykes with the help of Eleanor Cull and Neale Harrison.

To investigate the Tspan15 mAbs epitopes the four FLAG-tagged chimeras were transfected into Tspan15 KO HEK-293T cells alongside WT mouse and human Tspan15 controls. The cells were lysed using 1% Triton X-100 lysis buffer and lysates were western blotted under non-reducing condition (the non-reducing conditions preserves reactivity of mAbs, data not shown) for recognition and expression of the chimeras using four clones of

Tspan15 and FLAG mAbs respectively. Each mAb detected chimeras 1, 3 and 4, but not chimera 2, and as expected WT human but not mouse was detected (Figure 4.5B-C).

These results suggest the existence of a common epitope for the four Tspan15 mAbs, which is dependent on the FSV amino acid sequence in the main extracellular region.

A

```
hTspan15    MPRGDSEQVRYCARFSYLWLKFSLIIYSTVFWLIGALVLSVGIYAEVERQKYKTLESAFL
mTspan15    MPRGDSEQVRYCARFSYLWLKFSLIIYSTVFWLIGGLVLSVGIYAEAERQKYKTLESAFL
            ************************************.**********.**************

hTspan15    APAIILILLGVVMFMVSFIGVLASLRDNLYLLQAFMYILGICLIMELIGGVVALTFRNQT
mTspan15    APAIILILLGVVMFIVSFIGVLASLRDNLCLLQSFMYILGICLVMELIGGIVALIFRNQT
            **************:**************.***:*********:******:*** *****

hTspan15    IDFLNDNIRRGIENYYDDLDFKNIMDFVQKKFKCCGGEDYRDWSKNQYHDCSAPGPLACG
mTspan15    IDFLNDNIRRGIENYYDDLDFKNIMDFVQKKFKCCGGEDYRDWSKNQYHDCSAPGPLACG
            ************************************************************

hTspan15    VPYTCCIRNTTEVVNTMCGYKTIDKERFSVQDVIYVRGCTNAVIIWFMDNYTIMAGILLG
mTspan15    VPYTCCIRNTTDVVNTMCGYKTIDKERLNAQNIIHVRGCTNAVLIWFMDNYTIMAGLLLG
            ***********:***************:..*:::*:********:************:***

hTspan15    ILLPQFLGVLLTLLYITRVEDIIMEHSVTDGLLGPGAKPSVEAAGTGCCLCYPN
mTspan15    ILLPQFLGVLLTLLYITRVEDIILEHSVTDGLLGPGAKSRTDTAGTGCCLCYPD
            ************************:**************  .::***********:
```

B

```
hTspan15        TFRNQTIDFLNDNIRRGIENYYDDLDFKNIMDFVQKKFKCCGGEDYRDWSKNQYHDCSAP
mTspan15        TFRNQTIDFLNDNIRRGIENYYDDLDFKNIMDFVQKKFKCCGGEDYRDWSKNQYHDCSAP
                ************************************************************

hTspan15        GPLACGVPYTCCIRNTTEVVNTMCGYKTIDKERFSVQDVIYVRGCTNAVIIWFMDNYTIM
mTspan15        GPLACGVPYTCCIRNTTDVVNTMCGYKTIDKERLNAQNIIHVRGCTNAVLIWFMDNYTIM
                *****************:***************:..*:::*:********:**********
                                  1               222  33  3        4
```

Figure 4.4 Alignment of human (h) and mouse (m) Tspan15 sequences. The amino acid sequences comparison was performed using Clustal Omega. (A) The alignment of the full-length sequences. In light blue are highlighted the N-terminal tyrosine-based (YLWL) and C-terminal dileucine-based (LL) motifs, respectively. The putative N-glycosylation conserved residues are in pink. The four transmembrane regions are indicated in yellow. (B) The alignment of the large extracellular region only. The amino acids are grouped into four colour-coded regions to guide the generation of four chimeras.

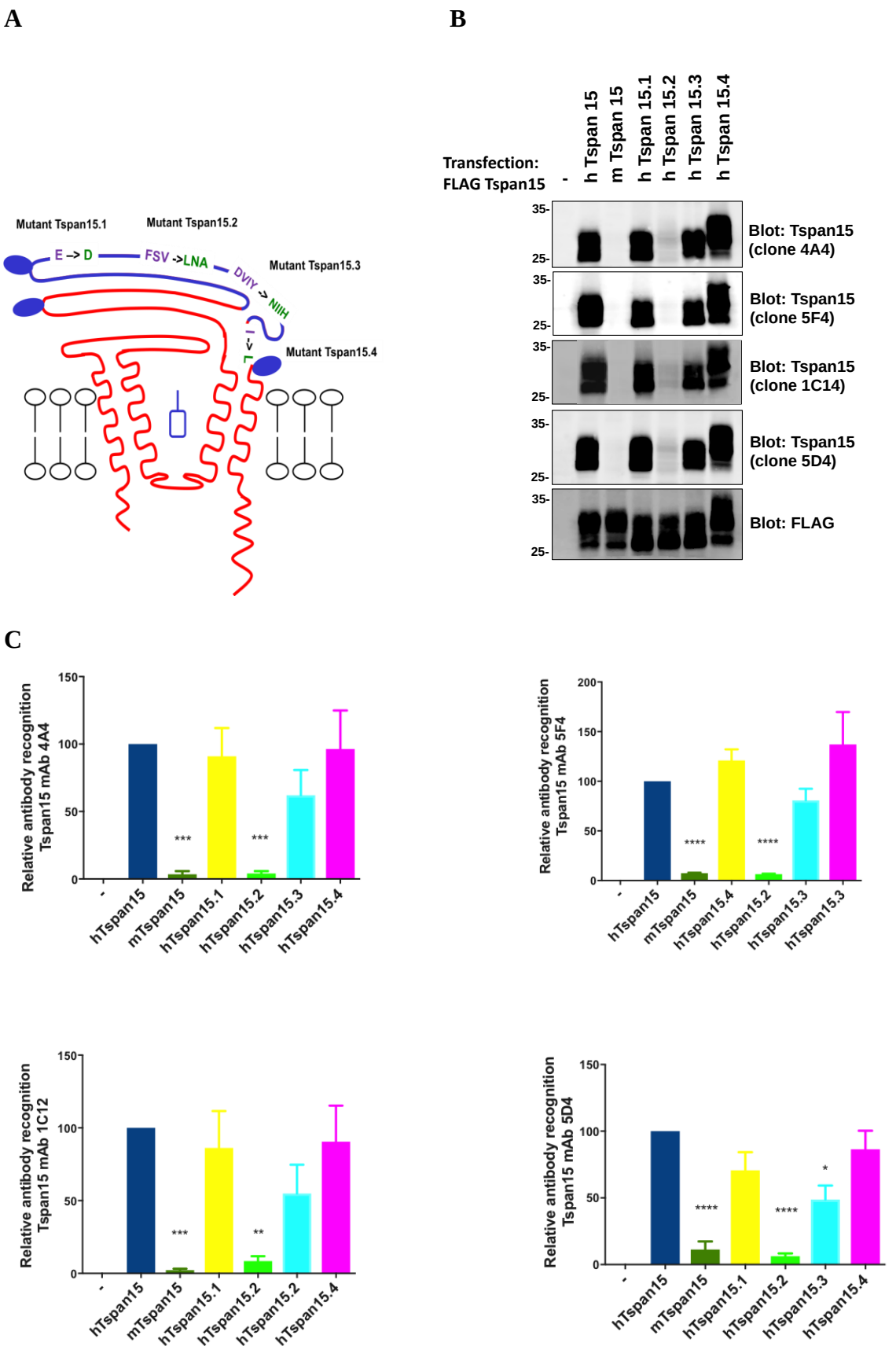
A
Mutant Tspan15.1
Mutant Tspan15.2
E -> D
FSV ->LNA
DVIY -> NIIH
Mutant Tspan15.3
L -> I
Mutant Tspan15.4
B
Transfection:
FLAG Tspan15
-
h Tspan 15
m Tspan 15
h Tspan 15.1
h Tspan 15.2
h Tspan 15.3
h Tspan 15.4
35-
25-
Blot: Tspan15 (clone 4A4)
Blot: Tspan15 (clone 5F4)
Blot: Tspan15 (clone 1C14)
Blot: Tspan15 (clone 5D4)
Blot: FLAG
C
Relative antibody recognition Tspan15 mAb 4A4
Relative antibody recognition Tspan15 mAb 5F4
Relative antibody recognition Tspan15 mAb 1C12
Relative antibody recognition Tspan15 mAb 5D4
hTspan15
mTspan15
hTspan15.1
hTspan15.2
hTspan15.3
hTspan15.4

Figure 4.5 Tspan15 epitope mapping suggests a common epitope for the four Tspan15 mAbs. [A] Schematic of human/mouse Tspan15 chimeras. The eight amino acid residues in the large extracellular region of human Tspan15 were divided into four regions (1-4) and substituted with the corresponding residues of mouse Tspan15. Chimeric constructs were generated by Neale Harrison, Michael Sykes and Eleanor Cull. [B] Tspan15 KO HEK-293T cells were transfected with FLAG-tagged WT human and mouse Tspan15 and human/mouse Tspan15 chimeras. The cells were lysed in 1% Triton X-100 lysis buffer and lysates western blotted under non-reducing conditions with each Tspan15 mAbs (used clones were in a form of purified antibodies) or FLAG mAb. [C] Tspan15 mAb data from panel B were quantified relative to FLAG blotting and relative to the WT human Tspan15 which was set to 100. Data were arcsine transformed and statistically analysed using a one-way ANOVA with Dunnett's multiple comparison test compared to WT human Tspan15 (*$p<0.05$, **$p<0.01$, ***$p<0.001$, ****$p<0.0001$). Error bars represent standard error of the mean for three independent experiments.

To investigate whether the human FSV sequence was sufficient for recognition by any of the Tspan15 mAbs, a chimera was generated in which FSV was introduced into mouse Tspan15 (Figure 4.6A). Western blotting was performed as described in the previous figure, but no detection of the chimera was observed for any of the mAbs, despite clear detection by FLAG blotting (Figure 4.6B-C). This indicates, that in the context of mouse Tspan15, the human FSV region is not sufficient to restore the binding and recognition by the Tspan15 antibodies. Therefore, while individual mAbs differed in their functional effects on VE-cadherin shedding, this did not correlate with distinct epitopes.

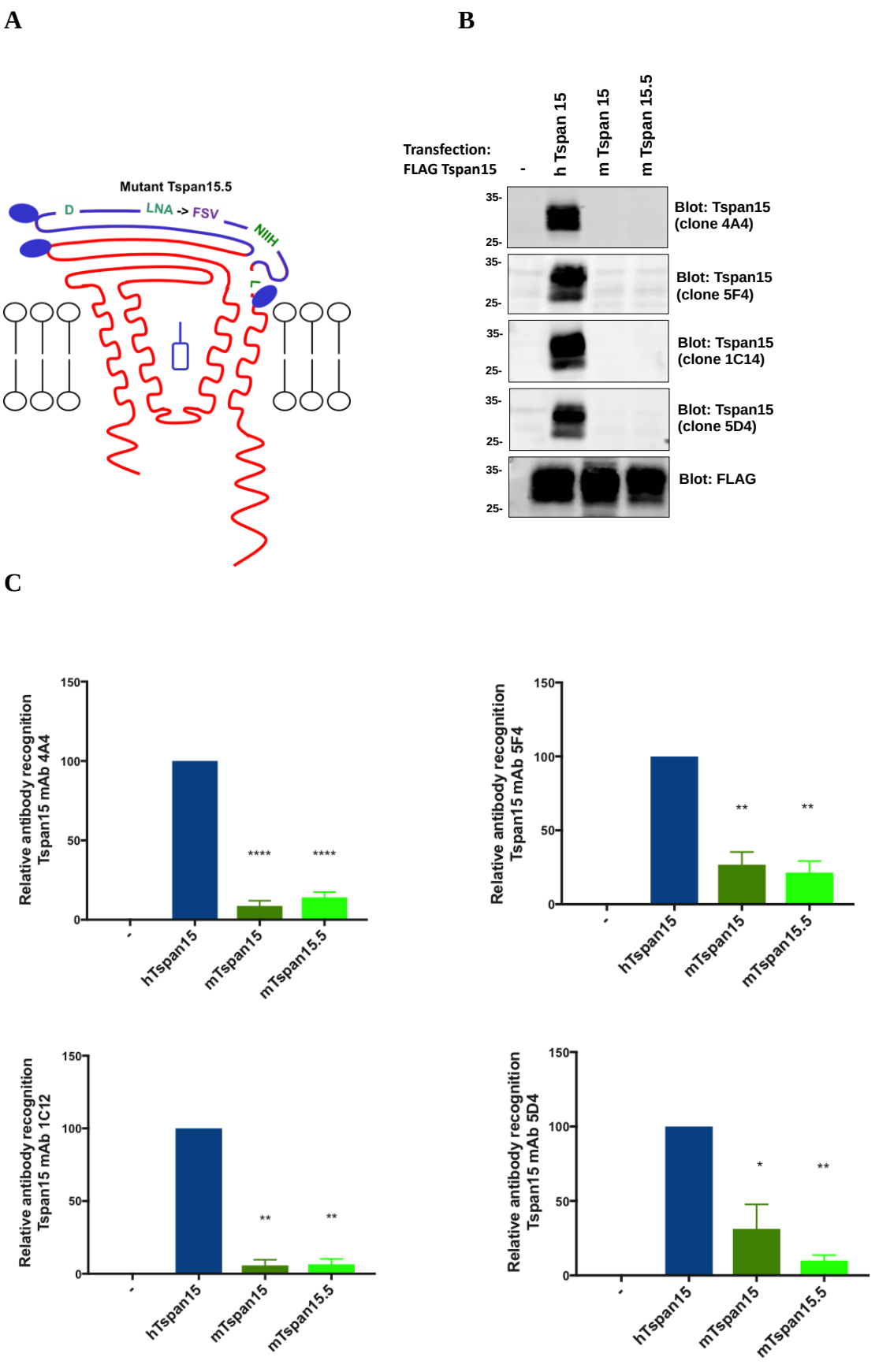
A
Mutant Tspan15.5
D
LNA -> FSV
NIIH
B
Transfection:
FLAG Tspan15
-
h Tspan 15
m Tspan 15
m Tspan 15.5
35-
25-
Blot: Tspan15 (clone 4A4)
Blot: Tspan15 (clone 5F4)
Blot: Tspan15 (clone 1C14)
Blot: Tspan15 (clone 5D4)
Blot: FLAG
C
Relative antibody recognition Tspan15 mAb 4A4
Relative antibody recognition Tspan15 mAb 5F4
Relative antibody recognition Tspan15 mAb 1C12
Relative antibody recognition Tspan15 mAb 5D4
150
100
50
0
-
hTspan15
mTspan15
mTspan15.5
****
**
*

Figure 4.6 The human FSV sequence not sufficient to restore binding of Tspan15 mAbs to mouse Tpan15. [A] Schematic of the mouse Tspan15 chimera. The three amino acid residues in the large extracellular region of the mouse Tspan15 were substituted with the corresponding residues of human Tspan15, and the FLAG-tagged chimeric construct was generated by Neale Harrison. The substitutions were as follow mouse leucine, asparagine and alanine to human phenylalanine, serine and valine. [B-C] Western blotting was performed as described in Figure 4.5. Data were arcsine transformed and statistically analysed using a one-way ANOVA with Dunnett's multiple comparison test compare to WT human Tspan15 (*p<0.05, **p<0.01, ***p<0.001, ****p<0.0001). Error bars represent standard error of the mean for three independent experiments.

4.2.5 Tspan15 mAbs induce similar level of Tspan15 internalisation

It is well established that mAbs to cell surface proteins commonly induce their internalisation (Latysheva et al., 2006, Xu et al., 2009, de Goeij et al., 2016, Li et al., 2015). To evaluate whether Tspan15 mAbs might differentially induce internalization, and thus potentially explain their different inhibitory effects, the four Tspan15 mAbs were used in conjunction with flow cytometry to measure a potential antibody internalisation effect. The Tspan15 mAbs were added directly to the HEK-293T cells at 4^0C for 30 min to allow mAb recognition. Next, the unbound mAbs were washed away. Internalization of Tspan15 and mAbs was enabled by incubating the cells at 37 ^{0}C for an additional 30 min. Following potential internalization, the remaining surface-bound mAbs were detected using anti-mouse-FITC and analysed by flow cytometry. As shown in Figure 4.7 A-B, the mAbs induced partial internalisation of Tspan15. However, the expression levels, post-internalisation, did not differ between the clones studied. Therefore, differential internalisation cannot explain the different functional effects of the mAbs.

A

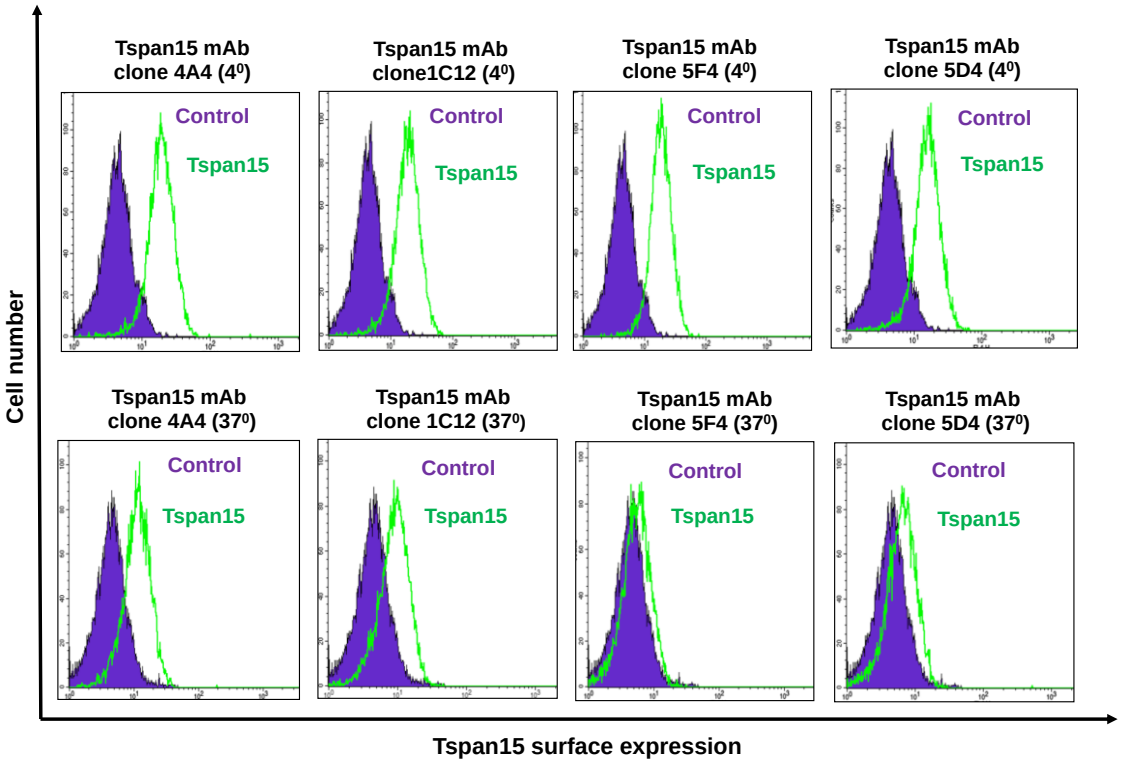
Tspan15 mAb clone 4A4 (4⁰)
Tspan15 mAb clone1C12 (4⁰)
Tspan15 mAb clone 5F4 (4⁰)
Tspan15 mAb clone 5D4 (4⁰)
Tspan15 mAb clone 4A4 (37⁰)
Tspan15 mAb clone 1C12 (37⁰)
Tspan15 mAb clone 5F4 (37⁰)
Tspan15 mAb clone 5D4 (37⁰)
Control
Tspan15
Cell number
Tspan15 surface expression

B

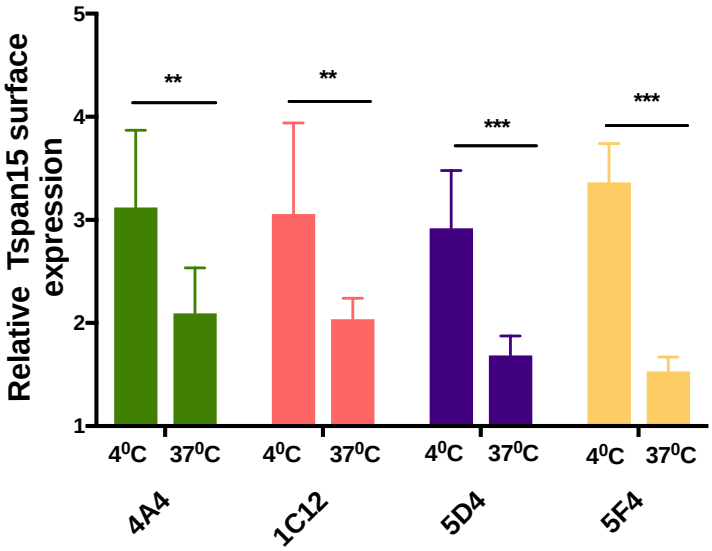
Relative Tspan15 surface expression
5
4
3
2
1
**
**
***
***
4⁰C
37⁰C
4A4
1C12
5D4
5F4

Figure 4.7 Tspan15 mAbs each cause a partial reduction in Tspan15 surface expression. [A] HEK-293T cells were treated with Tspan15 mAbs for 30 min (Tspan15 mAbs four clones were used in a form of purified antibodies). Tspan15 surface expression was measured by flow cytometry before (at 4^0C) and after (at 37^0C) the internalisation. Representative histograms of Tspan15 fluorescence intensities are plotted. The blue line represents isotype control staining while the green line represents Tspan15 staining (the cells were stained with four clones of Tspan15 mAbs in a form of tissue culture supernatants). [B] The average geometric mean of Tspan15 fluorescence intensities was quantified relative to the negative control and presented as a relative Tspan15 surface expression for each condition tested, such that a value of 1 represents no specific staining. The data were arcsine transformed before being statistically analysed using a two-way ANOVA with Sidak's multiple comparisons test (*p<0.05, **p<0.01, ***p<0.001, ****p<0.0001). Error bars represent standard error of the mean for four independent experiments.

The effect of Tspan15 mAbs on ADAM10 surface expression was also investigated since this could potentially explain the differential inhibitory effects on VE-cadherin cleavage. However, as shown in Figure 4.8, incubation with the Tspan15 mAbs did not alter the surface level of ADAM10.

Taken together, the inhibitory effects of Tspan15 mAbs 4A4 and 1C12, versus the non-inhibitory effects of 5F4 and 5D4, cannot be explained by different mAb epitopes, differential internalisation of Tspan15 or differential effects on ADAM10 surface expression.

A

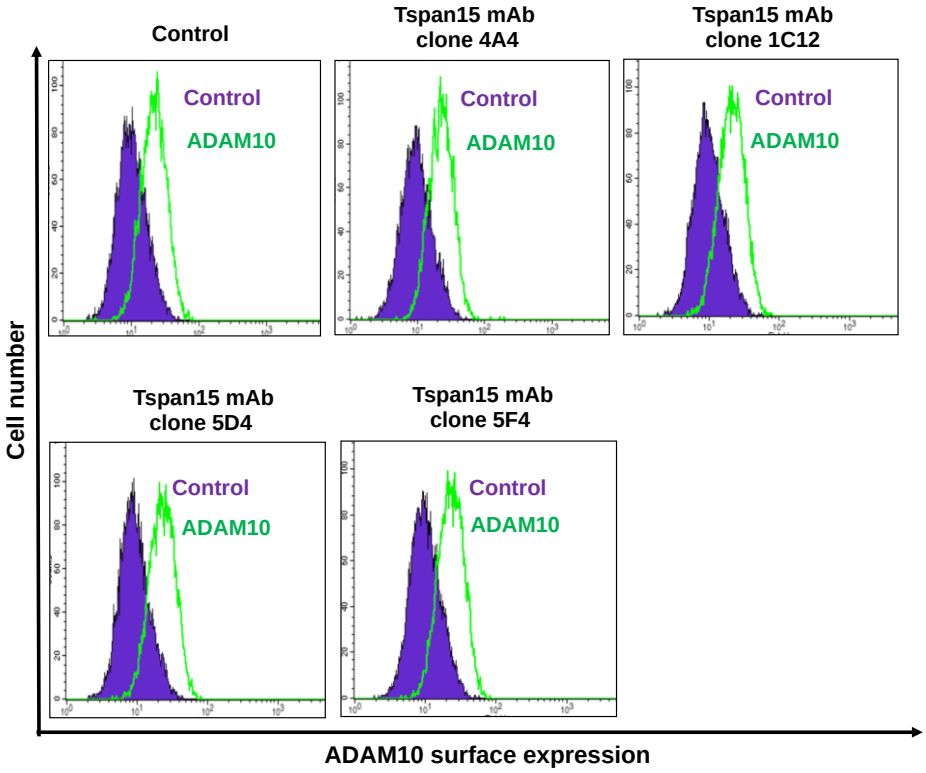
Control
Tspan15 mAb clone 4A4
Tspan15 mAb clone 1C12
Tspan15 mAb clone 5D4
Tspan15 mAb clone 5F4
Control
ADAM10
Cell number
ADAM10 surface expression

B

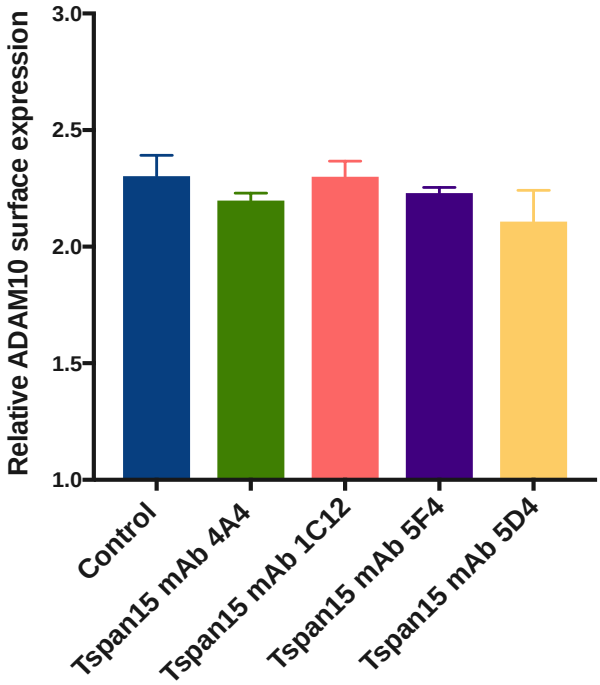
Relative ADAM10 surface expression
3.0
2.5
2.0
1.5
1.0
Control
Tspan15 mAb 4A4
Tspan15 mAb 1C12
Tspan15 mAb 5F4
Tspan15 mAb 5D4

Figure 4.8 ADAM10 surface expression is not affected by Tspan15 mAbs. [A] HEK-293T were incubated with Tspan15 mAbs at 37^0C for 30 min and analysed by flow cytometry for ADAM10 surface expression using ADAM10-conjugated mAbs. The blue lines represent isotype control staining, and green lines represent ADAM10 staining. [B] The average geometric mean fluorescence intensities of the samples were measured, and data were presented as a relative ADAM10 surface expression, as described for Figure 4.7. Data was arcsine transformed and statistically analysed using one-way ANOVA with Dunnett's multiple comparison test as compared with the control; no significant difference was detected. Error bars represent standard error of the mean for three independent experiments.

4.3 Discussion

The data in this chapter confirmed published reports suggesting that Tspan15/ADAM10 is the specific scissor for N-cadherin (Jouannet 2016; Noy 2016; Prox 2012), and extended these to show that Tspan15 was also required for E- and VE-cadherin cleavage. The latter was cell type dependent, because Tspan15 was required for cleavage in VE-cadherin-transfected HEK-293T cells, but not for the endogenous protein in HUVECs. Two of the Tspan15 mAbs, 1C12 and 4A4, impaired VE-cadherin cleavage in transfected HEK-293T cells by 50%, but 5D4 and 5F4 had not effect. No evidence was obtained to suggest that these differences are due to different mAb epitopes, because epitope mapping indicated epitopes dependent on the same three-amino acid sequence for all mAbs. The differences could also not be explained by differential internalisation of Tspan15, which was similar for all mAbs, or by loss of surface ADAM10, which was not induced by any of the mAbs.

In the absence of Tspan15 in A549 cells, the cleavage of endogenous N- and E-cadherin, respectively, was almost completely abolished, similar to ADAM10-KO cells. The cleavage of VE-cadherin in transfected HEK-293T cells was similarly abolished in the absence of Tspan15. Cleavage was induced in these experiments by the alkylating agent NEM, a powerful activator of ADAM10 (Loechel et al., 1999, Gardiner, 2018). These findings are consistent with a previous study from the Tomlinson lab, which showed that Tspan15 was unique amongst TspanC8s in being able to promote N-cadherin cleavage when over-expressed in HEK-293T cells (Noy et al., 2016). Two other groups have made observations consistent with this in different epithelial cell lines, using over-expression and siRNA knockdown of Tspan15 (Jouannet et al., 2016, Prox et al., 2012). More recently, the Saftig group reported the phenotype of Tspan15-KO mice, which were viable and healthy,

but the main phenotype reported was a 75-85% reduction in cleaved N-cadherin in the brain, despite only a 25-50% reduction in mature ADAM10; the variation was due to increases in effect size with age of the mice (Seipold et al., 2018). Taken together, this evidence implies that the cleavage of cadherins on epithelial cells is likely to rely on the regulation of ADAM10 by Tspan15. It remains to be determined how exactly the cleavage is affected by the complex. Whether it is an explicit structural conformation that ADAM10 adopts in association with Tspan15, or cellular localisation of the complex in close proximity with the cadherins, or capacity for Tspan15 to interact with cadherins, remains to be determined. In the absence of a consensus sequence for proteolytic cleavage by ADAM10, the specific cleavage of the cadherins could be caused by a distinct conformation change of ADAM10 in complex with Tspan15, which is supported by the Tomlinson lab's previous report that the 26 amino acid membrane-proximal stalk region of ADAM10 is sufficient for co-immunoprecipitation with Tspan15, but not other TspanC8s (Noy et al., 2016). Accordingly, the position of Tspan15 could be sufficient to 'lock' ADAM10 in the conformation that allows cleavage of the cadherins but not many other surface proteins such as Notch proteins which are preferentially cleaved and activated by Tspan5 and Tspan14 (Dornier et al., 2012, Jouannet et al., 2016, Saint-Pol et al., 2017). The role of Tspan15 in the cleavage of the cadherins could be further explained by Tspan15's preferential localization to the plasma membrane, where the cadherins are also predominantly localised. The relatively strong Tspan15 plasma membrane localisation, versus other TspanC8s, was apparent in transfected HeLa cells (Dornier et al., 2012) and HEK-293T cells (Matthews and Tomlinson, unpublished).

In contrast, to the observations in A549 and HEK-293T cells, Tspan15 knockdown in HUVECs had only a minor effect on endogenous VE-cadherin cleavage in response to NEM, as opposed to that seen in the ADAM10 knockdown cells where cleavage was reduced more profoundly. Indeed, the 30% reduction in cleavage following Tspan15 knockdown correlated with a 30% reduction in surface ADAM10 expression, suggesting that Tspan15/ADAM10 is not a specific scissor for VE-cadherin in primary endothelial cells. Previously, Haining *et al.* showed that knockdown of Tspan14, the major TspanC8 present in HUVECs, also caused a partial reduction (30%) in basal VE-cadherin cleavage, accompanied by an incomplete reduction (50%) in ADAM10 expression, which argues that Tspan14/ADAM10 is also not a specific scissor for VE-cadherin. More likely candidates are Tspan5 and Tspan17, which are the two most highly related TspanC8s, with 72% amino acid identity. As shown by a combination knockdown approach, the presence of either Tspan5 or Tspan17, with the other five TspanC8s knocked down, was sufficient to reduce basal surface levels of VE-cadherin by 30-40%, without affecting surface ADAM10 expression (Reyat et al., 2017). However, the mechanism by which Tspan5 and Tspan17 affect VE-cadherin expression remains unclear because no cleavage data was presented (Reyat et al., 2017). Indeed, experiments conducted during this thesis found that knockdown of Tspan5 and Tspan17 in HUVECs, either singly or in combination, had no effect on NEM-induced VE-cadherin cleavage (data not shown). Finally, it remains unclear why Tspan15/ADAM10 is the scissor for transfected VE-cadherin in HEK-293T cells, but not for endogenous VE-cadherin in HUVECs. A possible explanation is that HUVECs lack certain accessory proteins that are required for Tspan15/ADAM10 to cleave VE-cadherin.

Tetraspanin mAbs have a history of being used to gain functional insights and have often initiated a programme of work on particular tetraspanins. For example, CD81 was originally identified as the target of an anti-proliferative antibody (TAPA-1) in one of the earliest tetraspanin publications (Oren et al., 1990). More recently, a CD151 mAb was reported which disrupted the interaction of CD151 with integrin α3β1, to render CD151-free integrin less able to bind laminin (Nishiuchi et al., 2005). Of additional therapeutic interest is a mAb to Tspan12, which suppresses signalling through its Frizzled-4 partner and has therapeutic benefit in a mouse model of vasoproliferative retinopathy (Bucher et al., 2017). Of direct relevance to TspanC8s, a Tspan5 mAb inhibits Notch signalling in a cell line model (Saint-Pol et al., 2017a). In this chapter, two of the Tspan15 mAbs, clones 4A4 and 1C12, inhibited NEM-induced VE-cadherin cleavage in transfected HEK-293T cells by approximately 50%. In contrast, 5D4 and 5F4 mAbs had no such effect. The inhibitory effect was not due to any obvious difference in epitopes for these mAbs, which could enable ADAM10 inhibition by disruption of the Tspan15/ADAM10 complex or by steric hindrance of the ADAM10 active site. Indeed, the use of human/mouse chimeric Tspan15 constructs showed that all four mAbs require the FSV amino acid triplet, which is likely to be positioned near the top of the main extracellular region since its mutation to the LNA sequence of mouse Tspan15 prevented mAb recognition by western blotting. In more recent work by the Tomlinson group, this data was strengthened by a mAb competition experiment, in which all four mAbs competed with each other for Tspan15 binding by flow cytometry (Koo, unpublished). Furthermore, it does not appear likely that the mAbs can disrupt the Tspan15/ADAM10 interaction, because each co-immunoprecipitate ADAM10 effectively (Koo, unpublished). Also, the mAb differences are unlikely be to be due to changes in Tspan15 and ADAM10 surface expression, since the four Tspan15 mAbs

caused Tspan15 to be only partially internalised, and to a similar extent, while ADAM10 levels remained unchanged. It is possible that different affinities might explain the different functional effects of the mAbs, which has been established for other mAbs (Mortensen et al., 2012, Zhou et al., 2012). Alternatively, they might have epitopes that are overlapping, but distinct in terms of the way in which the bound mAb is orientated relative to ADAM10, thus allowing two to inhibit ADAM10 activity and two to have no effect. Further biochemical and structural experiments are required to investigate these possibilities.

CHAPTER 5
STRUCTURE-FUNCTION ANALYSIS OF TSPAN15

5.1 Introduction

In the previous chapter it was shown that ADAM10 activity towards cadherins on HEK-293T and A549 cells was specifically promoted by Tspan15. The underlying molecular mechanism by which Tspan15 promotes cadherin cleavage is not known. Indeed, the mechanism by which any TspanC8 promotes specificity in ADAM10 substrate recognition is unknown. This chapter starts with the hypothesis that Tspan15 promotes cadherin shedding by affecting ADAM10 conformation and/or cellular localisation. TspanC8s have been previously shown to have distinct localisations (Dornier et al., 2012) and to interact with ADAM10 through different mechanisms that could regulate the structural conformation of ADAM10 (Noy et al., 2016). Therefore, the chapter aims to extend these findings, using Tspan15-knockout cells stably reconstituted with various mutant forms of Tspan15 and the Tspan15/14 chimeric constructs (Figure 5.1). The information gathered in this chapter will increase our mechanistic understanding of the regulation of ADAM10 by Tspan15.

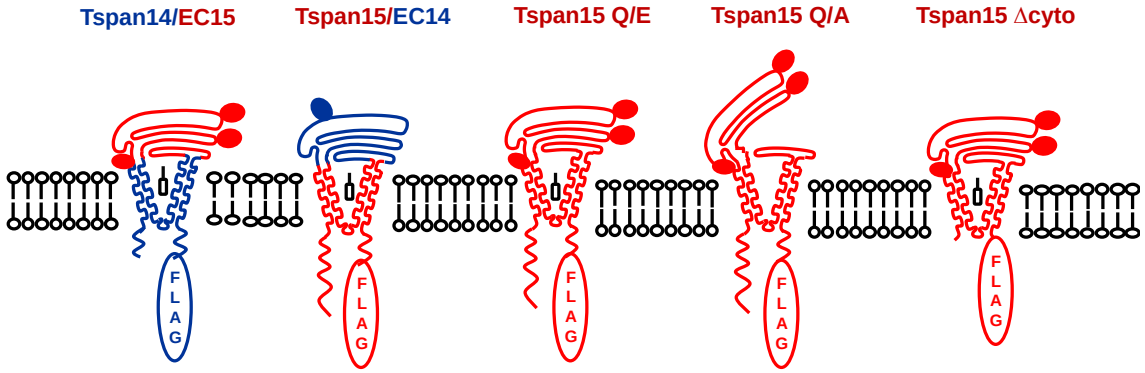

Figure 5.1 Schematic of Tspan15 chimeric and mutant constructs. From the left: human Tspan14 chimera with the extracellular region (EC) of human Tspan15 (Tspan14/EC15); Tspan15 chimera with EC of Tspan14 (Tspan15/EC14); Tspan15 with a glutamine (Q) to glutamic acid (E) point mutation at the predicted cholesterol-binding site at amino acid position 245 in the transmembrane region (Tspan15 Q/E); Tspan15 with a glutamine (Q) to alanine (A) point mutation at amino acid position 245 (Tspan15 Q/A); Tspan15 mutant with truncations in both N- and C- cytoplasmic tails (Tspan15 Δcyto). TspanC8 N-glycosylations are indicated by filled ovals**.** The putative 'open' conformation is shown for the Q/A mutant, based on structural analysis of CD81; the Q/E mutation may favour a 'closed' conformation (Zimmerman et al., 2016)

5.2 Results

5.2.1 The Tspan15 transmembrane and cytoplasmic regions are sufficient for promoting ADAM10 surface localisation, but the extracellular region is required for N-cadherin shedding

Noy *et al* have previously shown that different TspanC8s have distinct binding requirements for ADAM10; albeit, the requirements involve the extracellular region of TspanC8s and specific extracellular domains of ADAM10. Tspan15 is distinctive among TspanC8s in requiring only the 26 amino acid membrane-proximal "stalk" of ADAM10 for its interactions (Noy et al., 2016). To determine whether the extracellular region of Tspan15 confers its capacity to promote ADAM10-mediated shedding of N-cadherin, two Tspan15/14 chimeric constructs (Figure 5.1) were generated; Tspan14 was arbitrarily chosen as a representative TspanC8 that does not promote N-cadherin cleavage.

To confirm that the Tspan15/14 chimeras were functional in terms of interaction with ADAM10, HEK-293T cells were co-transfected with the FLAG-tagged chimeras and HA-tagged ADAM10. The cells were lysed in 1% digitonin lysis buffer, which has previously been used to demonstrate TspanC8 interactions with ADAM10 (Haining et al., 2012, Noy et al., 2016), and the tetraspanins were immunoprecipitated with an anti-FLAG antibody, separated by SDS-PAGE and probed with anti-HA and anti-FLAG for ADAM10 and tetraspanins respectively. As shown in Figure 5.2A Tspan14, 15 and chimeras co-immunoprecipitated ADAM10. Each of the tetraspanins interacted preferentially with a

lower molecular weight of ADAM10, which corresponds to the mature form of the protease, and their expression promoted ADAM10 maturation as reported previously (Haining et al., 2012). The cells co-transfected with the Tspan14/15 chimeras appeared to express less ADAM10, as detected by anti-HA blotting of the whole cell lysate. A possible explanation is that the chimeras are unstable, and thus the chimera-ADAM10 complex is unstable. The data presented suggest that the chimeric constructs act like WT TspanC8s in binding to ADAM10.

Since the overexpression of the chimeras promoted ADAM10 maturation, the process that precedes ADAM10 trafficking to the cell surface, the effect of the chimeras on ADAM10 surface expression was investigated by flow cytometry. Previous studies from the Tomlinson lab showed that over-expression of Tspan15, but not Tspan14, promotes localisation of ADAM10 to the cell surface in HEK-293T cells (unpublished). Because mAbs were not available for both of the TspanC8s tested, they were co-expressed with GFP, to label transfected cells. As shown in Figure 5.2B, only Tspan15 and the Tspan15/EC14 chimera significantly increased ADAM10 surface expression. This data suggested that the transmembrane and/or cytoplasmic regions of Tspan15 are important in promoting ADAM10 surface expression.

The functional role of the chimeras in promoting N-cadherin cleavage was next investigated using a well-established cleavage assay (Noy et al., 2016). HEK293T cells were transfected with the chimeric constructs, and the WT tetraspanins and western blotted with an antibody to the cytoplasmic tail of N-cadherin to measure the cleavage (as described in 2.4.1). As shown in Figure 5.2C, the chimeras failed to promote N-cadherin

cleavage; only Tspan15 promoted cleavage. This data suggests that the extracellular region of Tspan15 is required but not sufficient to promote ADAM10 cleavage of N-cadherin, in the context of the chimera with Tspan14. When considered alongside the localisation data, it can be concluded that the capacity of Tspan15 to promote ADAM10 cleavage of N-cadherin cannot be explained simply by its capacity to promote ADAM10 surface localisation. It is possible that the extracellular region of Tspan15 is important for inducing an ADAM10 conformation that is conducive to N-cadherin cleavage.

A

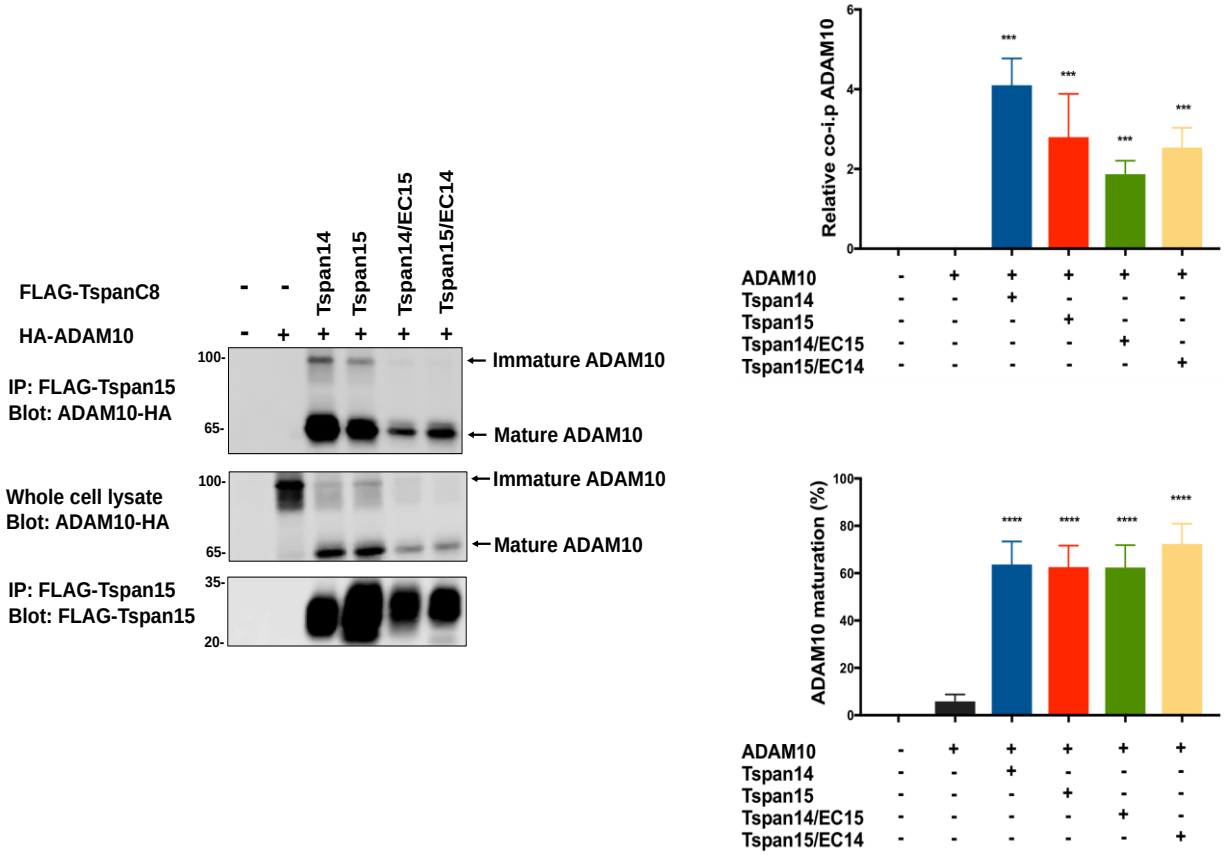
FLAG-TspanC8
HA-ADAM10
Tspan14
Tspan15
Tspan14/EC15
Tspan15/EC14
IP: FLAG-Tspan15
Blot: ADAM10-HA
Immature ADAM10
Mature ADAM10
Whole cell lysate
Blot: ADAM10-HA
IP: FLAG-Tspan15
Blot: FLAG-Tspan15
Relative co-i.p ADAM10
ADAM10 maturation (%)
ADAM10
Tspan14
Tspan15
Tspan14/EC15
Tspan15/EC14

B

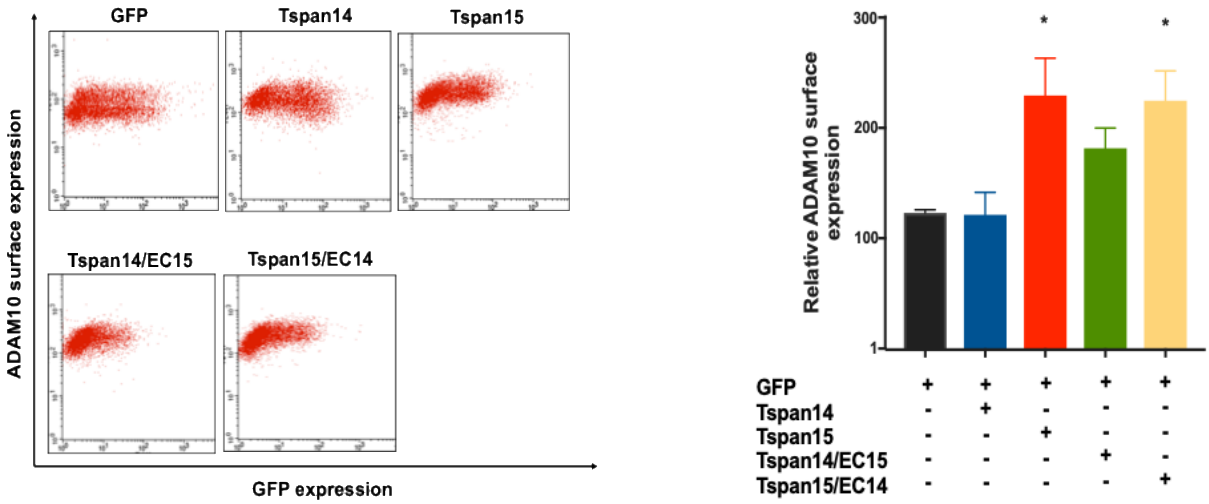
GFP
Tspan14
Tspan15
Tspan14/EC15
Tspan15/EC14
ADAM10 surface expression
GFP expression
Relative ADAM10 surface expression
GFP
Tspan14
Tspan15
Tspan14/EC15
Tspan15/EC14

C

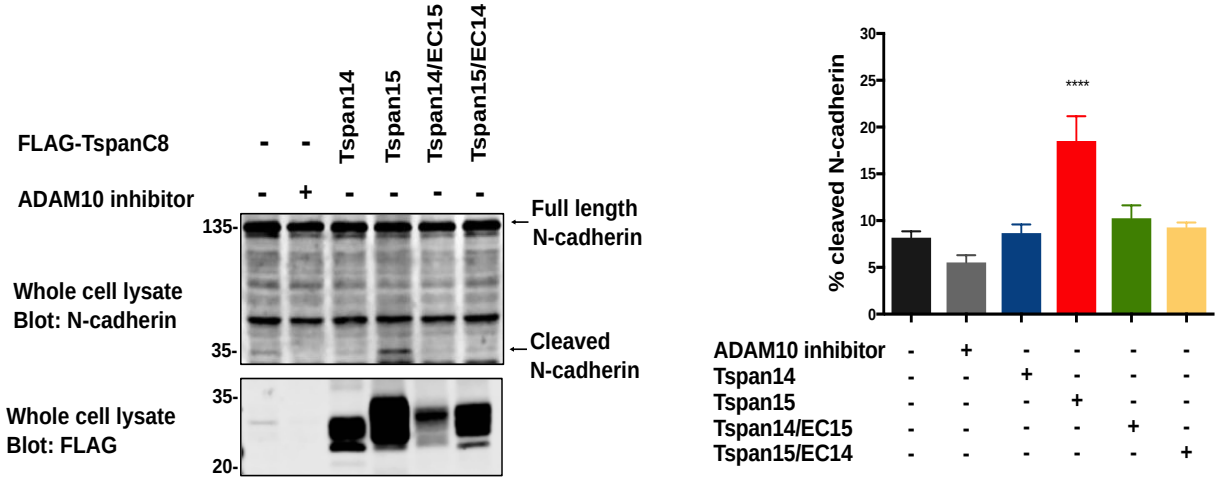

Figure 5.2 Tspan15 transmembrane and cytoplasmic regions are sufficient for promoting ADAM10 surface localisation, but the extracellular region is required for N-cadherin shedding. [A] Tspan14, 15, Tspan14/EC15 and Tspan15/EC14 co-immunoprecipitate mature ADAM10 in transfected HEK-293T cells. Co-immunoprecipitation was performed from 1% digitonin lysates of HEK-293T cells co-transfected with expression constructs for FLAG-tagged TspanC8s, chimeras and HA-tagged ADAM10. The amount of immunoprecipitated ADAM10 was quantified and showed as a relative amount of co-immunoprecipitated ADAM10 to the amount of ADAM10 present in the whole cell lysates. ADAM10 from whole cell lysate was measured and quantified as a percentage of mature ADAM10 detected in the presence of the tetraspanins. [B] The expression of WT Tspan15 and the Tspan15/EC14 chimera increases the surface expression of ADAM10. HEK-293T cells were transfected with the indicated TspanC8s, chimeras and GFP expression constructs. Cells were stained with APC-conjugated ADAM10 antibodies and analysed by flow cytometry. The geometric mean fluorescence intensities of ADAM10 from GFP-positive transfected populations of cells were quantified and presented as the relative ADAM10 surface expression. [C] The Tspan15 extracellular region is required for N-cadherin cleavage. HEK-293T cells were transiently transfected with the expression construct for FLAG-tagged WT Tspan14, 15 and the chimeras. The cells were lysed in 1% Triton X-100 lysis buffer, and western blotted with the antibodies against the cytoplasmic tail of N-cadherin and a FLAG-tagged epitope of the tetraspanins. The graph represents % cleaved N-cadherin calculated based on the intensities of the full-length and cleaved fragments. Error bars represent SEM for three independent experiments for shedding assay and flow cytometry; six independent experiments for co-i.p. The data was arcsine transformed and statistically analysed by one-way ANOVA with Dunnett's multiple comparison test, compared to the WT control for the flow cytometry and shedding assays, or to the ADAM10-HA transfection in the co-i.p experiment and whole cell lysates (*p<0.05, ***p<0.001, ****p<0.0001).

5.2.2 Mutation of the putative cholesterol-binding sites or truncation of cytoplasmic tails do not affect the ability of Tspan15 to interact with ADAM10

The previous section suggested the cytoplasmic tails and/or transmembranes are important for Tspan15 localisation. The cytoplasmic tails are the most divergent regions in sequence between TspanC8s but highly conserved between species of the same TspanC8 (Matthews et al., 2017b). Therefore, they are good candidates for regulating localisation and hence function. Through the generation of the Tspan15 tailless mutant construct (Figure 5.1), a suitable model was created for testing the tail truncations in the regulation of Tspan15. The recent structural characterisation of tetraspanin CD81 suggested that cholesterol binding within a transmembrane cavity is important for regulating conformational change and function (Zimmerman et al., 2016). To investigate this possibility, mutations in the putative cholesterol-binding sites of Tspan15 transmembranes were generated (Figure 5.1). It is expected that Q/E mutation would enhance a closed conformation, while Q/A would promote an open conformation.

To test whether Tspan15 mutants are functional in terms of ADAM10 binding, the co-transfection and immunoprecipitation approaches in 1% digitonin were used as previously described in section 5.2. As shown in Figure 5.3A, Tspan15 and the mutants co-immunoprecipitated with mature ADAM10, and each promoted the relative amount of this form versus immature. Next, the Tspan15 mutants were tested for their ability to promote endogenous ADAM10 surface expression. HEK-293T cells were mock transfected or transfected with WT Tspan15 and the mutants, labelled with Tspan15 and

ADAM10 mAbs and analysed by flow cytometry as previously described in section 5.2. As shown in Figure 5.3B, all the mutants increased ADAM10 surface expression by approximately two-fold on average, similar to WT Tspan15, and Tspan15 expression level correlated with that of ADAM10. None of these reached statistical significance from the five experiments, but the data suggests that the mutants are comparable to WT regarding promotion of ADAM10 trafficking in this over-expression system.

A

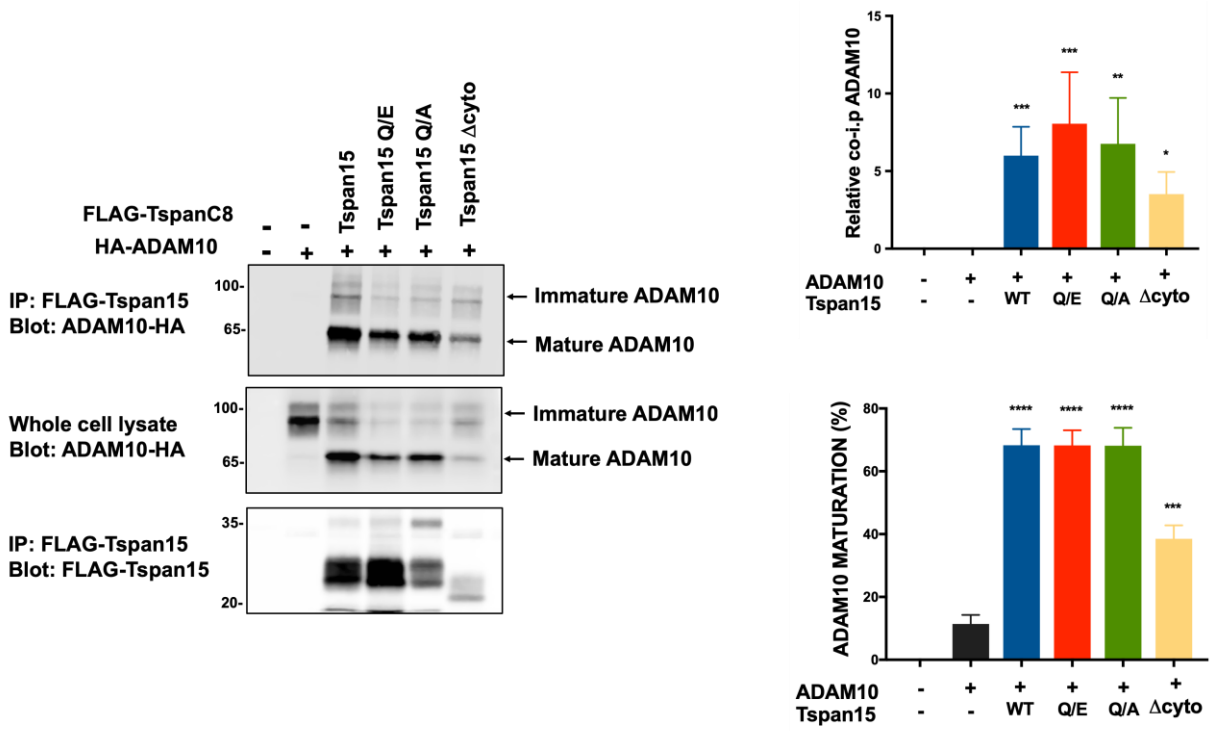
FLAG-TspanC8
HA-ADAM10
Tspan15
Tspan15 Q/E
Tspan15 Q/A
Tspan15 Δcyto
IP: FLAG-Tspan15
Blot: ADAM10-HA
Immature ADAM10
Mature ADAM10
Whole cell lysate
Blot: ADAM10-HA
IP: FLAG-Tspan15
Blot: FLAG-Tspan15
100-
65-
35-
20-
Relative co-i.p ADAM10
ADAM10 MATURATION (%)
ADAM10
Tspan15
WT
Q/E
Q/A
Δcyto

B

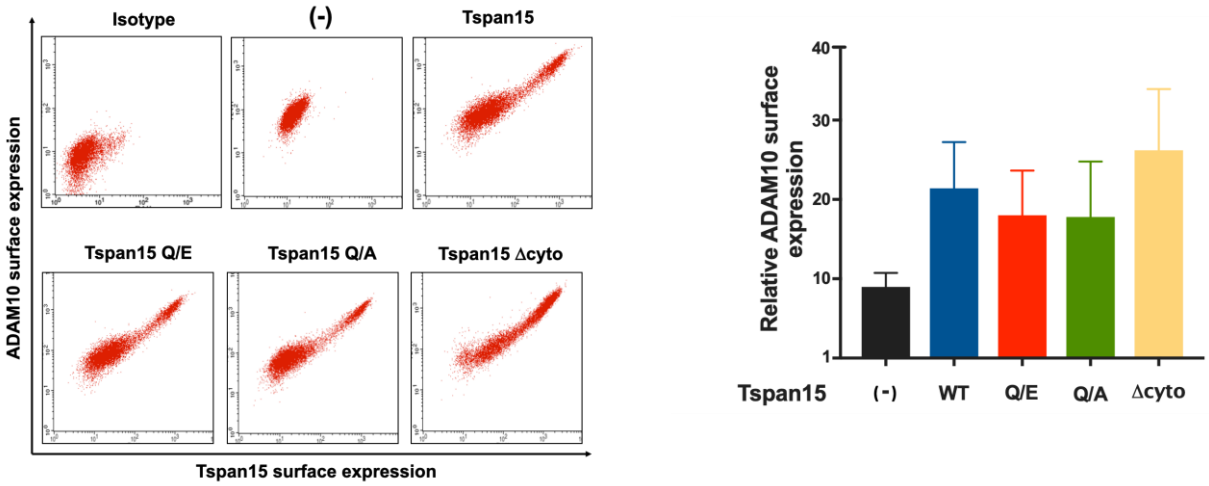
Isotype
(-)
Tspan15
Tspan15 Q/E
Tspan15 Q/A
Tspan15 Δcyto
ADAM10 surface expression
Tspan15 surface expression
Relative ADAM10 surface expression
Tspan15
(-)
WT
Q/E
Q/A
Δcyto

Figure 5.3 Mutation of the putative cholesterol-binding site or truncations of cytoplasmic tails do not affect the ability of Tspan15 to interact with ADAM10. [A] Tspan15 mutants interact with and promote ADAM10 maturation. HEK293T cells were mock transfected (-), transfected with FLAG-tagged Tspan15, the mutants and HA-tagged ADAM10. Cells were lysed in 1% digitonin and subjected to anti-FLAG immunoprecipitation (upper and lower panel) and anti-HA western blotting (middle panel). The co-precipitated immature and mature forms of ADAM10 were detected and quantified as a relative amount of ADAM10 co-immunoprecipitated to the amount of ADAM10 present in the whole cell lysate. ADAM10 in a whole cell lysate was quantified as a percentage of mature ADAM10 detected in the presence of the tetraspanins. [B] Tspan15 mutants retain the ability to traffic ADAM10 to the cell surface. HEK293T cells were transfected with FLAG-tagged Tspan15 constructs. Cells were stained with APC-conjugated ADAM0 antibody and Tspan15 mAbs (4A4 clone was used in a form of tissue culture supernatant) to identify transfected cells. The fluorescence intensities for ADAM10 surface expression, gated on live and positively transfected cells, for each construct were measured. [A, B] Data were arcsine transformed, and statistical significance was determined using one-way ANOVA with a Dunnett's multiple caparison test compare to WT control for flow cytometry or to ADAM10-HA for co-i.p (*$p<0.05$, **$p<0.01$, ***$p<0.001$, ****$p<0.0001$). The data are representative for three independent experiments for flow cytometry and six representative experiments for co-i.p.

5.2.3. Transfection of WT Tspan15 restores VE-cadherin cleavage in Tspan15 KO HEK-293T cells

As demonstrated in chapter 4.1, the cleavage of transfected VE-cadherin in Tspan15 KO HEK-293T cells was almost completely abrogated, and this was comparable to the extent observed in ADAM10 KO cells, suggesting a critical role for Tspan15 in the ADAM10-mediated shedding of this substrate. This VE-cadherin assay was more robust than the previously used N- and E-cadherin cleavage assays. Therefore, this assay was selected to functionally assess the Tspan15 chimeric and mutant constructs. To first confirm that Tspan15 could rescue VE-cadherin cleavage in Tspan15 KO cells, WT Tspan15 and VE-cadherin were co-transfected into WT, ADAM10 KO and Tspan15 KO cells, the latter of which served as a control. The cleavage assay used NEM stimulation (2 mM) for 30 min, followed by lysis in 1% Triton 100-X lysis buffer and Western blotting for VE-cadherin. VE-cadherin cleavage was rescued by over-expressed Tspan15 in Tspan15 KO HEK-293T cells, which was comparable to observations in WT (Figure 5.4).

Moreover, the percentage of cleaved VE-cadherin was significantly higher when Tspan15 was overexpressed in WT cells. As previously shown, VE-cadherin cleavage was minimal in ADAM10 and Tspan15 KO cells. It was noted in the experiment the appearance of some bands in the control samples in the FLAG blot. The weak band in the negative control (line 1) was most likely a result of non-specific binding of anti-FLAG mAb. The band in the positive control (line 2) was most likely caused by a strong signal of VE-cadherin in one channel that bled through to the other FLAG channel. As the VE-cadherin expression was always at relatively high levels in these experiments, this could be minimised in the future by using lower scan settings in a channel with a strong signal or reducing the amount of the

transfected construct. Nevertheless, the presence of the relatively weak background bands did not affect the VE-cadherin cleavage quantitation.

These data suggest that this VE-cadherin cleavage assay will be useful for testing the Tspan15 mutant constructs.

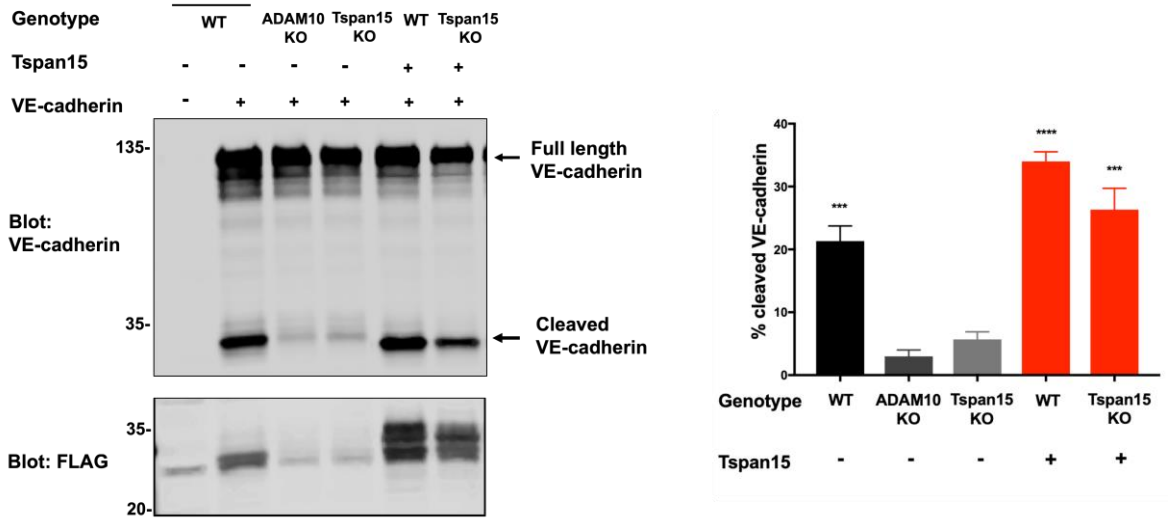

Figure 5.4 The reintroduced Tspan15 can rescue VE-cadherin cleavage in Tspan15 KO HEK-293T cells. WT, Tspan15 and ADAM10 KO HEK-293T cells were co-transfected with the FLAG-tagged WT Tspan15 and VE-cadherin. 2 mM of NEM was added to the cells for 30 min to induce cleavage. Cells were lysed in 1% Triton X-100 lysis buffer, and Western blotted with anti-VE-cadherin and anti-FLAG mAbs. The percentage of cleaved VE-cadherin was calculated based on fluorescence intensities of the cleaved fragment and full-length of VE-cadherin. The data was transformed by arcsine of the square root transformed, and statistical significance was determined by one-way ANOVA with Dunnett's multiple comparison test, as compared to Tspan15 KO HEK-293T cells. The error bars represent SEM for three independent experiments, (**p<0.01, ****p<0.0001).

5.2.4 Overexpression of cholesterol-binding mutants and tailless Tspan15, but not the Tspan15/EC14 chimera, rescues NEM-induced VE-cadherin cleavage in Tspan15-KO HEK-293T cells

Tspan15 KO HEK-293T cells were co-transfected with VE-cadherin and Tspan15/14 chimeras or Tspan15 mutant constructs, and NEM-induced VE-cadherin cleavage assay performed as described in the previous section. The Q/E and Q/A cholesterol-binding mutants, and the tailless Tspan15, were each able to rescue VE-cadherin cleavage like WT Tspan15 (Figure 5.5). In contrast, the two Tspan15/14 chimeras failed to rescue VE-cadherin cleavage, similar to WT Tspan14. However, expression of the Tspan14/EC15 chimera was not detected in these experiments (Figure 5.5), for reasons that are not clear, despite detectable expression previously (Figure 5.2A). Therefore, conclusions cannot be made for this chimera. The FLAG blotting showed that each construct was expressed at different levels. It was noted that Tspan14, chimera Tspan14/15 and mutant Q/A had considerably stronger expression levels than the other TspanC8s. However, this was consistent with other experiments.

A

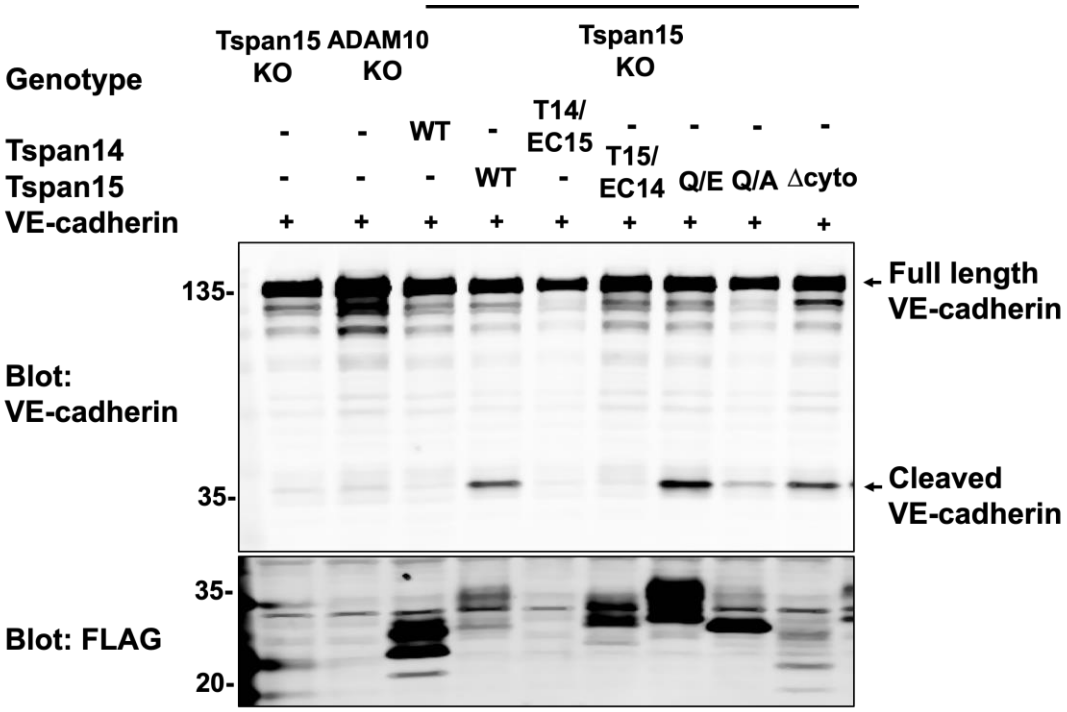
Genotype
Tspan15 KO
ADAM10 KO
Tspan15 KO
Tspan14
Tspan15
VE-cadherin
WT
T14/ EC15
T15/ EC14
Q/E
Q/A
Δcyto
135-
35-
Blot: VE-cadherin
Full length VE-cadherin
Cleaved VE-cadherin
35-
20-
Blot: FLAG

B

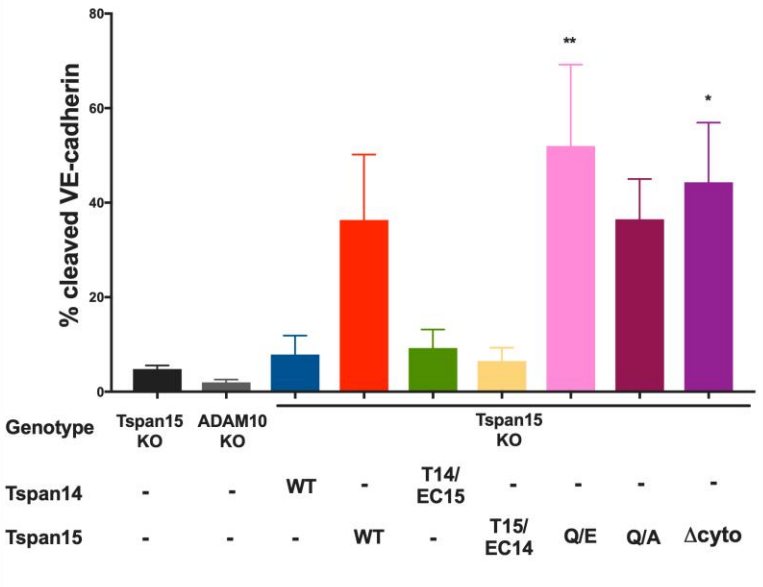
% cleaved VE-cadherin
80
60
40
20
0
**
*
Genotype
Tspan15 KO
ADAM10 KO
Tspan15 KO
Tspan14
Tspan15
WT
T14/ EC15
T15/ EC14
Q/E
Q/A
Δcyto

Figure 5.5 Over-expression of cholesterol-binding mutants and tailless Tspan15, but not the Tspan15/EC14 chimera, rescues NEM-induced VE-cadherin cleavage in Tspan15-KO HEK-293T cells. HEK-293T WT and Tspan15 KO cells were co-transfected with the Tspan15 mutant constructs FLAG-tagged and VE-cadherin. 2 mM NEM was added to the cells to induce the cleavage. Cells were lysed in 1% Triton X-100 lysis buffer, and Western blotted with anti-VE-cadherin and anti-FLAG mAbs. The percentage shed VE-cadherin was calculated based on fluorescence intensities of cleaved fragment and full-length of the cadherin. The data was transformed by arcsine of the square root and statistical significance was determined by one-way ANOVA with Dunnett's multiple comparison test as compared Tspan15 KO. The error bars represent SEM for three independent experiments, (*$p<0.05$, **$p<0.01$).

5.2.5 Generation of Tspan15-KO HEK-293T cell lines stably expressing mutant Tspan15 constructs

The overexpression system used to this point might not be an ideal model for determining the consequences of the mutations on ADAM10 activity. As all mutants were expressed at a much higher level than endogenous Tspan15, the overexpression may mask any defects in the mutants. Also, the level of over-expression differed between mutants. Therefore, the aim of this section was to generate Tspan15-knockout cell lines stably expressing Tspan15 mutants at the endogenous level.

To generate stable cell lines, Tspan15 WT, mutants and chimeras were first transiently expressed in Tspan15 KO and WT HEK-293T cells. The transfected cells were enriched by blasticidin selection, and clonal populations were isolated from a heterogeneous pool by serial dilution to one cell per well on 96-well plate. Only clones that appeared to originate from a single cell were expanded. The expression of the constructs was assessed by flow cytometry using mAbs against Tspan15 or Tspan14, for Tspan15/14EC construct; the Tspan14 mAb was recently made by the Tomlinson lab but may be a low affinity mAb because it only detects transfected Tspan14 by flow cytometry, not endogenous levels of the protein (Koo, unpublished). Two clones with a Tspan15 expression that resembled endogenous levels were chosen for future experiments (Figure 5.6A-B).

5.2.6 Tspan15 tailless and Q245A mutants support normal surface expression of ADAM10, but Q245E and Tspan15/14 chimeras do not

In order to determine whether stable expression of the Tspan15 mutants and chimeras could restore normal expression of surface ADAM10 in the Tspan15 KO cells, they were analysed by flow cytometry for ADAM10. As shown in Figure 5.6C-D, none of the stable Tspan15 KO clones expressing WT or mutant Tspan15 constructs had a significant increase in surface ADAM10 expression, compared to Tspan15 KO cells; ADAM10 was only significantly increased in the WT cells in which Tspan15 was stably expressed. However, when each pair of clones was grouped, the Tspan15 tailless and Q/A mutant reconstituted cells did show a significant increase in ADAM10 expression (Figure 5.6D), suggesting that individual clones would have reached significance if more repeats had been done. In contrast, the Tspan15 Q/E mutant and the two Tspan15/14 chimeras, when grouped, failed to show any significant rescue of ADAM10 expression (Figure 5.6D). The WT Tspan15 reconstituted cells did not reach significance for restoration of ADAM10 expression when grouped, but these probably would have reached significance with more repeats, because they were not significantly different from WT. These data demonstrate the importance of assessing Tspan15 mutants at endogenous expression levels, because all of these constructs, with the exception of the Tspan14/15 chimera, rescued ADAM10 expression when transiently over-expressed (Figures 5.2 and 5.3).

A

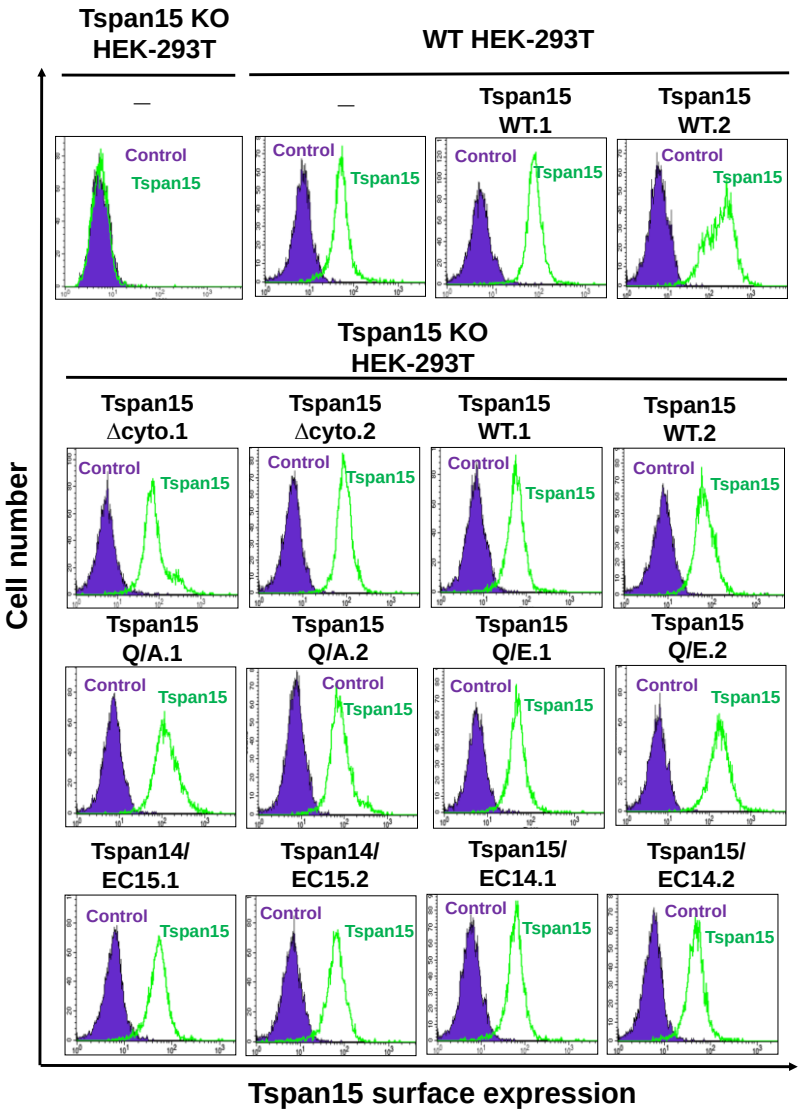
Tspan15 KO HEK-293T
WT HEK-293T
–
–
Tspan15 WT.1
Tspan15 WT.2
Control
Tspan15
Tspan15 KO HEK-293T
Tspan15 Δcyto.1
Tspan15 Δcyto.2
Tspan15 WT.1
Tspan15 WT.2
Tspan15 Q/A.1
Tspan15 Q/A.2
Tspan15 Q/E.1
Tspan15 Q/E.2
Tspan14/ EC15.1
Tspan14/ EC15.2
Tspan15/ EC14.1
Tspan15/ EC14.2
Cell number
Tspan15 surface expression

B

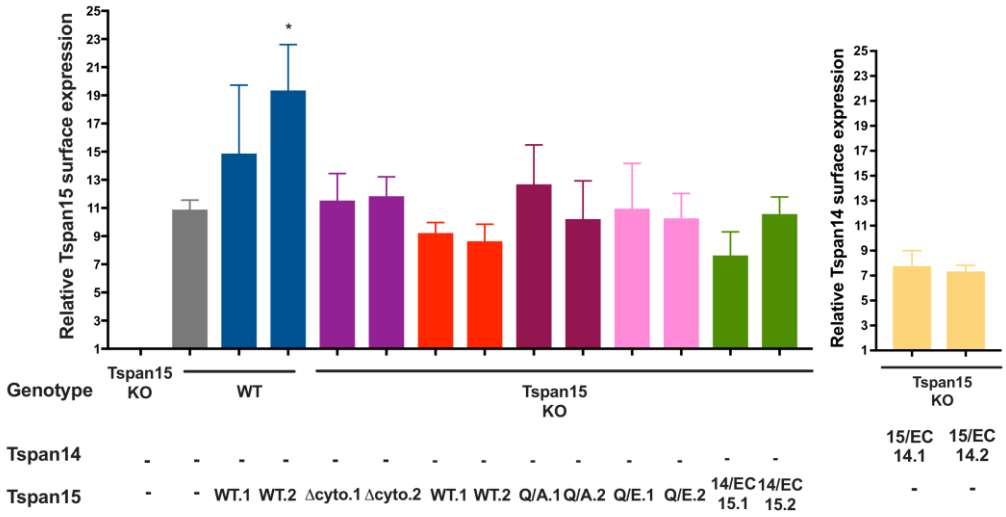
Relative Tspan15 surface expression
Relative Tspan14 surface expression
Genotype
Tspan15 KO
WT
Tspan15 KO
Tspan15 KO
Tspan14
Tspan15
WT.1 WT.2 Δcyto.1 Δcyto.2 WT.1 WT.2 Q/A.1 Q/A.2 Q/E.1 Q/E.2 14/EC 15.1 14/EC 15.2
15/EC 14.1
15/EC 14.2

C

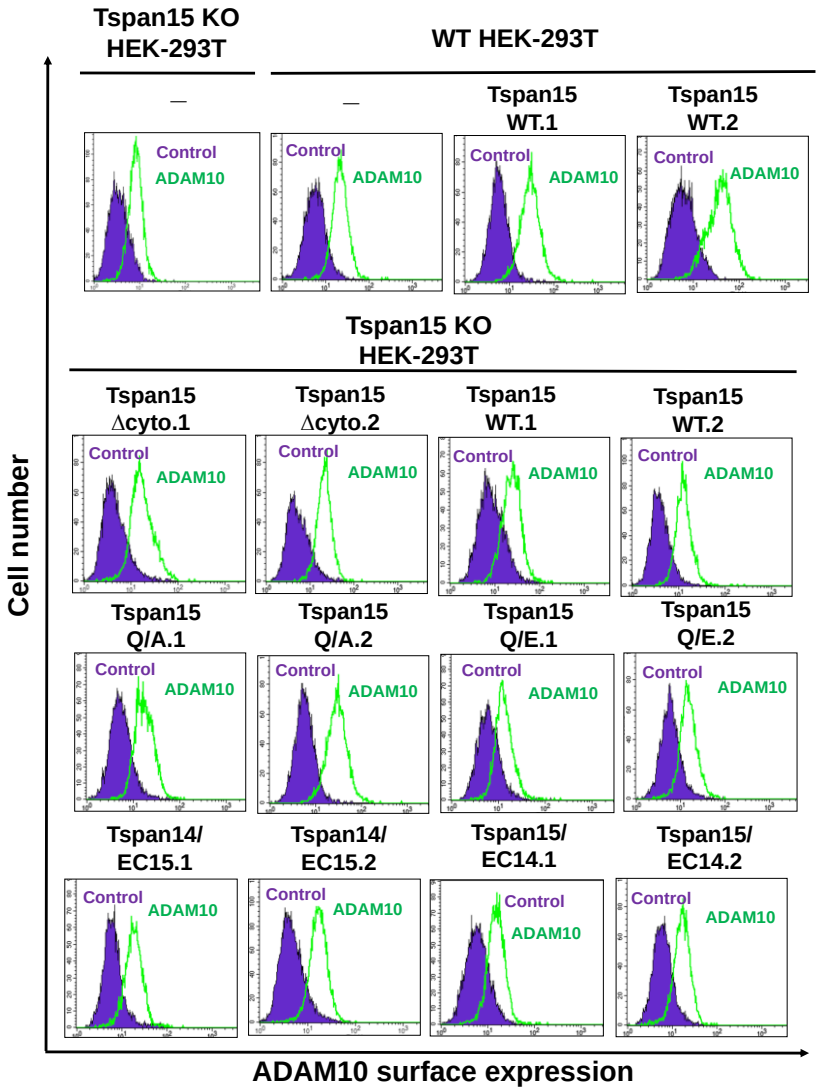
Tspan15 KO HEK-293T
WT HEK-293T
–
–
Tspan15 WT.1
Tspan15 WT.2
Control
ADAM10
Tspan15 KO HEK-293T
Tspan15 Δcyto.1
Tspan15 Δcyto.2
Tspan15 WT.1
Tspan15 WT.2
Tspan15 Q/A.1
Tspan15 Q/A.2
Tspan15 Q/E.1
Tspan15 Q/E.2
Tspan14/ EC15.1
Tspan14/ EC15.2
Tspan15/ EC14.1
Tspan15/ EC14.2
Cell number
ADAM10 surface expression

D

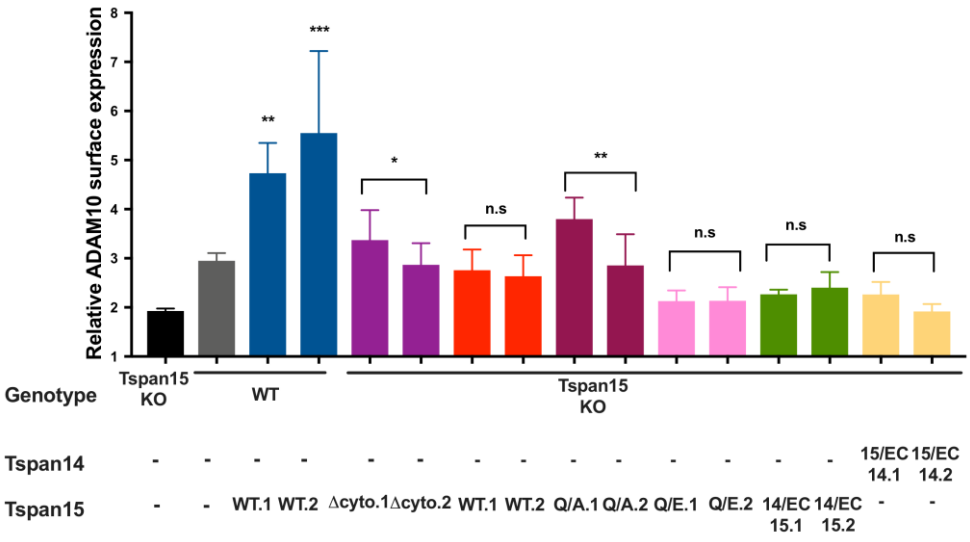
Relative ADAM10 surface expression
***
**
*
n.s
**
n.s
n.s
n.s
Genotype
Tspan15 KO
WT
Tspan15 KO
Tspan14
Tspan15
WT.1 WT.2 Δcyto.1 Δcyto.2 WT.1 WT.2 Q/A.1 Q/A.2 Q/E.1 Q/E.2 14/EC 15.1 14/EC 15.2
15/EC 14.1
15/EC 14.2

Figure 5.6 Validation of Tspan15 stables HEK-293T cell lines. WT and Tspan15 KO HEK-293T stably expressing Tspan15 WT, mutants and chimeric constructs were subjected to flow cytometry with mAbs against Tspan15 (clone 4A4 used in a form of tissue culture supernatant) and ADAM10. The surface expression of Tspan15 [A] and ADAM10 [C] was detected in the selected clones. [B, D] Data from panel A and C were normalised by arcsine transformation of the square root and analysed by a one-way ANOVA and Dunnett's multiple comparison test as compared to WT cells for Tspan15 expression or to Tspan15 KO cells for ADAM10 surface expression. The error bars represent standard error of the mean for six independent experiments (*$p<0.05$, **$p<0.01$, ***$p<0.001$).

5.2.7 Tspan15 tailless and Q245A mutants support NEM-induced VE-cadherin cleavage, but Q245E and Tspan15/14 chimeras do not

In order to determine whether stable expression of the Tspan15 mutants and chimeras could restore normal VE-cadherin cleavage, the reconstituted cell lines were analysed in the NEM-induced cleavage assay. As shown in Figure 5.7A-D, VE-cadherin cleavage was rescued by the tailless and Q/A Tspan15 mutants and WT Tspan15. In contrast, the Q/E Tspan15 mutant and chimeric constructs did not rescue VE-cadherin cleavage (Figure 5.7A-D), which is consistent with their inability to rescue ADAM10 surface expression (Figure 5.6). The expression of distinct Tspan15 mutants was not detectable in anti-FLAG blotting of the whole cell lysates, which was to be expected given that endogenous Tspan15 cannot be detected by Western blotting in these cells (data not shown).

Taken together, these data show that the tails of Tspan15 are not required for NEM-induced cleavage of VE-cadherin, and similarly the Q/A mutation of the Tspan15 putative cholesterol binding site does not affect NEM-induced VE-cadherin cleavage. In contrast, the Q/E mutation and Tspan15/14 chimera fail to rescue VE-cadherin cleavage, probably as a result of their failure to support ADAM10 surface expression.

A

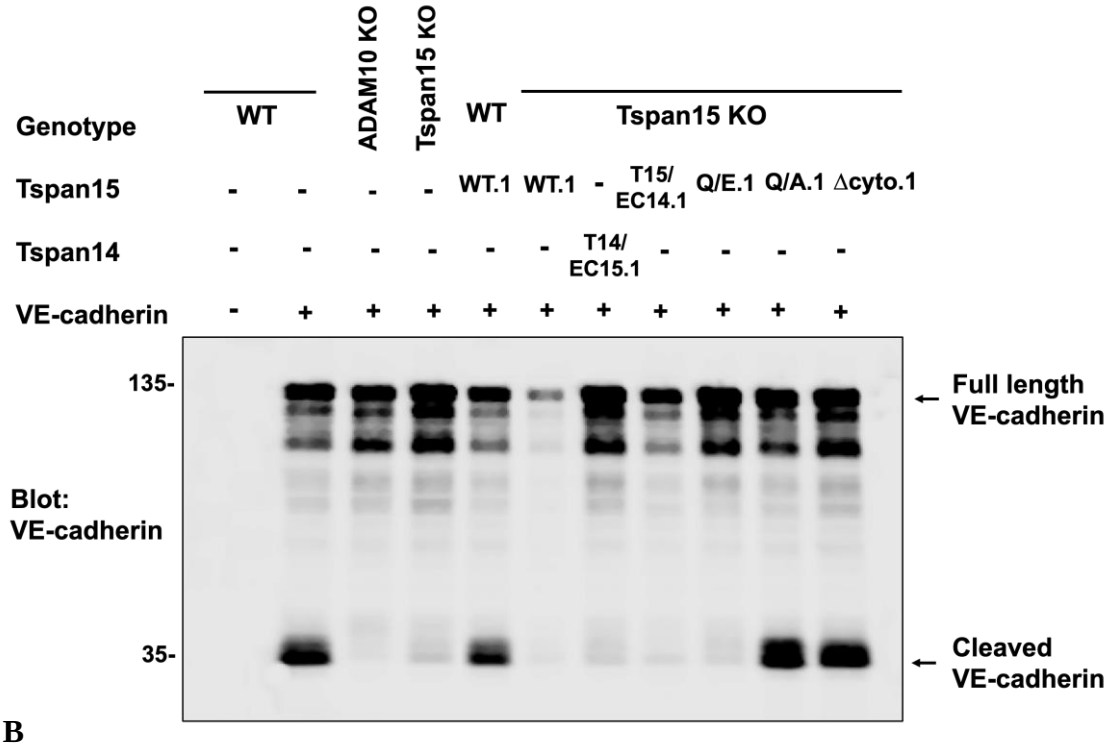
Genotype
WT
ADAM10 KO
Tspan15 KO
WT
Tspan15 KO
Tspan15
WT.1
WT.1
T15/ EC14.1
Q/E.1
Q/A.1
Δcyto.1
Tspan14
T14/ EC15.1
VE-cadherin
135-
35-
Blot: VE-cadherin
Full length VE-cadherin
Cleaved VE-cadherin

B

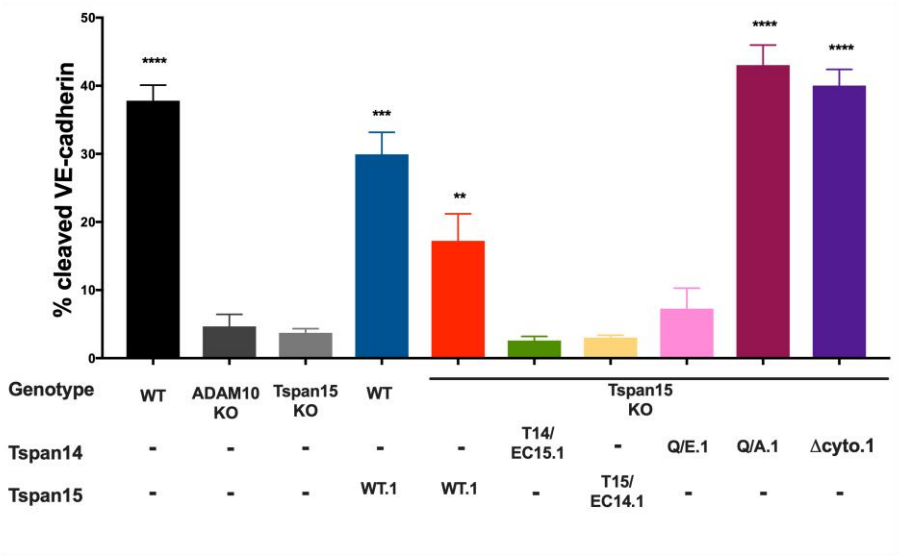
% cleaved VE-cadherin
50
40
30
20
10
0
****
***
**
****
****
Genotype
WT
ADAM10 KO
Tspan15 KO
WT
Tspan15 KO
Tspan14
T14/ EC15.1
Q/E.1
Q/A.1
Δcyto.1
Tspan15
WT.1
WT.1
T15/ EC14.1

C

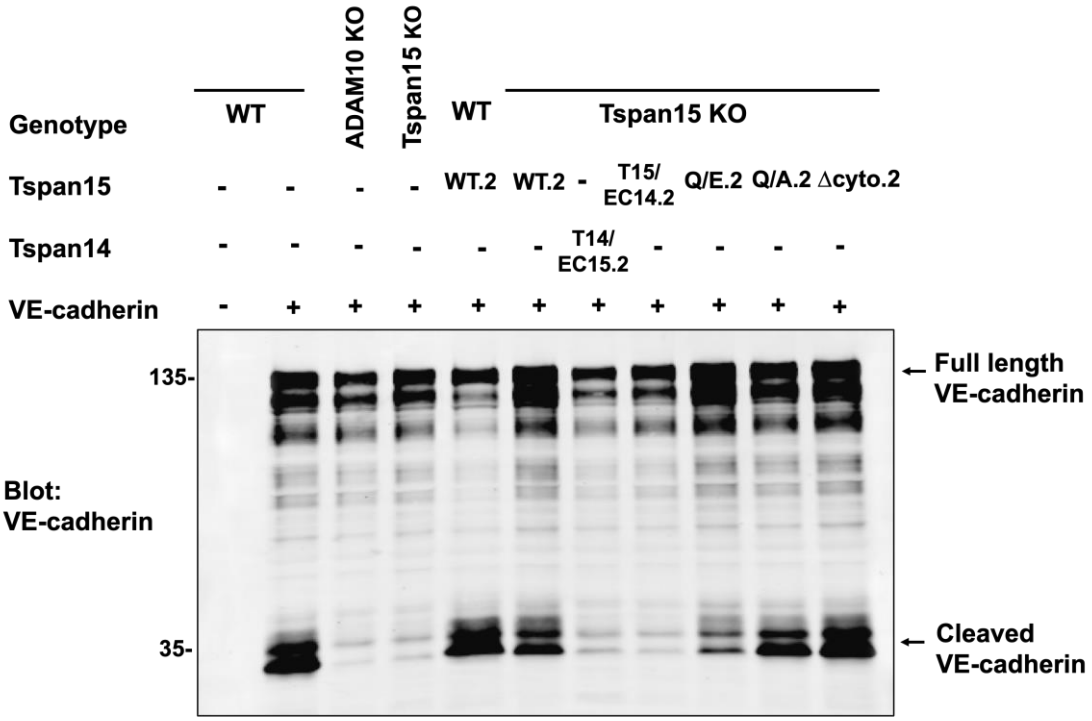

D

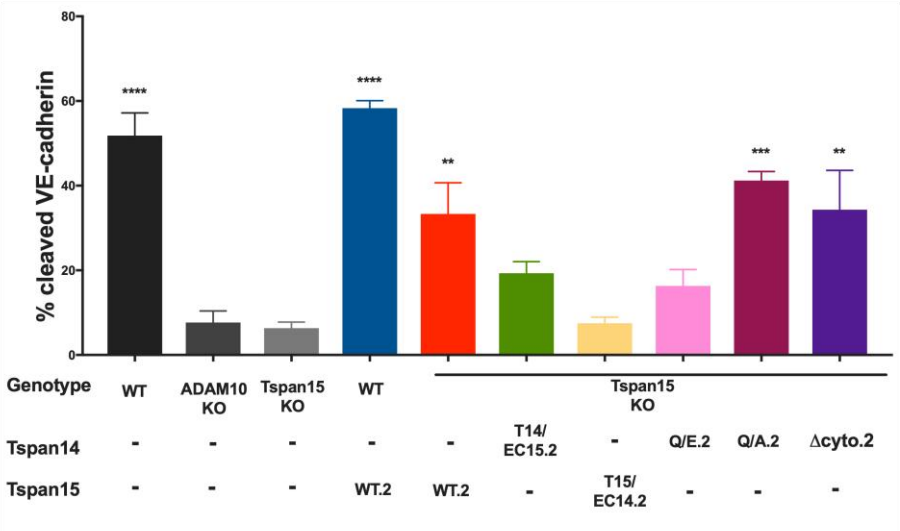

Figure 5.7 The cleavage of VE-cadherin is differentially affected by the stable expression of distinct Tspan15 mutants. [A-C] The NEM-induced cleavage assay was performed on the stable cell lines (two seperate clones for each cell line used) transfected with VE-cadherin as previously described. The cells were western blotted with VE-cadherin mAb and the percentage cleaved VE-cadherin was plotted [B-D]. Data were normalised by arcsine transformation of the square root and analysed by a one-way ANOVA and Dunnett's multiple comparison test as compared to Tspan15 KO cells. Error bars represent the standard error of the mean for three independent experiments (**p<0.01, ***p<0.001, ****p<0.0001).

5.3 Discussion

In this chapter, the first structure/function analyses on Tspan15 were carried out in WT and Tspan15-knockout HEK-293T cells using a range of Tspan15 mutant constructs to investigate the functions of the extracellular region, the putative cholesterol binding site and the cytoplasmic tails. Experiments with chimeric Tspan15/Tspan14 constructs, in which the extracellular regions were exchanged, showed that they could not function like WT Tspan15 in supporting ADAM10 surface expression and VE-cadherin cleavage, despite their co-immunoprecipitation with ADAM10. This indicates that the trafficking and function of Tspan15/ADAM10 complexes is dependent on the full Tspan15 molecule. In contrast, tail-less Tspan15 and a Q245A mutation in the putative cholesterol binding site supported ADAM10 surface expression and VE-cadherin cleavage following NEM stimulation. However, a Q245E mutation in the cholesterol binding site failed to support ADAM10 expression and VE-cadherin cleavage in response to NEM. These data suggest a potential functional role for the Tspan15 cholesterol binding site, but no role for the cytoplasmic tails, at least for NEM activation of the Tspan15/ADAM10 complex.

The Tomlinson lab previously showed that large extracellular region of TspanC8s is important for interaction with ADAM10 and for enabling its maturation and localisation to the cell surface (Noy et al., 2016). These experiments were conducted in HeLa cells with Tspan14 as a model TspanC8 (Noy et al., 2016). However, in the HEK-293T cells used in this chapter, Tspan15 over-expression promoted ADAM10 surface expression but Tspan14 did not, despite both being able to promote ADAM10 maturation (Haining et al., 2012). This discrepancy may be due to the expression of different repertoires of trafficking

proteins in the two cell types, such that Tspan14 is predominantly intracellularly-localised in HEK-293T cells. Nevertheless, the difference between Tspan15 and Tspan14 in HEK-293T cells allowed experiments to be conducted with chimeric forms of these proteins, in which the entire extracellular regions were exchanged. In initial over-expression studies, both chimeras co-immunoprecipitated with ADAM10 and promoted its maturation, demonstrating their correct folding and functionality as TspanC8s. However, only the construct with transmembrane/cytoplasmic regions of Tspan15 significantly increased ADAM10 surface expression, suggesting that these regions are driving localisation, possibly by interaction with as yet unidentified trafficking proteins. Candidates include Rab14 and its effector FAM116, which were reported to be required for ADAM10 trafficking to the cell surface in A549 cells (Linford et al., 2012). In Tspan15-knockout cells stably reconstituted with the two chimeras, neither restored normal ADAM10 surface expression, and neither supported cleavage of transfected VE-cadherin in response to NEM. This suggests that normal trafficking and shedding function of Tspan15/ADAM10 complexes is critically dependent on the entire Tspan15 protein, which cannot be substituted with either extracellular or transmembrane/cytoplasmic regions of Tspan14. This work also underscores the importance of working with stably reconstituted cell lines with endogenous levels of the mutant proteins, because 50-100-fold over-expression of the chimeras promoted ADAM10 surface expression, but endogenous-level expression did not. The former is likely to be an over-expression artefact.

Recent publication of the full-length structure of CD81 suggested that the tetraspanin-partner interactions may be regulated by cholesterol-mediated conformational state of the large extracellular region (Zimmerman et al., 2016). CD81 was shown to have a key polar

glutamic acid residue in transmembrane 4 (E219), which formed hydrogen bonds with the hydroxyl group of the cholesterol molecule. In molecular dynamics simulations, loss of cholesterol was predicted to cause a dramatic conformational change, in which the main extracellular region swings upwards (Zimmerman et al., 2016). Thus, CD81 may act as a 'molecular switch' to regulate partner proteins by inducing their conformational change. E219Q and E219A mutations, predicted to impair cholesterol binding, did indeed reduce cholesterol binding by 40%, in an experiment using immunoprecipitated CD81 and tritiated cholesterol (Zimmerman et al., 2016). Moreover, cell surface expression of transfected WT CD19, a CD81 partner, was increased two-fold in a HEK-293T model system overexpressing the mutants. Therefore, to investigate whether these observations hold true for the Tspan15/ADAM10 complex, Tspan15 Q245E and Q245A constructs were generated. Like most tetraspanins, Tspan15 lacks the glutamic acid residue in the precise location of that in CD81 (Zimmerman et al., 2016), but does have a conserved polar glutamine (Q245) on the preceding helix of the fourth transmembrane. Therefore, the Q245E mutant may interact with cholesterol more strongly than Q245A or WT Tspan15. The two mutant constructs were functional in terms of co-immunoprecipitation with ADAM10 and each promoted ADAM10 surface expression when over-expressed. In stably transfected Tspan15-knockout cells, the Q245A mutant restored ADAM10 surface expression and NEM-induced VE-cadherin cleavage, but the Q245E mutant did not, despite similar expression levels of each mutant at the cell surface that were similar to endogenous levels. Thus, the cleavage phenotype correlates with the ADAM10 trafficking phenotype. It is possible that Tspan15 Q245E, like for WT CD81 (E219) and CD19, binds cholesterol more strongly, cannot readily adopt an open conformation, and poorly traffics ADAM10 to the cell surface. In contrast, WT Tspan15 (Q245) or Q245A, like CD81

mutants E219Q or E219A and CD19, may weakly bind cholesterol and be more prone to adopt an open conformation and promote ADAM10 trafficking. Further experiments, including cholesterol-binding and subcellular localisation using fluorescence microscopy, are required to investigate this further.

Tspan15 is particularly efficient in promoting ADAM10 trafficking to the cell surface, as was shown in this chapter in comparison with Tspan14, and by fluorescence microscopy experiments that compared all TspanC8s (Dornier et al., 2012). To date the mechanism that controls the process remains unknown. As revealed by sequence line-ups of a full length of TspanC8s, the cytoplasmic tails are found to be relatively divergent in the sequence and length, but are highly conserved between species of a single TspanC8 (Matthews et al., 2017). Moreover, Tspan15 and Tspan10 possesses tyrosine- and dileucine-based motifs respectively, which can potentially engage to adaptor proteins capable of controlling subcellular localisation (Berditchevski and Odintsova, 2007). Therefore, the cytoplasmic tails are strong candidates for regulation of TspanC8 subcellular localisation. Indeed, this is a plausible scenario, as tail swaps between Tspan15 and Tspan10 were shown to be sufficient to alter the localisation of the respective TspanC8s (Matthews and Tomlinson, unpublished data). Thus, the importance of Tspan15 cytoplasmic tails in the regulation of ADAM10 activity was addressed in this study. Using Tspan15 tailless mutant stable transfectants in Tspan15-knockout cells, it was shown that interactions between Tspan15 and ADAM10 are not mediated by the cytoplasmic regions. In fact, neither NEM-induced cleavage of VE-cadherin nor surface expression of ADAM10 and Tspan15 were affected by the truncations. Therefore, the Tspan15 tails are not required for trafficking of Tspan15 or ADAM10 to the cell surface. However, a major

caveat to the cleavage data is that ADAM10 was activated with NEM, which is likely to directly activate ADAM10 via alkylation. Any requirement for the Tspan15 tails in, for example, growth factor- or Ca^{2+}-induced 'inside-out' ADAM10 activation, would not be determined using NEM. This will be discussed in Chapter 7 in the context of a proposed model for physiological ADAM10 activation.

Finally, it is interesting to note that in the overexpression system, the total expression level of the tailless mutant detected by western blot (Figure 5.5A) was relatively low compared to WT Tspan15, but its surface expression measured by flow cytometry was relatively high (Figure 5.3B). This could suggest that the tailless mutant, once trafficked to the cell surface, is not being degraded or recycled back as efficiently. Therefore, the Tspan15 tails may be important for endocytosis, potentially via the tyrosine-based motif in the N-terminus, as mentioned earlier. Future fluorescent microscopy experiments, or internalisation experiments similar to that used in the previous chapter, will help to address this interesting possibility.

In summary, this chapter has established Tspan15-knockout HEK-293T cells, stably reconstituted with Tspan15 mutants at endogenous expression levels, as a robust system to perform structure/function analyses. The data indicate that the capacity for Tspan15 to promote ADAM10 surface expression and activity towards a specific substrate is dependent on the extracellular region in combination with the transmembrane/cytoplasmic region, and that the putative cholesterol binding site may regulate ADAM10 trafficking in a manner similar to CD81 and CD19. The cytoplasmic tails are dispensable for Tspan15

for promoting ADAM10 trafficking to the cell surface and its activity in response to NEM, but they may play a role in Tspan15 internalisation.

CHAPTER 6
ROLE OF ADAM10 AND TSPAN15 IN ENODTHELIAL CELL FUNCTION

6.1 Introduction

The previous chapters have (1) characterised the first Tspan15 mAbs and shown that this TspanC8 requires ADAM10 for its expression, (2) shown that Tspan15 promotes cadherin shedding in cell lines and that two of the four mAbs have inhibitory function, and (3) initiated a structure-function analysis by stably reconstituting Tspan15-knockout cell lines with Tspan15 mutants. This chapter aimed to functionally characterise the Tspan15/ADAM10 scissor in primary cells. HUVECs were selected as an in vitro model system because siRNA knockdown is highly efficient in these cells, ADAM10 is known to be important for endothelial function in vivo (Alabi et al., 2018), and Tspan15 is largely unstudied in endothelial cells.

The molecular scissor ADAM10 is involved in many pathophysiological processes including angiogenesis. Through the proteolytic processing of growth factors, adhesion molecules and cytokines, it regulates many cellular functions relevant to the process. The consequences of ADAM10-mediated shedding on endothelial cells include initiation of

Notch signalling that is required for vascular development, removal of VE-cadherin to increase vascular permeability, and the release of transmembrane receptors VEGFR2 and Nrp-1 to direct angiogenesis by suppressing vessel sprouting and cell migration (van der Vorst et al., 2012, Mehta et al., 2018). The importance of ADAM10 in angiogenesis is underlined by the findings from knockout mice studies. Global ADAM10 inactivation is lethal at the embryonic stage due to developmental defects in the cardiovascular system (Hartmann et al., 2002), while its endothelial cell-specific deletion leads to abnormal vasculature sprouting and density (Caolo et al., 2015), and defects in multiple organs in both developing and adult mice (Glomski et al., 2011, Farber et al., 2018). These are similar to phenotypes observed by Notch deletion (Hartmann et al., 2002, Alabi et al., 2016), for which ADAM10 is essential for providing the initial cleavage event in the ligand-induced shedding of Notch proteins (van Tetering et al., 2009).

The role of TspanC8s in angiogenesis has not been previously investigated. However, HUVECs express five TspanC8s at the mRNA level and knockdown of the most highly expressed TspanC8, Tspan14, leads to a 30% decrease in basal VE-cadherin cleavage, which is most likely explained by a 50% decrease in surface expression of ADAM10 (Haining et al., 2012). Moreover, in a global study of HUVEC TspanC8s, Tspan5 and Tspan17 were found to negatively regulate VE-cadherin cell surface expression and to promote lymphocyte transmigration in an inflammatory model (Reyat et al., 2017). However, a role of Tspan5/17 in VE-cadherin cleavage was not investigated in this study.

The objectives of this chapter were firstly, to establish *in vitro* HUVEC assays in which ADAM10 activity is required, and secondly, to apply them to investigate the contribution of Tspan15.

6.2 Results

6.2.1 Inactivation of ADAM10, but not Tspan15, promotes HUVEC migration in an *in vitro* scratch wound assay

To assess the functional importance of ADAM10 on HUVEC migration, initially *in vitro* scratch wound assays were performed in the presence or absence of ADAM10 inhibitor (GI254023X). The concentration of 2.5 μM was chosen as it is commonly used at the similar concentration in the other studies (Hundhausen et al., 2003, Moss et al., 2007, Caolo et al., 2015, Mullooly et al., 2015). A confluent monolayer of the cells was wounded and immediately treated with the inhibitor or DMSO as vehicle control, and mitomycin (5 μg/ml) to inhibit proliferation. The images were taken every 6 hours until complete wound closure. As shown in Figure 6.1A-B, inhibition of ADAM10 promoted cell migration. The differences in the wounded area started to be apparent at the 6-hour time point and reached approximately 50% at 18 hours post-wounding, while at 24 hours the wound was completely closed for inhibitor-treated cells but not yet closed for DMSO controls.

To determine whether ADAM10 knockdown would yield a similar phenotype to the inhibitor, the assay was performed in a similar manner following siRNA knockdown of

ADAM10. As shown in Figure 6.1C-D, ADAM10 transfected cells were more motile as indicated by complete wound closure at 24 hours. Similar to the inhibitor, the effect was subtle but significant. Having shown that ADAM10 inhibitor and knockdown promoted cell migration, the assay was performed with Tspan15 siRNA knockdown to identify the effect of the tetraspanin on cell migration. As shown in Figure 6.1F-G, Tspan15 knockdown had no effect on cell migration, as no differences in the area covered by the cells were recorded at any time point. The efficiency of ADAM10 and Tspan15 knockdown was subsequently measured by flow cytometry and was found to be 80-90% (Figure 6.1E-H).

Taken together, these data suggest that ADAM10 is a negative regulator of cell migration in *in vitro* settings, while Tspan15 is not involved.

A

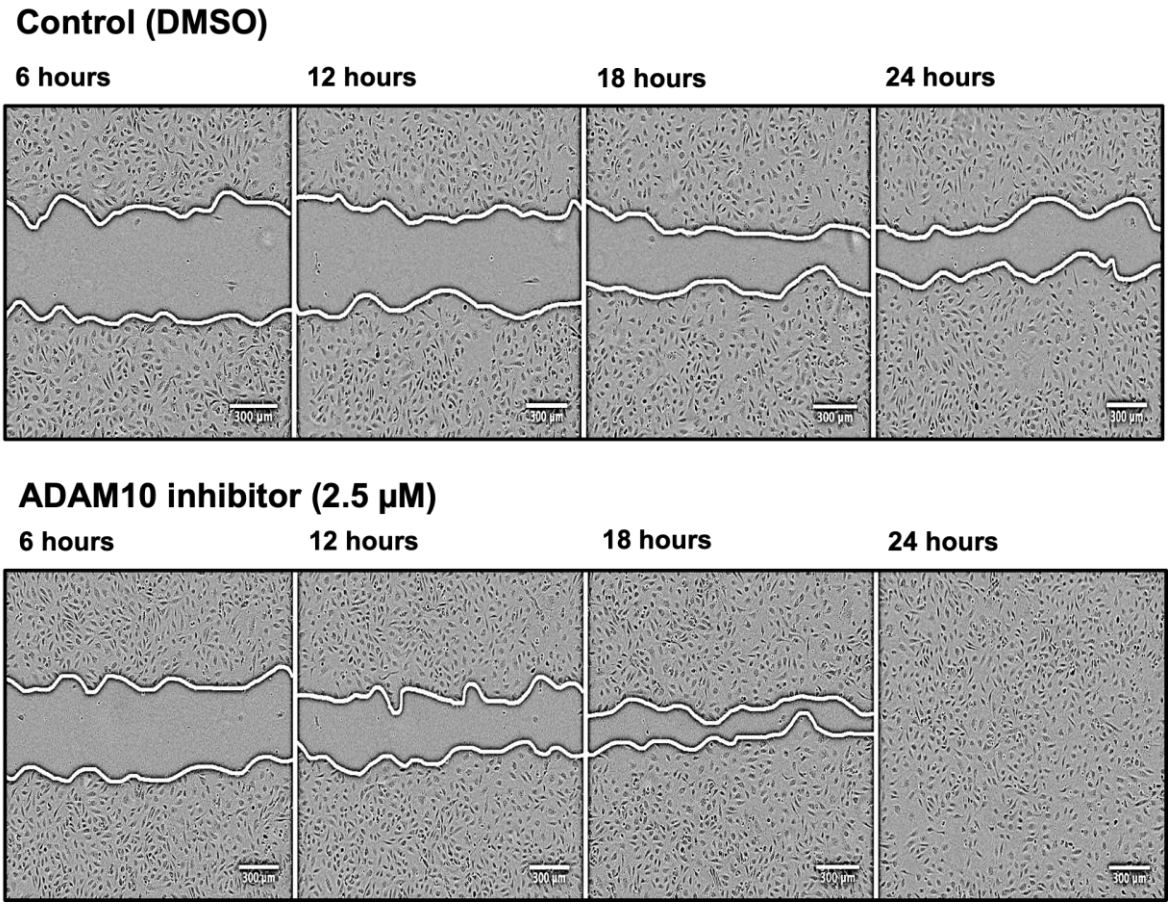
Control (DMSO)
6 hours
12 hours
18 hours
24 hours
ADAM10 inhibitor (2.5 μM)
6 hours
12 hours
18 hours
24 hours

B

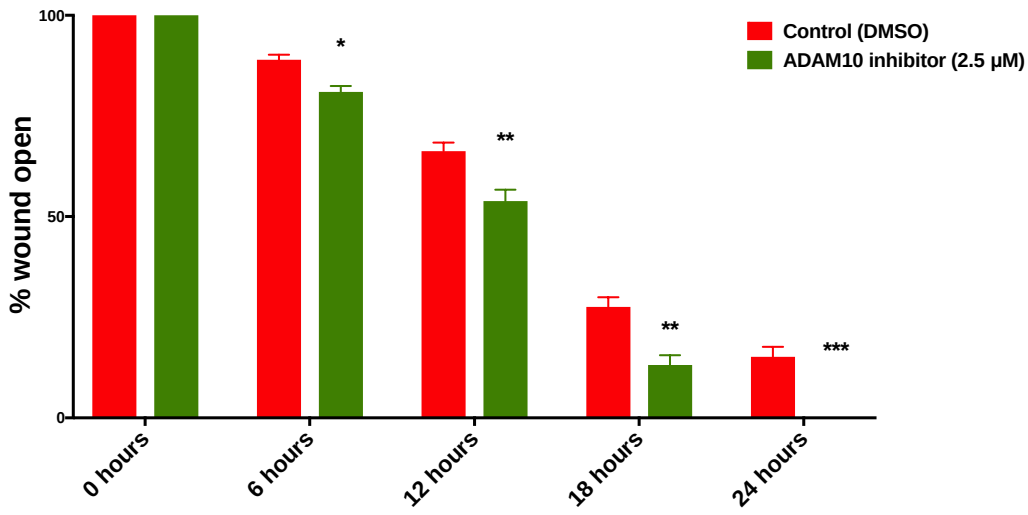
Control (DMSO)
ADAM10 inhibitor (2.5 μM)
% wound open
100
50
0
*
**
**
***
0 hours
6 hours
12 hours
18 hours
24 hours

C

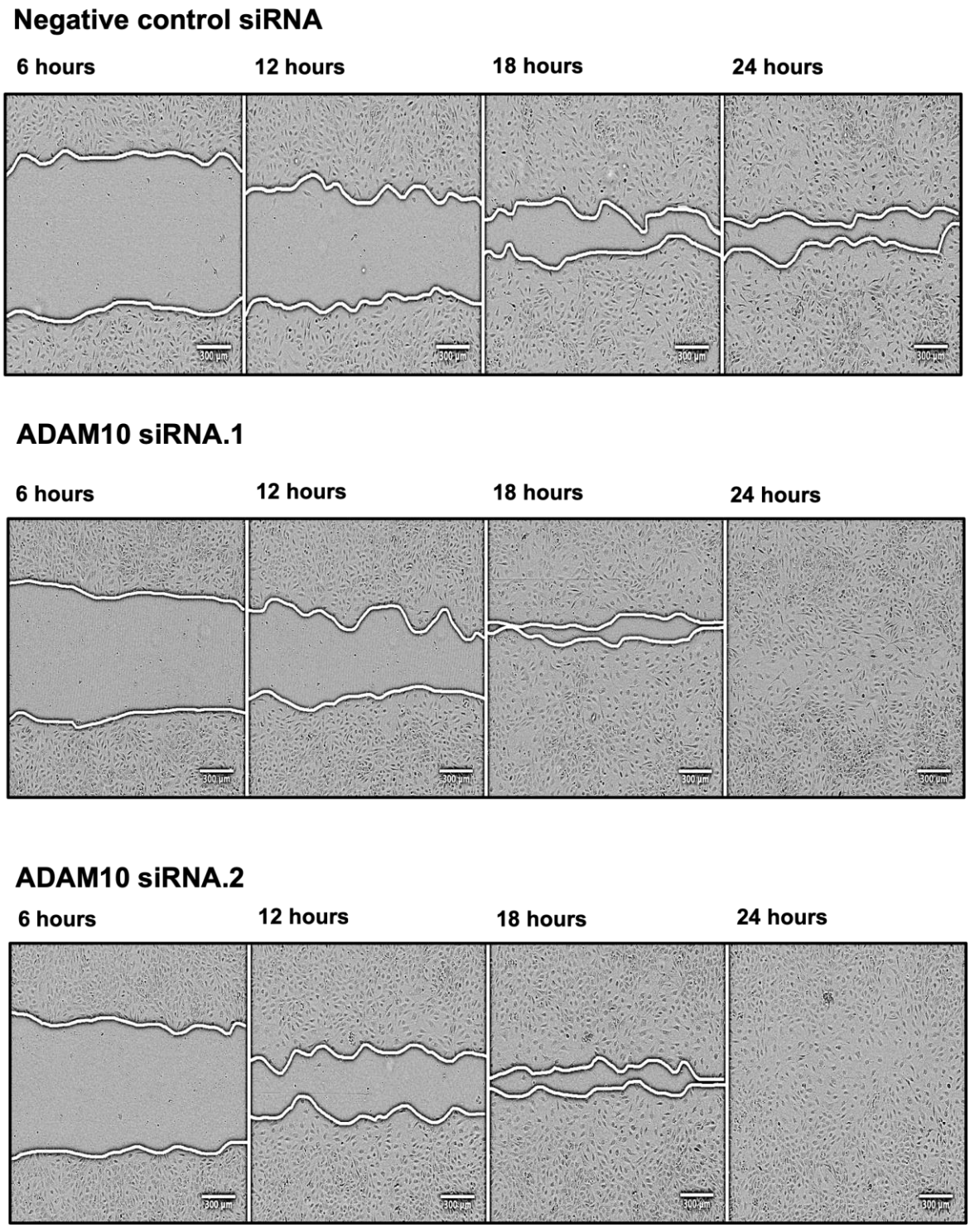
Negative control siRNA
6 hours
12 hours
18 hours
24 hours
ADAM10 siRNA.1
6 hours
12 hours
18 hours
24 hours
ADAM10 siRNA.2
6 hours
12 hours
18 hours
24 hours

D

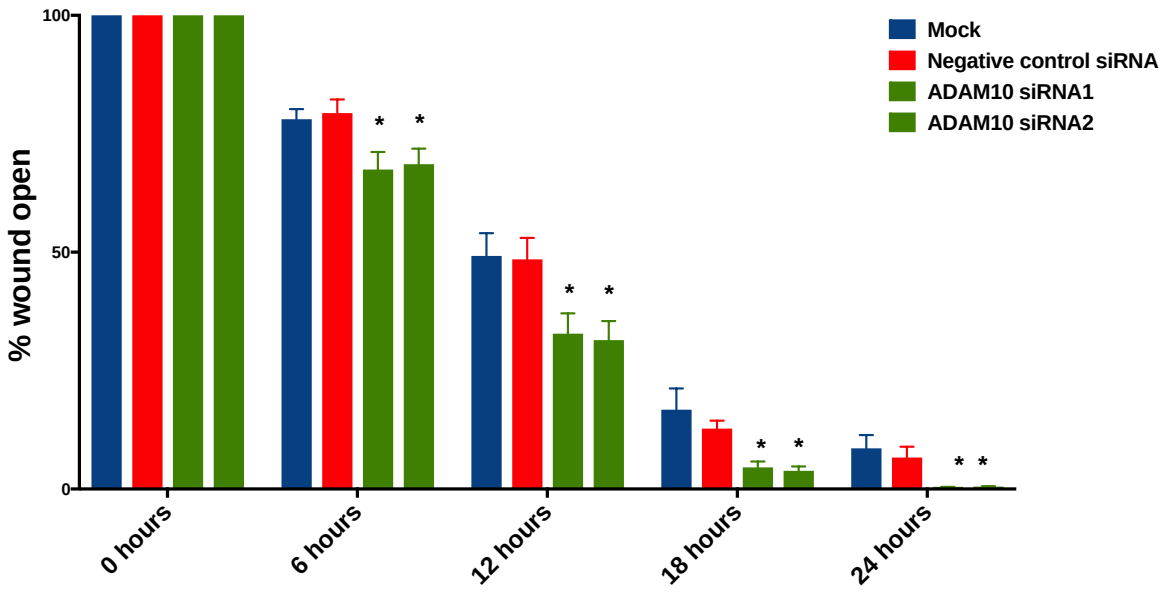
100
50
0
% wound open
Mock
Negative control siRNA
ADAM10 siRNA1
ADAM10 siRNA2
0 hours
6 hours
12 hours
18 hours
24 hours

E

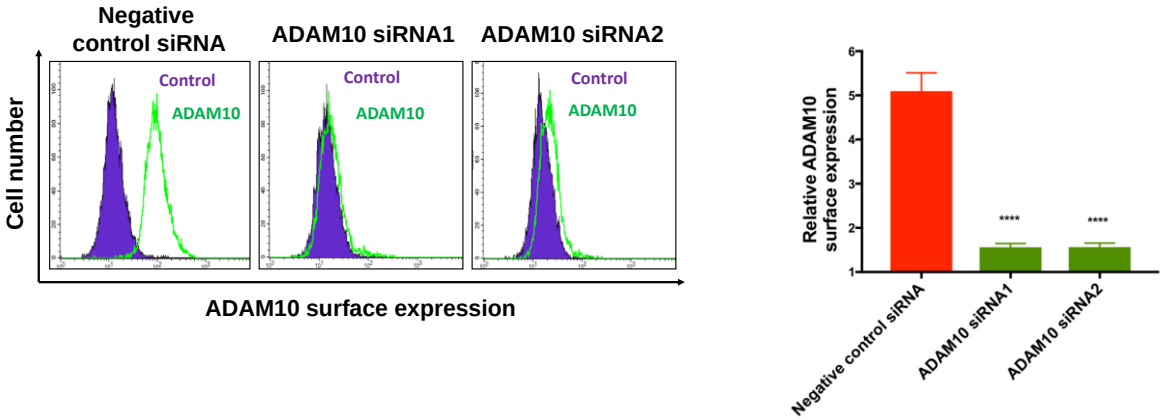
Negative control siRNA
ADAM10 siRNA1
ADAM10 siRNA2
Control
ADAM10
Cell number
ADAM10 surface expression
Relative ADAM10 surface expression
Negative control siRNA
ADAM10 siRNA1
ADAM10 siRNA2

F

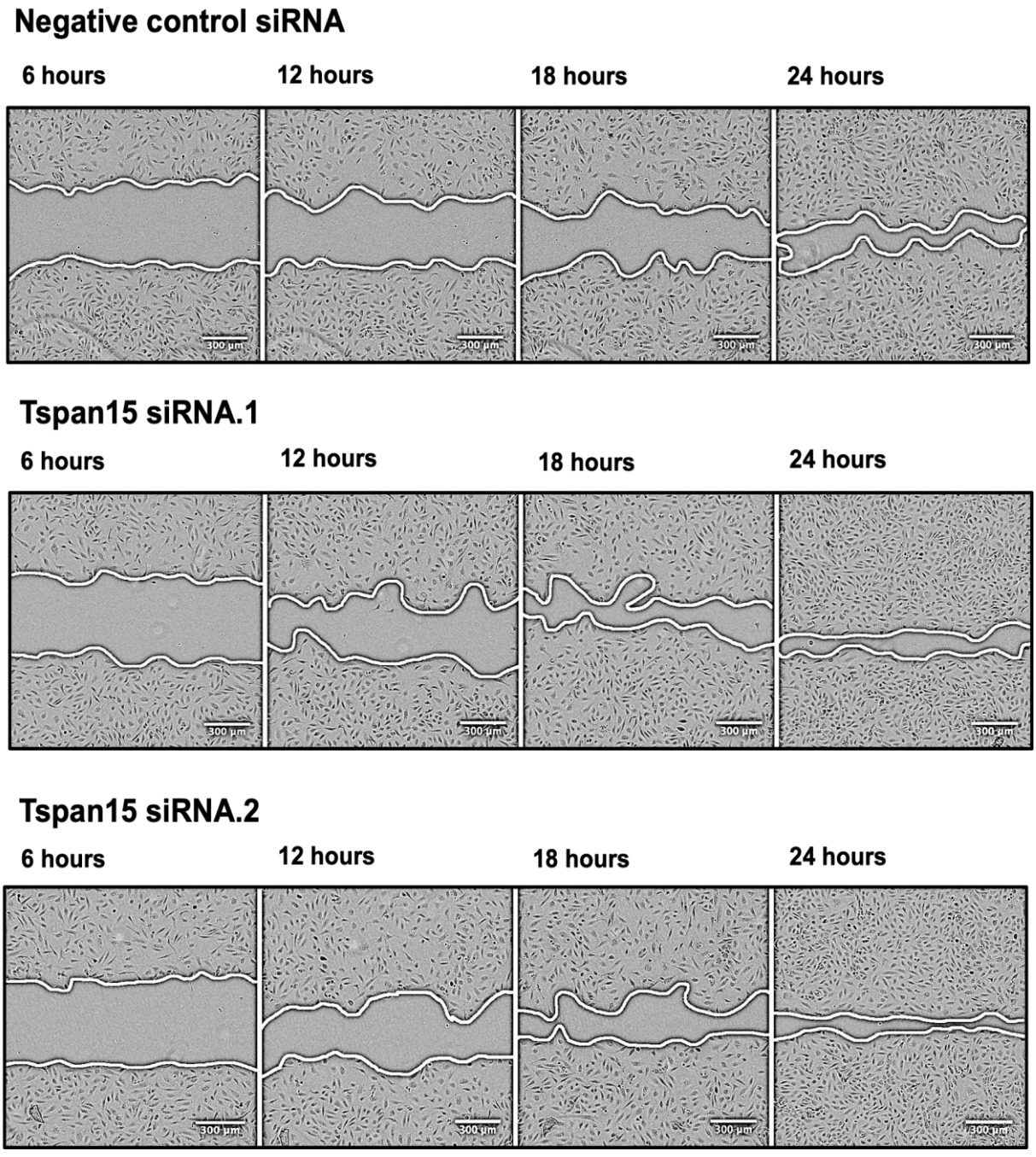
Negative control siRNA
6 hours
12 hours
18 hours
24 hours
300 µm
Tspan15 siRNA.1
6 hours
12 hours
18 hours
24 hours
300 µm
Tspan15 siRNA.2
6 hours
12 hours
18 hours
24 hours
300 µm

G

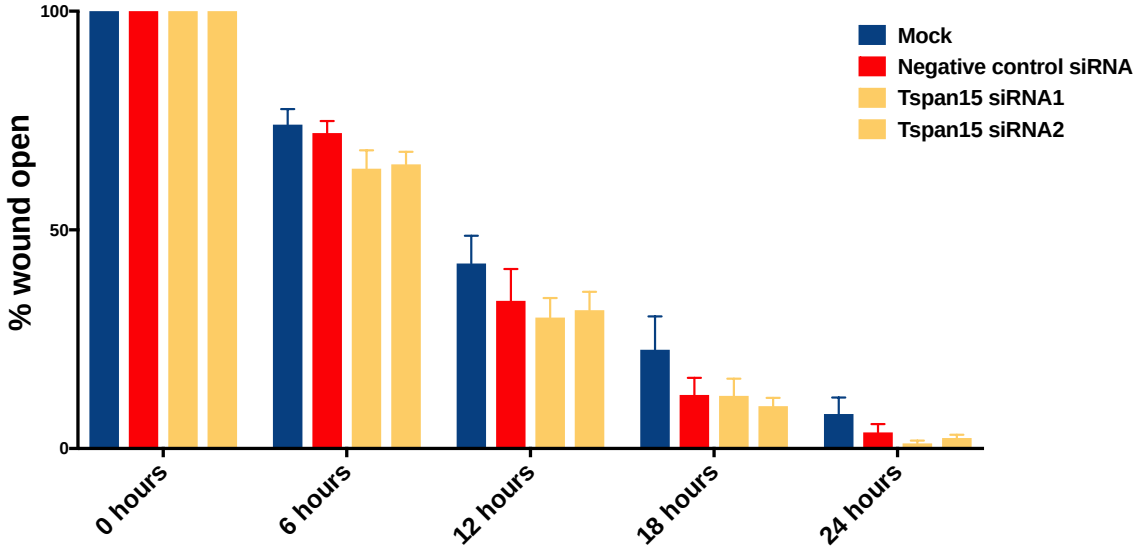

H

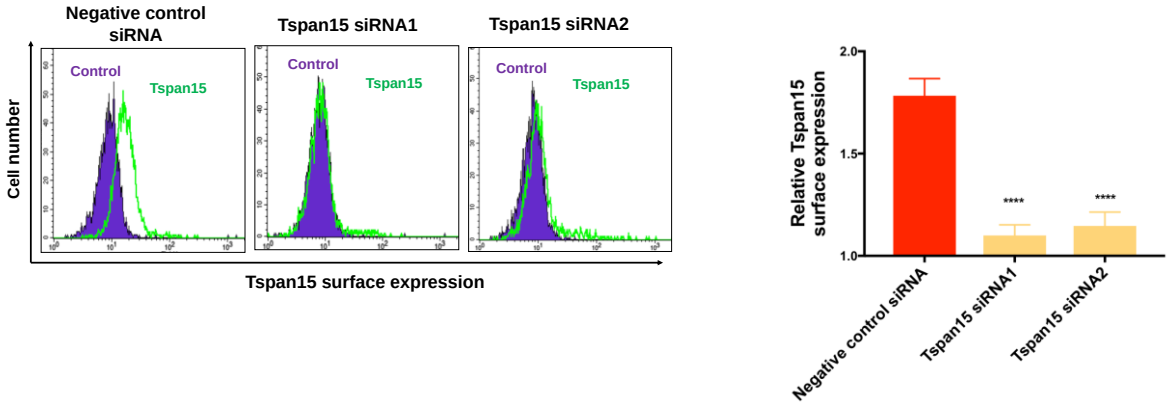

Figure 6.1 Inactivation of ADAM10, but not Tspan15, promotes HUVEC migration in an in vitro scratch wound assay. Migratory phenotypes of HUVEC cells treated with [A-B] 2.5 μM ADAM10 inhibitor (GI254023X), [C-D] ADAM10 siRNA duplexes and [F-G] Tspan15 siRNA duplexes were analysed using an in vitro scratch wound assay. The representative images of the wounded monolayer were taken using the IncuCyte Imaging System. The percentage of the wounded area for each time point was quantified by dividing the area at a given time point by the original area. The initial area was arbitrarily set as 100. Scale bar - 300 μm. [E, H] The ADAM10 and Tspan15 knockdown efficiencies were analysed by flow cytometry. Tspan15 mAb (4A4 clone) was used in a form of tissue culture supernatant. The bar charts represent the mean values from four to six independent experiments, and error bars are the standard error of the mean. Data were normalised by arcsine transformation of the square root and analysed by one-way ANOVA and Dunnett's multiple comparison test as compared to the control of each time point (*$p < 0.05$, **$p < 0.01$, ***$p < 0.001$, ****$p < 0.0001$).

6.2.2 Inactivation of ADAM10, but not Tspan15, impairs HUVEC network formation in an in vitro assay on Matrigel

To determine whether ADAM10 and Tspan15 affect the ability of HUVECs to form two-dimensional networks, cells were cultured on reduced growth factor gel matrix, Matrigel, in the presence of the ADAM10 inhibitor or after being transfected with ADAM10 or Tspan15 siRNA duplexes as previously described. Formation of characteristic networks of orderly branching structures was monitored every 6 hours until its complete decomposition. The stage of network formation was quantified by measuring the number of meshes. ADAM10 inhibition (Figure 6.2A-B) and siRNA-mediated knockdown (Figure 6.2C-D) impaired endothelial network formation. Efficient ADAM10 knockdown was confirmed by flow cytometry (Figure 6.2E). In contrast, Tspan15 knockdown had no significant effect on the network integrity (Figure 6.2F-G); knockdown was confirmed by flow cytometry (Figure 6.2H).

Together this data demonstrates that ADAM10 is required for normal endothelial tube formation *in vitro.* Tspan15 knockdown is not sufficient to mimic the phenotype seen when ADAM10 is knocked down.

A

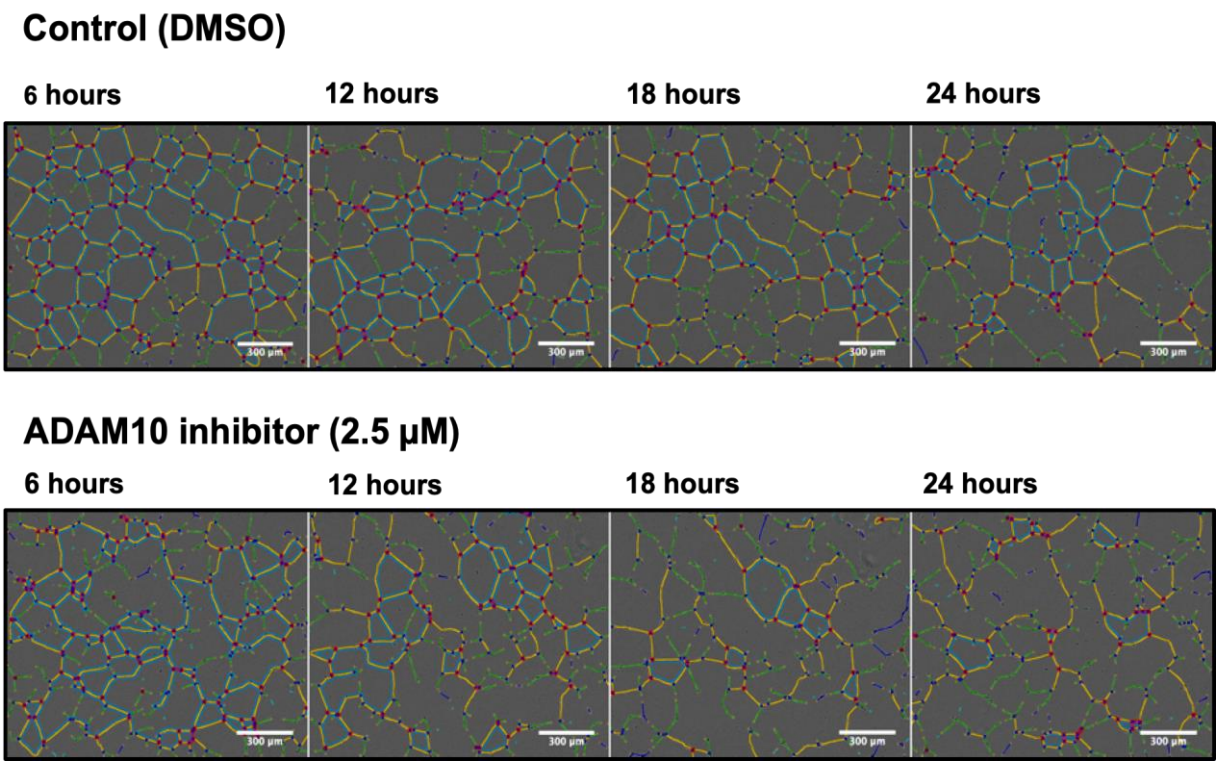
Control (DMSO)
6 hours
12 hours
18 hours
24 hours
ADAM10 inhibitor (2.5 µM)
6 hours
12 hours
18 hours
24 hours

B

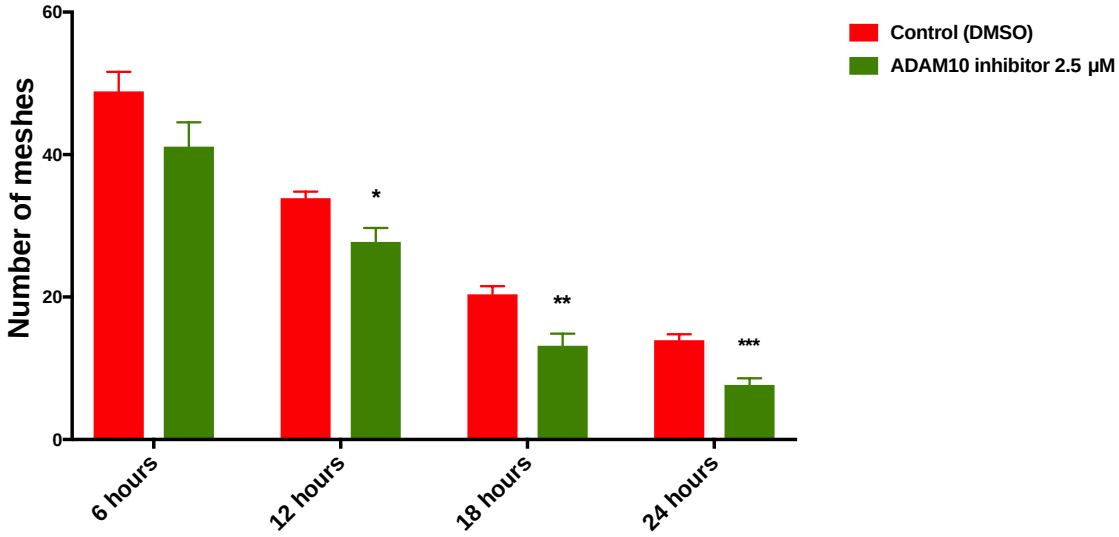
Number of meshes
60
40
20
0
*
**
***
6 hours
12 hours
18 hours
24 hours
Control (DMSO)
ADAM10 inhibitor 2.5 µM

C

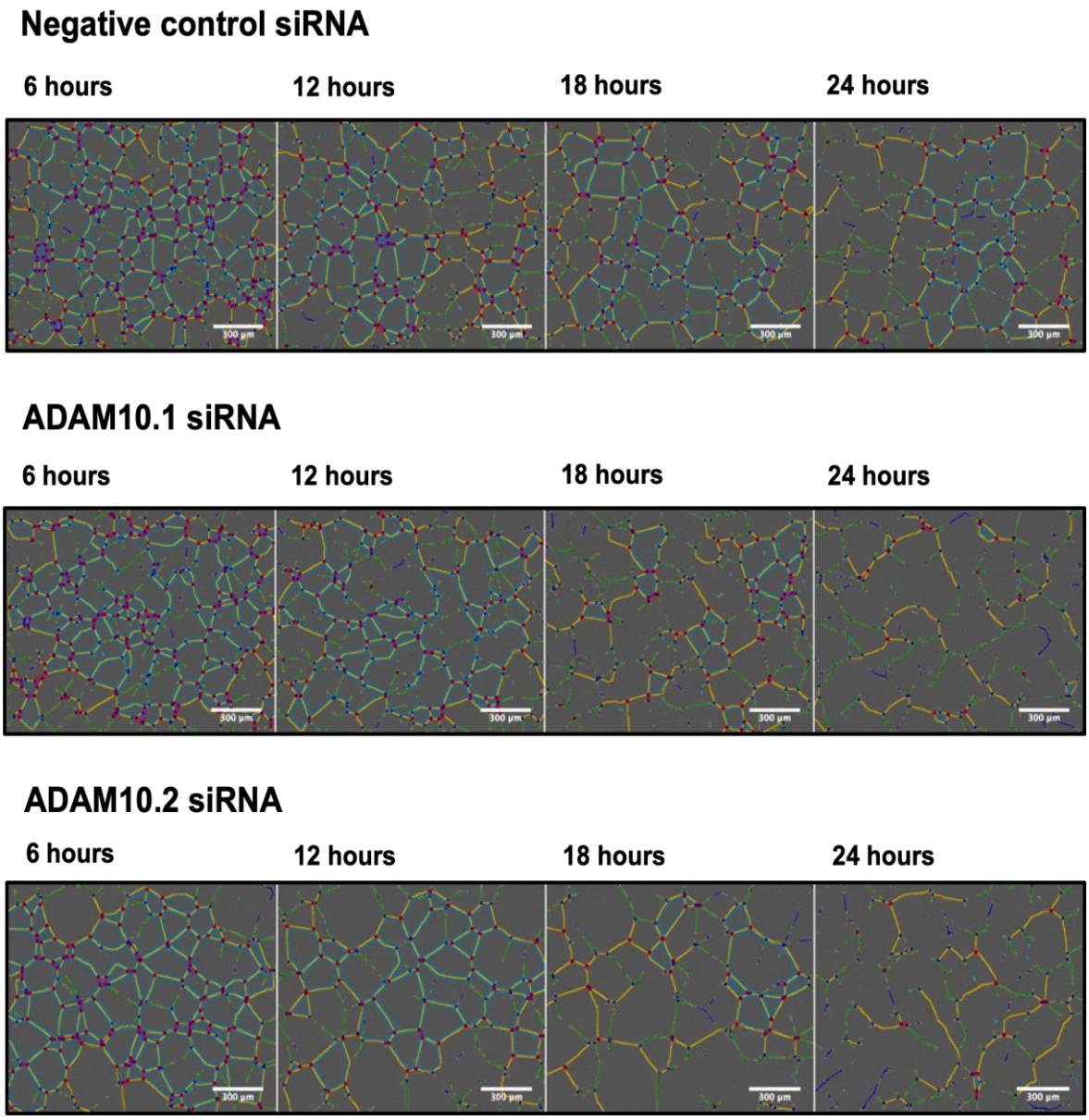
Negative control siRNA
6 hours
12 hours
18 hours
24 hours
ADAM10.1 siRNA
6 hours
12 hours
18 hours
24 hours
ADAM10.2 siRNA
6 hours
12 hours
18 hours
24 hours

D

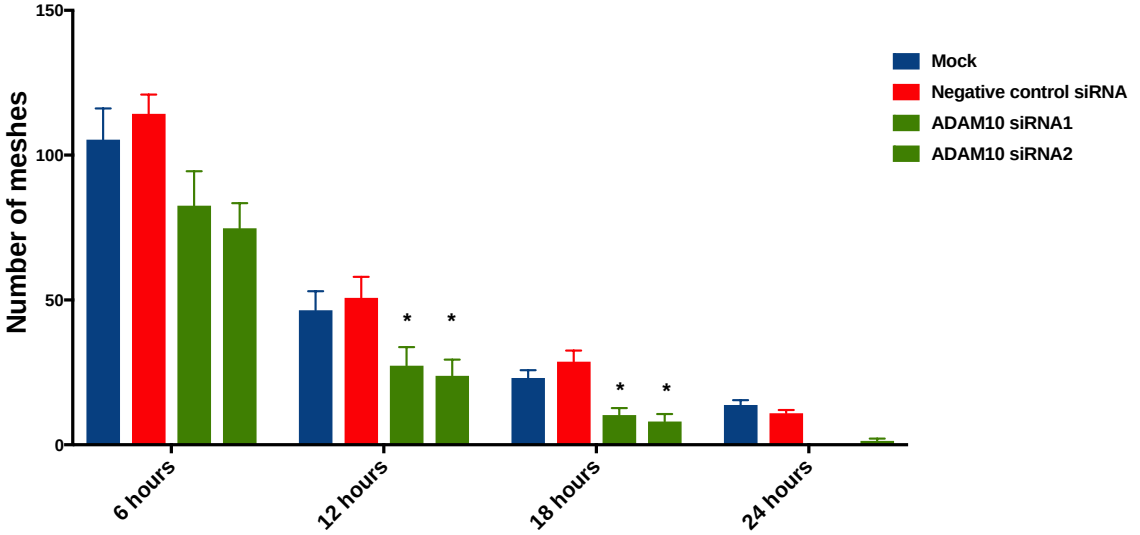
Number of meshes
150
100
50
0
Mock
Negative control siRNA
ADAM10 siRNA1
ADAM10 siRNA2
*
*
*
*
6 hours
12 hours
18 hours
24 hours

E

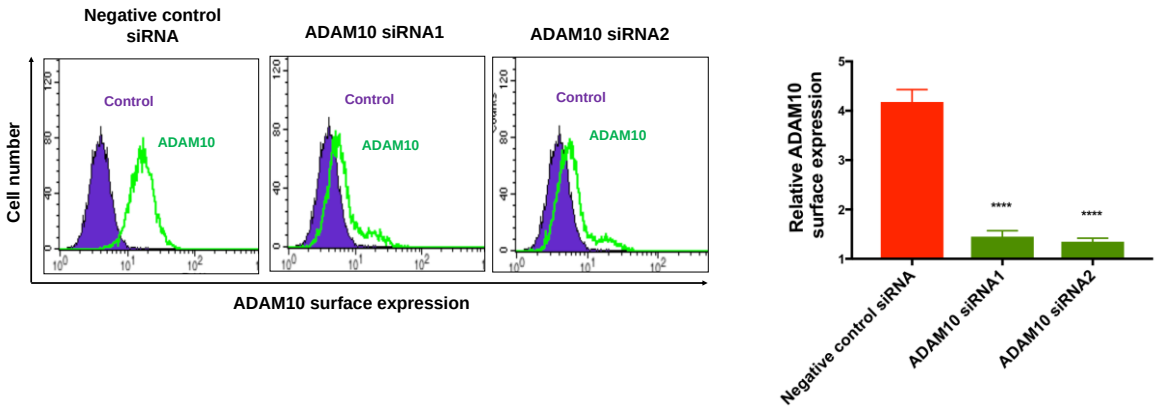
Negative control siRNA
ADAM10 siRNA1
ADAM10 siRNA2
Cell number
Control
ADAM10
ADAM10 surface expression
Relative ADAM10 surface expression
****
****
Negative control siRNA
ADAM10 siRNA1
ADAM10 siRNA2

F

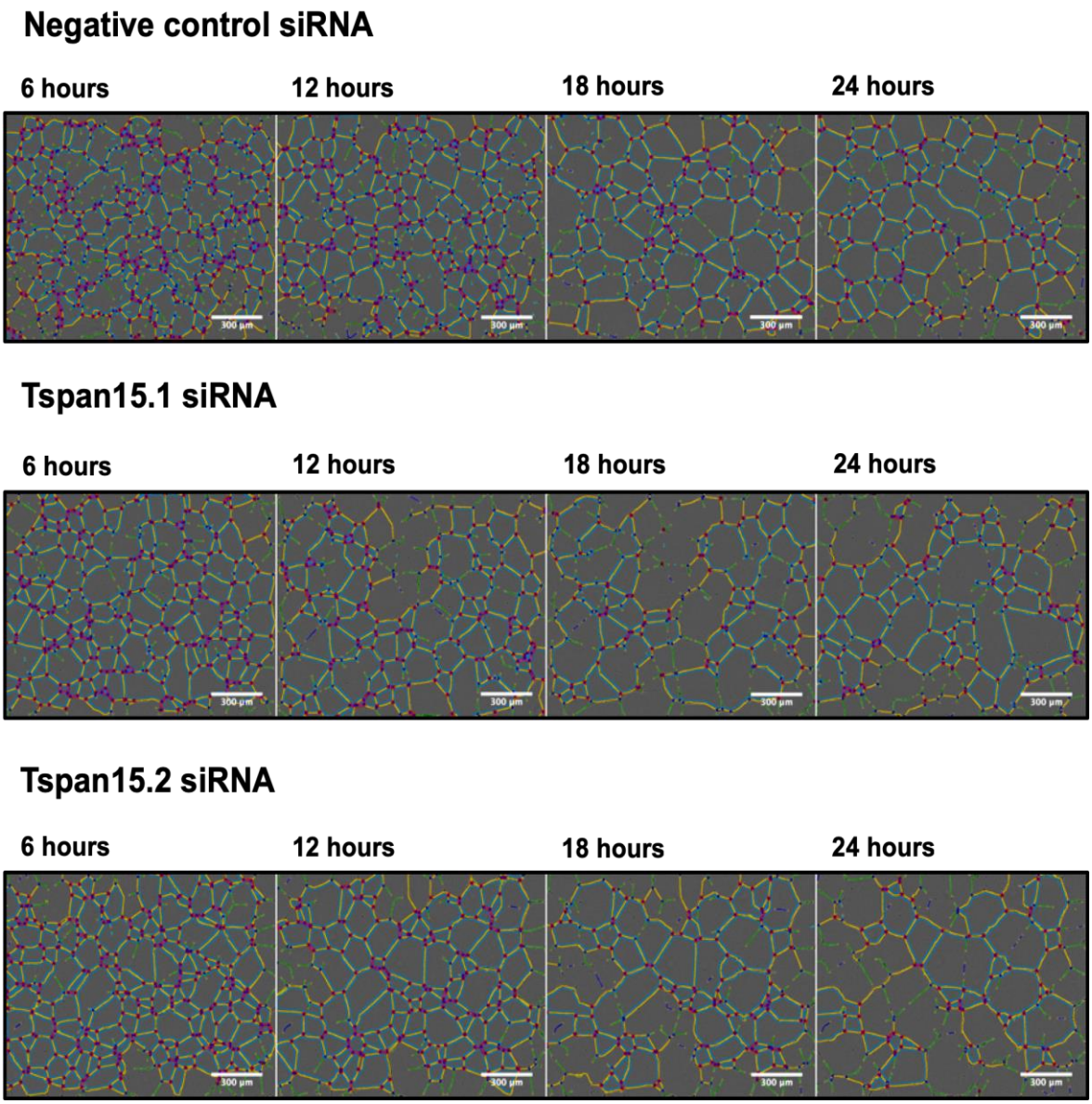
Negative control siRNA
6 hours
12 hours
18 hours
24 hours
Tspan15.1 siRNA
6 hours
12 hours
18 hours
24 hours
Tspan15.2 siRNA
6 hours
12 hours
18 hours
24 hours

G

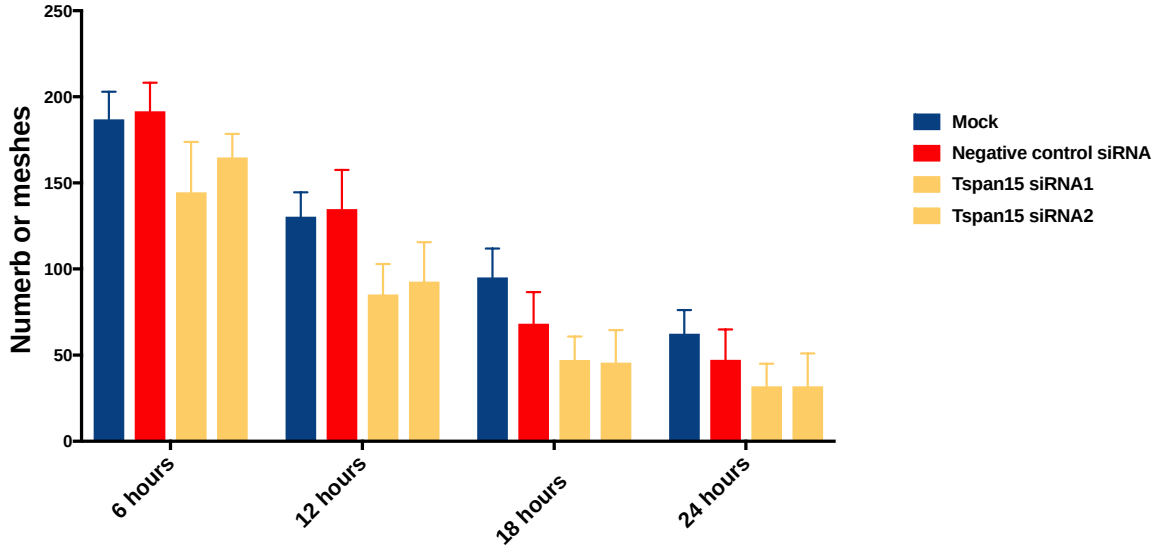

H

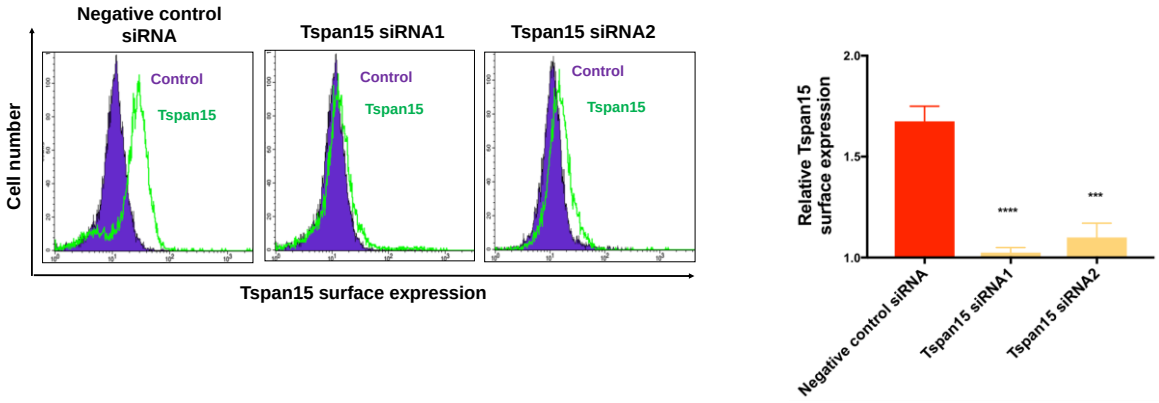

Figure 6.2 Inactivation of ADAM10, but not Tspan15, impairs endothelial network formation in an in vitro assay on Matrigel. HUVEC cells cultured on Matrigel were treated with 2.5 μM of ADAM10 inhibitor [A-B], ADAM10 siRNA duplexes [C-D] or Tspan15 siRNA duplexes [F-G]. The changes in the network were monitored every 6 hours, and representative images are shown. Scale bar - 300 μm. The bar charts represent the average number of meshes for four to six independent experiments, and error bars are the standard error of the mean. Data were normalised by arcsine transformation of the square root and analysed by one-way ANOVA and Dunnett's multiple comparison test as compared to the control (*p<0.05, **p<0.01, ***p < 0.001, ****p < 0.0001). The efficiency of ADAM10 and Tspan15 knockdown was analysed by flow cytometry [E, H]. Tspan15 mAb (clone 4A4) was used in a form of tissue culture supernatant.

6.2.3 HUVECs proliferate faster upon inactivation of ADAM10, but not Tspan15, in an *in vitro* proliferation assay

A role of ADAM10 and Tspan15 on HUVEC proliferation was measured by direct counting of viable cells (determined by the trypan blue exclusion method) following treatments with ADAM10 inhibitor or ADAM10 or Tspan15 siRNA duplexes for a 72-94-hour period. As shown in Figure 6.3A, inhibition of ADAM10 promoted cell proliferation, as did the ADAM10 knockdown (Figure 6.3B). In contrast, Tspan15 knockdown had no effect (Figure 6.3C). Efficient knockdown efficiency was confirmed by flow cytometry (Figure 6.3D-E).

In summary, ADAM10 appears to be a negative regulator of endothelial cell proliferation while Tspan15 is not required.

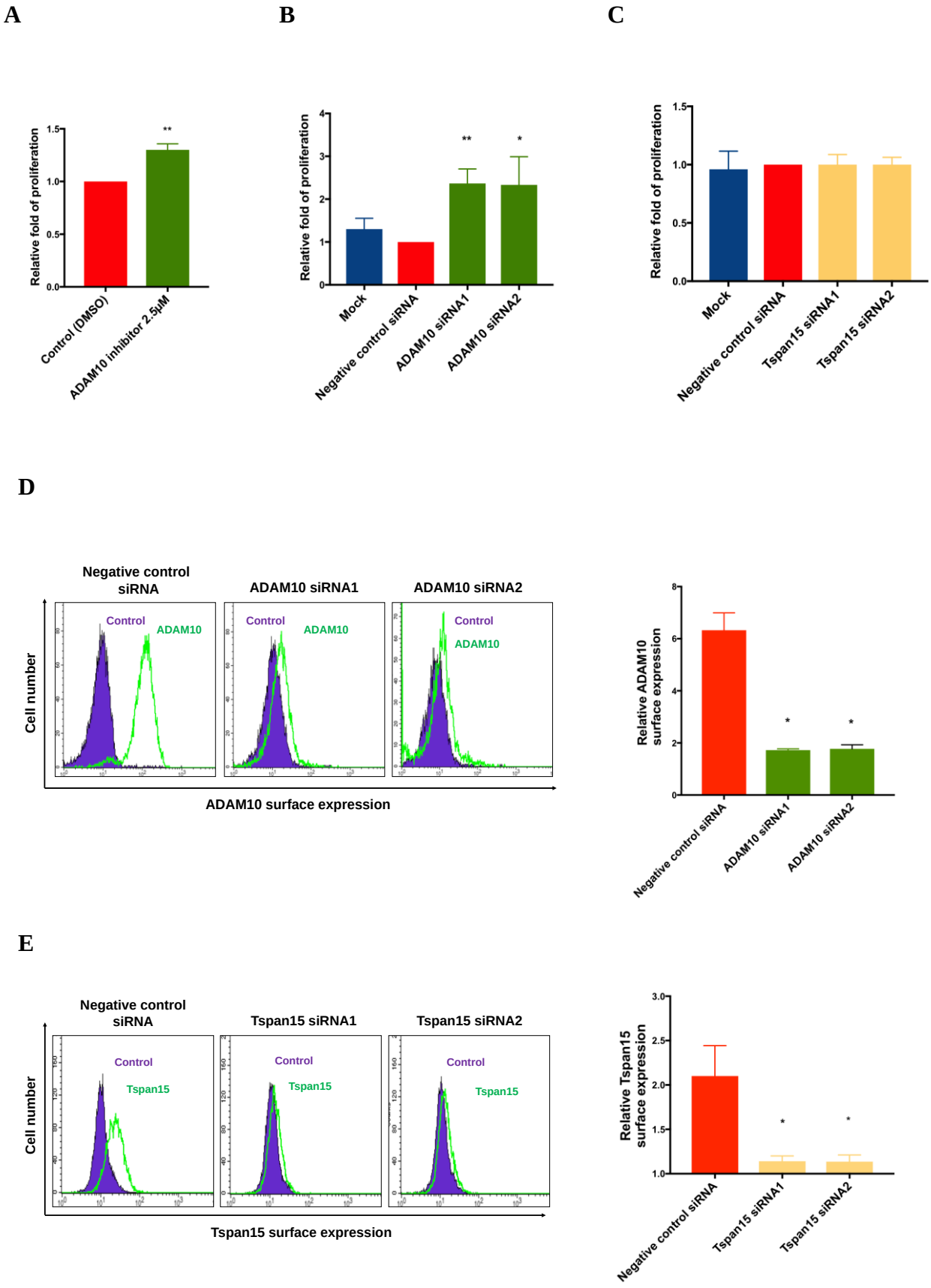
A
B
C
Relative fold of proliferation
Control (DMSO)
ADAM10 inhibitor 2.5μM
Mock
Negative control siRNA
ADAM10 siRNA1
ADAM10 siRNA2
Tspan15 siRNA1
Tspan15 siRNA2
D
Negative control siRNA
ADAM10 siRNA1
ADAM10 siRNA2
Control
ADAM10
Cell number
ADAM10 surface expression
Relative ADAM10 surface expression
E
Tspan15
Tspan15 surface expression
Relative Tspan15 surface expression

Figure 6.3 HUVECs proliferate faster upon inactivation of ADAM10, but not Tspan15, in an in vitro cell proliferation assay. HUVECs were treated with [A] ADAM10 inhibitor at 2.5 μM, [B] ADAM10 siRNA duplexes and [C] Tspan15 siRNA duplexes and cultured for an additional 72-94 hours. The difference in the cell number at the start and at the end of the time course was calculated and presented as a relative fold of proliferation relative to the control sample. The bar charts represent the mean fold of the proliferation from three to four independent experiments, and the error bars are the standard error of the mean. Data were normalised by arcsine transformation of the square root and analysed by a one-way ANOVA and Dunnett's multiple comparison test as compared to the control (*$p<0.05$, **$p<0.01$). The knockdown efficiency for ADAM10 and Tspan15 was determined by flow cytometry [D-E]. Tspan15 mAb (clone 4A4) was used in a form of a tissue culture supernatant.

6.3 Discussion

In this chapter, three *in vitro* angiogenesis assays were used to investigate the role of ADAM10 and Tspan15 in endothelial cell functions. In the assays, HUVEC cells were used as a model system and tested for their *in vitro* migration, proliferation and network formation. The results revealed that pharmacological inhibition, as well as siRNA knockdown, of ADAM10 promoted HUVEC proliferation and migration, but impaired their ability to form and maintain networks on Matrigel. In contrast, the inhibition of Tspan15 had no obvious effects in any of the functions studied.

The phenotypes observed following ADAM10 inhibition or knockdown are clear but not dramatic. The promotion of proliferation and migration were approximately two-fold and the impairment of network formation was about 50%. The latter is consistent with siRNA knockdown of ADAM10 in human microvascular endothelial cells (Isozaki et al., 2013). Therefore, ADAM10 appears to have a modulatory, not essential, role in these in vitro assays. Analysis of the in vitro endothelial cell literature suggests that impaired Notch activation is the mechanism responsible. For example, Williams *et al* showed that over-expression of DLL4 in HUVECs promotes Notch activation and decreases proliferation and migration (Williams et al., 2006), which is consistent with the opposite effects observed in this chapter following ADAM10 inhibition/knockdown to inhibit Notch signalling. Mechanistically, the Williams *et al* data could be explained by effects on gene expression of VEGFR2 and NRP1, since both were down-regulated following Notch activation (Williams et al., 2006). In agreement with the Williams *et al* study, Noseda *et al* found that expression in HUVECs of constitutively active Notch1 or Notch4, namely the

NICDs, decreases proliferation (Noseda et al., 2004). In an earlier paper by Taylor *et al*, expression of dominant negative Notch3 or dominant negative Jagged 1 in HUVECs was found to decrease network formation on Matrigel (Taylor et al., 2002).

In addition to Notch, VE-cadherin may partially explain the defects observed in network formation. Following ADAM10 knockdown, we have found VE-cadherin surface expression to increase by approximately 50% (Reyat et al., 2017). In a study by Abraham *et al*, a partial knockdown or antibody blockade of VE-cadherin increased HUVEC network formation on Matrigel (Abraham et al., 2009). Furthermore, VE-cadherin antibody blockade promoted tube formation in a HUVEC tube formation assay on fibroblasts, and VE-cadherin morpholino knockdown promoted vessel sprouting in a zebrafish model. The proposed mechanism was impaired VE-cadherin signalling, thus impaired Rho-kinase-dependent myosin light-chain 2 phosphorylation, and impaired actomyosin contractility at cell junctions, allowing sprouting to occur (Abraham et al., 2009).

This chapter includes the first functional analysis of Tspan15 in endothelial cells. No effect of Tspan15 knockdown was detected for HUVEC migration, proliferation or network formation, suggesting that one or more of Tspan5/ADAM10, Tspan10/ADAM10, Tspan14/ADAM10 or Tspan17/ADAM10 complexes are regulating these aspects of endothelial cell function. It is likely that Tspan15 regulates N-cadherin shedding in endothelial cells, given its clear role in other cell types (Jouannet et al., 2016, Noy et al., 2016, Prox et al., 2012). This was not examined in this study, but an approximate 50% increase in expression of full-length N-cadherin can be speculated on, in line with the VE-

cadherin data (Reyat et al., 2017). Generation of endothelial-specific N-cadherin knockout mice demonstrated the importance of N-cadherin in endothelial cells, since the mice are embryonic lethal at about day 9.5, due to severe defects in the vasculature, and this is accompanied by a dramatic reduction in VE-cadherin expression, for reasons that are not clear (Luo and Radice, 2005). However, any potential endothelial phenotype in mice with increased N-cadherin expression, due to defective shedding, may be subtle. Indeed, no endothelial cell phenotype was reported in the recent characterisation of Tspan15-knockout mice (Seipold et al., 2018).

In conclusion, this chapter indicates that HUVECs are not a suitable model system to investigate the functional effects of Tspan15/ADAM10 complexes. In future studies, it would be interesting to assess Tspan5, Tspan10 and Tspan14 in HUVECs, using single and combinatorial knockdowns, since they are reported to promote ADAM10-induced Notch signalling in other cell types (Dornier et al., 2012, Jouannet et al., 2016, Saint-Pol et al., 2017(Zhou et al., 2014). It is tempting to speculate that knockdown of one or more of these TspanC8s would impair Notch signalling, and would phenocopy the effects of ADAM10 inhibition/knockdown reported in this chapter.

CHAPTER 7
GENERAL DISCUSSION

7.1 Project overview

The ubiquitously expressed ‘molecular scissor’ ADAM10 can be regarded as a master regulator of health and disease through its role as a sheddase for over 40 proteins, some of which are life-essential (Dreymueller et al., 2015). As such, therapeutic targeting of ADAM10 has a vast potential. However, unlocking that potential is at present impossible because of toxicity which would result from the inactivation of ADAM10 on every cell in the body. The recent identification of the TspanC8 tetraspanins as crucial regulators of ADAM10 has opened the possibility to overcome this problem. The association of ADAM10 with TspanC8s is providing a further understanding of the molecular mechanism behind ADAM10 function on human cells (Saint-Pol et al., 2017b, Matthews et al., 2017b). Therefore, targeting of specific ADAM10/TspanC8 complexes could provide a substrate- and disease-specific therapeutic intervention in diseases where ADAM10’s proteolytic activity is driving disease, or when its activity could be exploited to prevent disease. However, the mechanisms by which ADAM10 is regulated by specific TspanC8s are only just beginning to be interrogated. At present, there is a lack of antibody and knockout mouse

reagents to investigate the endogenous function of specific TspanC8s and their role in affecting ADAM10.

The major aim of the study was to provide new insights into TspanC8/ADAM10 function, using Tspan15 as a model TspanC8. To investigate the function of Tspan15 in regulating ADAM10 activity, mAbs to Tspan15 were generated and validated in-house. In addition, the function of Tspan15 was interrogated using Tspan15 CRISPR/Cas9 knockout cells and siRNA, in epithelial-like cell lines and primary endothelial cells, respectively. Finally, various Tspan15 mutants and chimeric constructs were stably expressed in Tspan15-knockout HEK-293T cells at endogenous levels for structure/function analyses. The main findings showed:

(1) A reciprocal requirement for the regulation of Tspan15 and ADAM10 surface expression exists with the complex (Chapter 3, section 3.2.2).

(2) Tspan15 is required for cleavage of N-, E- and VE-cadherin in epithelial-like cell lines (Chapter 4.1, 4.2).

(3) Two of the four anti-Tspan15 mAbs have inhibitory activity, but this cannot be explained by different epitopes or differential effects on Tspan15 internalisation or ADAM10 expression (Chapter 4.3).

(4) The cytoplasmic tails of Tspan15 are not required for promotion of ADAM10 cell surface localisation and capacity to cleave VE-cadherin following activation by NEM. The Tspan14/15 chimeras appear not to support Tspan15 surface localization or cleavage of VE-cadherin, while mutation of the putative cholesterol binding site has effects that depend on the nature of the mutation: glutamine to glutamic acid substitution at amino acid

position 245 does not support ADAM10 surface expression or VE-cadherin cleavage capacity, but substitution to alanine does (Chapter 5).

(5) Loss of ADAM10 in primary human endothelial cells promotes cell migration, increases proliferation and impairs network formation, but loss of Tspan15 has no effect in these assays.

Due to the fundamental role of ADAM10 and tetraspanins in cell biology, these findings offer a starting point for future studies in exploring the specific purpose of TspanC8/ADAM10 complexes, and their potential therapeutic targeting in a substrate and cell-specific context.

7.2 The Tspan15/ADAM10 molecular scissor

The existing information regarding ADAM10 paints a complex picture, where a single protease is the primary regulator for a broad spectrum of cell surface proteins, giving a wide range of diverse functional consequences in a tissue and substrate-specific manner (Kuhn et al., 2016). Due to the biological importance of substrates cleaved by ADAM10, this protease has essential developmental and tissue-maintenance functions and represents an attractive therapeutic target. ADAM10 targeting could give rise to significant benefits for disease prevention, for instance its ability for non-amyloidogenic α-secretase activity (Postina et al., 2004). Such a therapy may be beneficial to avoid the excessive production

of neurotoxic Aβ species and amyloid plaque formation that are responsible for Alzheimer's disease pathology. ADAM10 is also an attractive therapeutic target for a host of other diseases including, but not limited to, cancer, bacterial infections and inflammatory disease (Wetzel et al., 2017). However, so far, direct targeting of ADAM family members for therapeutic benefit remains a challenge. This failure appears to be a consequence of the ubiquitous nature of any ADAM proteases, and their redundancy, in addition to the physiological importance of the cleaved substrates. Also, global ADAM10 inhibition is likely to result in severe toxicity and may only be useful in topical applications to the skin (Andreas Ludwig, personal communication). To be able to apply ADAM10/protease-based therapies, it is first necessary to successfully discriminate between, or target, a particular protease. In particular, an in-depth understanding of the substrate-specific regulation of ADAM10 is required.

Previous studies have demonstrated that the interaction of ADAM10 with TspanC8 tetraspanins could potentially lead to selective proteolytic processing of different substrates (Matthews et al., 2017b, Saint-Pol et al., 2017). The concept of the 'six molecular scissors', where ADAM10 is regarded as a distinct protease when partnered with each of the TspanC8s, could be applied in therapy design to overcome problems associated with global targeting of ADAM10 (Matthews et al., 2017b). Thus, targeting specific TspanC8s may offer a way to modify ADAM10 functions in more subtle ways, with less likelihood of disrupting vital physiological functions and less unwanted toxic side-effects. In this study, the role of TspanC8s in determining ADAM10 substrate specificity was evaluated using a model of N-cadherin shedding by Tspan15/ADAM10. Tspan15 is of particular interest for several research groups, who have investigated its contribution to the shedding

of APP, Notch and N-cadherins, all involved in various pathologies (Prox et al., 2012, Noy et al., 2016, Dornier et al., 2016, Jouannet et al., 2016).

N-cadherin shedding by ADAM10/Tspan15 is a well-recognised phenomenon *in vitro* and *in vivo.* This was confirmed by multiple groups independently and in various cell line models, indicating that a particular relationship exists between the components of the complex that drives the shedding (Prox et al., 2012, Noy et al., 2016, Dornier et al., 2016, Jouannet et al., 2016). Tspan15 was chosen as the focus of this thesis because it is of particular interest in the Tomlinson lab due to its importance as a biomarker and potential therapeutic target for many pathologies (Germain et al., 2015, Seipold et al., 2018, Zhang et al., 2018).

An important question that arises from the present study concerns the mechanism by which the Tspan15/ADAM10 molecular scissor cleaved cadherins and why is it so efficient in the process?

7.2.1 The main role of Tspan15 is to regulate ADAM10

Direct association between ADAM10 and Tspan15 was previously confirmed in multiple cell lines, reviewed in Matthews et al., 2017b and Saint-Pol et al., 2017b. Importantly, the interaction is specific to ADAM10, as its close relative, ADAM17 does not associate with TspanC8s. In fact, ADAM17 associates with inactive rhomboids 1 and 2 (Adrain et al., 2012, Matthews et al., 2017b). Furthermore, Tspan15 was shown to have a positive effect on ADAM10 expression, and to increase shedding activity of the protease towards N-

cadherin when over-expressed (Prox et al.,2012, Noy et al., 2016, Jouannet et al., 2016). Interestingly, Saint-Pol *et al* have also shown the reciprocal effect whereby ADAM10 also contributes to Tspan5 trafficking and surface localisation, therefore implying that complex formation is a prerequisite for determining activity of the molecular scissor towards Notch (Saint-Pol et al., 2017a). Thus, the current study aimed to test the possible reciprocal dependency between Tspan15 and ADAM10 and investigate how this relationship affects the shedding specificity towards N-cadherin. The ADAM10 and Tspan15 KO cell lines, provided suitable model systems to investigate the reverse impact on ADAM10 and Tspan15 trafficking distributions. While ADAM10 surface expression was partially reduced in Tspan15 KO cells, a significant reduction in Tspan15 surface expression was observed in ADAM10 KO cells, which was also associated with almost complete loss of N-cadherin shedding in both cell lines (section 3.2 and 4.1). This data strongly implies that the primary function of Tspan15 is to regulate ADAM10 surface expression. Indeed, Jouannet *et al* have suggested that Tspan15 has a strong 'affinity' towards ADAM10, which appears to take priority over the interactions of the protease with other tetraspanins. This was established by the observation that the overexpression of Tspan15 inhibited to some extent the interaction of ADAM10 with other constituents of the tetraspanin web (Jouannet et al., 2016). More recently, the Tomlinson and Lichtenthaler groups have combined to show that in proteomic analyses of endogenous Tspan15 immunoprecipitates in the relatively stringent detergent 1% digitonin, ADAM10 was the only significant protein to be identified (unpublished). High levels of Tspan15 have been found in cancer cells (Zhang et al., 2018). Thus, Tspan15 may act, at least in cancer, to enhance the ADAM10-mediated shedding of N- and E-cadherin, as a tumour becomes metastatic following epithelial-mesenchymal-transition (EMT) (Radice, 2013, Wheelock et al., 2008).

Therefore, the regulation of the epithelial cadherins by Tspan15/ADAM10 could provide a potential therapeutic strategy.

7.2.2 Tspan15 localises ADAM10 to N-cadherin

Tspan15 has both positive and negative effect on APP cleavage expressed on different cells (Prox et al., 2012, Jouannet et al., 2016). However, the shedding of N-cadherin seems to be explicitly regulated by Tspan15 regardless of the cell type (Prox et al., 2012, Jouannet et al., 2016, Noy et al., 2016). The reason behind this is unknown, but a direct association between Tspan15 and N-cadherin could occur. Indeed, Jouannet *et al* have shown that N-cadherin was within the repertoire of proteins that were present in the membrane compartments within which Tspan15 resides (Jouannet et al., 2016). CD82 was also able to co-immunoprecipitate N-cadherin in mild detergent, suggesting that the protein is present in tetraspanin microdomains. The fact that CD82 could regulate N-cadherin was evidenced by the reduction of N-cadherin surface expression in CD82-deficient acute myeloid leukaemia (AML) cells (Marjon et al., 2016). Also, E-cadherin was found to interact with tetraspanins, since co-immunoprecipitation revealed that E-cadherin is associated with Tspan8 in colon carcinoma cells (Greco et al., 2010). These data suggest that preferential binding of the tetraspanins to the substrate could contribute to the substrate specificity of the TspanC8/ADAM10 complex.

The subcellular localisation of TspanC8/ADAM10 complexes has been analysed previously in the Tomlinson lab using HEK-293T cells as a model system. A comparison

of the individual molecules has shown the most striking difference between Tspan15, which had plasma membrane localisation, and Tspan10, which was mostly intracellular (unpublished data). Therefore, it could be speculated that as N-cadherin shedding takes place at the plasma membrane, Tspan15 specific surface localisation may contribute to the competence of ADAM10 for its processing. The fact that Tspan15 could bring ADAM10 to close proximity to N-cadherin is further evidenced in the current study utilising chimeric constructs generated by exchanging the extracellular regions between Tspan14 and Tspan15 (Chapter 5.2). The surface expression of the chimeras showed that the transmembrane and cytoplasmic regions of Tspan15 promoted expression of ADAM10 at the surface, and the extracellular regions were necessary for cadherin cleavage. The importance of the cytoplasmic tails was previously shown for CD9 in supporting tetraspanin functions, molecular organisation at the plasma membrane and assembly of its interacting partners into CD9 complexes (Wang et al., 2011). Additionally, the cytoplasmic tail structural determinants of tetraspanins, such as palmitoylation and binding/sorting motifs, turned out to also have a vital impact. For example, the palmitoylation of CD151 had the functional consequence of recruiting and sorting integrin $\alpha 3\beta 1$ within the tetraspanin web and contributed to integrin signalling (Berditchevski et al., 2002). As Tspan15 cytoplasmic tails do not share sequence similarity with other TspanC8s (Matthews et al., 2017b), it may engage with unique intracellular trafficking proteins which may account for why the ADAM10/Tspan15 complex localises to N-cadherin. Indeed, it was shown that specific motifs, like the PDZ-binding motifs in CD151, CD81 and CD9, were essential for controlling their subcellular localisation and protein-protein interactions by as yet unknown interactions (Cao et al., 1999, Hemler, 2005). CD63, through tyrosine-based sorting motifs, interacts with syntenin-1 and adaptor protein

complexes that mediate its intracellular transport (Berditchevski and Odintsova, 2007). Amino acid sequence analysis of the TspanC8s cytoplasmic tails showed the presence of characteristic motifs containing dileucine (LL) and/or leucine repeats (LX_6L) in Tspan10, or tyrosine-based like for Tspan15 (Berditchevski and Odintsova, 2007). The leucine-containing motifs have been shown to be recognised by Rab effectors, that function as regulators of intracellular trafficking pathways (Evans et al., 2002). Therefore, it may be speculated that the cytoplasmic tail of Tspan15 might engage with an intracellular trafficking protein to direct ADAM10 to N-cadherin at the plasma membrane. This could be supported by the observation that Rab14 was required for ADAM10 localisation at the plasma membrane in A549 cells, similar to TspanC8s (Linford et al., 2012). It is worth noting that different Rabs in different cells might be involved in Tspan15/ADAM10 trafficking.

The results presented in Chapter 5.3 and 5.4, using the Tspan15 mutants lacking intracellular N- and C-termini, showed that the tails are actually dispensable for trafficking of the complex and are not a driving factor in the interaction of Tspan15 and ADAM10. This could suggest that additional regulatory mechanisms are involved, presumably at the plasma membrane and independent of trafficking. Jouannet *et al* have indicated that the composition of the plasma membrane and lateral diffusion of the proteins within the nanoclusters could be an essential driving factor in regulating protease specificity. Using co-immunoprecipitation followed by proteomic identification of interacting proteins, it was found that the nanodomain formed by Tspan15 differs to that of Tspan5 in terms of the composition of auxiliary proteins (Jouannet et al., 2016). This may in return change the fluidity of the plasma membrane and allow ADAM10 to ‘intrude’ into the nanodomain

holding the intended substrate. Similarly, the physical properties of tetraspanin nanoclusters was shown to be modulated by cholesterol content. Cholesterol depletion from the nanoclusters was shown to enhance ADAM10 substrate accessibility and cleavage, probably due to disruption of the tetraspanin nanoclusters and/or increased fluidity of the membrane (Charrin et al., 2003, Reiss and Bhakdi, 2017). All of the above could contribute to different actions of ADAM10/Tspan15; when proximal to N-cadherin it promotes the shedding, but when near to Notch shedding is inhibited.

7.2.3 Tspan15 may induce a distinct ADAM10 conformation to promote N-cadherin shedding

Extracellular regions of ADAM10 and TspanC8 have been found to mediate interactions with each other, but the individual TspanC8s require distinct binding domains on ADAM10. In this regard, Tspan15 is unique by requiring a relatively short 'stalk' domain of ADAM10 for its interaction (Noy et al., 2016). Therefore, it was hypothesised that preferential substrate cleavage is dictated by the particular conformational state of ADAM10 induced by a specific TspanC8 (Matthews et al., 2017b). In the current work, it was shown (Chapter 5.2) that the Tspan15/EC14 chimeric contract, which has the localisation properties of Tspan15 but presumably the ADAM10 interaction of Tspan14, was not able to cut N-cadherin, as compared to WT Tspan15. Importantly, the study showed that the involvement of the extracellular regions in regulating ADAM10 activity was analogous to that previously reported for CD151 and $\alpha 3\beta 1$ integrin (Yauch et al., 2000, Berditchevski et al., 2001), CD81 and CD19 (Shoham et al., 2006) or between EWI2

and the related CD9 and CD81 (Montpellier et al., 2011). This type of interaction is well established to be a general feature within the tetraspanin family. The analysis of the TspanC8-specific motifs in the main extracellular region of Tspan5 provided new insight into the functionality of this domain. Indeed, Saint-Pol *et al* identified two conserved motifs that not only determined the specificity of the interactions mediated by the major extracellular region, but also contributed to ER exit and proper folding of the tetraspanin (Saint-Pol et al., 2017a).

In the recently proposed model by Zimmerman et al, the tetraspanins were suggested to be 'molecular switches' that regulate partner protein activity via conformational change (Zimmerman et al., 2016). In the study, the authors used molecular dynamic simulations to show the effect of cholesterol removal on CD81 conformational change, from a 'closed' to 'open' state, and its effect on the partner protein CD19 trafficking. Therefore, a similar strategy was employed with Tspan15 in this thesis, mutating the cholesterol-binding sites within the transmembrane regions. In section 5.8 it was shown that Q245E mutation of the Tspan15 putative cholesterol binding site impairs NEM-induced VE-cadherin cleavage, whereas Q245A mutation has no effect. This data indicates that the putative conformational change in the major extracellular region of Tspan15 could be a driving factor for ADAM10 proteolytic activity towards cadherins through cholesterol depletion.

ADAM10 substrate cleavage sites vary in their position from the plasma membrane, for example 5 amino acids for GPVI (Gardiner et al., 2007), 9 and 10 amino acids for E- and N-cadherin (Uemura et al., 2006, Marambaud et al., 2002), respectively, and 15 amino acids for Notch (van Tetering et al., 2009). It is possible that Tspan15 constrains the ADAM10 catalytic domain to a particular position for optimal shedding of a substrate 9-10

amino acids from the plasma membrane, such as the cadherins. Similarly, Tspan5 and Tspan14 may constrain ADAM10 into a slightly different position for optimal cutting of Notch at 15 amino acids from the plasma membrane. Future experiments could investigate whether changing the distance of the cleavage site on N-cadherin, relative to the plasma membrane, affects shedding by Tspan15/ADAM10. In particular, could N-cadherin be converted into a Tspan5/ADAM10 or Tspan14/ADAM10 substrate by extending the cut site by 5 amino acids? Riethmueller *et al* have suggested that cleavage site localisation regulates substrate proteolysis (Riethmueller et al., 2016). Therefore, this experiment could begin to investigate if distinct modes of interactions within ADAM10/TspanC8 complexes indeed contribute to substrate specificity.

In the present study, the regulatory function of the Tspan15 mutants on ADAM10-mediated VE-cadherin cleavage was tested following NEM stimulation to activate ADAM10 (Chapter 5.7). However, NEM is thought to directly activate ADAM10 by alkylation of cysteine residues, so bypassing the intracellular signalling events, including Ca^{2+} elevation, that activate ADAM10 under physiological conditions. The cytoplasmic tails of Tspan15 were found not to be required for Tspan15/ADAM10 cleavage of VE-cadherin in response to NEM, but the use of NEM may have failed to reveal the true importance of the Tspan15 cytoplasmic tails in inducing ADAM10 activity. A hypothetical model for Tspan15 triggering of ADAM10 activity is shown in Figure 7.1A. The general idea behind the regulation could be that growth factors, for example VEGF, induce signalling to activate phospholipase Cγ (PLCγ), which results in elevation of intracellular Ca^{2+}. This could activate serine/threonine kinases that phosphorylate serine and threonine residues in the Tspan15 cytoplasmic tail. The phosphorylation may induce a

conformational change in Tspan15, which in turn causes a conformational change in the ADAM10 ectodomain, hence activating it. In contrast, NEM stimulation would bypass this activation mechanism (Figure 7.1B). This hypothesis offers a starting point for future studies where the function of Tspan15 mutants could be tested by the use of physiologically relevant inducers of ADAM10 activity, such as growth factors.

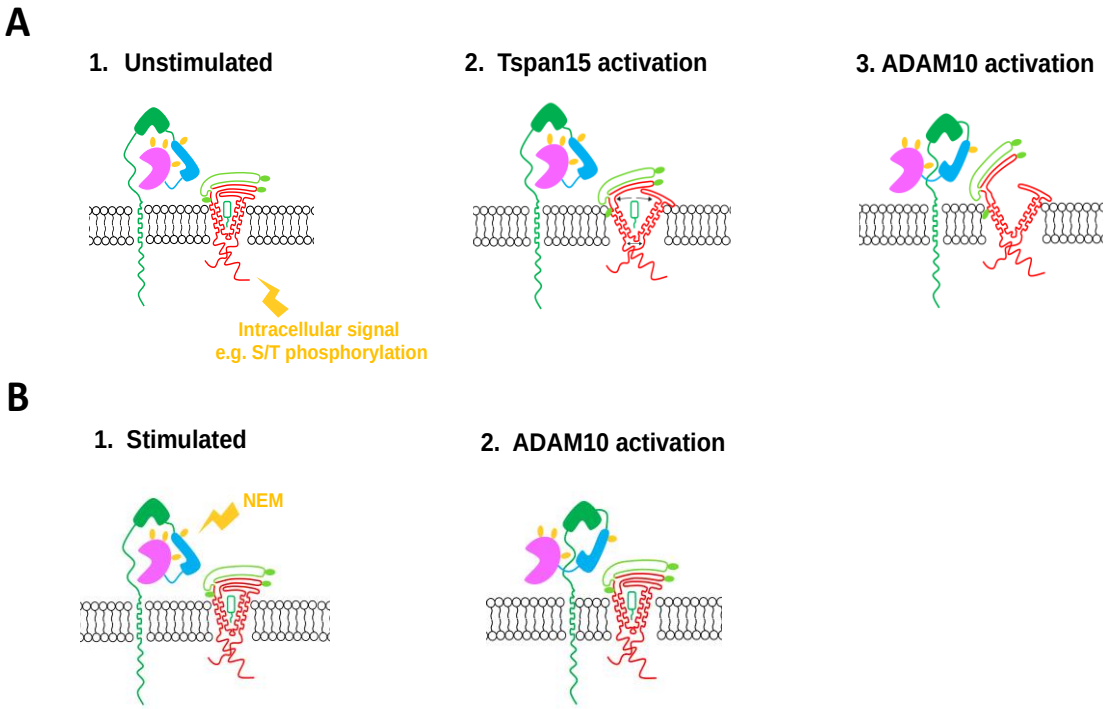

Figure 7.1 Speculative model of ADAM10 triggering by Tspan15 through intracellular signal activation [A] versus NEM stimulation [B]. [A-1] In the unstimulated state, ADAM10 and Tspan15 are expressed on the cell surface, but the constitutive sheddase activity is low. [A-2] Stimulation with growth factors or Ca^{2+} influx induces intracellular signalling that may lead to phosphorylation of serine/threonine residues in cytoplasmic tails of Tspan15. This may cause a conformational change in the tails that is transmitted to the transmembranes to slightly open the cholesterol-binding cavity and compromises cholesterol binding. [A-3] Loss of cholesterol changes the Tspan15 conformation from the closed to the open state. The open structure of Tspan15 induces a conformational change in ADAM10 that relieves the partial obscuring of the active site by the cysteine-rich region, so allowing it to cut substrate. [B-1 and B-2] Stimulation of ADAM10 with the alkylating agent NEM directly activates the metalloprotease domain, without any effect on the associated Tspan15.

7.3 What does the future hold for Tspan15?

7.3.1 Tspan15 and cancer

Tspan15 is substantially upregulated in cholangio carcinoma, pancreatic adenocarcinoma and ovarian serous cystadenocarcinoma, and Tspan15 expression is associated with poor patient survival in liver, kidney and pancreatic cancer (Tang et al., 2017). In addition, over-expression of Tspan15 was recently reported in oesophageal squamous cell carcinoma, which was associated with metastasis and poor survival. Indeed, Tspan15 over-expression in oesophageal cancer cell lines increased their migration in vitro and promoted their tumour formation in mice. Complementary to this, Tspan15 knockdown reduced in vivo tumour formation (Zhang et al., 2018). The authors presented evidence suggesting that the E3 ubiquitin ligase BTRC interacts with Tspan15 to promote NF-κB activation and drive tumour progression. However, these experiments were not definitive, as explained in section 1.4.2. It would informative in future to test whether Tspan15 interacts specifically with BTRC using Tspan15-knockout cells as the ideal control. In addition, both Tspan15-knockout and ADAM10-knockout cancer cell lines could be tested for tumour formation in mouse models; if both have reduced tumour formation it would suggest that Tspan15 exerts its oncogenic effects through ADAM10. Further experiments could then investigate which Tspan15/ADAM10 substrates are responsible. Potential candidates include E- and N-cadherin, due to their roles in epithelial-to-mesenchymal transition (EMT), and the growth factors EGF and betacellulin, which the Tomlinson lab have shown to be predominantly cleaved by Tspan15/ADAM10 (unpublished).

7.3.2 Tspan15 and bacterial infection

ADAM10 is activated by pore-forming bacterial toxins, including pneumolysin from *Streptococcus pneumoniae* and α-haemolysin from *Staphylococcus aureus*, the latter of which can interact with ADAM10. This causes ADAM10 cleavage of E-cadherin on epithelial cells and VE-cadherin on endothelial cells to weaken cell-cell junctions and promote bacterial spread (Berube and Bubeck Wardenburg, 2013, Powers et al., 2015, Thomer et al., 2016).

The data in this thesis suggest that Tspan15/ADAM10 is a critical mediator of bacterial toxin-induced cadherin shedding, at least for E-cadherin. Indeed, an exome sequencing project recently implicated a Tspan15 SNP as a susceptibility factor in *Streptococcus pneumoniae* infection (Salas et al., 2018). Future experiments could assess the Tspan15 knockout mouse (Seipold et al., 2018) for susceptibility to bacterial infection; a prediction is that they will be protected to a similar extent as ADAM10-knockout mice. If so, the Tspan15 mAbs 1C12 and 4A4, which this thesis has shown to impair Tspan15/ADAM10 activity towards cadherins, could be tested for a capacity to reduce bacterial infection. This could initially be done in A549, a lung epithelial cell line model that is used in the *Streptococcus pneumoniae* field, and our existing ADAM10- and Tspan15-knockout cells would provide useful confirmatory data. Ultimately a mouse infection model would be ideal to test the mAbs, but since they recognise mouse Tspan15 relatively weakly, a Tspan15-humanised mouse would be required.

7.4 Concluding remarks

Overall, the results presented in this thesis contribute to the broader understanding of the regulation of ADAM10 by the TspanC8s. Each results chapter opens new avenues for future research into the potential therapeutic targeting of Tspan15. This may provide novel means of improving specificity and reducing toxicity, compared to global inhibition of ADAM10.

Reference list

ABRAHAM, S., YEO, M., MONTERO-BALAGUER, M., PATERSON, H., DEJANA, E., MARSHALL, C. J. & MAVRIA, G. 2009. VE-Cadherin-mediated cell-cell interaction suppresses sprouting via signaling to MLC2 phosphorylation. *Curr Biol,* 19**,** 668-74.

ADAIR, T. H. & MONTANI, J. P. 2010. *Angiogenesis.* San Rafael (CA).

ADRAIN, C., ZETTL, M., CHRISTOVA, Y., TAYLOR, N. & FREEMAN, M. 2012. Tumor necrosis factor signaling requires iRhom2 to promote trafficking and activation of TACE. *Science,* 335**,** 225-8.

AIRD, W. C. 2012. Endothelial cell heterogeneity. *Cold Spring Harb Perspect Med,* 2**,** a006429.

ALABI, R. O., FARBER, G. & BLOBEL, C. P. 2018. Intriguing Roles for Endothelial ADAM10/Notch Signaling in the Development of Organ-Specific Vascular Beds. *Physiol Rev,* 98**,** 2025-2061.

ALABI, R. O., GLOMSKI, K., HAXAIRE, C., WESKAMP, G., MONETTE, S. & BLOBEL, C. P. 2016. ADAM10-Dependent Signaling Through Notch1 and Notch4 Controls Development of Organ-Specific Vascular Beds. *Circ Res,* 119**,** 519-31.

ALTMEPPEN, H. C., PROX, J., KRASEMANN, S., PUIG, B., KRUSZEWSKI, K., DOHLER, F., BERNREUTHER, C., HOXHA, A., LINSENMEIER, L., SIKORSKA, B., LIBERSKI, P. P., BARTSCH, U., SAFTIG, P. & GLATZEL, M. 2015. The sheddase ADAM10 is a potent modulator of prion disease. *Elife,* 4.

AMOUR, A., KNIGHT, C. G., WEBSTER, A., SLOCOMBE, P. M., STEPHENS, P. E., KNAUPER, V., DOCHERTY, A. J. & MURPHY, G. 2000. The in vitro activity ADAM-10 is inhibited by TIMP-1 and TIMP-3. *FEBS Lett,* 473**,** 275-9.

ANDERS, A., GILBERT, S., GARTEN, W., POSTINA, R. & FAHRENHOLZ, F. 2001. Regulation of the alpha-secretase ADAM10 by its prodomain and proprotein convertases. *FASEB J,* 15**,** 1837-9.

ARDUISE, C., ABACHE, T., LI, L., BILLARD, M., CHABANON, A., LUDWIG, A., MAUDUIT, P., BOUCHEIX, C., RUBINSTEIN, E. & LE NAOUR, F. 2008. Tetraspanins regulate ADAM10-mediated cleavage of TNF-alpha and epidermal growth factor. *J Immunol,* 181**,** 7002-13.

ASHINA, K., TSUBOSAKA, Y., NAKAMURA, T., OMORI, K., KOBAYASHI, K., HORI, M., OZAKI, H. & MURATA, T. 2015. Histamine Induces Vascular Hyperpermeability by Increasing Blood Flow and Endothelial Barrier Disruption In Vivo. *PLoS ONE,* 10**,** e0132367.

ATAPATTU, L., LACKMANN, M. & JANES, P. W. 2014. The role of proteases in regulating Eph/ephrin signaling. *Cell Adhesion & Migration,* 8**,** 294-307.

BAI, S., NASSER, M. W., WANG, B., HSU, S. H., DATTA, J., KUTAY, H., YADAV, A., NUOVO, G., KUMAR, P. & GHOSHAL, K. 2009. MicroRNA-122 inhibits tumorigenic properties of hepatocellular carcinoma cells and sensitizes these cells to sorafenib. *J Biol Chem,* 284**,** 32015-27.

BARREIRO, O., ZAMAI, M., YANEZ-MO, M., TEJERA, E., LOPEZ-ROMERO, P., MONK, P. N., GRATTON, E., CAIOLFA, V. R. & SANCHEZ-MADRID, F. 2008.

Endothelial adhesion receptors are recruited to adherent leukocytes by inclusion in preformed tetraspanin nanoplatforms. *J Cell Biol,* 183**,** 527-42.

BENDER, M., HOFMANN, S., STEGNER, D., CHALARIS, A., BOSL, M., BRAUN, A., SCHELLER, J., ROSE-JOHN, S. & NIESWANDT, B. 2010. Differentially regulated GPVI ectodomain shedding by multiple platelet-expressed proteinases. *Blood,* 116**,** 3347-55.

BERDITCHEVSKI, F., GILBERT, E., GRIFFITHS, M. R., FITTER, S., ASHMAN, L. & JENNER, S. J. 2001. Analysis of the CD151-alpha3beta1 integrin and CD151-tetraspanin interactions by mutagenesis. *J Biol Chem,* 276**,** 41165-74.

BERDITCHEVSKI, F. & ODINTSOVA, E. 2007. Tetraspanins as regulators of protein trafficking. *Traffic,* 8**,** 89-96.

BERDITCHEVSKI, F., ODINTSOVA, E., SAWADA, S. & GILBERT, E. 2002. Expression of the palmitoylation-deficient CD151 weakens the association of alpha 3 beta 1 integrin with the tetraspanin-enriched microdomains and affects integrin-dependent signaling. *J Biol Chem,* 277**,** 36991-7000.

BERUBE, B. J. & BUBECK WARDENBURG, J. 2013. Staphylococcus aureus alpha-toxin: nearly a century of intrigue. *Toxins (Basel),* 5**,** 1140-66.

BLANCO, R. & GERHARDT, H. 2013. VEGF and Notch in Tip and Stalk Cell Selection. *Cold Spring Harbor Perspectives in Medicine,* 3.

BLOBEL, C. P. 2005. ADAMs: key components in EGFR signalling and development. *Nat Rev Mol Cell Biol,* 6**,** 32-43.

BRASCH, J., HARRISON, O. J., HONIG, B. & SHAPIRO, L. 2012. Thinking outside the cell: how cadherins drive adhesion. *Trends Cell Biol,* 22**,** 299-310.

BUCHER, F., FRIEDLANDER, M. & YEA, K. 2018. Antibody targeting TSPAN12/beta-catenin signaling in vasoproliferative retinopathy. *Oncotarget,* 9**,** 12538-12539.

BUCHER, F., ZHANG, D., AGUILAR, E., SAKIMOTO, S., DIAZ-AGUILAR, S., ROSENFELD, M., ZHA, Z., ZHANG, H., FRIEDLANDER, M. & YEA, K. 2017. Antibody-Mediated Inhibition of Tspan12 Ameliorates Vasoproliferative Retinopathy Through Suppression of beta-Catenin Signaling. *Circulation,* 136**,** 180-195.

CAESCU, C. I., JESCHKE, G. R. & TURK, B. E. 2009. Active-site determinants of substrate recognition by the metalloproteinases TACE and ADAM10. *Biochem J,* 424**,** 79-88.

CANOBBIO, I., VISCONTE, C., MOMI, S., GUIDETTI, G. F., ZARA, M., CANINO, J., FALCINELLI, E., GRESELE, P. & TORTI, M. 2017. Platelet amyloid precursor protein is a modulator of venous thromboembolism in mice. *Blood,* 130**,** 527-536.

CAO, T. T., DEACON, H. W., RECZEK, D., BRETSCHER, A. & VON ZASTROW, M. 1999. A kinase-regulated PDZ-domain interaction controls endocytic sorting of the beta2-adrenergic receptor. *Nature,* 401**,** 286-90.

CAOLO, V., SWENNEN, G., CHALARIS, A., WAGENAAR, A., VERBRUGGEN, S., ROSE-JOHN, S., MOLIN, D. G., VOOIJS, M. & POST, M. J. 2015. ADAM10 and ADAM17 have opposite roles during sprouting angiogenesis. *Angiogenesis,* 18**,** 13-22.

CARMELIET, P. 2005a. Angiogenesis in life, disease and medicine. *Nature,* 438**,** 932-6.

CARMELIET, P. 2005b. VEGF as a key mediator of angiogenesis in cancer. *Oncology,* 69 Suppl 3**,** 4-10.

CARMELIET, P. & JAIN, R. K. 2000. Angiogenesis in cancer and other diseases. *Nature,* 407**,** 249-57.

CARMELIET, P., LAMPUGNANI, M.-G., MOONS, L., BREVIARIO, F., COMPERNOLLE, V., BONO, F., BALCONI, G., SPAGNUOLO, R., OOSTHUYSE, B., DEWERCHIN, M., ZANETTI, A., ANGELLILO, A., MATTOT, V., NUYENS, D., LUTGENS, E., CLOTMAN, F., DE RUITER, M. C., GITTENBERGER-DE GROOT, A., POELMANN, R., LUPU, F., HERBERT, J.-M., COLLEN, D. & DEJANA, E. 1999. Targeted Deficiency or Cytosolic Truncation of the VE-cadherin Gene in Mice Impairs VEGF-Mediated Endothelial Survival and Angiogenesis. *Cell,* 98**,** 147-157.

CHALARIS, A., ADAM, N., SINA, C., ROSENSTIEL, P., LEHMANN-KOCH, J., SCHIRMACHER, P., HARTMANN, D., CICHY, J., GAVRILOVA, O., SCHREIBER, S., JOSTOCK, T., MATTHEWS, V., HASLER, R., BECKER, C., NEURATH, M. F., REISS, K., SAFTIG, P., SCHELLER, J. & ROSE-JOHN, S. 2010. Critical role of the disintegrin metalloprotease ADAM17 for intestinal inflammation and regeneration in mice. *J Exp Med,* 207**,** 1617-24.

CHARRIN, S., JOUANNET, S., BOUCHEIX, C. & RUBINSTEIN, E. 2014. Tetraspanins at a glance. *J Cell Sci,* 127**,** 3641-8.

CHARRIN, S., MANIE, S., THIELE, C., BILLARD, M., GERLIER, D., BOUCHEIX, C. & RUBINSTEIN, E. 2003. A physical and functional link between cholesterol and tetraspanins. *Eur J Immunol,* 33**,** 2479-89.

CHU, H. & WANG, Y. 2012. Therapeutic angiogenesis: controlled delivery of angiogenic factors. *Ther Deliv,* 3**,** 693-714.

CLARK, P. 2014. Protease-mediated ectodomain shedding. *Thorax,* 69**,** 682-4.

CORADA, M., MARIOTTI, M., THURSTON, G., SMITH, K., KUNKEL, R., BROCKHAUS, M., LAMPUGNANI, M. G., MARTIN-PADURA, I., STOPPACCIARO, A., RUCO, L., MCDONALD, D. M., WARD, P. A. & DEJANA, E. 1999. Vascular endothelial–cadherin is an important determinant of microvascular integrity in vivo. *Proceedings of the National Academy of Sciences,* 96**,** 9815-9820.

CROSBY, C. V., FLEMING, P. A., ARGRAVES, W. S., CORADA, M., ZANETTA, L., DEJANA, E. & DRAKE, C. J. 2005. VE-cadherin is not required for the formation of nascent blood vessels but acts to prevent their disassembly. *Blood,* 105**,** 2771-6.

DE GOEIJ, B. E., VINK, T., TEN NAPEL, H., BREIJ, E. C., SATIJN, D., WUBBOLTS, R., MIAO, D. & PARREN, P. W. 2016. Efficient Payload Delivery by a Bispecific Antibody-Drug Conjugate Targeting HER2 and CD63. *Mol Cancer Ther,* 15**,** 2688-2697.

DEJANA, E. & ORSENIGO, F. 2013. Endothelial adherens junctions at a glance. *J Cell Sci,* 126**,** 2545-9.

DERYCKE, L., MORBIDELLI, L., ZICHE, M., DE WEVER, O., BRACKE, M. & VAN AKEN, E. 2006. Soluble N-cadherin fragment promotes angiogenesis. *Clin Exp Metastasis,* 23**,** 187-201.

DONNERS, M. M., WOLFS, I. M., OLIESLAGERS, S., MOHAMMADI-MOTAHHARI, Z., TCHAIKOVSKI, V., HEENEMAN, S., VAN BUUL, J. D., CAOLO, V., MOLIN, D. G., POST, M. J. & WALTENBERGER, J. 2010. A disintegrin and metalloprotease 10 is a novel mediator of vascular endothelial growth factor-induced endothelial

cell function in angiogenesis and is associated with atherosclerosis. *Arterioscler Thromb Vasc Biol,* 30**,** 2188-95.

DORNIER, E., COUMAILLEAU, F., OTTAVI, J. F., MORETTI, J., BOUCHEIX, C., MAUDUIT, P., SCHWEISGUTH, F. & RUBINSTEIN, E. 2012. TspanC8 tetraspanins regulate ADAM10/Kuzbanian trafficking and promote Notch activation in flies and mammals. *J Cell Biol,* 199**,** 481-96.

DORNIER, E., COUMAILLEAU, F., OTTAVI, J. F., MORETTI, J., BOUCHEIX, C., MAUDUIT, P., SCHWEISGUTH, F. & RUBINSTEIN, E. 2016. Correction: TspanC8 tetraspanins regulate ADAM10/Kuzbanian trafficking and promote Notch activation in flies and mammals. *J Cell Biol,* 213**,** 495-6.

DREYMUELLER, D., UHLIG, S. & LUDWIG, A. 2015. ADAM-family metalloproteinases in lung inflammation: potential therapeutic targets. *Am J Physiol Lung Cell Mol Physiol,* 308**,** L325-43.

EDWARDS, D. R., HANDSLEY, M. M. & PENNINGTON, C. J. 2008. The ADAM metalloproteinases. *Mol Aspects Med,* 29**,** 258-89.

EELEN, G., DE ZEEUW, P., SIMONS, M. & CARMELIET, P. 2015. Endothelial cell metabolism in normal and diseased vasculature. *Circ Res,* 116**,** 1231-44.

EHRHARDT, C., SCHMOLKE, M., MATZKE, A., KNOBLAUCH, A., WILL, C., WIXLER, V. & LUDWIG, S. 2006. Polyethylenimine, a cost-effective transfection reagent. *Signal Transduction,* 6**,** 179-184.

EILKEN, H. M. & ADAMS, R. H. 2010. Dynamics of endothelial cell behavior in sprouting angiogenesis. *Curr Opin Cell Biol,* 22**,** 617-25.

ENDRES, K. & DELLER, T. 2017. Regulation of Alpha-Secretase ADAM10 In vitro and In vivo: Genetic, Epigenetic, and Protein-Based Mechanisms. *Front Mol Neurosci,* 10**,** 56.

EVANS, D. T., TILLMAN, K. C. & DESROSIERS, R. C. 2002. Envelope glycoprotein cytoplasmic domains from diverse lentiviruses interact with the prenylated Rab acceptor. *J Virol,* 76**,** 327-37.

FACEY, A., PINAR, I., ARTHUR, J. F., QIAO, J., JING, J., MADO, B., CARBERRY, J., ANDREWS, R. K. & GARDINER, E. E. 2016. A-Disintegrin-And-Metalloproteinase (ADAM) 10 Activity on Resting and Activated Platelets. *Biochemistry,* 55**,** 1187-94.

FARBER, G., HURTADO, R., LOH, S., MONETTE, S., MTUI, J., KOPAN, R., QUAGGIN, S., MEYER-SCHWESINGER, C., HERZLINGER, D., SCOTT, R. P. & BLOBEL, C. P. 2018. Glomerular endothelial cell maturation depends on ADAM10, a key regulator of Notch signaling. *Angiogenesis,* 21**,** 335-347.

FENEANT, L., LEVY, S. & COCQUEREL, L. 2014. CD81 and hepatitis C virus (HCV) infection. *Viruses,* 6**,** 535-72.

FERRARA, N. & KERBEL, R. S. 2005. Angiogenesis as a therapeutic target. *Nature,* 438**,** 967-974.

FERRERI, D. M., MINNEAR, F. L., YIN, T., KOWALCZYK, A. P. & VINCENT, P. A. 2008. N-cadherin levels in endothelial cells are regulated by monolayer maturity and p120 availability. *Cell Commun Adhes,* 15**,** 333-49.

FLEMMING, S., BURKARD, N., RENSCHLER, M., VIELMUTH, F., MEIR, M., SCHICK, M. A., WUNDER, C., GERMER, C. T., SPINDLER, V., WASCHKE, J. & SCHLEGEL, N. 2015. Soluble VE-cadherin is involved in endothelial barrier breakdown in systemic inflammation and sepsis. *Cardiovasc Res,* 107**,** 32-44.

FOLKMAN, J. 1971. Tumor angiogenesis: therapeutic implications. *N Engl J Med,* 285**,** 1182-6.

FRANZKE, C. W., COBZARU, C., TRIANTAFYLLOPOULOU, A., LOFFEK, S., HORIUCHI, K., THREADGILL, D. W., KURZ, T., VAN ROOIJEN, N., BRUCKNER-TUDERMAN, L. & BLOBEL, C. P. 2012. Epidermal ADAM17 maintains the skin barrier by regulating EGFR ligand-dependent terminal keratinocyte differentiation. *J Exp Med,* 209**,** 1105-19.

GALLEY, H. F. & WEBSTER, N. R. 2004. Physiology of the endothelium. *Br J Anaesth,* 93**,** 105-13.

GARDINER, E. E. 2018. Proteolytic processing of platelet receptors. *Res Pract Thromb Haemost,* 2**,** 240-250.

GARDINER, E. E., KARUNAKARAN, D., SHEN, Y., ARTHUR, J. F., ANDREWS, R. K. & BERNDT, M. C. 2007. Controlled shedding of platelet glycoprotein (GP)VI and GPIb-IX-V by ADAM family metalloproteinases. *J Thromb Haemost,* 5**,** 1530-7.

GARTNER, A., FORNASIERO, E. F. & DOTTI, C. G. 2015. Cadherins as regulators of neuronal polarity. *Cell Adh Migr,* 9**,** 175-82.

GAVARD, J. & GUTKIND, J. S. 2006. VEGF controls endothelial-cell permeability by promoting the beta-arrestin-dependent endocytosis of VE-cadherin. *Nat Cell Biol,* 8**,** 1223-34.

GERHARDT, H., WOLBURG, H. & REDIES, C. 2000. N-cadherin mediates pericytic-endothelial interaction during brain angiogenesis in the chicken. *Dev Dyn,* 218**,** 472-9.

GERMAIN, M., CHASMAN, D. I., DE HAAN, H., TANG, W., LINDSTROM, S., WENG, L. C., DE ANDRADE, M., DE VISSER, M. C., WIGGINS, K. L., SUCHON, P., SAUT, N., SMADJA, D. M., LE GAL, G., VAN HYLCKAMA VLIEG, A., DI NARZO, A., HAO, K., NELSON, C. P., ROCANIN-ARJO, A., FOLKERSEN, L., MONAJEMI, R., ROSE, L. M., BRODY, J. A., SLAGBOOM, E., AISSI, D., GAGNON, F., DELEUZE, J. F., DELOUKAS, P., TZOURIO, C., DARTIGUES, J. F., BERR, C., TAYLOR, K. D., CIVELEK, M., ERIKSSON, P., CARDIOGENICS, C., PSATY, B. M., HOUWING-DUITERMAAT, J., GOODALL, A. H., CAMBIEN, F., KRAFT, P., AMOUYEL, P., SAMANI, N. J., BASU, S., RIDKER, P. M., ROSENDAAL, F. R., KABRHEL, C., FOLSOM, A. R., HEIT, J., REITSMA, P. H., TREGOUET, D. A., SMITH, N. L. & MORANGE, P. E. 2015. Meta-analysis of 65,734 individuals identifies TSPAN15 and SLC44A2 as two susceptibility loci for venous thromboembolism. *Am J Hum Genet,* 96**,** 532-42.

GIAMPIETRO, C., TADDEI, A., CORADA, M., SARRA-FERRARIS, G. M., ALCALAY, M., CAVALLARO, U., ORSENIGO, F., LAMPUGNANI, M. G. & DEJANA, E. 2012. Overlapping and divergent signaling pathways of N-cadherin and VE-cadherin in endothelial cells. *Blood,* 119**,** 2159-70.

GIANNOTTA, M., TRANI, M. & DEJANA, E. 2013. VE-cadherin and endothelial adherens junctions: active guardians of vascular integrity. *Dev Cell,* 26**,** 441-54.

GIEBELER, N. & ZIGRINO, P. 2016. A Disintegrin and Metalloprotease (ADAM): Historical Overview of Their Functions. *Toxins (Basel),* 8**,** 122.

GLOMSKI, K., MONETTE, S., MANOVA, K., DE STROOPER, B., SAFTIG, P. & BLOBEL, C. P. 2011. Deletion of Adam10 in endothelial cells leads to defects in organ-specific vascular structures. *Blood,* 118**,** 1163-74.

GRECO, C., BRALET, M. P., AILANE, N., DUBART-KUPPERSCHMITT, A., RUBINSTEIN, E., LE NAOUR, F. & BOUCHEIX, C. 2010. E-cadherin/p120-catenin and tetraspanin Co-029 cooperate for cell motility control in human colon carcinoma. *Cancer Res,* 70**,** 7674-83.

GREEN, L. R., MONK, P. N., PARTRIDGE, L. J., MORRIS, P., GORRINGE, A. R. & READ, R. C. 2011. Cooperative role for tetraspanins in adhesin-mediated attachment of bacterial species to human epithelial cells. *Infect Immun,* 79**,** 2241-9.

HAINING, E. J., YANG, J., BAILEY, R. L., KHAN, K., COLLIER, R., TSAI, S., WATSON, S. P., FRAMPTON, J., GARCIA, P. & TOMLINSON, M. G. 2012. The TspanC8 subgroup of tetraspanins interacts with A disintegrin and metalloprotease 10 (ADAM10) and regulates its maturation and cell surface expression. *J Biol Chem,* 287**,** 39753-65.

HARTMANN, D., DE STROOPER, B., SERNEELS, L., CRAESSAERTS, K., HERREMAN, A., ANNAERT, W., UMANS, L., LUBKE, T., LENA ILLERT, A., VON FIGURA, K. & SAFTIG, P. 2002. The disintegrin/metalloprotease ADAM 10 is essential for Notch signalling but not for alpha-secretase activity in fibroblasts. *Hum Mol Genet,* 11**,** 2615-24.

HARTMANN, M., HERRLICH, A. & HERRLICH, P. 2013. Who decides when to cleave an ectodomain? *Trends Biochem Sci,* 38**,** 111-20.

HASSUNA, N. A., MONK, P. N., ALI, F., READ, R. C. & PARTRIDGE, L. J. 2017. A role for the tetraspanin proteins in Salmonella infection of human macrophages. *J Infect,* 75**,** 115-124.

HAZAN, R. B., PHILLIPS, G. R., QIAO, R. F., NORTON, L. & AARONSON, S. A. 2000. Exogenous Expression of N-Cadherin in Breast Cancer Cells Induces Cell Migration, Invasion, and Metastasis. *The Journal of Cell Biology,* 148**,** 779-790.

HEIKENS, M. J., CAO, T. M., MORITA, C., DEHART, S. L. & TSAI, S. 2007. Penumbra encodes a novel tetraspanin that is highly expressed in erythroid progenitors and promotes effective erythropoiesis. *Blood,* 109**,** 3244-52.

HEMLER, M. E. 2005. Tetraspanin functions and associated microdomains. *Nat Rev Mol Cell Biol,* 6**,** 801-11.

HEMLER, M. E. 2008. Targeting of tetraspanin proteins--potential benefits and strategies. *Nat Rev Drug Discov,* 7**,** 747-58.

HEMLER, M. E. 2014. Tetraspanin proteins promote multiple cancer stages. *Nat Rev Cancer,* 14**,** 49-60.

HERBERT, S. P. & STAINIER, D. Y. 2011. Molecular control of endothelial cell behaviour during blood vessel morphogenesis. *Nat Rev Mol Cell Biol,* 12**,** 551-64.

HOFMANN, J. J. & IRUELA-ARISPE, M. L. 2007. Notch Signaling in Blood Vessels: Who Is Talking to Whom About What? *Circulation Research,* 100**,** 1556-1568.

HOGL, S., KUHN, P. H., COLOMBO, A. & LICHTENTHALER, S. F. 2011. Determination of the proteolytic cleavage sites of the amyloid precursor-like protein 2 by the proteases ADAM10, BACE1 and gamma-secretase. *PLoS One,* 6**,** e21337.

HOLDERFIELD, M. T. & HUGHES, C. C. 2008. Crosstalk between vascular endothelial growth factor, notch, and transforming growth factor-beta in vascular morphogenesis. *Circ Res,* 102**,** 637-52.

HORIUCHI, K., LE GALL, S., SCHULTE, M., YAMAGUCHI, T., REISS, K., MURPHY, G., TOYAMA, Y., HARTMANN, D., SAFTIG, P. & BLOBEL, C. P. 2007. Substrate selectivity of epidermal growth factor-receptor ligand sheddases and their regulation by phorbol esters and calcium influx. *Mol Biol Cell,* 18**,** 176-88.

HULME, R. S., HIGGINBOTTOM, A., PALMER, J., PARTRIDGE, L. J. & MONK, P. N. 2014. Distinct regions of the large extracellular domain of tetraspanin CD9 are involved in the control of human multinucleated giant cell formation. *PLoS One,* 9**,** e116289.

HUNDHAUSEN, C., MISZTELA, D., BERKHOUT, T. A., BROADWAY, N., SAFTIG, P., , K., HARTMANN, D., FAHRENHOLZ, F., POSTINA, R., MATTHEWS, V., KALLEN, K. J., ROSE-JOHN, S. & LUDWIG, A. 2003. The disintegrin-like metalloproteinase ADAM10 is involved in constitutive cleavage of CX3CL1 (fractalkine) and regulates CX3CL1-mediated cell-cell adhesion. *Blood,* 102**,** 1186-95.

HUNDHAUSEN, C., SCHULTE, A., SCHULZ, B., ANDRZEJEWSKI, M. G., SCHWARZ, N., VON HUNDELSHAUSEN, P., WINTER, U., PALIGA, K., REISS, K., SAFTIG, P., WEBER, C. & LUDWIG, A. 2007. Regulated shedding of transmembrane chemokines by the disintegrin and metalloproteinase 10 facilitates detachment of adherent leukocytes. *J Immunol,* 178**,** 8064-72.

HUNTLEY, G. W. 2002. Dynamic aspects of cadherin-mediated adhesion in synapse development and plasticity. *Biol Cell,* 94**,** 335-44.

INDURUWA, I., JUNG, S. M. & WARBURTON, E. A. 2016. Beyond antiplatelets: The role of glycoprotein VI in ischemic stroke. *Int J Stroke,* 11**,** 618-25.

INOSHIMA, I., INOSHIMA, N., WILKE, G. A., POWERS, M. E., FRANK, K. M., WANG, Y. & BUBECK WARDENBURG, J. 2011. A Staphylococcus aureus pore-forming toxin subverts the activity of ADAM10 to cause lethal infection in mice. *Nat Med,* 17**,** 1310-4.

ISOZAKI, T., RABQUER, B. J., RUTH, J. H., HAINES, G. K., 3RD & KOCH, A. E. 2013. ADAM-10 is overexpressed in rheumatoid arthritis synovial tissue and mediates angiogenesis. *Arthritis Rheum,* 65**,** 98-108.

ISRAELS, S. J. & MCMILLAN-WARD, E. M. 2010. Palmitoylation supports the association of tetraspanin CD63 with CD9 and integrin alphaIIbbeta3 in activated platelets. *Thromb Res,* 125**,** 152-8.

JACKSON, L. F., QIU, T. H., SUNNARBORG, S. W., CHANG, A., ZHANG, C., PATTERSON, C. & LEE, D. C. 2003. Defective valvulogenesis in HB-EGF and TACE-null mice is associated with aberrant BMP signaling. *EMBO J,* 22**,** 2704-16.

JAIN, R. K. & CARMELIET, P. F. 2001. Vessels of death or life. *Sci Am,* 285**,** 38-45.

JAKOBSSON, L., FRANCO, C. A., BENTLEY, K., COLLINS, R. T., PONSIOEN, B., ASPALTER, I. M., ROSEWELL, I., BUSSE, M., THURSTON, G., MEDVINSKY, A., SCHULTE-MERKER, S. & GERHARDT, H. 2010. Endothelial cells dynamically compete for the tip cell position during angiogenic sprouting. *Nat Cell Biol,* 12**,** 943-53.

JANES, P. W., SAHA, N., BARTON, W. A., KOLEV, M. V., WIMMER-KLEIKAMP, S. H., NIEVERGALL, E., BLOBEL, C. P., HIMANEN, J. P., LACKMANN, M. & NIKOLOV, D. B. 2005. Adam meets Eph: an ADAM substrate recognition module acts as a molecular switch for ephrin cleavage in trans. *Cell,* 123**,** 291-304.

JANES, P. W., WIMMER-KLEIKAMP, S. H., FRANGAKIS, A. S., TREBLE, K., GRIESSHABER, B., SABET, O., GRABENBAUER, M., TING, A. Y., SAFTIG, P., BASTIAENS, P. I. & LACKMANN, M. 2009. Cytoplasmic relaxation of active Eph controls ephrin shedding by ADAM10. *PLoS Biol,* 7**,** e1000215.

JOUANNET, S., SAINT-POL, J., FERNANDEZ, L., NGUYEN, V., CHARRIN, S., BOUCHEIX, C., BROU, C., MILHIET, P. E. & RUBINSTEIN, E. 2016. TspanC8 tetraspanins differentially regulate the cleavage of ADAM10 substrates, Notch activation and ADAM10 membrane compartmentalization. *Cell Mol Life Sci,* 73**,** 1895-915.

JUNGE, H. J., YANG, S., BURTON, J. B., PAES, K., SHU, X., FRENCH, D. M., COSTA, M., RICE, D. S. & YE, W. 2009. TSPAN12 regulates retinal vascular development by promoting Norrin- but not Wnt-induced FZD4/beta-catenin signaling. *Cell,* 139**,** 299-311.

KARAMATIC CREW, V., BURTON, N., KAGAN, A., GREEN, C. A., LEVENE, C., FLINTER, F., BRADY, R. L., DANIELS, G. & ANSTEE, D. J. 2004. CD151, the first member of the tetraspanin (TM4) superfamily detected on erythrocytes, is essential for the correct assembly of human basement membranes in kidney and skin. *Blood,* 104**,** 2217.

KHOKHA, R., MURTHY, A. & WEISS, A. 2013. Metalloproteinases and their natural inhibitors in inflammation and immunity. *Nature Reviews Immunology,* 13**,** 649.

KITADOKORO, K., BORDO, D., GALLI, G., PETRACCA, R., FALUGI, F., ABRIGNANI, S., GRANDI, G. & BOLOGNESI, M. 2001. CD81 extracellular domain 3D structure: insight into the tetraspanin superfamily structural motifs. *EMBO J,* 20**,** 12-8.

KLINGENER, M., CHAVALI, M., SINGH, J., MCMILLAN, N., COOMES, A., DEMPSEY, P. J., CHEN, E. I. & AGUIRRE, A. 2014. N-cadherin promotes recruitment and migration of neural progenitor cells from the SVZ neural stem cell niche into demyelinated lesions. *J Neurosci,* 34**,** 9590-606.

KOGEL, D., DELLER, T. & BEHL, C. 2012. Roles of amyloid precursor protein family members in neuroprotection, stress signaling and aging. *Exp Brain Res,* 217**,** 471-9.

KOJRO, E., FUGER, P., PRINZEN, C., KANAREK, A. M., RAT, D., ENDRES, K., FAHRENHOLZ, F. & POSTINA, R. 2010. Statins and the squalene synthase inhibitor zaragozic acid stimulate the non-amyloidogenic pathway of amyloid-beta protein precursor processing by suppression of cholesterol synthesis. *J Alzheimers Dis,* 20**,** 1215-31.

KOPAN, R. & ILAGAN, M. X. 2009. The canonical Notch signaling pathway: unfolding the activation mechanism. *Cell,* 137**,** 216-33.

KOVALENKO, O. V., METCALF, D. G., DEGRADO, W. F. & HEMLER, M. E. 2005. Structural organization and interactions of transmembrane domains in tetraspanin proteins. *BMC Structural Biology,* 5**,** 11-11.

KREBS, L. T., XUE, Y., NORTON, C. R., SHUTTER, J. R., MAGUIRE, M., SUNDBERG, J. P., GALLAHAN, D., CLOSSON, V., KITAJEWSKI, J., CALLAHAN, R., SMITH, G. H., STARK, K. L. & GRIDLEY, T. 2000. Notch signaling is essential for vascular morphogenesis in mice. *Genes Dev,* 14**,** 1343-52.

KUHN, P. H., COLOMBO, A. V., SCHUSSER, B., DREYMUELLER, D., WETZEL, S., SCHEPERS, U., HERBER, J., LUDWIG, A., KREMMER, E., MONTAG, D.,

MULLER, U., SCHWEIZER, M., SAFTIG, P., BRASE, S. & LICHTENTHALER, S. F. 2016. Systematic substrate identification indicates a central role for the metalloprotease ADAM10 in axon targeting and synapse function. *Elife,* 5.

LAMMERDING, J., KAZAROV, A. R., HUANG, H., LEE, R. T. & HEMLER, M. E. 2003. Tetraspanin CD151 regulates alpha6beta1 integrin adhesion strengthening. *Proc Natl Acad Sci U S A,* 100**,** 7616-21.

LAMPUGNANI, M. G., ZANETTI, A., CORADA, M., TAKAHASHI, T., BALCONI, G., BREVIARIO, F., ORSENIGO, F., CATTELINO, A., KEMLER, R., DANIEL, T. O. & DEJANA, E. 2003. Contact inhibition of VEGF-induced proliferation requires vascular endothelial cadherin, β-catenin, and the phosphatase DEP-1/CD148. *The Journal of Cell Biology,* 161**,** 793-804.

LATYSHEVA, N., MURATOV, G., RAJESH, S., PADGETT, M., HOTCHIN, N. A., OVERDUIN, M. & BERDITCHEVSKI, F. 2006. Syntenin-1 is a new component of tetraspanin-enriched microdomains: mechanisms and consequences of the interaction of syntenin-1 with CD63. *Mol Cell Biol,* 26**,** 7707-18.

LE GALL, S. M., BOBÉ, P., REISS, K., HORIUCHI, K., NIU, X. D., LUNDELL, D., GIBB, D. R., CONRAD, D., SAFTIG, P. & BLOBEL, C. P. 2009. ADAMs 10 and 17 Represent Differentially Regulated Components of a General Shedding Machinery for Membrane Proteins Such as Transforming Growth Factor α, L-Selectin, and Tumor Necrosis Factor α. *Mol Biol Cell,* 20**,** 1785-94.

LE GALL, S. M., MARETZKY, T., ISSUREE, P. D., NIU, X. D., REISS, K., SAFTIG, P., KHOKHA, R., LUNDELL, D. & BLOBEL, C. P. 2010. ADAM17 is regulated by a rapid and reversible mechanism that controls access to its catalytic site. *J Cell Sci,* 123**,** 3913-22.

LECKBAND, D. E. & DE ROOIJ, J. 2014. Cadherin adhesion and mechanotransduction. *Annu Rev Cell Dev Biol,* 30**,** 291-315.

LEE, H. R., SHIN, H. K., PARK, S. Y., KIM, H. Y., LEE, W. S., RHIM, B. Y., HONG, K. W. & KIM, C. D. 2014. Cilostazol suppresses beta-amyloid production by activating a disintegrin and metalloproteinase 10 via the upregulation of SIRT1-coupled retinoic acid receptor-beta. *J Neurosci Res,* 92**,** 1581-90.

LEMIEUX, G. A., BLUMENKRON, F., YEUNG, N., ZHOU, P., WILLIAMS, J., GRAMMER, A. C., PETROVICH, R., LIPSKY, P. E., MOSS, M. L. & WERB, Z. 2007. The low affinity IgE receptor (CD23) is cleaved by the metalloproteinase ADAM10. *J Biol Chem,* 282**,** 14836-44.

LEVY, S. 2014. Function of the tetraspanin molecule CD81 in B and T cells. *Immunol Res,* 58**,** 179-85.

LI, J.-L. 2009. Crosstalk of VEGF and Notch pathways in tumour angiogenesis: therapeutic implications. *Frontiers in Bioscience,* Volume**,** 3094.

LI, Y., LIU, P. C., SHEN, Y., SNAVELY, M. D. & HIRAGA, K. 2015. A Cell-Based Internalization and Degradation Assay with an Activatable Fluorescence-Quencher Probe as a Tool for Functional Antibody Screening. *J Biomol Screen,* 20**,** 869-75.

LICHTENTHALER, S. F., HAASS, C. & STEINER, H. 2011. Regulated intramembrane proteolysis--lessons from amyloid precursor protein processing. *J Neurochem,* 117**,** 779-96.

LINFORD, A., YOSHIMURA, S., NUNES BASTOS, R., LANGEMEYER, L., GERONDOPOULOS, A., RIGDEN, D. J. & BARR, F. A. 2012. Rab14 and its

exchange factor FAM116 link endocytic recycling and adherens junction stability in migrating cells. *Dev Cell,* 22**,** 952-66.

LOECHEL, F., OVERGAARD, M. T., OXVIG, C., ALBRECHTSEN, R. & WEWER, U. M. 1999. Regulation of human ADAM 12 protease by the prodomain. Evidence for a functional cysteine switch. *J Biol Chem,* 274**,** 13427-33.

LOPEZ-OTIN, C. & BOND, J. S. 2008. Proteases: multifunctional enzymes in life and disease. *J Biol Chem,* 283**,** 30433-7.

LUCITTI, J. L., MACKEY, J. K., MORRISON, J. C., HAIGH, J. J., ADAMS, R. H. & FABER, J. E. 2012. Formation of the collateral circulation is regulated by vascular endothelial growth factor-A and a disintegrin and metalloprotease family members 10 and 17. *Circ Res,* 111**,** 1539-50.

LUDWIG, A., HUNDHAUSEN, C., LAMBERT, M. H., BROADWAY, N., ANDREWS, R. C., BICKETT, D. M., LEESNITZER, M. A. & BECHERER, J. D. 2005. Metalloproteinase inhibitors for the disintegrin-like metalloproteinases ADAM10 and ADAM17 that differentially block constitutive and phorbol ester-inducible shedding of cell surface molecules. *Comb Chem High Throughput Screen,* 8**,** 161-71.

LUO, Y. & RADICE, G. L. 2005. N-cadherin acts upstream of VE-cadherin in controlling vascular morphogenesis. *J Cell Biol,* 169**,** 29-34.

MARAMBAUD, P., SHIOI, J., SERBAN, G., GEORGAKOPOULOS, A., SARNER, S., NAGY, V., BAKI, L., WEN, P., EFTHIMIOPOULOS, S., SHAO, Z., WISNIEWSKI, T. & ROBAKIS, N. K. 2002. A presenilin-1/gamma-secretase cleavage releases the E-cadherin intracellular domain and regulates disassembly of adherens junctions. *EMBO J,* 21**,** 1948-56.

MARCELLO, E., BORRONI, B., PELUCCHI, S., GARDONI, F. & DI LUCA, M. 2017. ADAM10 as a therapeutic target for brain diseases: from developmental disorders to Alzheimer's disease. *Expert Opin Ther Targets,* 21**,** 1017-1026.

MARCELLO, E., SARACENO, C., MUSARDO, S., VARA, H., DE LA FUENTE, A. G., PELUCCHI, S., DI MARINO, D., BORRONI, B., TRAMONTANO, A., PEREZ-OTANO, I., PADOVANI, A., GIUSTETTO, M., GARDONI, F. & DI LUCA, M. 2013. Endocytosis of synaptic ADAM10 in neuronal plasticity and Alzheimer's disease. *J Clin Invest,* 123**,** 2523-38.

MARETZKY, T., EVERS, A., LE GALL, S., ALABI, R. O., SPECK, N., REISS, K. & BLOBEL, C. P. 2015. The cytoplasmic domain of a disintegrin and metalloproteinase 10 (ADAM10) regulates its constitutive activity but is dispensable for stimulated ADAM10-dependent shedding. *J Biol Chem,* 290**,** 7416-25.

MARETZKY, T., REISS, K., LUDWIG, A., BUCHHOLZ, J., SCHOLZ, F., PROKSCH, E., DE STROOPER, B., HARTMANN, D. & SAFTIG, P. 2005. ADAM10 mediates E-cadherin shedding and regulates epithelial cell-cell adhesion, migration, and beta-catenin translocation. *Proc Natl Acad Sci U S A,* 102**,** 9182-7.

MARETZKY, T., SCHOLZ, F., KOTEN, B., PROKSCH, E., SAFTIG, P. & REISS, K. 2008. ADAM10-mediated E-cadherin release is regulated by proinflammatory cytokines and modulates keratinocyte cohesion in eczematous dermatitis. *J Invest Dermatol,* 128**,** 1737-46.

MARJON, K. D., TERMINI, C. M., KARLEN, K. L., SAITO-REIS, C., SORIA, C. E., LIDKE, K. A. & GILLETTE, J. M. 2016. Tetraspanin CD82 regulates bone marrow

homing of acute myeloid leukemia by modulating the molecular organization of N-cadherin. *Oncogene,* 35**,** 4132-40.

MARTIN, S. & MURRAY, J. C. 2009. *Angiogenesis protocols*, Springer.

MATTHEWS, A. L., KOO, C. Z., SZYROKA, J., HARRISON, N., KANHERE, A. & TOMLINSON, M. G. 2018. Regulation of Leukocytes by TspanC8 Tetraspanins and the "Molecular Scissor" ADAM10. *Front Immunol,* 9**,** 1451.

MATTHEWS, A. L., NOY, P. J., REYAT, J. S. & TOMLINSON, M. G. 2017a. Regulation of A disintegrin and metalloproteinase (ADAM) family sheddases ADAM10 and ADAM17: The emerging role of tetraspanins and rhomboids. *Platelets,* 28**,** 333-341.

MATTHEWS, A. L., SZYROKA, J., COLLIER, R., NOY, P. J. & TOMLINSON, M. G. 2017b. Scissor sisters: regulation of ADAM10 by the TspanC8 tetraspanins. *Biochem Soc Trans,* 45**,** 719-730.

MATTHEWS, V., SCHUSTER, B., SCHUTZE, S., BUSSMEYER, I., LUDWIG, A., HUNDHAUSEN, C., SADOWSKI, T., SAFTIG, P., HARTMANN, D., KALLEN, K. J. & ROSE-JOHN, S. 2003. Cellular cholesterol depletion triggers shedding of the human interleukin-6 receptor by ADAM10 and ADAM17 (TACE). *J Biol Chem,* 278**,** 38829-39.

MEHTA, V., FIELDS, L., EVANS, I. M., YAMAJI, M., PELLET-MANY, C., JONES, T., MAHMOUD, M. & ZACHARY, I. 2018. VEGF (Vascular Endothelial Growth Factor) Induces NRP1 (Neuropilin-1) Cleavage via ADAMs (a Disintegrin and Metalloproteinase) 9 and 10 to Generate Novel Carboxy-Terminal NRP1 Fragments That Regulate Angiogenic Signaling. *Arterioscler Thromb Vasc Biol*.

MENSAH, G. A. 2007. Healthy endothelium: The scientific basis for cardiovascular health promotion and chronic disease prevention. *Vascular Pharmacology,* 46**,** 310-314.

MONK, P. N. & PARTRIDGE, L. J. 2012. Tetraspanins: gateways for infection. *Infect Disord Drug Targets,* 12**,** 4-17.

MONTPELLIER, C., TEWS, B. A., POITRIMOLE, J., ROCHA-PERUGINI, V., D'ARIENZO, V., POTEL, J., ZHANG, X. A., RUBINSTEIN, E., DUBUISSON, J. & COCQUEREL, L. 2011. Interacting regions of CD81 and two of its partners, EWI-2 and EWI-2wint, and their effect on hepatitis C virus infection. *J Biol Chem,* 286**,** 13954-65.

MORTENSEN, D. L., PRABHU, S., STEFANICH, E. G., KADKHODAYAN-FISCHER, S., GELZLEICHTER, T. R., BAKER, D., JIANG, J., WALLACE, K., IYER, S., FIELDER, P. J. & PUTNAM, W. S. 2012. Effect of antigen binding affinity and effector function on the pharmacokinetics and pharmacodynamics of anti-IgE monoclonal antibodies. *MAbs,* 4**,** 724-31.

MOSS, M. L., BOMAR, M., LIU, Q., SAGE, H., DEMPSEY, P., LENHART, P. M., GILLISPIE, P. A., STOECK, A., WILDEBOER, D., BARTSCH, J. W., PALMISANO, R. & ZHOU, P. 2007. The ADAM10 prodomain is a specific inhibitor of ADAM10 proteolytic activity and inhibits cellular shedding events. *J Biol Chem,* 282**,** 35712-21.

MULLOOLY, M., MCGOWAN, P. M., KENNEDY, S. A., MADDEN, S. F., CROWN, J., N, O. D. & DUFFY, M. J. 2015. ADAM10: a new player in breast cancer progression? *Br J Cancer,* 113**,** 945-51.

MURAI, T., MARUYAMA, Y., MIO, K., NISHIYAMA, H., SUGA, M. & SATO, C. 2011. Low cholesterol triggers membrane microdomain-dependent CD44 shedding and suppresses tumor cell migration. *J Biol Chem,* 286**,** 1999-2007.

MURPHY, G. 2011. Tissue inhibitors of metalloproteinases. *Genome Biol,* 12**,** 233.

NAGANO, O., MURAKAMI, D., HARTMANN, D., DE STROOPER, B., SAFTIG, P., IWATSUBO, T., NAKAJIMA, M., SHINOHARA, M. & SAYA, H. 2004. Cell-matrix interaction via CD44 is independently regulated by different metalloproteinases activated in response to extracellular Ca(2+) influx and PKC activation. *J Cell Biol,* 165**,** 893-902.

NANBA, D., MAMMOTO, A., HASHIMOTO, K. & HIGASHIYAMA, S. 2003. Proteolytic release of the carboxy-terminal fragment of proHB-EGF causes nuclear export of PLZF. *The Journal of Cell Biology,* 163**,** 489-502.

NAVARRO, P., RUCO, L. & DEJANA, E. 1998. Differential Localization of VE- and N-Cadherins in Human Endothelial Cells: VE-Cadherin Competes with N-Cadherin for Junctional Localization. *The Journal of Cell Biology,* 140**,** 1475-1484.

NISHIUCHI, R., SANZEN, N., NADA, S., SUMIDA, Y., WADA, Y., OKADA, M., TAKAGI, J., HASEGAWA, H. & SEKIGUCHI, K. 2005. Potentiation of the ligand-binding activity of integrin alpha3beta1 via association with tetraspanin CD151. *Proc Natl Acad Sci U S A,* 102**,** 1939-44.

NOSEDA, M., CHANG, L., MCLEAN, G., GRIM, J. E., CLURMAN, B. E., SMITH, L. L. & KARSAN, A. 2004. Notch activation induces endothelial cell cycle arrest and participates in contact inhibition: role of p21Cip1 repression. *Mol Cell Biol,* 24**,** 8813-22.

NOY, P. J., YANG, J., REYAT, J. S., MATTHEWS, A. L., CHARLTON, A. E., FURMSTON, J., ROGERS, D. A., RAINGER, G. E. & TOMLINSON, M. G. 2016. TspanC8 Tetraspanins and A Disintegrin and Metalloprotease 10 (ADAM10) Interact via Their Extracellular Regions: EVIDENCE FOR DISTINCT BINDING MECHANISMS FOR DIFFERENT TspanC8 PROTEINS. *J Biol Chem,* 291**,** 3145-57.

NUSSE, R. & CLEVERS, H. 2017. Wnt/beta-Catenin Signaling, Disease, and Emerging Therapeutic Modalities. *Cell,* 169**,** 985-999.

OREN, R., TAKAHASHI, S., DOSS, C., LEVY, R. & LEVY, S. 1990. TAPA-1, the target of an antiproliferative antibody, defines a new family of transmembrane proteins. *Mol Cell Biol,* 10**,** 4007-15.

OTROCK, Z. K., MAHFOUZ, R. A., MAKAREM, J. A. & SHAMSEDDINE, A. I. 2007. Understanding the biology of angiogenesis: review of the most important molecular mechanisms. *Blood Cells Mol Dis,* 39**,** 212-20.

PASCIUTO, E., AHMED, T., WAHLE, T., GARDONI, F., D'ANDREA, L., PACINI, L., JACQUEMONT, S., TASSONE, F., BALSCHUN, D., DOTTI, C. G., CALLAERTS-VEGH, Z., D'HOOGE, R., MULLER, U. C., DI LUCA, M., DE STROOPER, B. & BAGNI, C. 2015. Dysregulated ADAM10-Mediated Processing of APP during a Critical Time Window Leads to Synaptic Deficits in Fragile X Syndrome. *Neuron,* 87**,** 382-98.

PECINA-SLAUS, N. 2003. Tumor suppressor gene E-cadherin and its role in normal and malignant cells. *Cancer Cell Int,* 3**,** 17.

PERON, R., VATANABE, I., MANZINE, P., CAMINS, A. & COMINETTI, M. 2018. Alpha-Secretase ADAM10 Regulation: Insights into Alzheimer's Disease Treatment. *Pharmaceuticals,* 11**,** 12.

PHNG, L. K. & GERHARDT, H. 2009. Angiogenesis: a team effort coordinated by notch. *Dev Cell,* 16**,** 196-208.

POSTINA, R., SCHROEDER, A., DEWACHTER, I., BOHL, J., SCHMITT, U., KOJRO, E., PRINZEN, C., ENDRES, K., HIEMKE, C., BLESSING, M., FLAMEZ, P., DEQUENNE, A., GODAUX, E., VAN LEUVEN, F. & FAHRENHOLZ, F. 2004. A disintegrin-metalloproteinase prevents amyloid plaque formation and hippocampal defects in an Alzheimer disease mouse model. *J Clin Invest,* 113**,** 1456-64.

POULTER, J. A., ALI, M., GILMOUR, D. F., RICE, A., KONDO, H., HAYASHI, K., MACKEY, D. A., KEARNS, L. S., RUDDLE, J. B., CRAIG, J. E., PIERCE, E. A., DOWNEY, L. M., MOHAMED, M. D., MARKHAM, A. F., INGLEHEARN, C. F. & TOOMES, C. 2010. Mutations in TSPAN12 Cause Autosomal-Dominant Familial Exudative Vitreoretinopathy. *The American Journal of Human Genetics,* 86**,** 248-253.

POWERS, M. E., BECKER, R. E., SAILER, A., TURNER, J. R. & BUBECK WARDENBURG, J. 2015. Synergistic Action of Staphylococcus aureus alpha-Toxin on Platelets and Myeloid Lineage Cells Contributes to Lethal Sepsis. *Cell Host Microbe,* 17**,** 775-87.

POWERS, M. E., KIM, H. K., WANG, Y. & BUBECK WARDENBURG, J. 2012. ADAM10 mediates vascular injury induced by Staphylococcus aureus alpha-hemolysin. *J Infect Dis,* 206**,** 352-6.

PROX, J., WILLENBROCK, M., WEBER, S., LEHMANN, T., SCHMIDT-ARRAS, D., SCHWANBECK, R., SAFTIG, P. & SCHWAKE, M. 2012. Tetraspanin15 regulates cellular trafficking and activity of the ectodomain sheddase ADAM10. *Cell Mol Life Sci,* 69**,** 2919-32.

PRUESSMEYER, J. & LUDWIG, A. 2009. The good, the bad and the ugly substrates for ADAM10 and ADAM17 in brain pathology, inflammation and cancer. *Semin Cell Dev Biol,* 20**,** 164-74.

RADICE, G. L. 2013. N-cadherin-mediated adhesion and signaling from development to disease: lessons from mice. *Prog Mol Biol Transl Sci,* 116**,** 263-89.

RADICE, G. L., RAYBURN, H., MATSUNAMI, H., KNUDSEN, K. A., TAKEICHI, M. & HYNES, R. O. 1997. Developmental defects in mouse embryos lacking N-cadherin. *Dev Biol,* 181**,** 64-78.

RAJESH, S., SRIDHAR, P., TEWS, B. A., FENEANT, L., COCQUEREL, L., WARD, D. G., BERDITCHEVSKI, F. & OVERDUIN, M. 2012. Structural basis of ligand interactions of the large extracellular domain of tetraspanin CD81. *J Virol,* 86**,** 9606-16.

REISS, K. & BHAKDI, S. 2017. The plasma membrane: Penultimate regulator of ADAM sheddase function. *Biochim Biophys Acta Mol Cell Res,* 1864**,** 2082-2087.

REISS, K., MARETZKY, T., LUDWIG, A., TOUSSEYN, T., DE STROOPER, B., HARTMANN, D. & SAFTIG, P. 2005. ADAM10 cleavage of N-cadherin and regulation of cell-cell adhesion and beta-catenin nuclear signalling. *EMBO J,* 24**,** 742-52.

REISS, K. & SAFTIG, P. 2009. The "a disintegrin and metalloprotease" (ADAM) family of sheddases: physiological and cellular functions. *Semin Cell Dev Biol,* 20**,** 126-37.

REYAT, J. S., CHIMEN, M., NOY, P. J., SZYROKA, J., RAINGER, G. E. & TOMLINSON, M. G. 2017. ADAM10-Interacting Tetraspanins Tspan5 and Tspan17 Regulate VE-Cadherin Expression and Promote T Lymphocyte Transmigration. *J Immunol,* 199**,** 666-676.

RIETHMUELLER, S., EHLERS, J. C., LOKAU, J., DUSTERHOFT, S., KNITTLER, K., DOMBROWSKY, G., GROTZINGER, J., RABE, B., ROSE-JOHN, S. & GARBERS, C. 2016. Cleavage Site Localization Differentially Controls Interleukin-6 Receptor Proteolysis by ADAM10 and ADAM17. *Sci Rep,* 6**,** 25550.

ROOKE, J., PAN, D., XU, T. & RUBIN, G. M. 1996. KUZ, a conserved metalloprotease-disintegrin protein with two roles in Drosophila neurogenesis. *Science,* 273**,** 1227-31.

RUBINSTEIN, E., CHARRIN, S. & TOMLINSON, M. G. 2013. Organisation of the Tetraspanin Web. *In:* BERDITCHEVSKI, F. & RUBINSTEIN, E. (eds.) *Tetraspanins.* Dordrecht: Springer Netherlands.

SACHS, N., KREFT, M., VAN DEN BERGH WEERMAN, M. A., BEYNON, A. J., PETERS, T. A., WEENING, J. J. & SONNENBERG, A. 2006. Kidney failure in mice lacking the tetraspanin CD151. *J Cell Biol,* 175**,** 33-9.

SAFTIG, P. & LICHTENTHALER, S. F. 2015. The alpha secretase ADAM10: A metalloprotease with multiple functions in the brain. *Prog Neurobiol,* 135**,** 1-20.

SAHIN, U., WESKAMP, G., KELLY, K., ZHOU, H. M., HIGASHIYAMA, S., PESCHON, J., HARTMANN, D., SAFTIG, P. & BLOBEL, C. P. 2004. Distinct roles for ADAM10 and ADAM17 in ectodomain shedding of six EGFR ligands. *J Cell Biol,* 164**,** 769-79.

SAINT-POL, J., BILLARD, M., DORNIER, E., ESCHENBRENNER, E., DANGLOT, L., BOUCHEIX, C., CHARRIN, S. & RUBINSTEIN, E. 2017a. New insights into the tetraspanin Tspan5 using novel monoclonal antibodies. *J Biol Chem,* 292**,** 9551-9566.

SAINT-POL, J., ESCHENBRENNER, E., DORNIER, E., BOUCHEIX, C., CHARRIN, S. & RUBINSTEIN, E. 2017b. Regulation of the trafficking and the function of the metalloprotease ADAM10 by tetraspanins. *Biochem Soc Trans,* 45**,** 937-44.

SALAS, A., PARDO-SECO, J., BARRAL-ARCA, R., CEBEY-LOPEZ, M., GOMEZ-CARBALLA, A., RIVERO-CALLE, I., PISCHEDDA, S., CURRAS-TUALA, M. J., AMIGO, J., GOMEZ-RIAL, J., MARTINON-TORRES, F. & NETWORK, G. 2018. Whole Exome Sequencing Identifies New Host Genomic Susceptibility Factors in Empyema Caused by Streptococcus pneumoniae in Children: A Pilot Study. *Genes (Basel),* 9.

SALOMON, D., AYALON, O., PATEL-KING, R., HYNES, R. O. & GEIGER, B. 1992. Extrajunctional distribution of N-cadherin in cultured human endothelial cells. *J Cell Sci,* 102 (Pt 1)**,** 7-17.

SANDERSON, M. P., ERICKSON, S. N., GOUGH, P. J., GARTON, K. J., WILLE, P. T., RAINES, E. W., DUNBAR, A. J. & DEMPSEY, P. J. 2005. ADAM10 mediates ectodomain shedding of the betacellulin precursor activated by

p-aminophenylmercuric acetate and extracellular calcium influx. *J Biol Chem,* 280**,** 1826-37.

SARACENO, C., MARCELLO, E., DI MARINO, D., BORRONI, B., CLAEYSEN, S., PERROY, J., PADOVANI, A., TRAMONTANO, A., GARDONI, F. & DI LUCA, M. 2014. SAP97-mediated ADAM10 trafficking from Golgi outposts depends on PKC phosphorylation. *Cell Death Dis,* 5**,** e1547.

SATHYA, M., MOORTHI, P., PREMKUMAR, P., KANDASAMY, M., JAYACHANDRAN, K. S. & ANUSUYADEVI, M. 2017. Resveratrol Intervenes Cholesterol- and Isoprenoid-Mediated Amyloidogenic Processing of AbetaPP in Familial Alzheimer's Disease. *J Alzheimers Dis,* 60**,** S3-S23.

SCHNEIDER, M. R. & KOLLIGS, F. T. 2015. E-cadherin's role in development, tissue homeostasis and disease: Insights from mouse models: Tissue-specific inactivation of the adhesion protein E-cadherin in mice reveals its functions in health and disease. *Bioessays,* 37**,** 294-304.

SCHNOOR, M. 2015. E-cadherin Is Important for the Maintenance of Intestinal Epithelial Homeostasis Under Basal and Inflammatory Conditions. *Digestive Diseases and Sciences,* 60**,** 816-818.

SCHULZ, B., PRUESSMEYER, J., MARETZKY, T., LUDWIG, A., BLOBEL, C. P., SAFTIG, P. & REISS, K. 2008. ADAM10 regulates endothelial permeability and T-Cell transmigration by proteolysis of vascular endothelial cadherin. *Circ Res,* 102**,** 1192-201.

SEEGAR, T. C. M., KILLINGSWORTH, L. B., SAHA, N., MEYER, P. A., PATRA, D., ZIMMERMAN, B., JANES, P. W., RUBINSTEIN, E., NIKOLOV, D. B., SKINIOTIS, G., KRUSE, A. C. & BLACKLOW, S. C. 2017. Structural Basis for Regulated Proteolysis by the alpha-Secretase ADAM10. *Cell,* 171**,** 1638-1648 e7.

SEIPOLD, L., ALTMEPPEN, H., KOUDELKA, T., THOLEY, A., KASPAREK, P., SEDLACEK, R., SCHWEIZER, M., BAR, J., MIKHAYLOVA, M., GLATZEL, M. & SAFTIG, P. 2018. In vivo regulation of the A disintegrin and metalloproteinase 10 (ADAM10) by the tetraspanin 15. *Cell Mol Life Sci,* 75**,** 3251-3267.

SHALABY, F., ROSSANT, J., YAMAGUCHI, T. P., GERTSENSTEIN, M., WU, X. F., BREITMAN, M. L. & SCHUH, A. C. 1995. Failure of blood-island formation and vasculogenesis in Flk-1-deficient mice. *Nature,* 376**,** 62-6.

SHAPIRO, L. & WEIS, W. I. 2009. Structure and biochemistry of cadherins and catenins. *Cold Spring Harb Perspect Biol,* 1**,** a003053.

SHERER, D. M. & ABULAFIA, O. 2001. Angiogenesis during implantation, and placental and early embryonic development. *Placenta,* 22**,** 1-13.

SHIBUYA, M. 2013. Vascular endothelial growth factor and its receptor system: physiological functions in angiogenesis and pathological roles in various diseases. *J Biochem,* 153**,** 13-9.

SHOHAM, T., RAJAPAKSA, R., BOUCHEIX, C., RUBINSTEIN, E., POE, J. C., TEDDER, T. F. & LEVY, S. 2003. The tetraspanin CD81 regulates the expression of CD19 during B cell development in a postendoplasmic reticulum compartment. *J Immunol,* 171**,** 4062-72.

SHOHAM, T., RAJAPAKSA, R., KUO, C. C., HAIMOVICH, J. & LEVY, S. 2006. Building of the tetraspanin web: distinct structural domains of CD81 function in different cellular compartments. *Mol Cell Biol,* 26**,** 1373-85.

SILVIE, O., RUBINSTEIN, E., FRANETICH, J. F., PRENANT, M., BELNOUE, E., RENIA, L., HANNOUN, L., ELING, W., LEVY, S., BOUCHEIX, C. & MAZIER, D. 2003. Hepatocyte CD81 is required for Plasmodium falciparum and Plasmodium yoelii sporozoite infectivity. *Nat Med,* 9**,** 93-6.

SIMONS, M., GORDON, E. & CLAESSON-WELSH, L. 2016. Mechanisms and regulation of endothelial VEGF receptor signalling. *Nat Rev Mol Cell Biol,* 17**,** 611-25.

SOLANAS, G., CORTINA, C., SEVILLANO, M. & BATLLE, E. 2011. Cleavage of E-cadherin by ADAM10 mediates epithelial cell sorting downstream of EphB signalling. *Nat Cell Biol,* 13**,** 1100-7.

SOTILLOS, S., ROCH, F. & CAMPUZANO, S. 1997. The metalloprotease-disintegrin Kuzbanian participates in Notch activation during growth and patterning of Drosophila imaginal discs. *Development,* 124**,** 4769.

STERK, L. M., GEUIJEN, C. A., VAN DEN BERG, J. G., CLAESSEN, N., WEENING, J. J. & SONNENBERG, A. 2002. Association of the tetraspanin CD151 with the laminin-binding integrins alpha3beta1, alpha6beta1, alpha6beta4 and alpha7beta1 in cells in culture and in vivo. *J Cell Sci,* 115**,** 1161-73.

STERNLICHT, M. D., SUNNARBORG, S. W., KOUROS-MEHR, H., YU, Y., LEE, D. C. & WERB, Z. 2005. Mammary ductal morphogenesis requires paracrine activation of stromal EGFR via ADAM17-dependent shedding of epithelial amphiregulin. *Development,* 132**,** 3923-33.

STIPP, C. S., KOLESNIKOVA, T. V. & HEMLER, M. E. 2003. Functional domains in tetraspanin proteins. *Trends in Biochemical Sciences,* 28**,** 106-112.

TANG, Z. 2017. GEPIA: a web server for cancer and normal gene expression profiling and interactive analyses. 45**,** W98-w102.

TANG, Z., LI, C., KANG, B., GAO, G., LI, C. & ZHANG, Z. 2017. GEPIA: a web server for cancer and normal gene expression profiling and interactive analyses. *Nucleic Acids Res,* 45**,** W98-W102.

TAYLOR, K. L., HENDERSON, A. M. & HUGHES, C. C. 2002. Notch activation during endothelial cell network formation in vitro targets the basic HLH transcription factor HESR-1 and downregulates VEGFR-2/KDR expression. *Microvasc Res,* 64**,** 372-83.

TEJERA, E., ROCHA-PERUGINI, V., LOPEZ-MARTIN, S., PEREZ-HERNANDEZ, D., BACHIR, A. I., HORWITZ, A. R., VAZQUEZ, J., SANCHEZ-MADRID, F. & YANEZ-MO, M. 2013. CD81 regulates cell migration through its association with Rac GTPase. *Mol Biol Cell,* 24**,** 261-73.

THOMER, L., SCHNEEWIND, O. & MISSIAKAS, D. 2016. Pathogenesis of Staphylococcus aureus Bloodstream Infections. *Annu Rev Pathol,* 11**,** 343-64.

TIPPMANN, F., HUNDT, J., SCHNEIDER, A., ENDRES, K. & FAHRENHOLZ, F. 2009. Up-regulation of the alpha-secretase ADAM10 by retinoic acid receptors and acitretin. *FASEB J,* 23**,** 1643-54.

TOMLINSON, M. G., HANKE, T., HUGHES, D. A., BARCLAY, A. N., SCHOLL, E., HUNIG, T. & WRIGHT, M. D. 1995. Characterization of mouse CD53: epitope mapping, cellular distribution and induction by T cell receptor engagement during repertoire selection. *Eur J Immunol,* 25**,** 2201-5.

TOMLINSON, M. G., WILLIAMS, A. F. & WRIGHT, M. D. 1993. Epitope mapping of anti-rat CD53 monoclonal antibodies. Implications for the membrane orientation of the Transmembrane 4 Superfamily. *Eur J Immunol,* 23**,** 136-40.

TOUSSEYN, T., THATHIAH, A., JORISSEN, E., RAEMAEKERS, T., KONIETZKO, U., REISS, K., MAES, E., SNELLINX, A., SERNEELS, L., NYABI, O., ANNAERT, W., SAFTIG, P., HARTMANN, D. & DE STROOPER, B. 2009. ADAM10, the rate-limiting protease of regulated intramembrane proteolysis of Notch and other proteins, is processed by ADAMS-9, ADAMS-15, and the gamma-secretase. *J Biol Chem,* 284**,** 11738-47.

TUCHER, J., LINKE, D., KOUDELKA, T., CASSIDY, L., TREDUP, C., WICHERT, R., PIETRZIK, C., BECKER-PAULY, C. & THOLEY, A. 2014. LC-MS based cleavage site profiling of the proteases ADAM10 and ADAM17 using proteome-derived peptide libraries. *J Proteome Res,* 13**,** 2205-14.

UEMURA, K., KIHARA, T., KUZUYA, A., OKAWA, K., NISHIMOTO, T., NINOMIYA, H., SUGIMOTO, H., KINOSHITA, A. & SHIMOHAMA, S. 2006. Characterization of sequential N-cadherin cleavage by ADAM10 and PS1. *Neurosci Lett,* 402**,** 278-83.

UHLEN, M., FAGERBERG, L., HALLSTROM, B. M., LINDSKOG, C., OKSVOLD, P., MARDINOGLU, A., SIVERTSSON, A., KAMPF, C., SJOSTEDT, E., ASPLUND, A., OLSSON, I., EDLUND, K., LUNDBERG, E., NAVANI, S., SZIGYARTO, C. A., ODEBERG, J., DJUREINOVIC, D., TAKANEN, J. O., HOBER, S., ALM, T., EDQVIST, P. H., BERLING, H., TEGEL, H., MULDER, J., ROCKBERG, J., NILSSON, P., SCHWENK, J. M., HAMSTEN, M., VON FEILITZEN, K., FORSBERG, M., PERSSON, L., JOHANSSON, F., ZWAHLEN, M., VON HEIJNE, G., NIELSEN, J. & PONTEN, F. 2015. Proteomics. Tissue-based map of the human proteome. *Science,* 347**,** 1260419.

VAN DER VORST, E. P. C., KEIJBECK, A. A., DE WINTHER, M. P. J. & DONNERS, M. M. P. C. 2012. A disintegrin and metalloproteases: Molecular scissors in angiogenesis, inflammation and atherosclerosis. *Atherosclerosis,* 224**,** 302-308.

VAN DEVENTER, S. J., DUNLOCK, V. E. & VAN SPRIEL, A. B. 2017. Molecular interactions shaping the tetraspanin web. *Biochem Soc Trans,* 45**,** 741-750.

VAN TETERING, G., VAN DIEST, P., VERLAAN, I., VAN DER WALL, E., KOPAN, R. & VOOIJS, M. 2009. Metalloprotease ADAM10 is required for Notch1 site 2 cleavage. *J Biol Chem,* 284**,** 31018-27.

VAN ZELM, M. C., SMET, J., ADAMS, B., MASCART, F., SCHANDENE, L., JANSSEN, F., FERSTER, A., KUO, C. C., LEVY, S., VAN DONGEN, J. J. & VAN DER BURG, M. 2010. CD81 gene defect in humans disrupts CD19 complex formation and leads to antibody deficiency. *J Clin Invest,* 120**,** 1265-74.

VASSILEV, V. S., MANDAI, M., YONEMURA, S. & TAKEICHI, M. 2012. Loss of N-Cadherin from the Endothelium Causes Stromal Edema and Epithelial Dysgenesis in the Mouse Cornea. *Investigative Ophthalmology & Visual Science,* 53**,** 7183-7193.

VENTRESS, J. K., PARTRIDGE, L. J., READ, R. C., COZENS, D., MACNEIL, S. & MONK, P. N. 2016. Peptides from Tetraspanin CD9 Are Potent Inhibitors of Staphylococcus Aureus Adherence to Keratinocytes. *PLoS One,* 11**,** e0160387.

VIRREIRA WINTER, S., ZYCHLINSKY, A. & BARDOEL, B. W. 2016. Genome-wide CRISPR screen reveals novel host factors required for Staphylococcus aureus α-hemolysin-mediated toxicity. *Scientific Reports,* 6**,** 24242.

WANG, H. X., KOLESNIKOVA, T. V., DENISON, C., GYGI, S. P. & HEMLER, M. E. 2011. The C-terminal tail of tetraspanin protein CD9 contributes to its function and molecular organization. *J Cell Sci,* 124**,** 2702-10.

WEBER, S. & SAFTIG, P. 2012. Ectodomain shedding and ADAMs in development. *Development,* 139**,** 3693-709.

WELTI, J., LOGES, S., DIMMELER, S. & CARMELIET, P. 2013. Recent molecular discoveries in angiogenesis and antiangiogenic therapies in cancer. *J Clin Invest,* 123**,** 3190-200.

WETZEL, S., SEIPOLD, L. & SAFTIG, P. 2017. The metalloproteinase ADAM10: A useful therapeutic target? *Biochim Biophys Acta Mol Cell Res,* 1864**,** 2071-2081.

WHEELOCK, M. J., SHINTANI, Y., MAEDA, M., FUKUMOTO, Y. & JOHNSON, K. R. 2008. Cadherin switching. *J Cell Sci,* 121**,** 727-35.

WHO. 2007. *Cardiovascular diseases (CVDs)* [Online]. World Health Organization. [Accessed 14.11.15].

WILLIAMS, C. K., LI, J. L., MURGA, M., HARRIS, A. L. & TOSATO, G. 2006. Up-regulation of the Notch ligand Delta-like 4 inhibits VEGF-induced endothelial cell function. *Blood,* 107**,** 931-9.

WINTERWOOD, N. E., VARZAVAND, A., MELAND, M. N., ASHMAN, L. K. & STIPP, C. S. 2006. A critical role for tetraspanin CD151 in alpha3beta1 and alpha6beta4 integrin-dependent tumor cell functions on laminin-5. *Mol Biol Cell,* 17**,** 2707-21.

WONG, E., MARETZKY, T., PELEG, Y., BLOBEL, C. P. & SAGI, I. 2015. The Functional Maturation of A Disintegrin and Metalloproteinase (ADAM) 9, 10, and 17 Requires Processing at a Newly Identified Proprotein Convertase (PC) Cleavage Site. *J Biol Chem,* 290**,** 12135-46.

XU, C., ZHANG, Y. H., THANGAVEL, M., RICHARDSON, M. M., LIU, L., ZHOU, B., ZHENG, Y., OSTROM, R. S. & ZHANG, X. A. 2009. CD82 endocytosis and cholesterol-dependent reorganization of tetraspanin webs and lipid rafts. *FASEB J,* 23**,** 3273-88.

YAN, Y., SHIRAKABE, K. & WERB, Z. 2002. The metalloprotease Kuzbanian (ADAM10) mediates the transactivation of EGF receptor by G protein-coupled receptors. *J Cell Biol,* 158**,** 221-6.

YANG, X. H., MIRCHEV, R., DENG, X., YACONO, P., YANG, H. L., GOLAN, D. E. & HEMLER, M. E. 2012. CD151 restricts the alpha6 integrin diffusion mode. *J Cell Sci,* 125**,** 1478-87.

YANG, X. H., RICHARDSON, A. L., TORRES-ARZAYUS, M. I., ZHOU, P., SHARMA, C., KAZAROV, A. R., ANDZELM, M. M., STROMINGER, J. L., BROWN, M. & HEMLER, M. E. 2008. CD151 accelerates breast cancer by regulating alpha 6 integrin function, signaling, and molecular organization. *Cancer Res,* 68**,** 3204-13.

YAUCH, R. L., KAZAROV, A. R., DESAI, B., LEE, R. T. & HEMLER, M. E. 2000. Direct extracellular contact between integrin alpha(3)beta(1) and TM4SF protein CD151. *J Biol Chem,* 275**,** 9230-8.

YOSHIDA, T., EBINA, H. & KOYANAGI, Y. 2009. N-linked glycan-dependent interaction of CD63 with CXCR4 at the Golgi apparatus induces downregulation of CXCR4. *Microbiol Immunol,* 53**,** 629-35.

ZHANG, B., ZHANG, Z., LI, L., QIN, Y. R., LIU, H., JIANG, C., ZENG, T. T., LI, M. Q., XIE, D., LI, Y., GUAN, X. Y. & ZHU, Y. H. 2018. TSPAN15 interacts with BTRC to promote

oesophageal squamous cell carcinoma metastasis via activating NF-kappaB signaling. *Nat Commun,* 9**,** 1423.

ZHANG, C., TIAN, L., CHI, C., WU, X., YANG, X., HAN, M., XU, T., ZHUANG, Y. & DENG, K. 2010. Adam10 is essential for early embryonic cardiovascular development. *Dev Dyn,* 239**,** 2594-602.

ZHOU, J., FUJIWARA, T., YE, S., LI, X. & ZHAO, H. 2014. Downregulation of Notch modulators, tetraspanin 5 and 10, inhibits osteoclastogenesis in vitro. *Calcif Tissue Int,* 95**,** 209-17.

ZHOU, Y., GOENAGA, A. L., HARMS, B. D., ZOU, H., LOU, J., CONRAD, F., ADAMS, G. P., SCHOEBERL, B., NIELSEN, U. B. & MARKS, J. D. 2012. Impact of intrinsic affinity on functional binding and biological activity of EGFR antibodies. *Mol Cancer Ther,* 11**,** 1467-76.

ZIMMERMAN, B., KELLY, B., MCMILLAN, B. J., SEEGAR, T. C. M., DROR, R. O., KRUSE, A. C. & BLACKLOW, S. C. 2016. Crystal Structure of a Full-Length Human Tetraspanin Reveals a Cholesterol-Binding Pocket. *Cell,* 167**,** 1041-1051 e11.

ZUIDSCHERWOUDE, M., DUNLOCK, V.-M. E., VAN DEN BOGAART, G., VAN DEVENTER, S. J., VAN DER SCHAAF, A., VAN OOSTRUM, J., GOEDHART, J., IN 'T HOUT, J., HÄMMERLING, G. J., TANAKA, S., NADLER, A., SCHULTZ, C., WRIGHT, M. D., ADJOBO-HERMANS, M. J. W. & VAN SPRIEL, A. B. 2017. Tetraspanin microdomains control localized protein kinase C signaling in B cells. *Science Signaling,* 10.

ZUIDSCHERWOUDE, M., GÖTTFERT, F., DUNLOCK, V. M. E., FIGDOR, C. G., VAN DEN BOGAART, G. & VAN SPRIEL, A. B. 2015. The tetraspanin web revisited by super-resolution microscopy. *Scientific reports,* 5.